Repurposing Dichloroacetate for the Treatment of Multiple Myeloma

Dandan Tian

June 2018

A thesis submitted for the degree of Doctor of Philosophy of
The Australian National University

Declaration

This thesis contains no material which has been accepted for the award of any other degree or diploma in any university with the exception of the patients 005 and 006 data in Figure 4.3, Table 4.10, and Table 4.11, which formed part of the thesis submitted for the degree of Master of Biotechnology of Ms Niloofar Pooryousef, Nov 2017 (awarded). To the best of the author's knowledge, it contains no material previously published or written by another person, except where due reference is made in the text.

Dandan Tian

June 2018

Acknowledgments

This research is supported by Cancer Council ACT, Cancer Australia and the Canberra Hospital (TCH) Private Practice Trust Fund.

I would like to express my gratitude to my supervisory panel: A/Prof. Anneke Blackburn, Dr James D'Rozario, Prof. Stefan Broer, Dr Lucy Coupland and Dr Nadine Hein. I especially want to thank my main supervisor Anneke who not only guided me through this uphill journey of medical research but also taught me how to be an independent researcher.

I wish to thank the funding body of the Australia National University for offering me a scholarship, which allowed me to focus on my research and I also want to thank James and Anneke for their generous support of my scholarship extension which allowed me to finish the final part of my research without worrying about finance difficulty.

I would like to thank our collaborators from the Haematology Department of The Canberra Hospital who generously offered their time and expertise and the patients who participated in our trial. I enjoyed working together with Dr Sam Bennett, Dr Yadanar Lwin, Dr Kathryn Forwood and Dr Fathima Ayyalil to facilitate patients' samples collection and medical records collating. I enjoyed the discussions with Dr Philip Crispin about how to find the best way to test the yield of plasma cell from patients' bone marrow samples. I want to thank Dr Euan McNaughton for his technique support.

I also want to say a special thanks to Ms Melissa Rooke for her patient help with my experiments. I am highly appreciative of the support I received from all members of the Blackburn, Board, Hannan and Gardiner groups, from the ACRF Cancer Biology & Therapeutics Department, during my study time here.

I have made strong connections and valuable friendships throughout my study here. I want to thank my colleagues from John Curtin School of Medical Research and friends from University House and Graduate House. I would also like to thank my family in China for their support of my decision to change my clinical medical career into medical research.

Abstract

Multiple myeloma (MM) is an incurable B-cell malignancy and the second most common haematological cancer in the world. MM patients easily develop innate and acquired chemotherapy resistance due to the dynamic gene mutations. The current standard MM treatment is not promising as patients go through cycles of remission and relapse and eventually treatment failure. Therefore, new treatments and management approaches are needed.

MM displays a glycolytic phenotype (Warburg effect) that contributes to cancer development, survival, and drug resistance. Dichloroacetate (DCA) is a pyruvate dehydrogenase kinase (PDK) inhibitor that can reverse the glycolytic phenotype. DCA is an inexpensive and bioavailable drug that has been used to treat mitochondrial malfunctions in humans for decades. Studies have shown DCA to have metabolic modulatory and cytotoxicity effects when used at clinically unachievable concentrations (>10 mM) in various cancer types including MM, but there is a lack of evidence of the on-target and anti-cancer effects of DCA when it is used at clinically achievable concentrations. DCA inhibits its own metabolism through inactivation of its only known metabolising enzyme, GSTZ1. It has been hypothesised that *GSTZ1* polymorphisms alter a patient's ability to metabolise DCA, thus it has been proposed that a personalized DCA dose regimen based on *GSTZ1* genotype be applied for clinical use.

This study examined the on-target and anti-cancer effects of DCA at mechanistically relevant concentrations under clinically relevant conditions in MM cell lines, and investigated the factors contributing to the variable sensitivity to DCA. The clinical implication of DCA was examined in a phase-2 clinical trial in MM patients and the pharmacokinetics and pharmacogenetics of DCA were evaluated.

Results of this study showed that DCA at mechanistically relevant concentrations inhibited glycolysis and cell proliferation but did not induce apoptosis in MM cell lines. DCA can act on-target by reducing phosphorylated pyruvate dehydrogenase (pPDH) when used at concentrations achieved in our clinical trial. The effect of DCA in reducing pPDH was cumulative *in vitro* over time.

This study demonstrated that MM cells displayed heterogeneous metabolic profiles. The degree of dependence on glycolysis was a key contributing factor in the sensitivity of MM cells to DCA. Moreover, the growth inhibition effect of DCA required glucose and an active glycolysis pathway. Under hypoxic conditions that mimic the bone marrow (BM) microenvironment (BMM), DCA can induce apoptosis in a non-glycolytic cell line that has the greatest glycolytic reserve and the highest increase in the targets of DCA, PDK1 and PDK3. Thus, DCA can have greater growth inhibition effect and even cytotoxic effects in hypoxic cancers.

The clinical use of DCA in cancer had been tested in four clinical trials in solid tumours, with results showing that DCA was well tolerated but there was no direct efficacy information. The clinical use of DCA in haematological cancer patients was investigated through our world-first trial of DCA in MM patients. The results demonstrated that DCA was quickly absorbed and maintained at mechanistically relevant concentrations for inhibition of PDK2. MM patients tolerated DCA well despite having baseline neuropathy. The main side effect of DCA was neuropathy but this was reversible. The disease burden was reduced, and a response was achieved on day 28 in 33% of patients, but this effect was not maintained. A *GSTZ1* promoter polymorphism correlated with one patient's elevated DCA serum levels and side effects, and it may be the driving variant in determining the serum levels of DCA in long-term use. This trial suggested that the DCA dosing regimen needs to be increased in order for it to inhibit the targets PDK1 and PDK3 in cancer patients in future trials. The combination of DCA with common chemotherapy drugs, such as dexamethasone (DEX) and lenalidomide (LEN), significantly decreased the total viable cells numbers compared to when DEX or LEN was used as a single agent. This indicates that DCA is not interfering with the conventional chemotherapy agents.

Thus, DCA has the potential to be used as a low-toxicity addition to conventional chemotherapy for the treatment of MM. This study provides DCA dosing guidance and opens windows for future clinical trials in cancers that display a glycolytic phenotype.

Conference Proceedings and Manuscripts

Oral Conference Presentations

Dichloroacetate (DCA) at clinically achievable concentrations can reduce pPDH and inhibit growth in Multiple Myeloma (MM) cells. In Canberra Health Annual Research Meeting, ACT, Australia. 2017.

GSTZ1 genotypes correlate with DCA levels and chronic side effects in MM patients. In Canberra Health Annual Research Meeting, ACT, Australia. 2017.

Targeting the Dexamethasone Resistance in MM with DCA. In Canberra Health Annual Research Meeting, ACT, Australia. 2016.

Targeting the Glycolytic Phenotype of MM with DCA. In ASMR New Investigator Forum, JCSMR, ACT, Australia. 2016.

Poster Conference Presentations

D. Tian, M. Rooke, A. C. Blackburn. DCA at clinically achievable concentrations can reduce pPDH and reverse the glycolytic phenotype in MM cells. In Proceedings of 2nd Australian Cancer Metabolism Meeting. VIC, Australia. 2017

D. Tian, S. K. Bennett, L. A. Coupland, K. Forwood, Y. Lwin, I. Tea, T. Neeman, P. Crispin, J. D'Rozario, A. C. Blackburn. DiCAM (DiChloroAcetate in Myeloma): a trial of DCA efficacy and pharmacogenetics in MM patients in partial remission. In Proceedings of 2nd Australian Cancer Metabolism Meeting. VIC, Australia. 2017

D. Tian, A. C. Blackburn. Targeting the Dexamethasone Resistance in MM with DCA. In Proceedings of International Cell Conference: Hallmarks of Cancer. Ghent, Belgium. 2016.

D. Tian, L. A. Coupland, J. D'Rozario, A. C. Blackburn. Targeting the Glycolytic Phenotype of MM with DCA. In Proceedings of 28th Lorne Cancer Conference. VIC, Australia. 2016.

Manuscript in Preparation

GSTZ1 genotypes correlate with dichloroacetate levels and chronic side effects in multiple myeloma patients.

Dandan Tian, Samuel K. Bennett, Lucy A. Coupland, Kathryn Forwood, Yadanar Lwin, Niloofar Pooryousef, Illa Tea, Teresa Neeman, Philip Crispin, and James D'Rozario, Anneke C. Blackburn.

In preparation for submission to British Journal of Clinical Pharmacology.

Table of Contents

List of Abbreviations

^{18}F-FDG: ^{18}F- fluorodeoxyglucose
2-DG: 2-deoxy-D-glucose
2-ME: 2-mercaptoethanol
Acetyl CoA: acetyl coenzyme A
ADP: adenosine diphosphate
ASCT: autologous stem cell transplant
ATCC: American Type Culture Collection
ATP: adenosine triphosphate
Bak: Bcl-2 homologous antagonist killer
Bax: Bcl-2-associated X protein
Bcl-2: B-cell lymphoma 2
BM: bone marrow
BMM: bone marrow microenvironment
BrdU: Bromodeoxyuridine
cDNA: complementary DNA
CFSE: Carboxyfluorescein Diacetate Succinimidyl Ester
CI: combination index
CO_2: carbon dioxide
CRBN: cereblon
DCA: dichloroacetate
DEX: dexamethasone
ECAR: extracellular acidification rate
EGFR: epidermal growth factor receptor
ETC: electron transport chain
FA: fatty acid
FACS: fluorescence-activated cell sorting
$FADH_2$: flavin adenine dinucleotide
FAO: fatty acid oxidation
FASN: fatty acid synthase
FCCP: carbonyl cyanide-4 (trifluoromethoxy) phenylhydrazone
FLC: free light chain
G6P: glucose-6-phosphate
GAPDH: glyceraldehyde 3-phosphate dehydrogenase
GC: glucocorticoid
GLS: glutaminase
GLUD: glutamate dehydrogenase
GLUT: glucose transporters
GR: glucocorticoid receptor
GSTZ1: glutathione transferase Zeta 1
HIF: hypoxia inducible factor
HK: hexokinase
HRE: hypoxia-responsive element
HSC: haematopoietic stem cell
Ig: immunoglobulin
IL-6: interleukin-6
IMWG: International Myeloma Working Group
LC/MS: liquid chromatography–mass spectrometry

LDHA: lactate dehydrogenase A
LEN: lenalidomide
MAPK: mitogen activated protein kinase
MCT: monocarboxylate transporter
MGUS: monoclonal gammopathy of undetermined significance
MM: multiple myeloma
MPC: mitochondria pyruvate carrier
mRNA: messenger ribonucleic acid
mTOR: mammalian target of rapamycin
NADH: reduced nicotinamide adenine dinucleotide
NADPH: reduced nicotinamide adenine dinucleotide phosphate
NF-κB: nuclear factor kappa-light-chain-enhancer of activated B cells
NIH: National Institutes of Health
NK cells: natural killer cells
OCR: oxygen consumption rate
OXPHOS: oxidative phosphorylation
PBMC: peripheral blood mononuclear cell
PCR: polymerase chain reaction
PDC: pyruvate dehydrogenase complex
PDH: pyruvate dehydrogenase
PDK: pyruvate dehydrogenase kinase
PDP: pyruvate dehydrogenase phosphatase
PDT: cell population-doubling time
PET: positron emission tomography
PHD: prolyl hydroxylases
PI: propidium iodide
PI3K: phosphatidylinositol3-kinase
PKM: pyruvate kinase
pPDH: phosphorylated pyruvate dehydrogenase
PPP: pentose phosphate pathway
Puma: p53-upregulated modulator of apoptosis
ROS: reactive oxygen species
SD: standard deviation
SMM: smouldering multiple myeloma
SNP: single nucleotide polymorphism
TCA: tricarboxylic acid cycle
TIGAR: TP53-induced glycolysis and apoptosis regulator
TNSc: total neuropathy score
tPDH: total pyruvate dehydrogenase
VEGF: vascular endothelial growth factor
α-KG: α-ketoglutarate

Chapter 1 Introduction

Overview: Deregulated cancer metabolism is recognised as a hallmark of cancer. The genetic aberrations of cancer cells are recognised as drivers of the abnormal metabolism phenotypes, which provide selective advantages for cancer cell survival (section 1.2). One of the most studied metabolic phenotypes is known as the glycolytic phenotype (Warburg effect), where cancer cells rely on glycolysis instead of mitochondrial respiration, even in the presence of oxygen (section 1.2). This glycolytic phenotype is present in a majority of cancer types, making it a promising therapeutic target in cancer treatment [1, 2]. There are metabolic modulatory drugs that are clinically usable or are used as experimental tools for targeting the glycolytic phenotype in cancer, as well as other commonly deregulated metabolic pathways including the mitochondrial metabolism, glutamine metabolism and fatty acid synthesis (section 1.3). Compared to other metabolic modulatory drugs, dichloroacetate (DCA), an investigational drug that has been used for the treatment of lactate acidosis and mitochondrial malfunction for decades in humans, has potential to be repurposed in cancer therapy for its merit of targeting the PDH/PDK axis central to metabolic control, its low toxic, established safety profile in patients and relatively low cost (section 1.4) [3, 4]. DCA has been shown to have anti-growth effects both *in vitro* and *in vivo* in various cancer types [5-10]. Multiple myeloma (MM), an incurable B cell malignancy with a complex genetic profile, also displays a glycolytic phenotype, which can be targeted by DCA [11-13]. The rationale behind the repurposing of DCA in the treatment of myeloma patients is discussed in section 1.5, leading to the hypothesis and aims of this thesis (section 1.6).

1.1 Normal glucose metabolism

Cancer cells present with a different metabolic phenotype compared to that of normal cells. Targeting cancer cell metabolism has been investigated as a new treatment approach. One of the most studied phenotypes in cancer is the glycolytic phenotype. To understand the glycolytic phenotype in cancer, this section will first explain the glucose metabolism in normal cells.

1.1.1 Glycolysis

Glucose, a simple six-carbon sugar, is the most abundant and important energy-producing organic molecule for living cells. Glycolysis is a multi-step process, which occurs in the cytoplasm to metabolise glucose into two molecules of the three-carbon compound pyruvate. The glycolysis pathway contains 10 steps of biochemical reactions, and each reaction is catalysed by a specific enzyme as follows: hexokinase (HK), phosphoglucose isomerase, phosphofructokinase (PFK), aldolase, triosephosphate isomerase, glyceraldehyde 3-phosphate dehydrogenase (GAPDH), phosphoglycerate kinase, phosphoglycerate mutase, enolase, and pyruvate kinase (PKM) (**Figure 1.1**) [14, 15]. This process results in the production of two molecules of adenosine triphosphate (ATP, energy-containing molecules), two molecules of pyruvate, and two molecules of nicotinamide adenine dinucleotide reduced form (NADH) (electron-carrying molecules) [14].

Glycolysis is a process independent of the presence of oxygen. When oxygen is sufficient, pyruvate is transported across the mitochondrial membranes into the mitochondrial matrix to get completely oxidized through the tricarboxylic acid (TCA) cycle, also known as the citric acid cycle or Krebs cycle, which is followed by oxidative phosphorylation to create 34 ATP molecules. This process is known as oxidative glucose metabolism. But in hypoxia, glycolysis is the dominant metabolic pathway and the pyruvate generated through glycolysis is converted into lactate instead of going through the oxidative phosphorylation. This process is known as anaerobic glycolysis [14]. Many other metabolic pathways involved in the synthesis of macromolecules such as lipids, proteins and nucleotides synthesis are strongly dependent on glycolysis for their source of metabolic precursors.

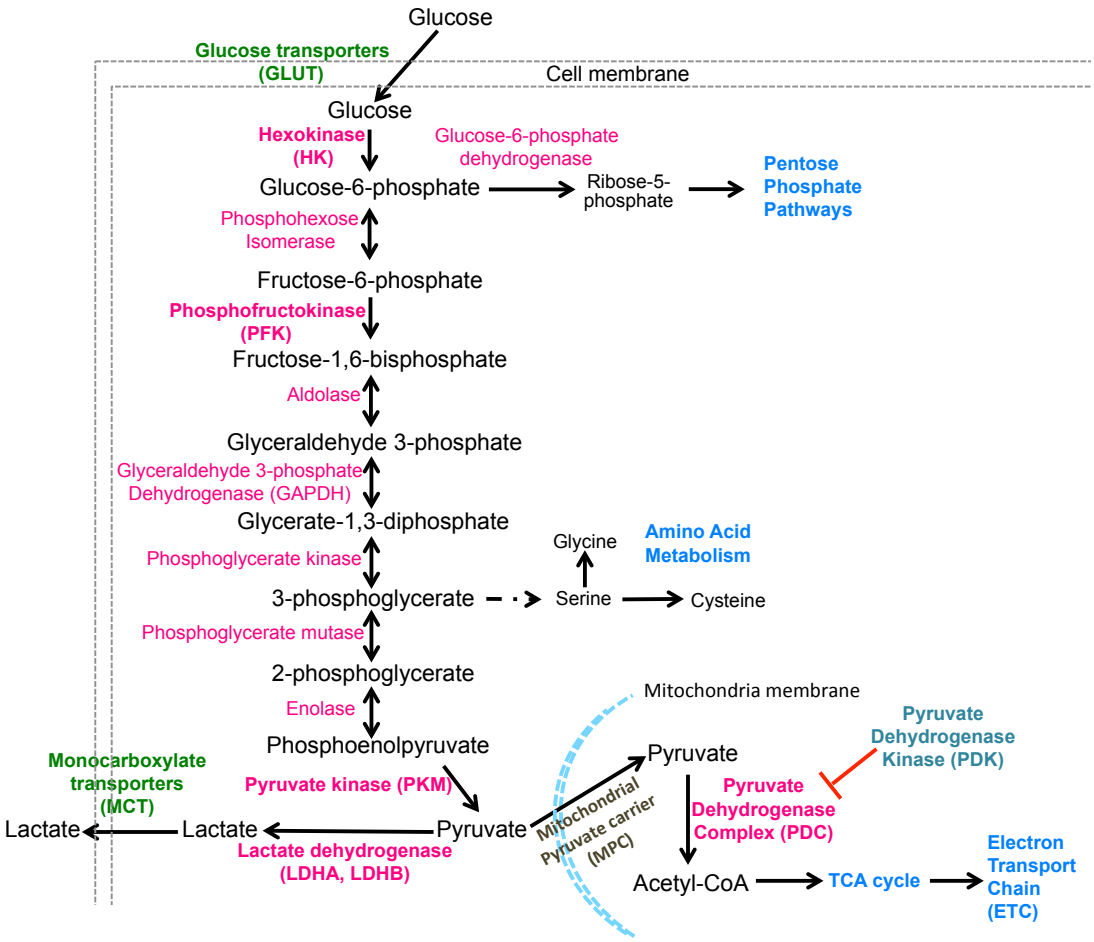

Figure 1.1 Glucose metabolism. The key enzymes and transporter of substrates of the glycolysis pathway are marked in pink. Glucose is transported into the cells through the glucose transporters (GLUT), where it is metabolised to pyruvate through glycolysis. When oxygen is sufficient, pyruvate enters the mitochondria and is fully metabolised in the TCA cycle. This process provides NADH and electrons for the electron transport chain (ETC) to generate ATP (34 ATP/1 molecule glucose). In hypoxia, pyruvate produced by glycolysis will be metabolised to lactate by lactate dehydrogenase (LDH) and is transported out of cells through the monocarboxylate transporters (MCT). Glycolysis intermediates also provide substrates and precursors for nucleic acid and amino acid synthesis. Diagram modified from Nelson et al. [14].

1.1.2 TCA cycle, electron transport chain and oxidative phosphorylation

After glycolysis, the first stage of cellular respiration, pyruvate is further oxidized inside the mitochondria matrix via a series of biochemical reactions, called the TCA cycle, producing two molecules of ATP, six molecules of NADH and two molecules of flavin adenine dinucleotide ($FADH_2$). Pyruvate is transported through the mitochondrial membrane and is used to form acetyl coenzyme A (Acetyl CoA). Acetyl CoA is then used in the TCA cycle to form citrate. Each step of the TCA cycle is catalysed by a specific enzyme (**Figure 1.2**) [16].

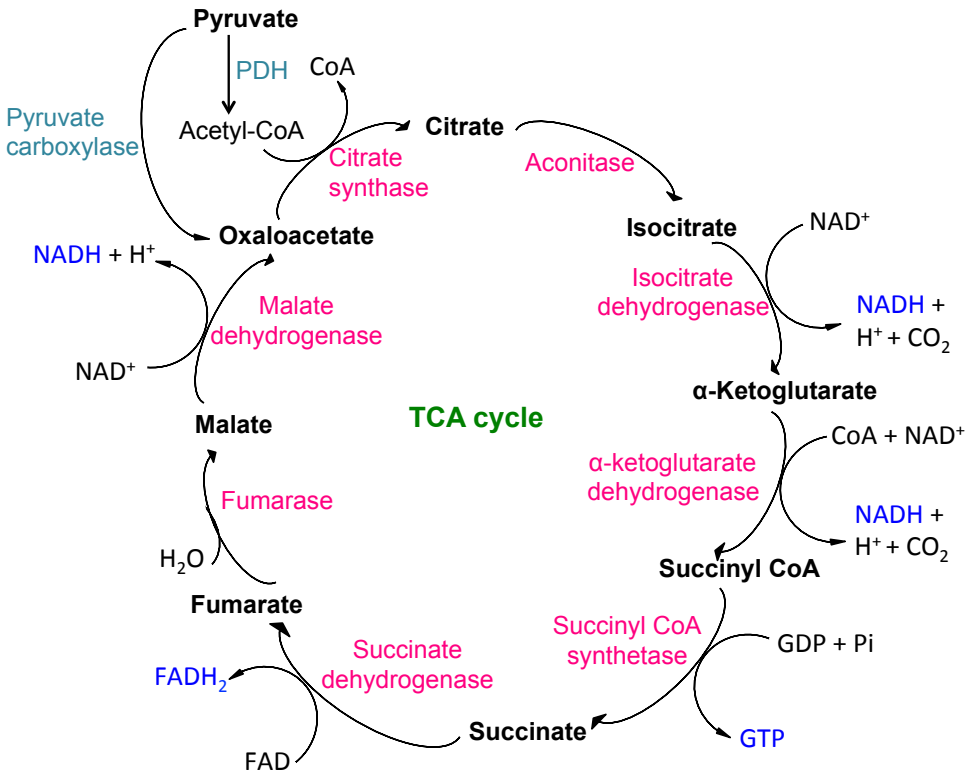

Figure 1.2 The TCA cycle. Pyruvate generated from glycolysis enters the TCA cycle and is fully metabolised when there is sufficient oxygen. The TCA cycle generates NADH and $FADH_2$ to enter the mitochondrial ETC. Illustration modified from Nelson et al. [14].

Electrons from NADH and $FADH_2$ are transferred to the third and last stage of cellular respiration, the electron transport chain (ETC), and undergo oxidative phosphorylation to generate more ATP in a series of reactions that require oxygen. The ETC is the last step of cellular respiration and oxygen is required. The ETC uses the NADH and $FADH_2$ produced by the TCA cycle to generate ATP. The ETC generates most of the

ATP that cells need in order to function, and this entire metabolic pathway is known as oxidative phosphorylation. Electrons from NADH and $FADH_2$ are transferred through protein complexes embedded in the inner mitochondrial membrane by a series of enzymatic reactions. The ETC is composed of five protein complexes (Complex I/NADH-Q oxidoreductase, Complex II/Succinate-Q reductase, Complex III/Q-cytochrome c oxidoreductase, Complex IV/cytochrome c oxidase, and Complex V/ATP synthase) and two coenzymes (ubiquinone (Q) and Cytochrome c), which act as electron carriers and proton pumps for transferring H^+ ions in and out of the intermembrane space of mitochondria (**Figure 1.3**). Electrons are donated to the ETC by NADH and $FADH_2$ and passed along the chain from protein complex to protein complex until they are donated to the final electron acceptor, oxygen, to form H_2O. During electron transport, protons/hydrogen ions (H^+) are pumped out of the matrix, across the inner membrane and into the intermembrane space. The accumulation of protons in the intermembrane space creates an electrochemical gradient that causes protons to flow down the gradient and back into the matrix through ATP synthase (Complex V) (**Figure 1.3**). ATP synthase uses the energy generated from the movement of H^+ ions into the matrix for the conversion of ADP to ATP. For every NADH molecule that is oxidized, ten H^+ ions are pumped into the intermembrane space and yield three ATP. $FADH_2$ enters the chain at a later stage (Complex II), six H^+ ions are transferred to the intermembrane space and yield two ATP. A total of 34 ATP molecules per molecule of glucose are generated in electron transport and oxidative phosphorylation [17, 18].

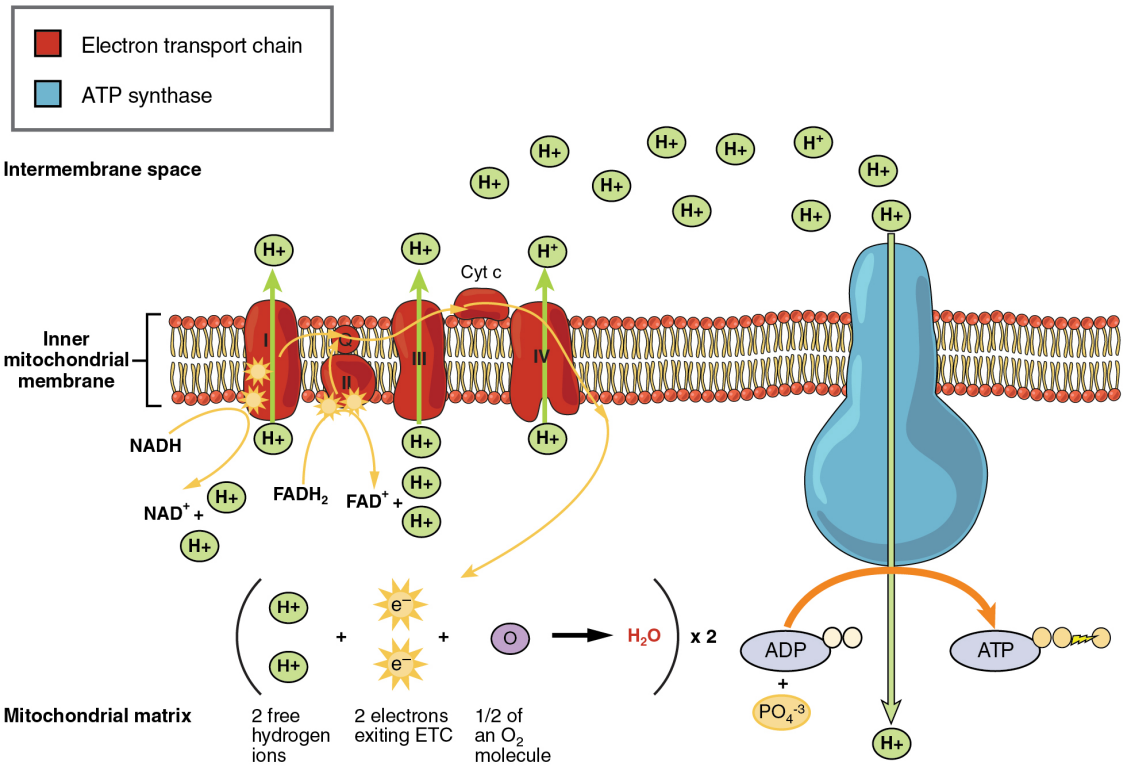

Figure 1.3 Mitochondrial electron transport chain and oxidative phosphorylation. NADH transfers two electrons to Complex I resulting in four H^+ ions being pumped across the inner membrane. NADH is oxidized to NAD^+, which is recycled back into the TCA cycle. Electrons are transferred from Complex I to a carrier molecule ubiquinone (Q), which is reduced to ubiquinol (QH2). QH2 carries the electrons to Complex III. $FADH_2$ transfers electrons to Complex II and the electrons are passed along to Q and reduced to QH2 which carries the electrons to Complex III. No H^+ ions are transported to the intermembrane space in this process. The passage of electrons to Complex III drives the transport of four more H^+ ions across the inner membrane. QH2 is oxidized and electrons are passed to another electron carrier protein cytochrome C. Cytochrome C passes electrons to the final protein complex in the chain, Complex IV. Two H^+ ions are pumped across the inner membrane. The electrons are then passed from Complex IV to an oxygen molecule to form water. ATP synthase moves H^+ ions, which were pumped out of the matrix by the ETC, back into the matrix. The energy from the influx of protons into the matrix is used to generate ATP by the phosphorylation of ADP. Illustration from Anatomy & Physiology, http://cnx.org/content/col11496/1.6/.

1.2 Cancer glycolytic phenotype

To find effective anti-cancer targets within the glycolytic pathway, it is necessary to understand what the differences are between cancer cells and normal non-proliferating cells and what advantages the glycolytic phenotype would enable in cancer cells.

1.2.1 Difference between cancer and normal cells

There are fundamental differences between the metabolic pathways of cancer cells and normal non-proliferating cells. Otto Warburg initially observed that cancer cells prefer to metabolise glucose through glycolysis rather than use the more efficient oxidative phosphorylation even with sufficient oxygen present (known as "Warburg Effect") [1]. Most normal non-proliferating (differentiated) cells primarily rely on mitochondrial oxidative phosphorylation to generate the energy needed for cellular activities. Normal cells generally only rely on glycolysis to generate ATP and large amounts of lactate under anaerobic conditions, while most cancer cells use glycolysis regardless of whether there is abundant oxygen present or not (**Figure 1.4**) [19].

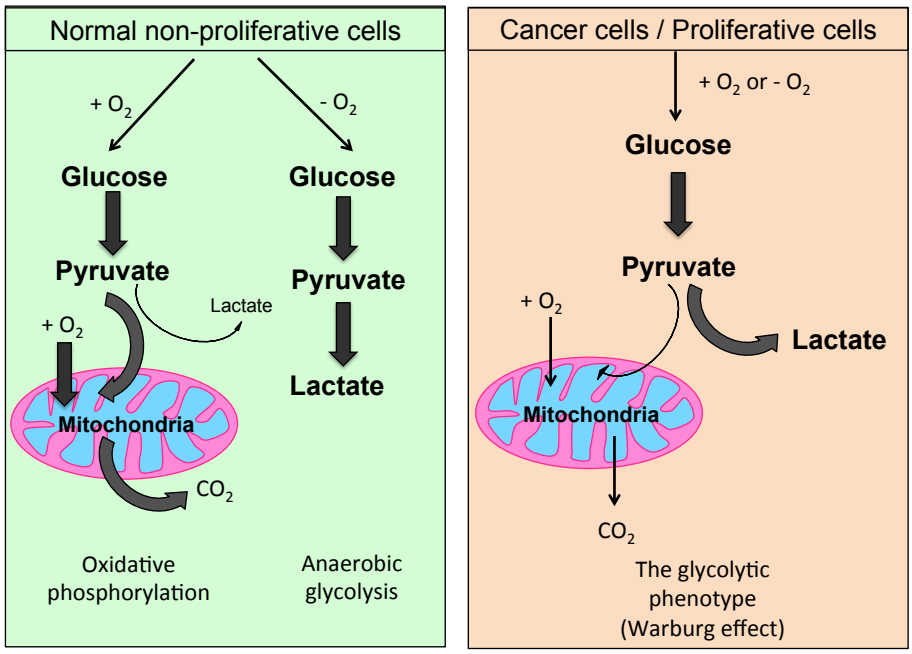

Figure 1.4 The difference in glucose metabolism between cancer cells and normal non-proliferating cells. Differentiated tissue metabolizes glucose mainly through oxidative phosphorylation and only depends on glycolysis under hypoxia. In contrast, cancer or proliferating cells depend on glycolysis regardless of the presence of oxygen. Illustration modified based on the review by Vander-Heiden et al. [19].

Genes of the glycolysis pathway are overexpressed in 24 types of cancer that represent about 70% of global cancer cases. This was discovered by analyzing microarray gene expression data available from National Institutes of Health (NIH) [2]. This study found that the overexpression of glycolytic genes seems to be ubiquitous among different cancer types, whereas other biochemical pathways such as the citric acid cycle do not have a consistent pattern of overexpression [2]. This highlighted the importance of the glycolytic phenotype for cancer cells, suggesting it could be targeted in the development of new anti-cancer metabolic therapies.

1.2.2 Oncogene activation, tumour suppressor mutations and the glycolytic phenotype

The proliferating cancer cells utilise a metabolic pathway that is less efficient, in terms of ATP generation, than the oxidative phosphorylation pathway [14]. The cancer glycolytic phenotype is linked to oncogene activation and tumour suppressor gene mutation, which are associated with genes coding key enzymes in metabolism and thus have profound effects on cancer metabolism, resulting in selective advantages for cancer cells [1, 20, 21]. In the following sections, some of the most studied mechanisms are introduced [1, 22]. The glycolytic phenotype of the cancer cells provides selective advantages in the cancer microenvironment, which is often characterized by hypoxia, nutrient deprivation and acidity due to insufficient nutrition supply in highly proliferative cancer tissues [23]. Oncogenic changes in the cancer cells, the unique cancer microenvironment, and the cancer cell glycolytic phenotype are all interacting with each other [24].

1.2.2.1 Hypoxia inducible factors

Oncogene transformations enable cancer cells to undergo uncontrolled proliferation, which then causes the cancer microenvironment to become hypoxic and acidic. Hypoxia inducible factors (HIFs) are the key primary transcriptional factors produced by the cells in response to hypoxia. Hypoxia induces the stabilization and activation of HIFs that lead to adaptation to hypoxic stress and enhance the glycolytic phenotype by inducing genes responsible for glucose transport and metabolism [25]. HIFs are upregulated and expressed in various types of cancers such as bladder, brain, breast, colon, ovarian, pancreatic, prostate, and renal carcinomas in a heterogeneous pattern, while in normal

tissue HIFs are not detectable [26]. The HIFs are heterodimeric complexes composed of a constitutively expressed β subunit and an O_2-regulated α subunit (either HIF-1α, HIF-2α or HIF-3α) [27-29]. HIF-1 primarily mediates a rapid response to acute hypoxia, while HIF-2 responds in an accumulative manner and is dominated by chronic hypoxic gene activation. In neuroblastoma, HIF-2 can be stabilized and localized in the nucleus under both normal growth conditions and chronic hypoxic conditions. In contrast, the levels and activities of HIF-1 were transiently and rapidly induced to the highest levels under acute hypoxia and diminished or disappeared after prolonged hypoxia, and were very low in non-hypoxic conditions [30-33]. HIFs activate the transcription of more than 60 genes coding for proteins that are involved in many biological functions such as erythropoiesis, angiogenesis, glycolysis, cell survival, proliferation, apoptosis, and metastasis [34].

HIFs are hydroxylated by prolyl hydroxylases (PHD) in the presence of O_2 and α-ketoglutarate substrates resulting in conformational changes to promote HIF-α binding to the von Hippel Lindau (VHL) protein E3 ligase complex, thus leading to ubiquitylation and proteasome degradation. In hypoxia, PHD activity is inhibited; VHL can no longer bind to HIF-α, preventing the ubiquitylation of HIF-α, thus resulting in HIF-α stabilization and accumulation [27, 34-36]. The expression of HIFs can be induced and stabilized by hypoxia or chemical hydroxylase inhibitors (dimethyloxalylglycine, cobalt). HIF protein synthesis can also be regulated in an oxygen-independent manner by PI3K-mTOR signalling pathway, growth factors, hormones, oncogene activation (e.g. AKT/mTOR, MAPK, MYC), or tumour suppressor mutations [29, 35, 37, 38]. Non-hypoxic factors, such as insulin-like growth factor-1 (IGF-1) can also significantly increase HIF-1α expression through activation of the AKT and MAPK signalling pathways in normoxia [39]. The stabilized HIF-α dimerizes with β subunit to form the complete HIF transcription factor and then translocates to the nucleus. Together with the co-activator p300-CBP, the HIF transcription factor activates the transcription of its target genes promoters or enhancer regions via hypoxia-responsive elements (HREs) to mediate adaptive cellular responses to hypoxia [34].

Upon activation, HIFs can stimulate the transcription of genes encoding glucose transporters and most glycolytic enzymes, thereby increasing the capacity of the cell to

carry out glycolysis [40]. In cancer cells, HIF-1 induces over-expression and increased activity of several cancer-specific glycolytic protein isoforms, including glucose transporters and key glycolysis enzymes such as HK, PFK, phosphoglycerate kinase, enolase, lactate dehydrogenase A (LDHA), and 6-phosphofructo-2-kinase/F2 (PFKFB3), that participate in cancer cell survival, apoptosis inhibition and metastasis promotion [40]. HIF and overexpressed oncogenic MYC have been shown to collaborate to enhance the glycolytic phenotype by activation of glycolytic enzymes including pyruvate dehydrogenase kinase 1 (PDK1) and HK in human P493 Burkitt's lymphoma cells [41]. HIF and MYC can also enhance the glycolytic phenotype in cancer cells *in vitro* by independently activating key glycolysis enzymes such as glucose-6-phosphate isomerase (GPI), PFK1, aldolase, fructose bisphosphate, triose phosphate isomerase, LDHA, GAPDH, and phosphoglycerate kinase [42-47].

Activation of HIFs can also inhibit mitochondrial function and oxygen consumption by activating PDK1 and PDK3. PDKs inactivate the pyruvate dehydrogenase complex (PDH), reducing the flow of pyruvate generated from glycolysis into the TCA cycle. This reduction in pyruvate flux into the TCA cycle suppresses oxidative phosphorylation and oxygen consumption, reinforcing the glycolytic phenotype, also reducing ROS damage and contributing to drug resistance [40, 48-50]. Inhibitors of HIFs or the PDKs could potentially reverse the metabolic effects of tumourigenic HIF1 signalling and thus are potential treatment options. One of several such candidates is the PDK inhibitor dichloroacetate (DCA), which is the focus of this thesis (section 1.4).

1.2.2.2 p53

Tumour suppressor gene mutation can also regulate cancer cell metabolism. *p53* is a well-studied tumour suppressor gene and the most commonly mutated gene in human cancer [51]. In cellular stressed conditions, p53 is stabilized and activated by dissociation from its ubiquitin ligase, MDM2, via various post-translational modifications to avoid degradation by the proteasome. Activated/stabilized p53 mediates the appropriate cellular response to various cellular stressed conditions such as genotoxicity, cytotoxicity, DNA damage, aberrant DNA replication, hypoxia, oxidative stress, nutrient stress, and oncogene activation by inducing cell-cycle arrest, apoptosis,

senescence, or differentiation, and thus plays a pivotal role in tumourigenesis, cell-death, and survival [51-54].

In addition to mediating the cellular fate in response to stress, p53 is now also known to regulate cancer metabolism. p53 has been demonstrated to suppress glycolysis through various mechanisms. Wild-type p53 suppresses the expression of glucose transporters (GLUT1, GLUT4) to decrease glucose uptake in breast cancer cells, while tumorigenic mutations in the p53 DNA-binding domain impair this effect, thereby resulting in increased glucose metabolism [55]. p53 can negatively regulate hypoxia-driven glycolysis via inhibiting the translocation of GLUT1 to the plasma membrane of lung cancer cells [56]. p53 induces TIGAR (TP53-induced glycolysis and apoptosis regulator, a fructose-2,6-bisphosphatase) which suppresses glycolysis by reducing fructose-2,6-bisphosphate levels, an activator of phosphofructokinase (third step of glycolysis). This redirects the flow of glucose-6-phosphate toward the pentose phosphate pathway (PPP) and NADPH production, thus resulting in an overall decrease in ROS levels [57]. p53 decreases PDK2 expression and thus that of its product, the inactive form of the pyruvate dehydrogenase complex (PDC), which in turn promotes conversion of pyruvate into acetyl-CoA instead of lactate [58]. p53 decreases the expression of MCT1 (monocarboxylate transporter 1) to inhibit lactate export produced by increased glycolysis, thereby preventing the facilitation of the shift from mitochondrial oxidative phosphorylation to the glycolysis pathway [59]. In addition to p53's role in suppressing glycolysis, it promotes mitochondrial oxidative phosphorylation by switching on the transcription of cytochrome c oxidase 2 (SCO2, an effector necessary for ETC function) [60-62]. Thus, mutation of the *p53* gene and the loss of function of the p53 protein in cancer can remove multiple mechanisms inhibiting glycolysis and contribute to reinforcing the glycolytic phenotype (**Figure 1.5**).

1.2.2.3 PI3K-AKT-mTOR

The phosphatidylinositol3-kinase (PI3K)-AKT and the mammalian target of rapamycin (mTOR) signalling pathways are heavily interrelated. They are hyperactivated in many cancer types and regulate cell survival, proliferation, metabolism, angiogenesis, and metastasis [63]. The activation of the PI3K-AKT pathway provides not only strong growth and survival signals to cancer cells but also provides profound effects on cancer

metabolism [64]. AKT is the most studied downstream effector of PI3K. The activation of the AKT oncogene is sufficient to stimulate cancer cell switching to glycolysis without affecting its oxidative phosphorylation rate. AKT activity causes cancer cells to be dependent on glycolysis for uncontrolled proliferation and survival [64, 65]. PI3K-AKT signalling stimulates glycolysis through different mechanisms, such as by increasing the expression and membrane translocation of glucose transporters (such as GLUT1, GLUT4) and by phosphorylating key glycolytic enzymes, such as HK and PFK [65, 66].

AKT also strongly stimulates signalling through the kinase mTOR by phosphorylating and inhibiting the negative regulator of mTOR [66]. mTOR is a kinase that plays a key role as a metabolic integration point, by coupling growth signals to nutrient availability. Activated mTOR can stimulate protein and lipid biosynthesis and cell growth when there are sufficient nutrients and energy. It is often constitutively activated during tumourigenesis [67]. mTOR directly stimulates mRNA translation and ribosome biogenesis, and indirectly affects metabolism by activating transcription factors, such as HIF, even under normoxia. The subsequent metabolic changes caused by activated HIF contribute to and reinforce the glycolytic phenotype downstream of PI3K-AKT and mTOR pathways (**Figure 1.5**) [63, 68].

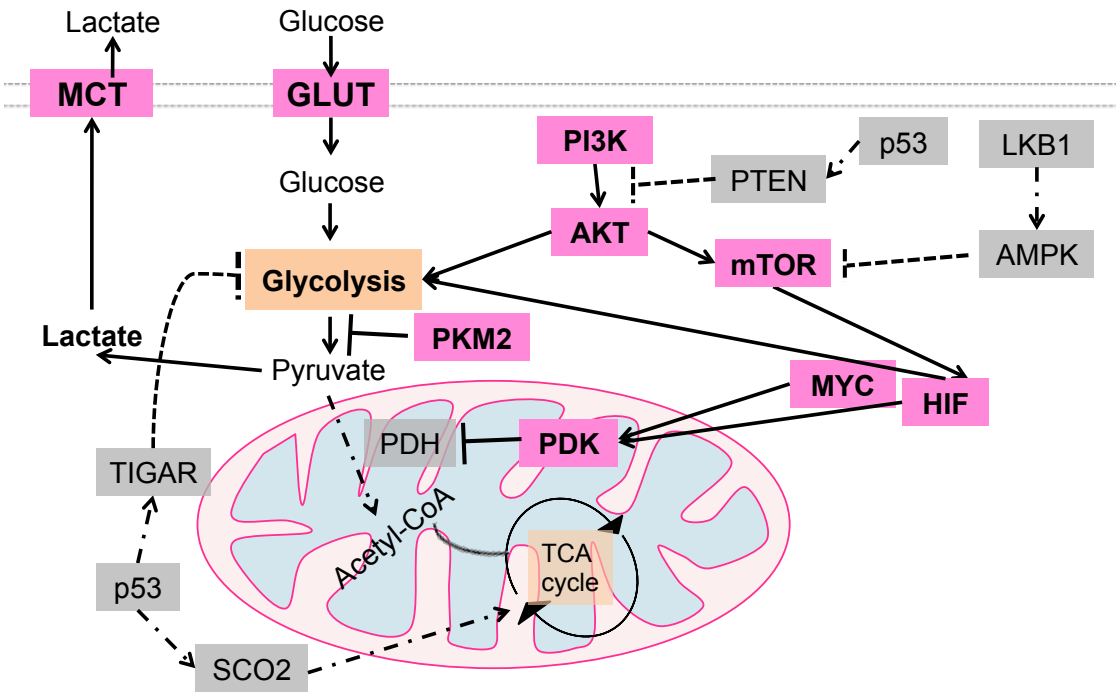

Figure 1.5 Summary of the molecular mechanisms driving the glycolytic phenotype. The glycolytic phenotype in cancer is driven by activation of multiple oncogenes and mutations of tumour suppressor genes. The dashed lines indicate loss of tumour suppressor function (p53 and liver kinase B1 (LKB1)). Pink colour indicates the upregulation of oncogene and transcription factors. mTOR enhances glycolysis by activating HIF activity. MYC cooperates with HIF to activate genes that encode glycolytic proteins. The PI3K-AKT-mTOR pathway stimulates glycolysis by directly regulating glycolytic enzymes. LKB1-AMPK results in loss of glycolysis inhibition. p53 can suppress glycolysis through TIGAR. The less active PKM2 isoform promotes the accumulation of upstream glycolytic intermediates. Illustration modified from Cairns et al. [1].

1.2.3 The glycolytic phenotype offers survival advantages for cancer cells

The glycolytic phenotype's selective advantages for cancer are viewed as a multi-purpose complex adapting system to fulfil the needs of cancer cells to proliferate, progress and invade. The glycolytic phenotype can fulfil the rapid energy requirements for cancer proliferation by generating ATP at a higher rate than oxidative phosphorylation which is to its advantage, as long as the glucose supply is not restricted [1]. Evidence strongly suggests that such ATP production is neither the sole nor the key benefit of the glycolytic phenotype to cancer cells, which is discussed in the following sections.

1.2.3.1 Bioenergetics and biosynthesis

The glycolytic phenotype provides a biosynthetic advantage for cancer cells due to a high flux of substrate from glycolysis that allows effective shunting of carbon nutrients to key biosynthetic pathways [19], thus to provide large amounts of macromolecules that fulfil the need of cancer cells for uncontrolled proliferation. The synthesis of macromolecules such as nucleotides, amino acids, and lipids, demands a large quantity of carbon and nitrogen sources. For example, the synthesis of palmitate, a major component of cellular membranes, requires 16 carbons from 8 acetyl-CoA molecules, and 28 electrons from 14 reduced nicotinamide adenine dinucleotide phosphate (NADPH) molecules but only 7 ATP [14]. The acetyl-CoA converted from the pyruvate produced in glycolysis, provides carbons in the above reaction to make fatty acids by the *de novo* lipogenesis [69]. Likewise, synthesis of amino acids and nucleotides consumes more equivalents of carbon and NADPH than that of ATP [19]. Pyruvate generated from glycolysis can be synthesized into alanine amino acid [70]. Glucose and glucose-6-phosphate are intermediates in the conversion to other sugars that are involved in nucleotide synthesis through the PPP, which is parallel to glycolysis. The PPP generates NADPH, which is used in many reductive biosynthesis reactions for the synthesis of fatty acids, cholesterol, and neurotransmitters [71]. It also generates 5-carbon sugars, such as pentose, as well as ribose 5-phosphate (R5P), which is a precursor for the synthesis of nucleotides and then nucleic acids [14, 72]. Upregulated glycolysis in cancer can offer abundant metabolic intermediates, carbon sources and rapid ATP needed for cancer cell proliferation.

1.2.3.2 Protection against oxidative stress

In highly proliferative cancer cells, the abnormal metabolic phenotype promoted by cancer oncogene activation causes reactive oxygen species (ROS) production and increases its rate of production. The mitochondrial ETC is responsible for generating the majority of the ROS in cells through partial reduction of oxygen [73]. ROS are a class of diverse radical species containing oxygen such as peroxides, superoxide, hydroxyl radical, and singlet oxygen, all of which are produced in all cells as a normal by-product of metabolic processes and have important roles in cell signalling and homeostasis [74, 75]. The effects of ROS on cells depend on the levels of ROS present; low levels of ROS can support cell proliferation and survival pathways, and excessively high levels

of ROS can cause detrimental oxidative stress that leads to cell apoptosis [76, 77]. Cells have endogenous antioxidant defence systems to prevent ROS from accumulating at high levels and to overcome this potential for oxidative stress, such as manganese superoxide dismutase (a mitochondrial matrix enzyme) and a variety of antioxidant molecules (e.g. glutathione (GSH), ascorbic acid) [78, 79].

Cancer cells exert tight regulation of ROS and antioxidants to reduce the levels of excessive ROS to ensure survival. The glycolytic phenotype enables cancer cells to counteract the accumulation of ROS by upregulating antioxidant systems [1]. For example, in cancer cells, cytochrome c (located at the inner mitochondria membrane where it serves as a redox carrier for the ETC) is reduced and kept inactive by intracellular GSH. GSH is one of the most abundant intracellular reducing molecules and maintains redox homeostasis by scavenging ROS [80]. GSH generation is increased in cancer cells as a result of the increased shunting to PPP that is parallel to the increased dependence on glycolysis. The cytochrome c can be activated by increased ROS and released into the cytosol to initiate apoptosome complex formation, leading to caspase activation and subsequent cell apoptosis. Thus cancer cells can evade cytochrome c-mediated apoptosis by GSH production through the increased glycolysis [81].

Cancer cells also counteract ROS stress by increasing the production of antioxidants. The dependence on glycolysis in cancer cells leads to excessive NADPH production through the increased PPP activity. NADPH provides reducing power in many enzymatic reactions that are crucial for macromolecular biosynthesis and it is also a crucial antioxidant, directly quenching the ROS produced during rapid cell proliferation [82-84]. Moreover, NADPH provides the reducing power for both the glutathione and thioredoxin systems that scavenge ROS and repair ROS-induced damage [82, 84]. The tight control of ROS allows cancer cells to avoid the detrimental effects of high levels of ROS and to also increase the chance of additional ROS-mediated gene mutations and stress responses that promote further tumourigenesis [1].

1.2.3.3 Invasion and immune escape

The glycolytic phenotype used to be considered as an adaptive mechanism to the hypoxic microenvironment during the early vascular phase of solid tumour development, as it enables ATP production in the absence of oxygen [85]. However, some cancer cells present with a glycolytic phenotype before exposure to hypoxia, for example, leukaemia cells reside in the bloodstream and lung cancer cells reside in the airway. Both have sufficient oxygen but nonetheless, these cancer cell types are highly glycolytic [86, 87]. Thus, the benefits to cancer development of the glycolytic phenotype must go beyond adapting to hypoxia. Increased glycolysis leads to excessive lactate production, which contributes to an acidic extracellular microenvironment and further changes in gene expression, which may promote cancer progression. The acidosis of the cancer microenvironment can be caused by the increased production of anabolic substrates, anti-oxidants and the production of H^+, which is toxic to the normal adjacent tissue and can alter the interface of the tumour and stroma, cause remodelling of normal tissue and then mediated invasion [88-90]. Both hypoxia and acidosis can contribute to increased somatic mutation levels that further drive cancer progression [35, 91].

An acidic microenvironment can heavily weaken immune cell responses, including effector T cells' normal functions, which are responsible for the anti-cancer immune response [92]. Tumour-specific $CD8^+$ T lymphocytes in a mouse model and in humans had been shown to become inactive and to arrest in an anergic state after the microenvironmental pH is slightly lowered to values representative of tumour masses (pH 6.0-6.5). This anergic state was characterized by weakened normal T cell functions such as the reduced cytolytic activity and impaired cytokine secretion, reduced IL-2Rα (CD25) and T-cell receptors expression. However, when the buffering pH was restored to normal physiological values, these above measures of T-cell functions were restored. This finding illustrated that the acidification of the tumour microenvironment can act as a mechanism of immune escape [93]. Moreover, the activation of T cells requires the T cell switching to a glycolytic phenotype. The normal activation of T cells requires the binding of the glycolysis enzyme GAPDH to IFN-gamma mRNA. Thus, GAPDH controls T cell cytokine production function by engaging/disengaging glycolysis and through fluctuations in its expression [94]. During T cell activation, T cells increase their glucose uptake and glycolytic rate by the upregulating glycolytic enzymes; this

process generates excessive lactate into the microenvironment [94]. When functioning normally, the activated T cells use glycolysis but also rely on the efficient secretion of lactate, as its intracellular accumulation disturbs T cell metabolism. The efficient exportation of lactate is through MCT1, which depends on a gradient between cytoplasmic and extracellular lactate levels [95]. The glycolytic phenotype causes high lactate concentrations in the tumour environment, which will block lactate export from T cells, resulting in impaired cytotoxic T cell function as indicated by reduced proliferation and reduced cytokine production. By disturbing the metabolism and function of T cells, cancer cells escape from immune surveillance [95]. These findings suggest that targeting the glycolytic phenotype in cancer is a promising strategy to enhance immunotherapy against tumours.

1.2.4 Clinical use of the glycolytic phenotype

The glycolytic phenotype is present in the majority of cancer cases worldwide, and is therefore, used in clinical medicine for tumour imaging. Positron emission tomography (PET) integrated with computed tomography (CT) scan using ^{18} Fluorodeoxyglucose (^{18}F-FDG) as a tracer has been widely used in cancer diagnosis, staging, and monitoring. As a glucose analogue, ^{18}F-FDG can be taken up and phosphorylated by hexokinase but cannot be further metabolised, and thus it accumulates intracellularly. Cancer cells with a glycolytic phenotype present with increased glucose transport and increased hexokinase activity so that they accumulate more ^{18}F-FDG intracellularly, allowing the cancer cells to be differentiated from the adjacent non-glycolytic benign tissues [96-98].

In summary, the glycolytic phenotype has selective advantages for cancer cell survival, proliferation, and metastasis. Not only does it offer rapid energy production for cell proliferation, it also provides important intermediates needed for synthesizing macromolecules such as nucleotides, amino acids and lipids (the building blocks for producing new cancer cells), and it offers protection against ROS damage [22].

1.3 Therapeutic agents targeting cancer metabolism

Although the glycolytic phenotype is the most studied metabolic phenotype in cancer, substantial evidence demonstrates that tumours exhibit heterogeneous metabolic alterations that extend beyond the glycolytic phenotype. For example, ^{18}F-FDG PET and ^{11}C-acetate–PET scans in patients demonstrated that cancer cells exhibit different uptake of nutrients [97, 99]. The heterogeneous uptake of nutrients has also been revealed by the differential uptake of radioactively labelled amino acid analogues and by the variable secretion of lactate in cancers that originate from the same tissue [100-103]. Abnormal tumour vasculature can result in gradients of nutrients, oxygen, and pH. The glycolytic phenotype of cancer cells is responsive to the microenvironment and is readily interchangeable with non-glycolytic metabolism. The adaptability of cancer cells to the available nutrients can ensure proliferation in heterogeneous cancer microenvironments [103, 104]. Thus, it is important to consider the metabolic heterogeneity in cancer treatment. Studies and clinical trials have been testing the therapeutical potential of metabolic modulatory drugs that target different metabolic pathways in various cancer types. This section briefly summarizes the agents that can target the abnormal metabolism of cancer cells.

1.3.1 Glycolysis

Cancer cells display increased glucose uptake and glucose metabolism compared to normal non-proliferating cells. The glycolytic phenotype offers cancer cells selective survival advantages. Many key enzymes of the glycolysis pathway such as HK, LDHA, GAPDH, and PDK as well as glucose transporters (GLUTs) are overexpressed in various cancer types due to changes in oncogene activation and tumour suppressor mutations such as the HIF, PI3K-AKT, MYC and p53 pathways, and thus have been studied as potential targets for cancer treatments (**Figure 1.6**) [1, 105].

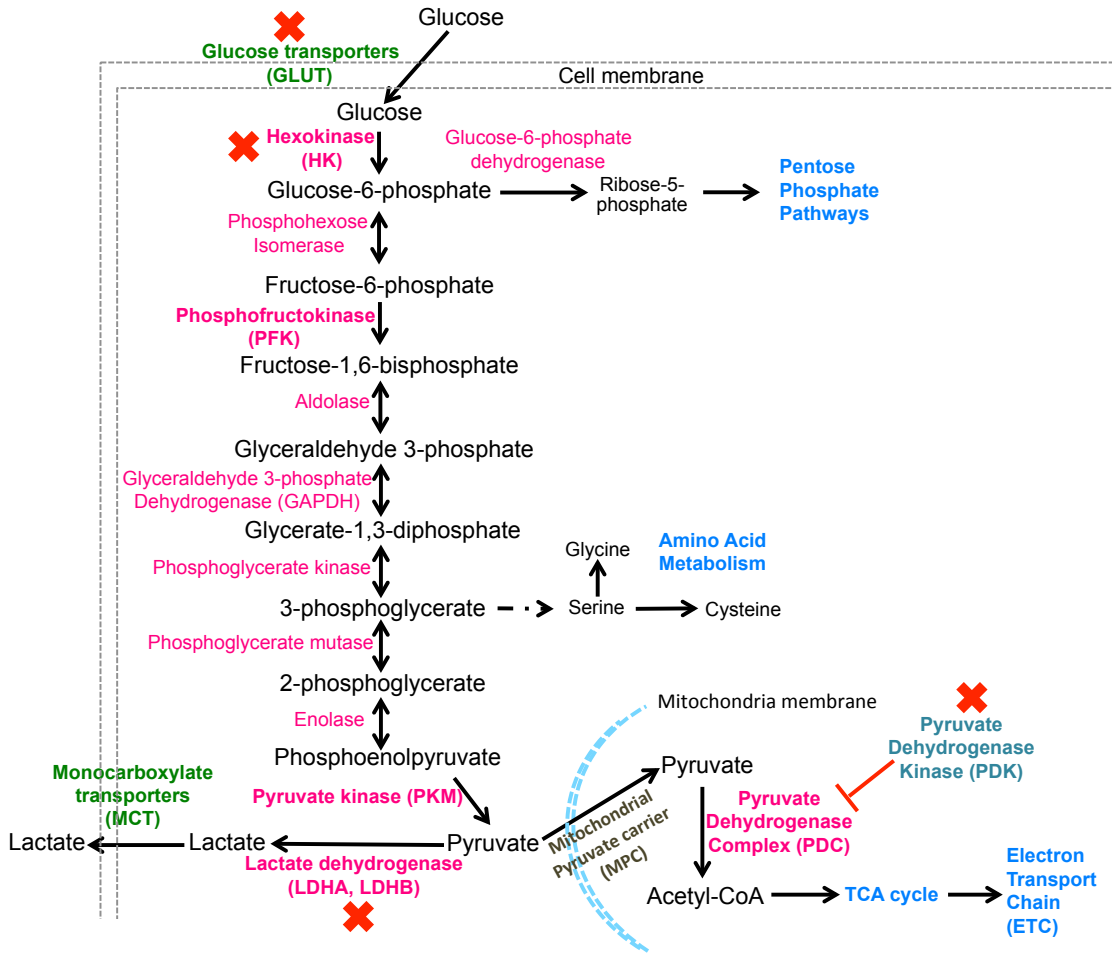

Figure 1.6 Potential targets of the glycolysis pathway in cancer therapy. This diagram shows the main enzymes involved in glycolysis. Some key enzymes of the glycolysis pathway such as GLUT, HK, LDHA, and PDKs can be targeted in cancer therapy. GLUT: glucose transporter. HK: hexokinase. LDHA: lactate dehydrogenase. PDK: pyruvate dehydrogenase kinase. Illustration modified from Nelson et al. [14].

The first rate-limiting step for glucose metabolism is glucose transportation across the plasma membrane. The glucose transporter (GLUT) family of proteins is responsible for this process and is found overexpressed in many cancer types. The human GLUT family consists of 14 members (GLUT1-14). Upregulated expression of GLUT and abnormal patterns of GLUT expression are found to contribute to the elevated glucose uptake and increased rate of glycolysis in cancer cells, thus GLUT could be a potential therapeutic target [106]. The natural flavonoid apigenin has been found to have anti-cancer effects through inhibiting GLUT1 mRNA and protein expression in pancreatic cancer [107], head and neck cancer [108]. Apigenin also enhanced the sensitivity of laryngeal carcinoma Hep-2 cells to cisplatin [109]. A specific GLUT1 inhibitor, fasentin, inhibits

glucose uptake and the transporter functions resulting in increased apoptosis in prostate cancer and leukaemia cells [110]. shRNA knockdown of GLUT4 and GLUT11 resulted in a downregulation of glucose consumption and an increase in cytotoxicity in multiple myeloma cells [111]. Although there is evidence to show that inhibiting GLUTs leads to anti-cancer effects, many GLUT family members are also expressed on normal cells, thus it is difficult to identify and inhibit only the isoforms associated with cancer cells.

Hexokinases (HK), the first family of enzymes in glycolysis, can phosphorylate glucose that entered the cells into glucose-6-phosphate (G6P). HKs are a family of four isoforms. The overexpression of HK2 is observed in some tumour tissues and is often associated with poor prognosis [112, 113]. The inhibitor of HK, 3-bromopyruvate (3-BrPA), has been found to have anti-cancer effects in breast cancer cells, melanoma cells, acute lymphoblastic leukaemia cells, and neuroblastoma [105, 114, 115]. However, 3-BrPA was demonstrated to have mitochondrial toxicity in non-cancerous primary hepatocytes from rats and mice [116], and its toxicity in humans remains to be determined. 2-deoxyglucose (2-DG), a glucose analogue, can enter cells through GLUT and be phosphorylated by HK to 2-DG-phosphate, but cannot be further metabolized through the glycolysis pathway. The accumulation of 2-DG inhibits HK through feedback inhibition, arresting glycolysis at the second step, causing decreased ATP levels, cell cycle arrest, growth inhibition and even cell death [117]. Continuous exposure of 2-DG in cell lines from human ovarian, squamous, cerebral, hepatic, colonic, and mesothelial malignancies resulted in various degrees of growth inhibition, ranging from slowing down proliferation, to proliferation arrest, cell cycle arrest, and massive apoptosis [118]. However, early phase clinical trials did not show efficacy of 2-DG in patients with prostate cancer or solid tumours, suggesting future studies of 2-DG would need to consider combination therapy [119]. 2-DG in combination with radiation therapy was tolerated well in glioma patients but its efficacy needs to be further studied [120]. A phase I dose-escalation trial of 2-DG in patients with advanced solid tumours demonstrated even with high dose of 2-DG at 63 mg/kg/day, 66% of patients had progressed disease and about 22% patients experienced cardiovascular toxicity (prolonged Q-T interval). The lack of efficacy of 2-DG at high doses and its cardiac side effects has reduced its likelihood of being used in future clinical trials [121].

Lactate dehydrogenase A (LDHA) catalyses the conversion of pyruvate and NADH to lactate, which is the final step of the glycolysis pathway. Many malignant tumours expressed higher LDHA levels compared to normal tissues [122]. LDHA can promote cancer cell growth and metastasis and it is an indicator of poor prognosis in various cancer types, making it a potential treatment target [12, 123-125]. shRNA (short hairpin RNA) knockdown of LDHA stimulated mitochondrial respiration and also impaired cell proliferation under hypoxia in mouse mammary gland tumour cells [126]. Knockdown of LDHA showed anti-cancer effects *in vitro* in various cancer types, such as increased apoptosis in hepatocellular carcinoma cells [127], inhibited invasion of breast cancer and head and neck cancer cells [128], and induced cell death in lymphoma and pancreatic cancer cell lines [129]. An *in vivo* study showed the inhibition of LDHA by siRNA significantly reduced metastatic potential in a liver cancer xenograft mouse model [127], and FX11, a small-molecule LDHA inhibitor, inhibited the progression of human lymphoma and pancreatic cancer xenograft models [129]. Sodium oxamate, a structural analogue of pyruvate that is an inhibitor of LDHA, has shown therapeutic potential in many different cancer types. For example, oxamate caused G2/M cell cycle arrest and promoted apoptosis through enhanced ROS production and sensitise head and neck cancer cells to radiotherapy [130], it inhibited tumour growth in a breast cancer mouse model and potentiated the effects of chemotherapy agent paclitaxel in breast cancer cells [131], and induced apoptosis in multiple myeloma cell lines with high LDHA activities [12]. While the laboratory studies are encouraging, the side effects and pharmacokinetics of oxamate in cancer patients are not yet clear and require further study before its clinical potential can be assessed.

Pyruvate dehydrogenase (PDH) is the enzyme responsible for the rate-limiting conversion of pyruvate to acetyl-CoA, which enters the TCA cycle. PDKs (PDK1-4) are a family of kinases that phosphorylate PDH and inhibit its enzymatic activity, resulting in reduced flow of the glucose-derived pyruvate into the TCA cycle. This diversion decreases the oxidative phosphorylation rate and oxygen consumption of the ETC, and thus reinforcing the glycolytic phenotype [48, 49, 132]. HIF-1α activation can induce PDK1 and PDK3 expression, resulting in a switch from mitochondrial respiration to glycolysis [40, 48-50]. In a study of cervical cancer cells (HeLa cells), HIF-mediated PDK3 induction or PDK3 overexpression significantly inhibited cell apoptosis and

increased resistance to cisplatin or paclitaxel, while PDK3 knockdown inhibited hypoxia-induced glycolysis and increased sensitivity of cancer cells to chemotherapy drugs [50]. In human colon cancer tissues, PDK3 levels are elevated and correlated with the HIF-1α level and strongly correlated with the severity of the cancer and can be used as a predictor of poor prognosis [133]. The expression levels of PDK1 were significantly higher in plasma cells from multiple myeloma patients than patients with a pre-myeloma condition, and the inhibition of PDK1 led to inhibition of myeloma cell growth and induction of apoptosis [12]. These findings indicate that PDKs are potentially novel targets for cancer therapy. Dichloroacetate (DCA), a pyruvate mimetic, is a small molecule developed for clinical use as a PDK inhibitor and has been used in mitochondria diseases for decades. DCA inhibits PDKs leading to reactivation of PDH and a metabolic switch from glycolysis to mitochondrial respiration and will be introduced in detail in section 1.4. The preclinical studies on DCA have shown its anti-cancer effects in a variety of cancer types, however, because DCA is not patentable, its clinical development as a cancer therapy lacks pharmaceutical support [134]. Although there are DCA-derivatives and other molecules have been developed to inhibit PDKs, many of them lack further preclinical study or have been shown to be too toxic to use, such as 2-chloropropionate [134]. The new PDK inhibitors lack *in vitro* and *in vivo* studies and the development of a new drug would be costly and time-consuming. Targeting PDK has potential as a viable cancer therapeutic approach and DCA is currently the most developed and suitable molecule, therefore, it warrants further investigation.

1.3.2 Mitochondria

It was originally thought that cancer cell had impaired mitochondria, and the glycolytic phenotype was a survival adaptation to cope with ATP depletion. However, cumulative evidence has now shown that the majority of the cancer types do not present with mitochondrial defects but retain their capacity for oxidative phosphorylation [135]. Mitochondria serve multifunctional roles in cancer such as in bioenergetics, redox regulation, calcium homeostasis, oncogenic signalling, innate immunity, and apoptosis [135, 136]. Different approaches to target mitochondria have been tested and recognised in cancer therapy.

Induction of mitochondria-led apoptosis is one of the common anti-cancer approaches. The B-cell lymphoma (Bcl)-2 protein family plays a crucial role in controlling mitochondrial apoptosis pathways (**Figure 1.7**). Within this Bcl-2 family, there are three subclasses: anti-apoptotic proteins (such as Bcl-2, Bcl-X_L, Bcl-B, Bcl-w); pro-apoptotic effectors (such as Bcl-2-associated X protein (Bax), Bcl-2 homologous antagonist killer (Bak), Bcl-2-related ovarian killer (Bok)); and pro-apoptotic Bcl-2-homology (BH)3-only proteins (such as Bcl-2-interacting mediator of cell death (Bim), Bcl-2-interacting domain death agonist (Bid) and p53-upregulated modulator of apoptosis (Puma)). Alterations in the expression and function of these proteins contribute to the pathogenesis and progression of human cancers, thus they provide therapeutic targets for cancer [137, 138]. Proteins of the Bcl-2 family have the capacity to regulate the permeability of intracellular membranes. Permeabilisation of mitochondrial membrane initiates the apoptosis process under the control of the permeability transition pore complex (mPTPC). Increased mitochondria outer membrane permeability (MOMP) releases a key apoptosis effector, cytochrome c, which induces apoptosis by activating the caspase cascade [139]. It was discovered that the pro-apoptotic members of the Bcl-2 family, such as Bax and Bid, alter the permeabilisation of the mitochondrial membrane by forming channels in membranes and regulating existing channels, whereas the anti-apoptotic proteins tend to have the opposing effect and can block the cytochrome c release [140].

There are many molecules in use or being tested in clinical trials that have an effect on mitochondria to induce apoptosis. Several clinically approved anticancer drugs such as paclitaxel, etoposide and vinorelbine as well as a number of experimental drugs such as, ceramide, MKT077, CD437, lonidamine, and betulinic acid have been found to act directly on mitochondria to trigger mitochondria-led apoptosis in cancer treatments [141]. Arsenic trioxide can act on the respiratory chain and induce caspases and thus cause apoptosis in leukaemia and myeloma cells [142]. The anti-apoptotic proteins of the Bcl-2 family such as Bcl-2, Bcl-X_L, can be targeted in cancer therapy as cancer cells express abundant amounts of such anti-apoptotic proteins to evade apoptosis [143, 144]. Compounds inhibiting the anti-apoptotic protein Bcl-2 have been studied in preclinical and clinical trials for their efficacy. Bcl-2 function can be inhibited by the binding of

selective Bcl-2 homology (BH)3-only proteins, BH3 mimetics, such as venetoclax, have already been used in the clinic to treat chronic lymphoid leukaemia patients [144-146].

Even though there is great potential in targeting mitochondria to induce apoptosis in cancer treatments, these compound may have uncontrolled distribution to non-cancer tissues and it is unclear whether they can be made to selectively accumulate in the tumours' mitochondria. The clinical use of some of the experimental compounds is limited due to the difficulty in managing their toxicity caused by mitochondria dysfunction [145].

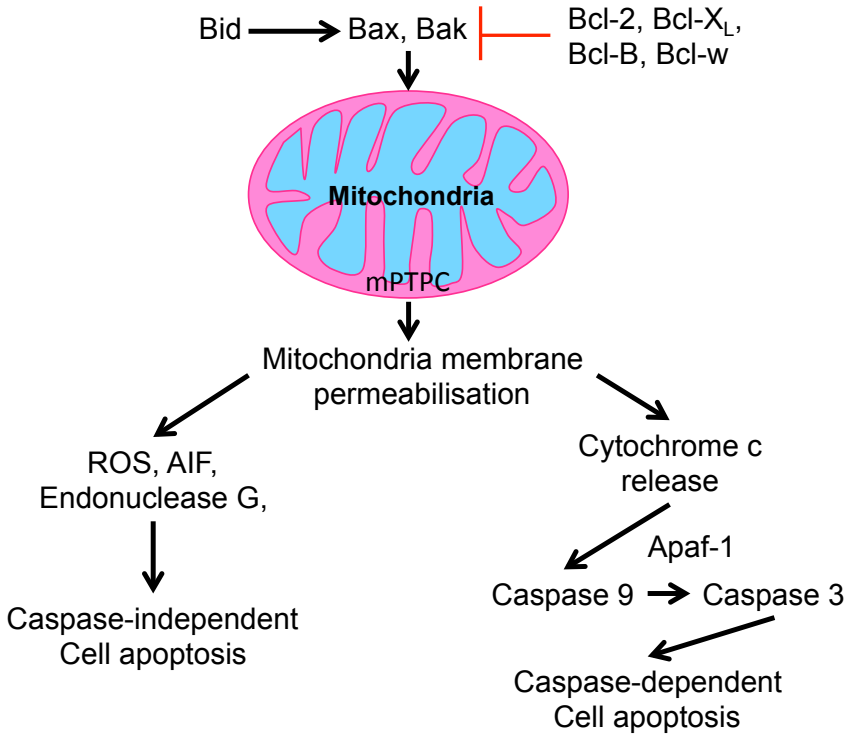

Figure 1.7 Mitochondria-led apoptosis pathways. The B-cell lymphoma (Bcl)-2 protein family plays a crucial role in regulating mitochondria membrane permeabilisation and controlling mitochondrial apoptosis pathways. There are three different subgroups of the Bcl-2 protein family, including the apoptotic proteins (such as Bcl-2, Bcl-X_L, Bcl-B, Bcl-w), pro-apoptotic effectors (Bax, Bak, and Bok) and pro-apoptotic BH3 only proteins (Bim, Bid, and Puma). AIF: apoptosis-inducing factor; AIF: apoptosis-inducing factor; Apaf-1: apoptotic protease-activating factor-1; Bcl-XL: Bcl-2-like. mPTPC: permeability transition pore complex.

Another novel approach to cancer treatment is to target mitochondria metabolism. Mitochondria play a central role in the production of ATP and metabolic intermediates. It uses multiple carbon sources such as pyruvate, amino acids, and fatty acids to feed into the TCA cycle inside the mitochondrial matrix, generating reduced NADH and $FADH_2$ to drive ETC, respiration and ROS control. The TCA cycle generates intermediates that can funnel into multiple biosynthetic metabolic pathways to produce glucose, amino acids, lipids, and nucleotides [135]. Accumulating evidence indicates that mitochondrial bioenergetics, biosynthesis and signalling are required for tumour growth, thus targeting mitochondrial metabolism has potential for cancer therapy (**Figure 1.8**) [147].

There have been preclinical compounds as well as some FDA (U.S. Food and Drug Administration) approved drugs used in non-cancer diseases that targeting mitochondria metabolism being studied in cancer therapy. Anti-diabetic biguanide drug Metformin was reported to induce cancer cell death upon glucose deprivation and to inhibit cancer growth by inhibiting mitochondria complex I activity [148]. Metformin can also inhibit cancer growth by decreasing the flux of glucose- and glutamine-derived metabolic intermediates into the TCA cycle, thus suppressing the production of mitochondrial-dependent metabolic intermediates required for cell growth [149]. Metformin has been reported to prevent cancer development and increase cancer patient survival; thus, it is being intensively studied in preclinical studies and clinical trials for cancer treatment [150]. A systematic meta-analysis of clinical trials and research data has showed that metformin intervention was associated with a significant benefit in patient outcomes of early-stage colorectal cancer and prostate cancer [151]. With a similar mechanism of action as metformin, phenformin is another biguanide that inhibits mitochondrial complex I. Although phenformin exhibits more potent anti-cancer effects than metformin in preclinical studies, its clinical use is limited due to the serious lactic acidosis side effect. In an *in vitro* study, oxamate, a lactate production inhibitor, showed to overcome the side effect of phenformin, and a synergism between these two compounds was discovered [152]. More studies are needed in cancer models and clinical trials to see if there is any potential.

In preclinical studies, compounds that target ETC such as VLX600 have been demonstrated to have anticancer activity by decreasing mitochondrial oxidative phosphorylation (OXPHOS) and can have greater effects on cancer cells in metabolically compromised microenvironments [153]. Compounds that target mitochondrial protein translation and stability have also been reported to have anti-cancer effects. FDA approved antibiotics Tigecycline was reported to have selective toxicity for human acute myeloid leukaemia (AML) cells both *in vitro* and *in vivo* by inhibiting mitochondrial ribosome and consequently the translation of ETC proteins subunits, as AML cells demonstrated higher mitochondria activities than normal haematopoietic cells [154]. Many studies are ongoing but the clinical trials haven't demonstrated efficacy yet [155]. Gamitrinib was shown to accumulate in the mitochondria of human cancer cell lines and to inhibit Hsp90 (chaperone protein assisting correct protein folding) activity by acting as an ATPase antagonist. It showed selective anticancer activity in a prostate cancer mouse model [156, 157].

Although targeting mitochondria metabolism appears to be promising, the heterogeneity of cancer cell metabolism and the cells' ability to adapt and bypass mitochondrial-dependent metabolism will lead to resistance to this novel therapy. Targeting multiple metabolic pathways, such as glycolysis and mitochondrial respiration together, has been proposed as a viable approach to cancer treatment.

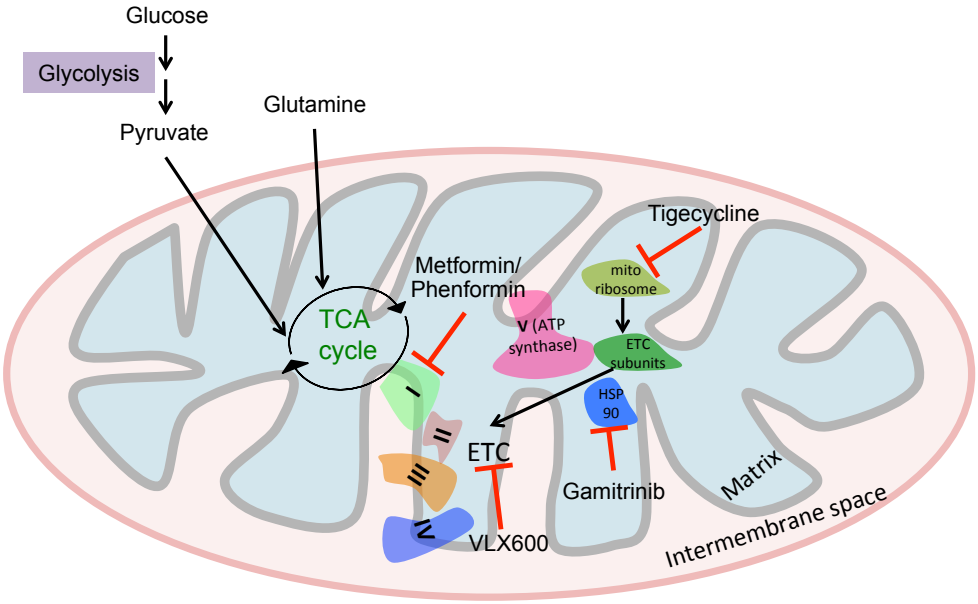

Figure 1.8 Targeting mitochondria bioenergetics for cancer therapy. Metformin and phenformin inhibit mitochondrial complex I; VLX600 inhibits multiple sites of the ETC; tigecycline inhibits the mitochondrial ribosome and affects the translation of ETC subunits; gamitrinib inhibits mitochondrial chaperone proteins, such as HSP-90, decreasing ETC complex stability and function. mtDNA: mitochondrial DNA. Illustration modified from Weinberg et al. [147].

1.3.3 Glutamine metabolism

Glutamine is the most abundant free amino acid in the human blood, and cancer consume and utilize glutamine at much higher rates than other amino acids. Glutamine is a major carbon source to replenish the TCA cycle, allowing it to sustain biosynthesis in many cancer cells [158, 159]. Glutamine is also a critical nitrogen source for the biosynthesis of purines, pyrimidines, NAD, asparagine, and glucosamine [160, 161]. Glutamine metabolism contributes to cancer cell proliferation by supporting ATP production and the biosynthesis of proteins, lipids, and nucleic acids.

Glucose and glutamine metabolism are interlinked and actively coordinated in cancer cells through the activation of oncogene pathways such as PI3K-AKT-mTOR, KRAS, and MYC. MYC can simultaneously increase the uptake and metabolism of both glucose and glutamine by regulating key transporters and enzymes involved in both metabolic pathways. Cancer cells that are driven by MYC would be reliant on glutamine metabolism as MYC induces the expression of glutamine transporters (solute carrier family 1 member 5 (SLC1A5), also known as ASCT2 and glutaminase (GLS)

[161]. Glutamine metabolism can play an essential role in maintaining cell survival and proliferation under oxygen and glucose deprived conditions. A tracer study has demonstrated that glutamine transportation and glutamine metabolism in the TCA cycle persisted under hypoxia, and that glutamine contributed significantly to citrate carbons. Under glucose-deprived conditions, glutamine-derived fumarate, malate, and citrate were significantly increased to provide the carbon source [162].

The glutamine metabolism (**Figure 1.9**) occurs mainly inside the mitochondria matrix and is related to the metabolism in the mitochondria. Glutamine can be transported into mitochondria through the glutamine transporter and converted by glutaminase into glutamate inside the mitochondria. Glutamate can then be converted by glutamate dehydrogenase (GLUD1, GLUD2) or aminotransferases into α-ketoglutarate (α-KG) to enter the TCA cycle. Other amino acids can be produced as by-products of the aminotransferase reactions. α-KG enters the TCA cycle to generate ATP, malate and oxaloacetate. Malate can exit the TCA cycle and be converted into pyruvate and NADPH, and oxaloacetate can be converted into aspartate to support nucleotide synthesis. The glutamine-derived α-KG can also be carboxylated to produce citrate, which can exit mitochondria and then being used to generate oxaloacetate and acetyl-CoA to fuel fatty acid synthesis (**Figure 1.9**) [163, 164].

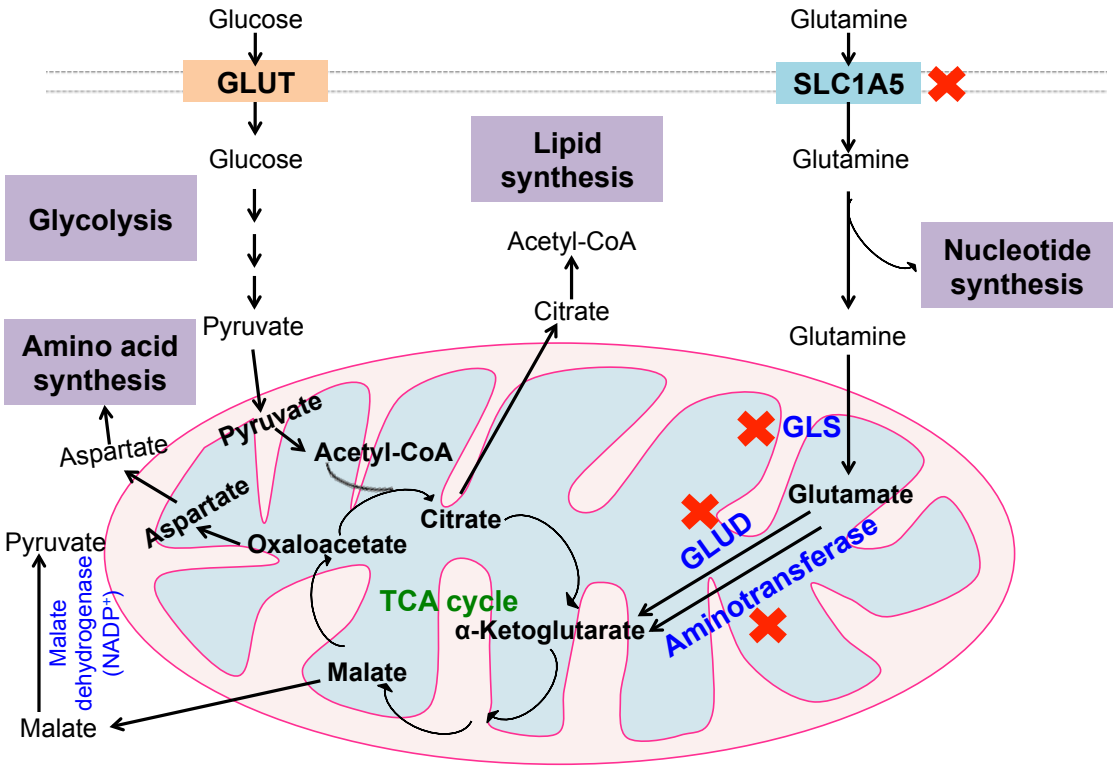

Figure 1.9 Glutamine metabolism and potential therapeutic targets. Glutamine enters the mammalian cell through transporters such as SLC1A5. Glutamine can be metabolized into glutamate by glutaminase (GLS), then further being transformed into α-ketoglutarate (α-KG) by either glutamate dehydrogenase (GLUD) or aminotransferases, and α-KG then enters the TCA cycle. Glutamine metabolism is interlinked with glucose metabolism, nucleotide synthesis, and fatty acid synthesis. Citrate produced in the TCA cycle can exit mitochondria and become a precursor for fatty acid synthesis. Oxaloacetate can be converted into aspartate to support nucleotide synthesis. Illustration modified from Choi et al. [165].

Because glutamine is important for cancer cell survival and proliferation, therapeutic targeting of glutamine metabolism has been studied as a novel anticancer approach. Many cancer types such as lung cancer, colon cancer, breast cancer, melanoma, neuroblastoma, glioblastoma, and prostate cancer have upregulated glutamine transporter expression. Therefore, they present with enhanced transportation of glutamine and a high dependency on glutamine metabolism [166, 167]. Inhibitors of the glutamine transporter SLC1A5 such as tamoxifen, raloxifene, benzylserine, γ-FBP (γ-folate binding protein), and GPNA (L-γ-glutamyl-p-nitroanilide) have been shown to be effective in suppressing glutamine-dependent cancer cells through inhibition of glutamine uptake [168-171]. Inhibitors of GLS, such as CB839 and compound 968, inhibit the first step of glutamine metabolism and demonstrated anticancer effects in

preclinical studies in various cancer cell types [172-174]. CB839 is currently undergoing phase I clinical trials in both haematological cancer and in several solid tumours (https://clinicaltrials.gov). Inhibition of the transformation of glutamate into α-KG has also been studied in cancer treatment, with GLUD inhibitor R162 [175], and aminotransferase inhibitor aminooxyacetic acid all showing anticancer growth effects in preclinical studies [176].

There are limitations of targeting glutamine metabolism. First of all, not all cancer cells display dependence on glutamine. Studies are needed to predict whether the cancer cells from patients would respond to therapies targeting glutamine metabolism or not. The cancer cells can potentially rewire their metabolic pathways to be independent of glutamine. Therapy that inhibits glutamine metabolism when used in combination with therapies that target other metabolic pathways such as glycolysis, mitochondria metabolism of cancer have shown synergistic potential in preclinical cancer studies and should be pursued further [160]. The studied compounds to inhibit glutamine metabolism often act off-target and induce toxicity in healthy cells that require glutamine [165]. Most of the molecules listed above are still in preclinical research. More clinical studies are needed to evaluate their efficacy and safety.

1.3.4 *de novo* fatty acid synthesis

Cancer cells prefer to synthesize lipids through *de novo* fatty acid (FA) synthesis rather than using dietary lipids, and this phenotype is independent of abundant dietary lipid supply [13]. FA synthesis study using ^{14}C labelled glucose as a tracer found that the vast majority of the esterified FA in the tumour models was derived from *de novo* FA synthesis. In contrast to normal cells that primarily rely on exogenous lipid sources, in mice Ehrlich ascites cancer cells, FA produced through *de novo* FA synthesis accounted for 93% of the triacylglycerol FA using ^{14}C labelled glucose as a tracer [177].

The abnormal FA metabolism of cancer cells is linked with a glycolytic phenotype, which was reflected by constitutively up-regulated glycolytic and lipogenic enzyme activities [178]. Both metabolism pathways can be constitutively upregulated through genetic or epigenetic changes [179]. The upregulated glucose metabolism in cancer provides both ATP and a carbon source which can be redirected towards the *de novo* FA synthesis to support lipid production [180]. The glutamine metabolism in cancer also provides precursors for FA synthesis. Increased glutamine metabolism in cancer cells enables the replenishment of citrate, which can then be used for the production of acetyl-groups for FA synthesis [181]. FAs can be taken up through FA translocase, CD36, or by passive diffusion (flip-flop). In the cytoplasm, FAs are either in free form or bound to FA binding proteins to transport FAs to fulfil multiple functions, such as elongation in endoplasmic reticulum, gene expression regulation inside the nucleus, and triglycerides formation in lipid droplets. FAs can be released through enzymes such as monoacylglycerol lipase during the process of lipolysis. FAs can be activated by acyl-CoA synthetase and then enter the mitochondria via carnitine palmitoyl transporters (CPT) for fatty acid oxidation (FAO)/β-oxidation, leading to acetyl-CoA formation. The large amount of acetyl-CoA generated enters the TCA cycle and contributes to ATP production in tumour cells. Intermediates of the TCA cycle can contribute to NADPH production, which contributes to protection against ROS. Citrate derived from the TCA cycle can be synthesized into FAs by the enzyme activities of ATP-citrate lyase (ACLY), acetyl-CoA carboxylase (ACC) and FA synthase (FASN) (**Figure 1.10**) [182]. FAs are essential for cancer cell proliferation, so limiting their availability and blocking the FAs synthesis could form novel therapeutic approaches. There could be multiple ways of limiting availability of FAs through the lipid metabolism pathways, such as

inhibiting FA degradation via β oxidation, blocking FA synthesis, diverting FAs to storage, or decreasing FA release from storage; these approaches could be used solely or in combinations [181].

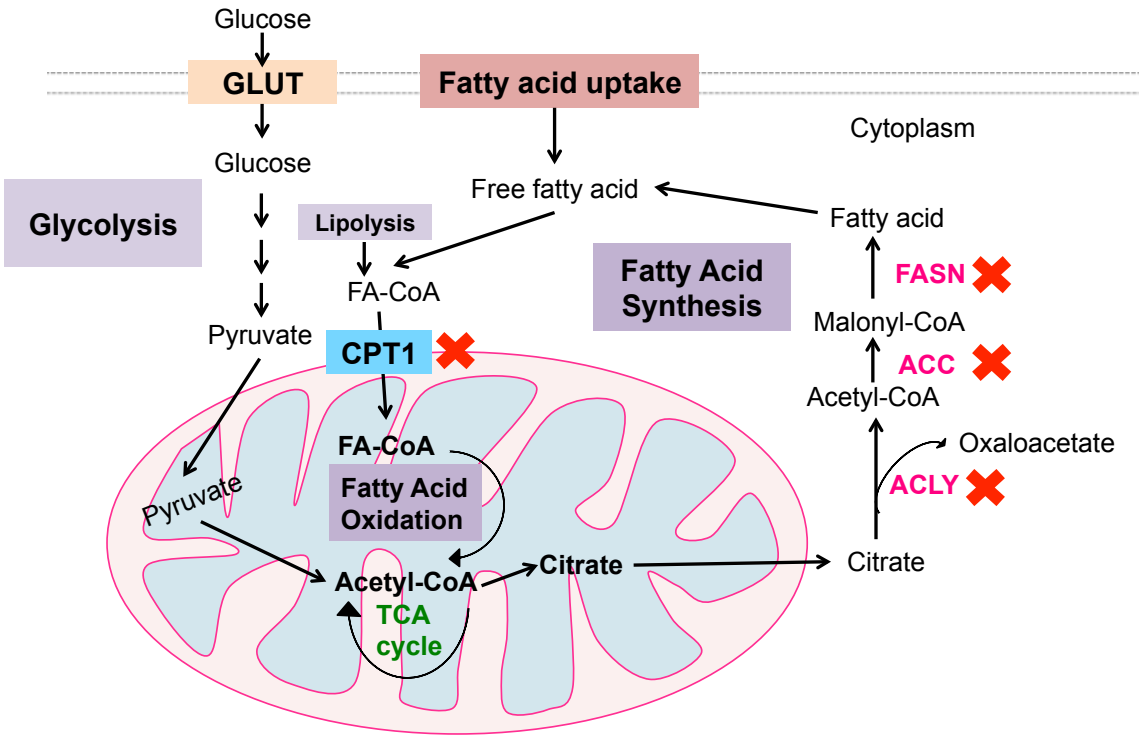

Figure 1.10 Fatty acid metabolism and the potential therapeutic targets against cancer. Fatty acid oxidation (FAO)/β-oxidation in cancer cells ultimately promotes redox and energy balance during metabolic stress in nutrient deprived or hypoxic conditions. CPT can be a target for inhibiting FAO, which leads to less acetyl-CoA formation to support cancer ATP production. Citrate derived from the TCA cycle can be converted into FAs through activity of ATP-citrate lyase (ACLY), acetyl-CoA carboxylase (ACC) and FA synthase (FASN). These enzymes (marked in red) are required for cancer growth and could be used as potential treatment targets. Illustration modified from Harjes et al. [182].

Fatty acid oxidation (FAO) in cancer cells was thought to provide protection against ROS and provide energy balance during metabolic stress situations, for example in nutrient deprivation or hypoxia. However, the responses of cancer cells to the inhibition of FAO were unclear. Carnitine palmitoyl transporters (CPT) is the first and rate-limiting step of the long chain FA transportation into mitochondria for FAO. Pharmacological inhibition of CPT1 by etomoxir inhibited cancer cell growth by inhibiting FAO which lead to the reduction of NADPH and GSH and consequently

increased ROS damage [183]. However, recent study showed that the anti-cancer effects of inhibition of CPT1 by etomoxir may not be due to the inhibition of FAO, as the use of low dose etomoxir yielded a 90 % inhibition of FAO but the cancer cell proliferation was unaffected. Instead, cancer cells utilized other nutrients to compensate for the loss of FAO; the high concentration of etomoxir used for inhibition of cancer cell growth may be acting through off-targets effects such as inhibition of the mitochondria complex I [184].

Another treatment approach is to block *de novo* FA synthesis in cancer through inhibiting the key enzymes in this pathway. Citrate derived from the TCA cycle fuels into FAs synthesis through the activities of enzymes such as ACLY, ACC, FASN, and acyl-CoA synthetase (ACS, ACSL, also known as fatty acid-CoA ligase (FACL)) [181]. The upregulated FA synthesis of cancer cells relies on the overexpression of these key enzymes of this pathway, thus inhibiting these enzymes would limit cancer cell growth.

ACLY is the enzyme that links glucose metabolism with FA metabolism by converting citrate into oxaloacetate and acetyl-CoA (the precursor for FA synthesis). ACLY was found to be overexpressed in many cancer types such as glioblastoma, colorectal cancer, breast cancer, lung cancer, and liver carcinoma [185]. shRNA knockdown of ACLY or the use of chemical ACLY inhibitor (SB-204990) in mice models was demonstrated to impair tumourigenesis [186], and an *in vitro* study showed siRNA knockdown of ACLY inhibited cancer cell growth and induced apoptosis [187], but the product of ACLY, acetyl-CoA, is an important metabolite for many other metabolic pathways, thus inhibiting ACLY could lead to negative consequences for the metabolism networks.

Fatty acid synthase (FASN) is a key enzyme for *de novo* FA synthesis and its expression is highly increased in various cancer types such as colon, prostate, ovary and breast cancers [188]. Overexpressed FASN is also strongly correlated with poor prognosis in soft tissue sarcoma and lung cancer patients [189, 190]. It has been shown that FASN overexpression contributed to increased drug resistance against adriamycin and mitoxantrone in breast cancer cell lines, and that reducing the FASN expression resulted in increased sensitivity to those drugs [191]. FASN protein and mRNA were highly expressed in plasma cells from myeloma patient BM samples as well as MM cell lines, while there was no detectable FASN levels in peripheral blood mononuclear cell

(PBMCs) from healthy donors; and the inhibition of FASN was demonstrated to be cytotoxic to myeloma cells [192]. Orlistat is an anti-obesity drug approved by FDA, which inhibits gastric and pancreatic lipases in the intestine. It is also an inhibitor of FASN and has been demonstrated to have cytotoxicity effects in various cancers [193]. Orlistat was shown to reduce myeloma cells proliferation by 40-70%; it caused cell cycle arrest and sensitized myeloma cells to apoptosis induction by bortezomib [194]. The low bioavailability of orlistat hinders its use in cancer treatment. Another concern of using FASN inhibitors (cerulenin and a synthetic compound C75) in cancer treatment is their side effect of affecting food intake and severe weight loss observed in mouse models [195]. Future clinical trials may be carried out in obese cancer patients and to research on how to improve the bioavailability of FASN inhibitors.

While targeting different aspects of FA metabolic pathways offers new approaches in cancer treatments, the chemical inhibitors currently available require further investigation. Fatty acid metabolism is a very complex network with many different feedback regulation processes. The adaptability of cancer cells' fatty acid metabolism also contributes to the difficulty of targeting fatty acid metabolism effectively in cancer. Future therapy studies need to understand the specific metabolism abnormalities of a particular cancer type.

1.4 Dichloroacetate

Dichloroacetate (DCA), a pyruvate dehydrogenase kinase (PDK) inhibitor, has many advantages compared to other metabolic modulatory drugs and is ready to be repurposed for clinical cancer treatment. The safety, toxicity and pharmacokinetics of DCA have been well established because of its use in human mitochondria diseases and lactic acidosis for decades. DCA has many advantages to be repurposed in cancer treatment as it can be easily administered orally, has high bioavailability, low toxicity and is relatively inexpensive. DCA has been proposed as a potential metabolic modulatory drug for potentiating cancer cells to chemotherapy or radiotherapy [3, 4, 196].

1.4.1 The mechanism of action

DCA is an inhibitor of PDKs. PDKs are a family of kinase enzymes that inactivate the pyruvate dehydrogenase complex (PDC) by phosphorylating pyruvate dehydrogenase (PDH), which is the first catalytic component of the PDC. The PDC in eukaryotes is composed of three catalytic enzymes: PDH (E1), dihydrolipoamide acetyltransferase (E2), and dihydrolipoamide dehydrogenase (E3). These three catalytic subunits work sequentially, catalysing the irreversible oxidative decarboxylation of pyruvate into acetyl-CoA, CO_2, and NADH. PDC plays a key role in glucose metabolism by linking the glycolytic pathway to the TCA cycle [132]. PDKs inactivate PDC to reduce the glucose-derived pyruvate flow into the TCA cycle. This diversion decreases the rate of oxidative phosphorylation and oxygen consumption and thus reinforces the glycolytic phenotype. Phosphatases (isoenzymes: PDP1 and PDP2) can readily dephosphorylate and reactivate the PDC [48, 49, 132]. The activity of PDC is tightly regulated by the PDKs and PDPs in tissues to adapt to specific nutritional conditions and disease status [197]. DCA, a pyruvate mimetic, can inhibit the activity of PDKs by binding to the allosteric pyruvate binding site of the PDKs. The binding of DCA to the N-terminal regulatory domain of PDK1 and PDK2, promotes local conformational changes which result in inactivation of the kinase activities [198, 199]. By inhibiting PDKs, DCA diverts the flux of glycolysis-generated pyruvate into the mitochondria, thereby promoting glucose oxidation through mitochondrial respiration. This metabolism shift reverses the glycolytic phenotype and would arrest the growth advantage of highly glycolytic cancer cells (**Figure 1.11**) [24, 196]. DCA can halt the inhibitory effect of

PDKs on PDH, but it cannot dephosphorylate and reactivate the already phosphorylated PDH, thus the effect of DCA requires the presence of PDPs. Although the deficiency of PDPs is extremely rare [200], it could be a factor affecting the ability of DCA to exert its effect in restoring PDH activity.

The effect of DCA as a PDK inhibitor may be affected by the distribution and expression of PDK isoforms. There are four isoforms of PDKs (PDK1, PDK2, PDK3, and PDK4) in humans, and they vary in tissue distribution, kinetic activities and sensitivity to DCA. PDK2 is the ubiquitous isoform, constitutively expressed in all tissues but at low levels in lung and spleen. PDK1 is expressed almost exclusively in the heart (in normoxia) while PDK3 presents most abundantly in the testis. PDK4 is predominantly expressed in the skeletal muscle and heart [4]. The enzyme activities of the different PDK isoforms differ by 25-fold and are largely determined by their binding capacities to the inner lipoyl-bearing domain L2 in the E2 (transacetylase) component of the PDC. The binding affinity of PDKs has been identified as PDK3 > PDK1 = PDK2 > PDK4 [201, 202]. The inhibitory constant (K_i) values of PDKs by DCA are different. The most prevalently expressed PDK2 is the most sensitive isoform to be inhibited by DCA (K_i: 0.2 mM), which is 40-fold lower than that of the least sensitive, PDK3 (K_i: 8 mM); the K_i values for PDK1 and PDK4 are 1.0 and 0.5 mM respectively [4]. Thus, the amount of DCA needed to successfully inhibit the PDKs may vary in tissues or cancers that express different PDKs.

The phosphorylation of PDH by PDKs is site specific. Human PDH (E1 subunit) has three serine residues, which can be phosphorylated, referred to as site 1 (Ser 264/293), site 2 (Ser 271/300), and site 3 (Ser 203/232) respectively (a segment of 29 amino acids is not present in the matured protein, giving rise to the two position numbers) [203]. The PDK isoenzymes show different specificities for these three phosphorylation sites of PDH E1. Studies showed that only PDK1 could phosphorylate site 3, whereas all four PDKs can phosphorylate sites 1 and 2 of PDH E1 at different rates in phosphate buffer (for site 1, PDK2 > PDK4 ≈ PDK1 > PDK3; for site 2, PDK3 > PDK4 > PDK2 > PDK1) [204-206]. Thus the effect of DCA in activating PDH may be influenced by the complexity of the tissue distributions and expressions of PDKs and PDPs in specific disease or biological conditions.

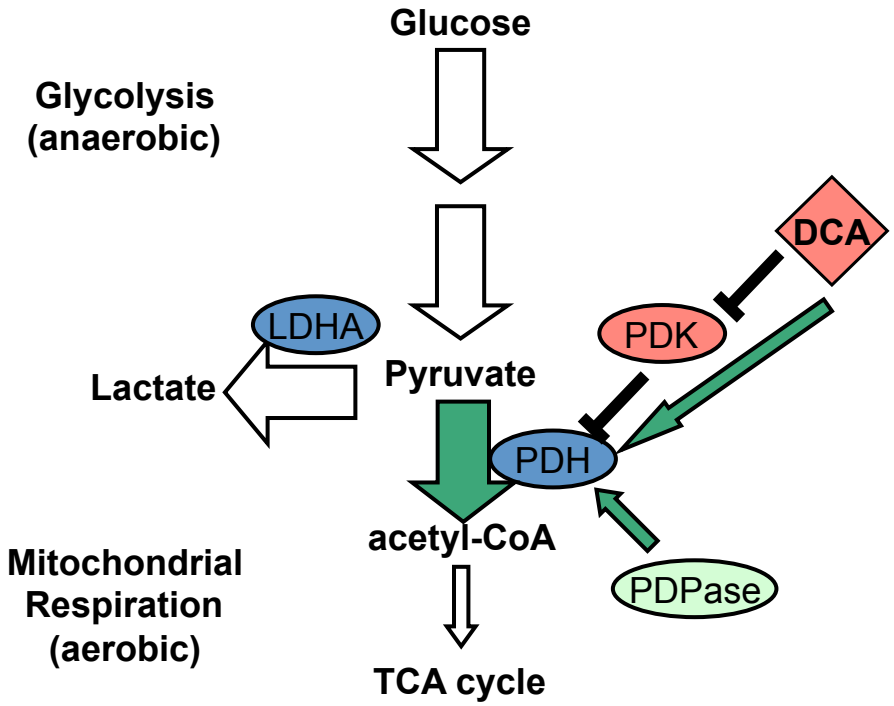

Figure 1.11 DCA mechanism of action. DCA inhibits PDKs, and thus activates the PDH complex indirectly, diverting the flow of glycolysis-derived pyruvate from lactate production into mitochondrial respiration. PDK: pyruvate dehydrogenase kinase. PDH: pyruvate dehydrogenase. TCA cycle: tricarboxylic acid cycle. LDHA: Lactate dehydrogenase A. PDP: pyruvate dehydrogenase phosphatase.

1.4.2 DCA metabolism

DCA can be rapidly and easily absorbed after oral administration in humans, as shown by pharmacokinetics studies [207, 208]. The major route of metabolism of DCA is through oxidative dechlorination by GSTZ1 (glutathione transferase Zeta 1, identical to maleylacetoacetate isomerase) to form glyoxylate [209]. DCA is an inhibitor of its own metabolism. Administration of DCA by different routes to healthy human subjects showed that subsequent doses of DCA yielded a much longer half-life than the first dose [208, 210-212]. This inhibition of DCA metabolism was found to be associated with the biotransformation of DCA into electrophilic metabolites that covalently modify and inactivate the GSTZ1 enzyme *in vitro* [213]. The inactivation of GSTZ1 by DCA was also demonstrated in an *in vivo* rat model where the hepatic GSTZ1 activity and the GSTZ1 protein level were reduced after DCA treatment in a dose-dependent manner. There was barely any detectable GSTZ1 protein remaining in rat liver after 12 weeks of 50 mg/kg DCA administration [214].

The *GSTZ1* haplotype can considerably influence GSTZ1 enzyme expression and function and thus affect DCA biotransformation and pharmacokinetics [215-219]. Thus it is suggested that the *GSTZ1* genotype needs to be considered in the clinical use of DCA. Many single nucleotide (nt) polymorphisms (SNPs) have been identified in both the protein-coding and promoter regions of the *GSTZ1* gene. Three non-synonymous SNPs in the protein-coding region (Exon 3 nt 94 and 124, Exon 5 nt 245) have been identified in people and found to give rise to five commonly found haplotypes of *GSTZ1* (**Table 1**) with significant variation in GSTZ1 activity [215, 219, 220]. Studies of expressed recombinant enzymes corresponding to the common variants showed that the amino acid changes resulted in alterations of enzyme activity with DCA (**Table 1**). The *GSTZ1*A* (KRT) haplotype displayed 3.6-fold higher activity towards DCA compared to other haplotypes tested as recombinant proteins *in vitro* [220]. *In vitro* study of human liver cytosol confirmed that individuals with at least one copy of the *GSTZ1*A* (KRT) haplotype exhibited higher activity with DCA than those without it [221]. Notably, *GSTZ1*A* did not metabolize DCA faster than other haplotypes following repeated doses of DCA [215]. However, there was no conclusive result in healthy humans regarding the higher activity of *GSTZ1*A* (KRT) haplotype. The heterozygous with KRT haplotype in healthy volunteers was associated with relatively rapid metabolism of the initial dose of DCA; in contrast, the homozygous KRT did not show a different rate of DCA clearance compared to persons with one or more of other haplotype alleles [215].

Table 1 GSTZ1 polymorphism, allele frequency and corresponding activity *in vitro*

Haplotype	**Variant nucleotides positions [219]**			**Variant amino acid positions [215]**			**Allele Frequency [219, 221]**	**DCA metabolism activity [220] *in vitro*** (nmol/min/mg prot)
	Exon3		**Exon5**					
	94	**124**	**245**	**32**	**42**	**82**		
*GSTZ1*A*	A	A	C	K	R	T	0.086	1610
*GSTZ1*B*	A	G	C	K	G	T	0.285	450
*GSTZ1*C*	G	G	C	E	G	T	0.473	450
*GSTZ1*D*	G	G	T	E	G	M	0.156	300
**GSTZ1*E*	G	G	C	E	G	T	------	-----
*GSTZ1*F*	A	G	T	K	G	M	0.004	-----

Standard amino acid abbreviations: K = lysine, R=Arginine, G = glycine, T = threonine, E = glutamic acid, M = methionine. *GSTZ1*E* is identical to *GSTZ1*C* in the protein sequence, only variant in the 5' non-coding region, and thus has no effect on enzyme function. No individual carrying this mutation has been identified yet [219].

Polymorphisms in the human *GSTZ1* promoter can also alter GSTZ1 expression and thus affect the pharmacokinetics of DCA. Among the ten polymorphisms identified in a 1.5 kb proximal region of *GSTZ1* promoter, -1002 G>A and -289 C>T significantly changed promoter activity in HepG2 cells transfected with luciferase reporter gene constructs; the -1002A allele had significantly lower transcription activity compared to the -1002G allele, while -289T had higher promoter activity compared to the -289C allele [218]. These promoter SNPs also affected GSTZ1 protein level in human liver cytosol. The GSTZ1 enzyme activity and protein level of the -1002A allele in human liver cytosol were significantly lower than that of the -1002G regardless of the donors' ethnicity (**Table 2**) [217]. The impact of these promoter polymorphisms on cancer patient DCA serum levels has not been investigated, but it is hypothesized that knowledge of *GSTZ1* genotype may be important when assigning dosing regimens to subjects participating in clinical trials of DCA.

Table 2 *GSTZ1* promoter -1002 polymorphism, allele frequency and corresponding promoter activity *in vitro*

Promoter nt -1002	Allele Frequency[219]	Promoter Activity[215, 217, 218]
A	0.33	low
G	0.67	high

1.4.3 The anti-cancer effects of DCA

Evidence of the anti-cancer effects of DCA has emerged from *in vitro* and *in vivo* research in various types of cancer. Through the main action of reversing the glycolytic phenotype, the anti-cancer mechanisms of DCA in published studies have concentrated on the following areas: inhibiting proliferation; increasing ROS and normalizing mitochondrial membrane potentials (MMP) to activate mitochondria-led apoptosis; counteracting HIF-activation-led adaptation; overcoming glycolytic phenotype-associated drug resistance and potentiating cancer cell responses to the cytotoxicity of chemotherapy agents.

Inhibition of proliferation and induction of apoptosis. Studies have demonstrated that DCA can inhibit cancer cell proliferation and/or induce apoptosis. Stacpoole et al. reviewed that the ability of DCA to inhibit cell proliferation and/or induce apoptosis *in vitro* in various solid tumours such as human breast, ovary, cervix, uterus, prostate, pancreas, colon, stomach, liver, lung, and brain cancers, as well as in haematological

cancers such as lymphoma, leukaemia, and multiple myeloma [222]. However, the extent of the anti-cancer effects of DCA are not consistent among the published studies, with effects ranging from merely growth inhibition, to cell cycle arrest, to apoptosis.

Several studies in human breast cancer, human colorectal cancer and canine mammary cell lines demonstrated that DCA when used at concentrations lower than 5 mM can inhibit cancer cell proliferation to various extents without inducing apoptosis [9, 10, 223, 224]. The anti-proliferative effect on human breast cancer cell lines was associated with the reversal of the glycolytic phenotype. Although DCA did not induce apoptosis *in vitro*, it did reduce tumour size in a metastatic breast cancer rat model [9, 10]. DCA may inhibit proliferation by reversing the glycolytic phenotype, which is independent of cell cycle arrest or apoptosis.

The mechanism of DCA inducing apoptosis in many cancer types has been demonstrated to be via increasing ROS production and reducing mitochondrial hyperpolarisation (which is associated with resistance to apoptosis) thus inducing mitochondria-led apoptosis. Some of these published studies are summarised below. In lung cancer, glioblastoma, and breast cancer cell lines, DCA caused increased glucose oxidation, induced apoptosis by decreasing MMP, increasing mitochondrial ROS production, and activating Kv channels [7]. In invasive human endometrial cell lines, an increase of the p53 upregulated modulator of apoptosis (PUMA, a pro-apoptotic protein) was also observed by DCA treatment [6]. In human prostate cancer cell lines, DCA at high concentration (>10 mM) caused apoptosis and G1 phase cell cycle arrest, and these anti-cancer effects were associated with the decreased MMP [225]. In colorectal cancer cell lines, DCA (20-50 mM) suppressed cell proliferation and caused G2 phase cell cycle arrest, which were associated with reduced lactate levels and pPDH; but these anti-cancer effects were not observed on non-cancerous cells [8].

In freshly isolated patient glioblastoma biopsy tissue (highly-expressed PDK2 compared to non-cancer brain tissue), DCA caused mitochondrial depolarization and increased ROS but there was no effect in non-cancer brain tissue from epilepsy patients *in vitro* [5]. In a clinical trial conducted in glioblastoma patients, post-DCA chronic treatment tissue in the patients showed decreased cell proliferation (% PCNA-positive cells), increased apoptosis (% TUNEL-positive cells), and increased tissue PDH enzymatic

activity compared to pre-DCA treatment glioblastoma tissue, suggesting the on-target and anti-cancer effects of DCA can be viable *in vivo* [5].

Based on these studies, it is proposed that whether DCA can cause cancer cell growth inhibition or induce apoptosis may be cell type specific and dose-dependent. The concentrations of DCA causing cytotoxic effects in the *in vitro* studies were typically used at clinically unachievable concentrations (10-50 mM) [222]. A viability screening study using C^{14}-leucine incorporation showed that the IC_{50} values to be inhibited by DCA (48 hour) ranging from 17-40 mM in a range of cancer cell lines including leukaemia, melanoma, ovarian, breast, prostate, lung and renal cancers [226]. Studies showed that when DCA used at concentrations in the range of its inhibitory constant for PDKs (mechanistic relevant concentrations), it mainly showed an anti-proliferative rather than an apoptosis-inducing effect. However, DCA has still been demonstrated to inhibit cancer growth *in vivo*, indicating its potential for clinical use [10, 222].

Counteracting HIF. Oncogene activation and adaptation to the hypoxic microenvironment in cancer can lead to the abnormal cancer glycolytic phenotype [1]. Rapidly growing solid tumours and haematological cancers originating in the BM and lymph nodes are representative of hypoxic cancers. HIF stabilisation is a key factor in the adaptive switch to glycolysis and is associated with chemoresistance in cancer [227, 228]. HIF enhances the glycolytic phenotype by inducing the expression of many glycolysis-associated genes such as *PDK1*, and *PDK3* [40, 45, 48, 50]. In a clinical trial using DCA in glioblastoma patients, DCA was found to inhibit HIF-1α expression in patient glioblastoma tissue, which was accompanied by suppression of angiogenesis [5]. DCA treatment reduced tumour vascularity and perfusion in a lung cancer mouse model, which led to smaller tumour size and increased survival [229]. Both *in vitro* and *in vivo* experiments showed that DCA inhibits HIF-1, either by inducing the production of the mitochondrial-derived α-KG (substrate of PHD) that leads to HIF-1α degradation, or by increasing p53 activity and nuclear localization through stimulation of mitochondrial-derived H_2O_2 production [229], as the activation of p53 inhibits HIF-1 transcriptional activity [230]. DCA (20 mM) was found to resensitize gastric cell lines with hypoxia-induced resistance to 5-fluorouracil through the alteration of the glycolytic phenotype

[231]. These results indicate DCA may have great potential in the treatment of hypoxic cancers.

Potentiating cytotoxicity and overcoming drug resistance. DCA was found in many studies to potentiate the effect of cytotoxic drugs or radiation therapy on cancer cells. The combination of DCA and arsenic trioxide (inhibitor of the complex IV of the ETC) was more effective at inhibiting cell proliferation and inducing cell death than either drug alone in breast cancer cell lines. This effect may be due to the two agents co-operatively suppressing MYC and HIF-1α protein levels and decreasing Bcl-2 anti-apoptotic protein [9]. PENAO (4-(N-(S-penicillaminylacetyl)amino)phenylarsonous acid) is an arsenic-based mitochondrial toxin currently in early phase clinical trials. When PENAO was combined with DCA, its cytotoxicity was enhanced and apoptosis was increased through a mechanism involving increased ROS production [232]. DCA reduced epidermal growth factor receptor (EGFR) levels in breast cancer cell lines in a dose-dependent manner. Consistent with this being an on-target effect, siRNA knockdown of each PDK isoform caused the downregulation of EGFR. The overexpression of EGFR was associated with resistant to tamoxifen in breast cancer. The combination treatment of DCA and tamoxifen resulted in enhanced apoptosis, and it resensitized cells to tamoxifen treatment by decreasing EGFR expression in breast cancer cells [233]. In human prostate cancer cells, DCA was found to sensitize wild type and over-expressing Bcl-2 cells to radiation therapy by modulating the expression of key members of the Bcl-2 family [225]. In MM cell lines, DCA combined with bortezomib showed additive cytotoxic effects, and re-sensitized a bortezomib-resistant myeloma cell line. The combination of DCA and bortezomib further improved survival of a myeloma mouse model compared to bortezomib alone [11].

These studies have demonstrated that the anti-cancer effects of DCA were cancer cell specific while sparing the non-cancerous cells [5, 8], however, the anti-cancer effects were observed in some but not all of the evaluated cancer cell lines. The contributing factors for different sensitivity to DCA remain unclear. The accumulated evidence from various cancer types clearly shows DCA has potential to be used as an addition to cancer therapy, and that more investigations are needed to find out the contributing factors to the sensitivity of DCA and the efficacy of DCA in cancers with a glycolytic

phenotype. Despite the concentrations of DCA used in the *in vitro* studies being 10-50 times higher than what can be achieved *in vivo*; DCA still demonstrated a clear effect in inhibiting cancer growth *in vivo* [5, 10, 222]. Due to the established safety profile of DCA, the optimal doses of DCA and its efficacy can be evaluated directly in suitable cancer patients in phase 1/2 clinical trials.

1.4.4 DCA in cancer clinical trials

There have been several phase 1/2 clinical trials and case series to study the safety and efficacy of DCA on various solid tumour types. The first published DCA clinical study in cancer patients was conducted by Michelakis et al. (2010). Five glioblastoma patients were treated with different doses of DCA through oral administration for up to 15 months. Their results showed that the dose-limiting side effect of DCA was a dose-dependent, reversible peripheral neuropathy and there was no haematological, hepatic, renal, or cardiac toxicity. The *in vitro* study of patients' brain tumour biopsy tissue after chronic DCA treatment showed that DCA can act on-target to increase PDH enzyme activity [5]. Dunbar et al. (2014) studied DCA in a phase-1 trial in adults with recurrent glioblastoma. In this trial, a dose-escalating study of DCA was carried out in patients with recurrent glioblastoma (n=9) or cancer metastases to the brain (n=3). The data demonstrated that chronic DCA treatment (average treatment time 75.5 days) was feasible and DCA was well tolerated when taken orally using the doses developed for treating metabolic diseases. The results recommend individualizing DCA doses for patients based on their *GSTZ1* genotype [234]. Although the chronic use of DCA was established in cancer patients, there were not enough patients to confirm its efficacy. These two trials warrant further clinical study of DCA in cancer patients.

The doses of DCA given to cancer patients have been further investigated. A phase 1 study by Chu et al. (2015) assessed the safety and pharmacokinetic profile of oral DCA in 24 patients with advanced solid tumours. The results recommended using 6.25 mg/kg *b.i.d.* as the dose for future phase 2 trials [235], however, Michelakis et al. reported the DCA serum trough concentrations were too low to be detected when taking this dose in the first 2-3 months of a trial in glioblastoma patients due to DCA being an inhibitor of its own metabolism. Later on in this trial though, serum DCA trough concentrations can

be detected and ranged from 0.26-0.63 mM [5]. This highlights the importance of finding the optimal DCA doses for cancer patients.

The importance of finding suitable patients that can potentially benefit from DCA was evident in another early phase trial of DCA in patients with metastatic breast cancer (n=1) and advanced stage non-small cell lung cancer (n=6) conducted by Garon et al (2014). Before entering the trial, the enrolled patients already went through several rounds of standard therapies because they all had advanced malignancies. This study was terminated prematurely after 7 patients enrolled because the disease rapidly progressed in those patients. The results indicated there was no benefit from the single-agent oral administration of DCA for patients with advanced malignancies and a short life expectancy. This study suggested DCA should be tested in patients with longer life expectancy, in whom sustainable therapeutic drug concentrations could be achieved [236].

Based on these trials, it has been suggested that the doses of DCA in cancer patients should be adjusted according to the *GSTZ1* genotype and that reversible neuropathy caused by DCA should be carefully monitored. Selecting suitable patients who can potentially benefit from DCA treatment should be considered in the early phase trials of DCA. These clinical trials have confirmed it is feasible to administer DCA in cancer patients, and have demonstrated the safety of using it chronically in cancer patients. DCA may be used as an addition to antineoplastic chemotherapy agents rather than as a single agent. There is clearly support in the medical community for clinical testing of DCA in cancer therapy, hence our proposal for a clinical trial in multiple myeloma patients.

1.5 Multiple myeloma

1.5.1 Epidemiology and Etiology

Multiple myeloma (MM) is a B-cell malignancy characterized by a multifocal neoplastic proliferation of monoclonal plasma cells (end-stage B cell, antibody-producing B cell) in the BM [237]. MM is a relatively rare cancer type; it accounts for approximately 1% of all cancer cases worldwide and is the 2nd most common haematological malignancy after non-Hodgkin lymphoma [238, 239]. Incidence rates of MM are lowest among the Asian countries and the Asian populations residing outside of Asia compared to the rates of the Caucasian populations. MM incidence is highest among the African American population which is twice that of the Caucasian American population [238]. The median age of diagnosis is approximately 66-70 years with a slight male predominance in incidence. About 99% of cases are diagnosed in persons over the age of 40 [238]. In America, 30,280 new cases and 12,590 deaths were estimated to occur in the year 2017 (American National Cancer Institute, https://seer.cancer.gov/statfacts/html/mulmy.html). In Australia, 1,637 patients were diagnosed in the year 2013 and this number is steadily increasing. The estimated incident of MM in 2018 is 1,876, the estimated mortality is 566 people; and the 5-year relative survival rate was 48.5% during the period of 2009-2013 (**Figure 1.12**).

The survival of MM patients has been improving gradually over the past couple of decades, in correlation with the use of autologous stem cell transplantation followed by availability of novel treatments such as immunomodulatory drugs and proteasome inhibitors [240]. According to the Surveillance, Epidemiology, and End Results (SEER) registries, the 5-year relative survival rates (RSRs) in the United States improved from 24.6% for patients diagnosed during 1975-1977 to 51% for MM patients diagnosed during 2007-2013. When comparing the 10-year RSRs of 1993-1997 (19.6%) to 2003-2007 (35%), there was an improvement for patients younger than 65 years but not for patients older than 75 years [240]. In Australia, the 5-year RSRs also improved from 29% during 1984-1988 to 48.5% during 2009-2013 (**Figure 1.12**). This improvement correlated with the FDA approval of the novel chemotherapy agents: thalidomide was reintroduced in MM treatment during 1998-2002, while bortezomib and lenalidomide

were introduced in 2003 and 2004 respectively. Despite this mild improvement, MM remains an incurable disease with poor prognosis.

Although the etiology of MM is still unclear, some of the accepted risk factors for developing MM, such as old age at diagnosis, positive familial history, and a precondition called monoclonal gammopathy of undetermined significance (MGUS). The other possible risk factors are generally life style cancer risk factors such as obesity and unhealthy diet. There are some sporadic reports of risk caused by exposure to environmental hazards, pesticides and radiation but all lack concrete significance due to small population numbers [238, 241].

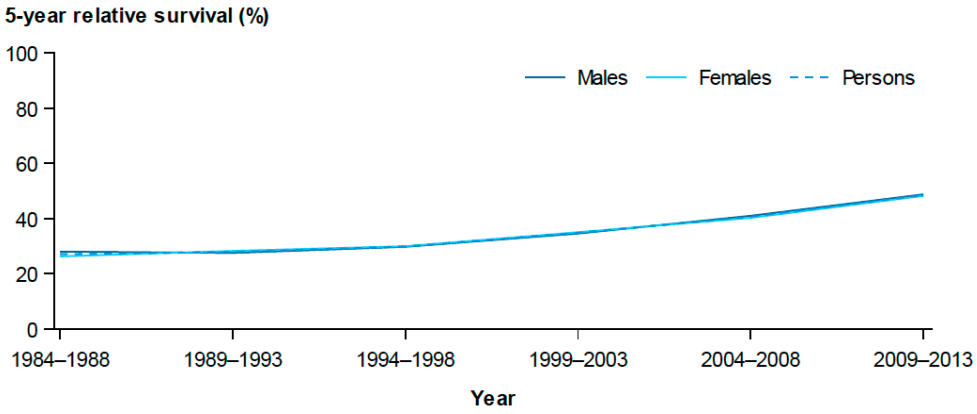

Figure 1.12 Slightly increase of the 5-year relative survival in patients with MM in Australia (from 1984-1988 to 2009-2013). The relative 5-year survival after diagnosis increased to 48.5% during 2009-2013. Sourced from Australian Institute of Health and Welfare (AIHW) 2017, Cancer in Australia 2017.

1.5.2 Pathology

The end-organ symptoms of MM are consequences of the expansion of the malignant plasma cells and the accumulation of a homogeneous immunoglobulin product, known as paraprotein or M protein, secreted by the malignant plasma cells. Patients with myeloma are often diagnosed upon presentation with bone pain and pathological fractures. This bone destruction is caused by the uncontrolled proliferation of the malignant plasma cells inside the BM, disruption of the normal BMM, and cytokine induced enhancement of normal osteoclast activity. The erosion of the bone structure results in the release of large amounts of calcium that subsequently causes hypercalcaemia. The accumulation of the malignant plasma cells can impair the normal white blood cell immune functions and interfere with the normal development of red blood cells, leading to immune deficiency as evidenced by hypogammaglobulinaemia and anaemia respectively. The accumulation and deposition in tissues of the paraprotein can cause multiple end-organ damage such as impaired renal function and ultimately renal failure [242].

MM develops from various preclinical stages (**Figure 1.13**). The initial condition is MGUS. MGUS patients present with a low level of paraprotein (< 30 g/L) and a low proportion of plasma cells in the BM (< 10%), but without organ impairment. The normal range of the plasma cells in the BM of healthy people is 0.4-3.9% with an average of 1.5%. MGUS is present in 3-4% of the general Caucasian population over 50 years old and has an average risk of 1% per year of progression to MM [243-246]. Smouldering myeloma (SMM), also known as asymptomatic myeloma, is an intermediate stage between MGUS and symptomatic MM. People diagnosed with SMM have higher levels of paraprotein (30 ≥ g/L) and a higher proportion of plasma cells (10-60%) in the BM than people with MGUS but without any end-organ damage symptoms [243-245]. The overall risk of progression to symptomatic MM from SMM is higher which is 73% at 15 years diagnosis (calculated as cumulative probability to progression) [247]. SMM has a heterogeneous profile. The two main high-risk factors for progression from SMM to symptomatic myeloma are a high proportion of BM plasma cells and a high serum monoclonal protein level at initial diagnosis [247]. The International Myeloma Working Group (IMWG) has updated the definition and diagnosis for MM to include some high-risk subgroups of the previous SMM with

clonal bone marrow plasma cells (BMPCs) ⩾60%, or serum free light chain (FLC) ratio ⩾100 (plus measurable involved FLC level ⩾100 mg/L), or more than one focal lesion on an MRI scan (each focal lesion size must be ≥ 5 mm). These indications are now considered as early-stage MM, and early interventions are suggested [248].

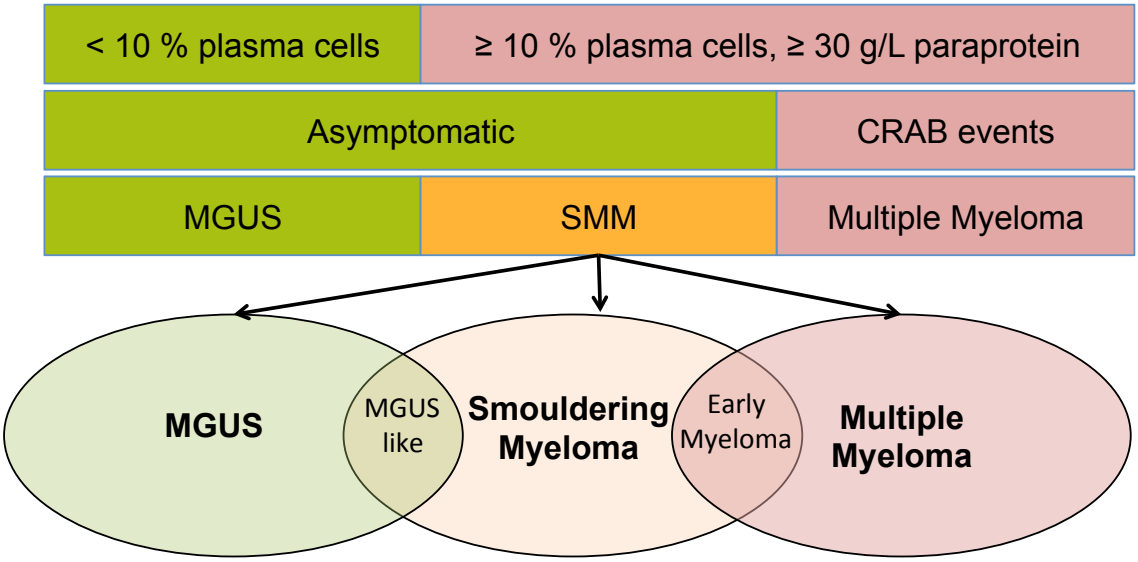

Figure 1.13 Clinical features of MGUS, SMM and MM. MM and SMM both have ⩾ 10% clonal bone marrow plasma cells and/or ⩾30 g/L of paraprotein. Similar to MGUS, SMM is characterized by an absence of end-organ damage-defining CRAB events (hypercalcemia, renal impairment, anemia or bone lesions). Illustration modified from Bhutani et al. [249].

1.5.3 Pathogenesis

The development of myeloma is a multiple-step process that requires accumulation of genome alterations in the neoplastic plasma cell clone, and changes in the BMM that facilitate the clone's expansion.

1.5.3.1 Aberrant gene mutations

The normal counterparts of the malignant plasma cells (myeloma cells) are the terminally differentiated B cells, which are known as the plasma cells or antibody-producing B cells. The molecular basis underlying the initiation of myeloma is mainly due to the normal biological functions of the B cells. B cells acquire the ability to produce specific immunoglobulin (Ig) through multiple rounds of somatic hypermutation, rearrangement of the Ig genes, and class switch recombination. B cells

become activated when in contact with antigens, otherwise, these B cells normally arrest in the G0/G1 phase of the cell cycle as long-lived plasma cells in the BM or as memory B-cells in the lymph nodes until the next antigen stimulation. The genetic events needed for B cell development into plasma cells require DNA double strand breaks which can result in aberrant chromosomal translocations, some of which could lead to oncogene activation and tumour suppressors mutations [250, 251].

The progression to MM requires the accumulation of aberrant gene mutations. The primary early genetic abnormalities initiated in myeloma development are defined as the immunoglobulin heavy chain translocations, which are shared by MM and MGUS. In addition to the primary early gene mutations, the secondary late-onset gene mutations promote further myeloma progression from MGUS to MM. Complex chromosomal abnormalities generated by abnormal class switch recombination can result in the activation of oncogenes such as *MYC* and fibroblast growth factor receptor 3 (*FGFR3*) [252], loss of expression or mutation in tumour suppressor *p53*, and the inactivation of cyclin-dependent kinase inhibitors. These abnormalities are normally found in MM but rarely in MGUS.

Certain chromosomal abnormalities such as t(4;14), t(14;16), t(14;20), chromosome 13 deletion, chromosome 1 abnormalities and 17p13 deletion are associated with poor prognosis and resistance to therapy [253-256]. The t(14;16), t(14;20) chromosome abnormalities are associated with increased oncogene *c-MAF* expression and indicate poor prognosis in MM but not in MGUS [257]. The high expression of MAF protein in myeloma due to t(14;16), t(14;20) translocation confers innate resistance to proteasome inhibitor (bortezomib) [258]. The t(4;14) translocation occurs frequently in MM and results in the simultaneous deregulated expression of two oncogenes, *FGFR3* and multiple myeloma SET domain protein/Wolf-Hirschhorn syndrome candidate gene 1 [252]. Deletions of 17p13, the genomic locus of the tumour suppressor gene *p53*, have been associated with a poor patient outcome [259]. Other genetic abnormalities involve epigenetic dysregulation and copy number abnormalities. Chromosomal abnormalities are present in 20-60% of newly diagnosed MM patients and in 60-70% of patients with progressive disease, indicating their importance in the pathogenesis of the disease [242]. This feature of dynamic gene mutations and chromosomes abnormalities makes MM

patients vulnerable to disease progression and prone to disease relapse, as patients easily present innate and develop acquired drug resistance [260, 261].

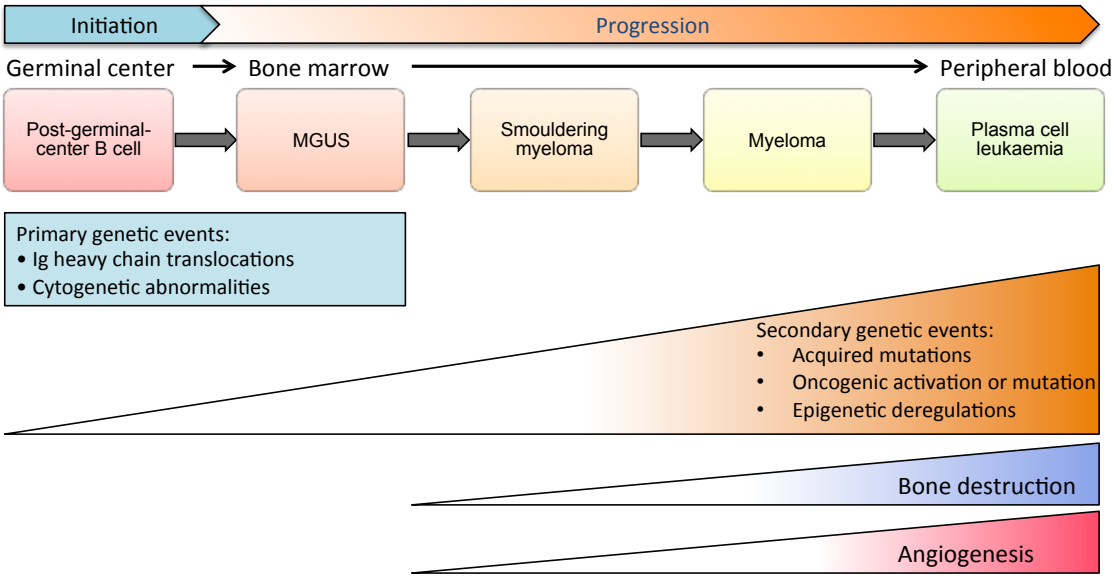

Figure 1.14 The pathogenesis of multiple myeloma. The progression of MM requires the accumulation of gene mutations and chromosomal abnormalities. Primary early mutation of the late stage matured B cells initiate the MM disease. The secondary accumulation of further gene abnormalities drives further disease progression. In rare cases, MM cells can also metastasise from the bone marrow into the blood stream causing plasma cell leukaemia. Illustration modified from Morgan et al. [251].

1.5.3.2 Bone marrow microenvironment and pathogenesis

Besides genetic mutations of myeloma cells, the hallmarks of MM progression include abnormal interactions between myeloma cells and the BMM, as well as aberrant angiogenesis [262]. BM is the semi-solid, spongy, gelatinous compartmentalized tissue found in the hollow spaces within the interior of bones. It is the major haematopoietic organ and a primary lymphoid tissue. BM consists of haematopoietic tissue and the associated supporting stroma. The BM haematopoietic tissue contains haematopoietic stem cells (HSCs), which can differentiate into precursors of all types of blood cells, erythrocytes, granulocytes, monocytes, lymphocytes and platelets [263]. The mesenchymal stem cells of the stroma can differentiate into a variety of supportive cells, such as osteoblasts, osteoclasts, chondrocytes, myocytes, fibroblasts, macrophages,

adipocytes, and endothelial cells [264-268]. Myeloma cells can manipulate and hijack this BM microenvironment for their own survival and progression.

Genetic abnormalities can alter the expression of adhesion molecules such as vascular-cell adhesion molecule 1 (VCAM1), intercellular adhesion molecule-1 (ICAM- 1), and integrin alpha 4 (VLA-4) on myeloma cell surfaces. The adhesion of myeloma cells to hematopoietic and stromal cells induces the production of cytokines and growth factors that are produced and secreted by cells in the BM microenvironment, such as interleukin-6 (IL-6), vascular endothelial growth factor (VEGF), insulin like growth factor 1, tumour necrosis factor, transforming growth factor β1, and interleukin-10, which stimulates myeloma cells growth, survival, migration, and angiogenesis [269-271]. The adhesion of myeloma cells to extracellular matrix proteins (e.g. collagen, fibronectin, laminin, and vitronectin) triggers the upregulation of cell-cycle regulatory proteins and anti-apoptotic proteins [262].

The approximate levels of oxygen found in normal tissues are lower than the 20% oxygen level in the air (normoxia), which averages at about 5% oxygen (ranging from 3-7.4%). Most untreated cancers are hypoxic with median oxygen levels around 2% (approximately ranging from 0.3-4.2%) [272]. The normal BM is hypoxic, but a study has shown that the myeloma-infiltrated BM has decreased hypoxia indicating that myeloma-associated angiogenesis is functional [273]. Despite high vascular density in MM, the absolute BM oxygen level is still low, ranging from 1.5-4.2% oxygen with 2.7% on average [274]. Using pimonidazole hydrochloride as a nontoxic hypoxia marker, the BM HSCs niche is hypoxic (1.3% O_2) and the pimonidazole hydrochloride staining pattern correlates with that of the HIF-1α protein [275]. These hypoxic niches inside the BM harbour quiescent HSCs and are critical for HSCs self-renewal, maintenance and function [268]. The disruption of the niches can affect the normal differentiation process and could potentially lead to myeloma malignancy [268].

The hypoxic BM environment offers a favourable environment for the development and survival of haematological malignancies such as MM. Under BM hypoxic conditions, the glycolytic phenotype can be enhanced via HIF-dependent transcription activities thus providing critical advantages for cell survival under hypoxia [27, 34, 48, 276]. Strong HIF-2α expression was seen in myeloma cells (surface marker: CD 138^+) but not

in MGUS cells from BM biopsy samples, indicating that up-regulated HIF-2α expression may be correlated with the malignant status of MM cells [277]. The up-regulated expression of HIFs in MM can promote angiogenesis and thus provide a beneficial microenvironment for MM cells evolving. Strong HIFs expression correlated with high vascular density and VEGF up-regulation in BM samples from 106 MM patients. High vascular density in 37 MM patients showed a significantly worse prognosis [278]. Reviewed by Irigoyen et al., hypoxia and HIF-mediated signalling pathways promote haematological tumour progression and relapse; and the inhibition of HIF can be explored as a treatment approach [279].

In solid tumours, cancer cells in regions with restricted supply of nutrients and oxygen would rely on different metabolic pathways such as glycolysis to support their growth [25, 280]. Similar to that of the solid tumour, different vasculature perfusions and complicated structure in the BM result in the malignant cells having only varied access to nutrients and oxygen, and therefor the malignant cells in the BM also presents with metabolic heterogeneity to ensure survival. A metabolomics study has indeed shown that biopsy specimens of osteolytic lesions display heterogeneous metabolism profiles from pathological fracture sites caused by MM [281].

To summarize, MM cells originate from and reside inside the BM before developing into circulating MM cells. The hypoxic BM microenvironment and the different types of supportive cells that coexist inside the niches provide ideal growth conditions to harbour MM cells, promote their growth and metastasis, and to assist resistance to chemotherapies by a complex network of cytokines, chemokines, adhesion molecules, proteolytic enzymes and other components of the extracellular matrix [262, 265, 266, 282]. The BM microenvironment is heterogeneous in structure, physiology, and metabolism. This complicated environment offers advantages for myeloma cell progression and survival. Treatment of MM should take this complicated microenvironment into consideration. Some novel agents used in the MM treatment can target the interaction between myeloma cells and stroma, such as the proteasome inhibitor and immunomodulatory drugs. There is metabolism context in the pathogenesis of MM in the BM microenvironment. Manipulating the metabolic phenotypes should be investigated as a possible approach to myeloma therapy.

1.5.4 Treatment

1.5.4.1 Treatment guidelines

Current consensus treatments in Australia are based on the clinical practice guideline for MM established by the Australian Medical Scientific Advisory Group. The current standard of care is monitoring and observation for MGUS patients and SMM. However, a randomized clinical trial showed early intervention using LEN and DEX improved overall survival in high-risk SMM compared to no-intervention observation group [283].

The focus of this thesis is the treatment of symptomatic/active MM. The commonly used novel agents in MM treatment include immunomodulatory drugs (thalidomide, lenalidomide (LEN), Pomalidomide), and proteasome inhibitor (bortezomib). Other backbone chemotherapy agents such as the alkylating agents (e.g. cyclophosphamide, melphalan), and glucocorticoids (e.g. dexamethasone (DEX)) are commonly used in combination with the novel agents in the induction therapy for newly diagnosed patients, maintenance therapy, and salvage therapies for relapsed patients.

Currently, the standard treatments for patients with symptomatic MM depend on their eligibility for autologous stem cell transplant (ASCT), which in turn depends on patients' age, comorbidities, and performance status. Patients eligible for transplant will be treated with 3-6 cycles of initial induction therapy (e.g. CyBorD: bortezomib+ cyclophosphamide+DEX), followed by the ASCT. Maintenance therapy such as thalidomide with or without glucocorticoids may be recommended for patients, depending on patients' response to ASCT and their comorbidities. For ASCT non-eligible patients, the induction therapy will be different, for example, BCD (bortezomib+cyclophosphamide+DEX), CTD (cyclophosphamide+thalidomide+DEX). The purposes of induction therapy are to bring a rapid reduction of tumour burden and reversal of disease related complications, thus preparing patients to proceed to transplant without antecedent toxicities. For relapsed/refractory patients, salvage treatment regimens are given to patients including a novel agent with other backbone chemotherapy agents in combinations, such as CTD, CyBortD, TD (thalidomide+DEX), and RD (LEN+DEX) [284].

New treatments are becoming available in Australia as the result of advancements in medical research. The up-to-date clinical practice guideline for myeloma in Australia (2017) listed new drugs that have been approved for the treatment of relapsed/refractory MM by the FDA; but they are not yet reimbursed by the Pharmaceutical Benefits Scheme (PBS) for the treatment of MM in Australia. These new drugs include the second-generation proteasome inhibitor ixazomib, the monoclonal antibodies daratumumab and elotuzumab, and the histone deacetylase inhibitor panabinostat. Some novel immune therapies are in the early phase of developments include of chimeric antigen receptors (CAR-T) and bispecific T cell engagers (BiTEs) [284]. The treatment choices available for MM patients will depend upon what country they are in and their country's health care scheme. For example, in Australia, LEN is not reimbursed as induction therapy for transplant eligible patients, but is reimbursed when used in non-responsive patients after one prior therapy or in patients who are not eligible for ASCT.

1.5.4.2 MM chemotherapy drugs

Glucocorticoid: dexamethasone

As a backbone agent of the MM therapy, Dexamethasone (DEX) is often used in combination with novel agents and other chemotherapy agents. DEX belongs to the family of glucocorticoids (GCs) involved in the regulation of a wide range of biological functions, such as immune responses, glucose and fatty acid metabolism, cell growth and proliferation. DEX has strong anti-proliferative effects, can induce apoptosis, and has been used in the treatment of many haematological malignancies including MM [285-287]. High doses of DEX are normally used in combination with novel agents such as lenalidomide, thalidomide, and bortezomib, and lead to significant anti-proliferative and pro-apoptosis effects in MM [287, 288]; however, DEX resistance is common [285].

DEX-induced apoptosis is mediated through a specific cytoplasmic glucocorticoid receptor (GR) which can mediate the receptor functions of hormone binding, nuclear translocation, DNA binding and transcriptional modulation. Thus, the binding of DEX to GR induces the activation or repression of a network of glucocorticoid responsive genes and produces a specific cellular response. DEX can reduce MM cell survival by inhibiting IL6 and NF-kB (nuclear factor kappa-light-chain-enhancer of activated B

cells) pathways, which contribute to MM cell survival and proliferation [289, 290]. DEX treatment of MM also triggers mitochondria to release Smac (a mitochondria-derived activator of caspases) into the cytosol which activates caspase-9 leading to apoptosis [291]. Chronic exposure to GCs ultimately leads to the development of resistance; as the binding affinity to GR is weakened, the GR mRNA expression is reduced or truncated and the GR protein is reduced in the resistant MM cell line [285, 289]. DEX treatment can change glucose metabolism and increase fatty acid synthesis, [292], and the altered metabolism also assists with drug resistance. Given the important position of DEX in the treatment of MM, more studies are needed to focus on how to overcome the resistance to DEX in MM treatment; for example, manipulation of the metabolic phenotype associated with DEX resistance could be a treatment option.

Immunomodulatory drugs: thalidomide & lenalidomide

Immunomodulatory drugs are a type of novel agent that are routinely used in induction and maintenance therapies for both newly diagnosed and relapsed or refractory MM patients. Thalidomide is the first of the immunomodulatory drugs used for MM treatment, and it is used in Australia as an upfront treatment option. The thalidomide-based treatment regimens, such as CTD, are among the effective treatment options for induction therapy in transplant ineligible patients; however, the toxic side effects such as venous thromboembolism and peripheral neuropathy are common. The thalidomide can cause sedation and cognition impairment on patients which can limit its use as a maintenance therapy [284]. Lenalidomide (LEN) is a second generation of immunomodulatory drug (an analogue of thalidomide) with different side effects to thalidomide. In Australia, LEN is either used as mono-therapy or in combination with glucocorticoids for MM patients who are progressing after at least one prior therapy, have experienced thalidomide-based treatment failure, and who are ineligible for a primary stem cell transplant [284].

The immunomodulatory drugs thalidomide and LEN have similar mechanisms of actions against cancer, such as modulating the immune system, interfering with BM stromal cell growth factors, anti-angiogenesis activity and direct anti-tumour activities. The anti-myeloma effects of thalidomide and LEN can be summarized: inhibition of adhesion of myeloma cells to the BM stroma by decreasing cell surface adhesion

molecules (e.g. ICAM1, VCAM1); inhibition of cytokines and growth factors production in the BM (e.g. IL-6, VEGF, TNF-α); inhibition of angiogenesis; stimulation of T cell cytotoxicity and host natural killer (NK) cell immune activities against myeloma; and direct apoptotic effects on myeloma cells [293-295]. Recently cereblon (CRBN) was identified as a direct binding target of immunomodulatory drugs. In normal tissue, CRBN is a 442-amino acid protein with multiple functions that locates in the cytoplasm, nucleus, and peripheral membrane of the human brain and other tissues [296]. Down regulation of CRBN is strongly associated with resistance to LEN in human myeloma cell lines, and CRBN levels correlate with patients' response to LEN [297].

LEN has similar immunomodulatory and anti-cancer effects to thalidomide, but has more potency in its direct apoptotic effects against myeloma cells, as well as in its inhibition of inflammatory cytokine production and stimulation of T cells and NK cells, furthermore, LEN has a different toxicity profile compared to thalidomide [295]. Beside the teratogenic effects, thalidomide has many adverse effects, such as sedation and drowsiness, constipation, subclinical hypothyroidism, peripheral neuropathy and venous thromboembolism. LEN does not cause sedation or constipation, and the incidence of neuropathy is lower than with thalidomide; but LEN has a more myelosuppressive effect than thalidomide [298]. LEN therapy was reported to have equal, if not better, outcomes than thalidomide therapy according to different clinical trials and population cohort analysis. A comparison of LEN+DEX and thalidomide+DEX in newly diagnosed MM patients found that patients on LEN+DEX had longer remission time, longer progression-free survival and overall survival, than patients who received thalidomide+DEX therapy [299]. A retrospective observational cohort study compared the survival and rates of peripheral neuropathy in MM patients who were new users of either thalidomide or LEN showed that there were no significant differences in overall survival outcomes, but LEN therapy was associated with less neurotoxicity in MM patients [300].

LEN is commonly used in combination with DEX; LEN and DEX act synergistically to inhibit cell proliferation and induce apoptosis in MM cells. LEN and DEX combination therapy has been approved for MM patients who have relapsed after initial therapy. In a

phase III clinical trials, the combination improved patients' response, prolonged their remission and overall survival [301]. Two phase III clinical trials in relapsed/refractory MM patients (not resistant to DEX) showed that the combination of LEN and DEX resulted in a significant improvement in overall response and gave longer remission time compared to DEX treatment alone [302]. Moreover, the combination of LEN and DEX is shown to be effective as a first-line treatment option for newly diagnosed MM patients in several clinical trials [303, 304], and in 2015, the FDA approved the combination of LEN and DEX to treat patients with newly diagnosed MM in the USA.

Despite the evidence showing thalidomide and LEN's abilities to inhibit MM, the patients eventually develop drug resistance and relapse. The resistance to LEN is common, with approximately 40% of MM cell lines found to be resistant to LEN treatment [305]. When used as single agents, MM patients taking thalidomide or LEN have only a 30% or 47% overall response rates respectively [306, 307]; the overall response rates were improved when used in combination with DEX or cyclophosphamide, yet invariably all patients develop drug resistance and relapse [307-309]. More studies are needed before we can understand how to overcome the development of resistance to immunomodulatory drugs in cancer cells.

Proteasome inhibitor: bortezomib

Bortezomib is the first proteasome inhibitor being approved for clinical use by the FDA. The proteasome is a proteolytic complex for intracellular degradation of ubiquitinated proteins that are involved in cell-cycle regulation, apoptosis, transcription, DNA repair, protein quality control and antigen presentation. More than 80% of cellular proteins are degraded through this ubiquitin proteasome pathway [310]. Cancer cells are highly proliferative compared to normal cells and their rate of protein translation and degradation is also higher. The blockade of protein degradation through proteasome pathways leads to accumulation of unwanted proteins and thus activates the caspases and the endoplasmic reticulum stress pathways that induce cell death [311, 312]. MM patients have elevated circulating serum proteasome (the 20S complex) compared to MGUS and healthy people, correlating with advanced disease, and thus this can be used as an independent prognostic factor in MM [313].

Bortezomib has been extensively studied either as a single agent or in combination with glucocorticoids, cytotoxic agents, immunomodulatory drugs and radiation as treatment options for MM and other haematological malignancies. It has ben found to have efficacy in haematological cancers including MM but not in solid tumours. Bortezomib proved to be potent against MM as demonstrated in several clinical trials [314-317]. While bortezomib exhibits activity as a single agent, it can overcome chemotherapy resistance and induce sensitivity to a variety of commonly used chemotherapeutic agents [318-321]. Despite good clinical results of initial treatment, many patients acquired resistance to bortezomib and eventually relapse. The mechanism underlying resistance to bortezomib could be due to impaired binding of the drug, adaptation to the disruptions of proteasomal pathways [322]. The altered metabolic pathways also have been found to contribute to the bortezomib resistance. A study showed that the altered glucose metabolism of MM cells, which resulted in higher activity of both the PPP and serine synthesis pathway, contributing to bortezomib resistance; and an enhanced cytotoxicity of bortezomib was achieved by limiting the serine access to MM cells [323]. Targeting the glycolytic phenotype can be further studied in reversing bortezomib resistance in future studies.

1.5.5 Chemotherapy resistance and correlation to glycolytic phenotype

Despite the use of novel agents such as proteasome inhibitors and immunomodulatory drugs, myeloma therapies are generally unsatisfactory, following a pattern of regression and remission, and ultimately ending in treatment failure. The various gene mutations make MM patients either present with innate, or develop, acquired drug resistance [260, 261].

There is growing evidence to show that an altered cancer metabolic phenotype is associated with drug resistance in cancer treatment via different mechanisms such as expanded cellular growth, activated export of chemotherapy drugs by the ATP-binding cassette transporters, and an acidified microenvironment for the cancer cells resulting in decreased passive transport of basic drugs. Furthermore, signalling pathways activated by dysregulated metabolism contribute to drug resistance by repressing pro-apoptotic signalling pathways and activating compensatory oncogene pathways [227].

More studies have indicated that resistance to chemotherapy in cancer is associated with altered metabolism, and that the glycolytic phenotype is one of the contributing factors. The increased glycolysis ratio has been associated with drug resistance in leukaemia and myeloma, and studies have shown that resistance to glucocorticoids, bortezomib and melphalan can be overcome by manipulation of glycolysis [11, 125, 324, 325]. Further, the combination of DCA and bortezomib showed additive cytotoxic effects in MM cell lines and improved outcomes in a myeloma-bearing mouse model [11]. This suggests that targeting the glycolytic phenotype in cancer cells can potentially overcome the drug resistance.

1.5.6 Target glycolytic phenotype in MM

Both myeloma cells from myeloma patients and human myeloma cell lines present with a glycolytic phenotype, thus it is feasible to target the glycolytic phenotype in MM. Based on the analysis of the gene expression data available from NIH, the glycolysis related genes (such as *HK, GPI, PFKL, GADPH, LDHA, GLUT1*) are overexpressed in cancers such as lymphoma and MM [2]. The expression of glycolysis-related genes such as *LDHA*, *PDK1*, and oncogene *MYC* was significantly higher in plasma cells collected from BM samples of 59 MM patients than that from 13 MGUS patients [12]. Analysis of MM cell lines showed a heterogeneous pattern of the glycolysis-related gene expression; where 4 of the 6 evaluated cell lines demonstrated a strong glycolytic phenotype, which was confirmed by the lactate production levels, glucose consumption levels, and LDHA mRNA expression and LDHA enzyme activities [12]. In another study, 3 of the 6 MM cell lines display a glycolytic phenotype [11]. The presence of the glycolytic phenotype in MM offers multiple potential therapeutic targets.

LDHA is an enzyme that can convert pyruvate into lactate. Many malignant tumours express higher LDHA levels compared to normal tissues [122]. LDHA can promote cancer cell growth and metastasis and it is an indicator of poor prognosis in various cancer types [12, 123-125]. Patients' LDHA serum levels positively correlate with the mRNA expression levels in myeloma cells isolated from patients. Higher levels of LDHA are associated with poor prognosis in MM patients [12]. Lactate used to be considered as a waste product of the glycolytic phenotype, but recent evidence showed that lactate can act as an important source of carbon for MM. Inhibition of LDHA by

oxamate (compete with pyruvate for the binding site on the enzyme) has been shown to reduce lactate production induced apoptosis in a dose-dependent manner in MM cell lines [12].

Myeloma cells and normal plasma cells isolated from MM patient BM constitutively express HIF even under normoxic conditions, while the normal peripheral blood mononuclear cells (PBMCs) did not express HIF [39, 326]. Suppression of HIF-1α with EZN2968, an antisense oligodeoxynucleotide that specifically targets HIF-1α, reduced MM cell viability by inducing cell cycle arrest and diverting myeloma cells towards mitochondrial respiration [326]. In preclinical studies, the inhibition of HIF-1 function either by HIF-1 inhibitor (echinomycin), or siRNA knockdown, enhanced sensitivity to melphalan in MM cells [39]. Down-regulation of HIF-1α expression has been reported to sensitize MM cells to LEN, and to significantly increase the anti-tumour effect of LEN in a xenograft MM mouse model [327, 328].

MM cells have elevated glucose uptake activity as a result of GLUT upregulation. MM cell lines and the primary myeloma cells overexpress various GLUTs (GLUT 1, 4, 8, 11) of the glucose transporter family because the GLUT overexpression is required for MM cell growth [111, 329]. High risk MM with poor prognosis is associated with high intensity of the ^{18}F-FDG-PET scan (reflects the glucose uptake rate) [330, 331]. Inhibition of GLUT can suppress the glucose uptake activity and induce apoptosis in myeloma cells while not showing cytotoxicity in normal PBMCs. Inhibition of GLUT could also synergistically enhance myeloma cell death induced by melphalan, doxorubicin, and bortezomib [111, 329].

1.5.7 DCA as a novel agent in MM treatment

MM displays a glycolytic phenotype, and it is feasible to be manipulated using glycolysis inhibitors as a novel therapy. As a metabolic modulatory drug, there are multiple advantages to repurpose DCA as an anti-cancer drug for clinical use. Firstly, DCA has been studied comprehensively in humans and it has been used to treat acidosis and mitochondrial malfunction in humans for decades; secondly, DCA has low toxicity compared to most chemotherapy agents; and thirdly, DCA is an inexpensive, small molecule that can be easily absorbed by patients (section 1.4).

There are two studies describing the effects of DCA on MM cell lines and MM patients' plasma cells [11, 12]. DCA, as a PDK1 inhibitor, could serve as a novel therapeutic drug as PDK1 is overexpressed in myeloma cells from MM patients, DCA (10-40 mM) induced apoptosis in MM cell lines by stimulating ROS production and the caspase cascade. DCA (40 mM) selectively induced apoptosis in patients' myeloma cells but did not have any cytotoxicity to the PBMCs from MM patients. The combination of DCA (40 mM) with bortezomib (4 nM) had greater effect in inducing apoptosis on MM cell line [12]. Furthermore, studies showed that DCA at lower (5-10 mM) could suppress anaerobic glycolysis and improve cellular respiration that associated with activation of the PDC, meanwhile higher concentrations of DCA (10-25 mM) could induce apoptosis and suppress proliferation in MM cell lines. DCA can re-sensitize bortezomib resistant MM cell line, and the DCA and bortezomib combined treatment improved the survival of myeloma-bearing mice [11]. To summarize, DCA at high concentrations was demonstrated to have anti-proliferation and cytotoxic effects on MM cells. However, the concentrations of DCA used in these published *in vitro* studies were approximately 10-50 times higher than what can be achieved in patients, thus the anti-cancer effects of DCA observed might not be due to its on-target effects. There is also lack of clinically relevant information regarding the use of DCA in MM patients.

1.6 Hypothesis and Aims

Hypothesis

We hypothesize that by inhibition of PDKs, DCA can reverse the glycolytic phenotype of multiple myeloma cells and result in biochemical and gene expression changes that can inhibit myeloma cell proliferation and thus can be used as a low toxicity addition to myeloma chemotherapy.

To examine this hypothesis, this thesis has addressed the following aims:

Aims

Aim 1: Determine the effects of DCA on human MM cell lines (**Chapter 2**).

This study will determine the effect of DCA on representative human MM cell lines and confirm the on-target effects of DCA. It will also examine key factors contributing to different sensitivities to DCA in MM cell lines.

Aim 2: Determine the impact of stress conditions that mimic the bone marrow microenvironment on the effects of DCA (**Chapter 3**).

This study will determine the effect of nutrient (glucose, glutamine) deprivation conditions or hypoxia on the effects of DCA on MM cell lines to shed light on if there is potential for DCA to be effective in heterogeneous *in vivo* MM microenvironments.

Aim 3: Determine the effects of DCA combined with chemotherapy drugs (**Chapter 4**).

This study will determine if DCA can enhance the effects of MM drugs in MM cell lines.

Aim 4: Determine the effects of DCA in MM patients at plateau phase in a phase-2 clinical trial (**Chapter 4**).

This study will determine if the proposed DCA dosing regimen achieves and maintains the desired drug levels in the clinical trial and correlate DCA pharmacokinetics with *GSTZ1* genotype. The patient response to DCA treatment will be analysed and correlated with DCA serum levels.

Chapter 2

Anti-cancer activities and metabolic modulatory effects of DCA in MM cells

Abstract

Background: MM is a B-cell malignancy that displays a glycolytic phenotype. DCA is a PDK inhibitor that can reverse the glycolytic phenotype and has potential to be utilized in MM treatment. Previous *in vitro* and *in vivo* studies have shown the cytotoxic effects of using high-dose DCA (>10 mM) in MM, but evidence is needed of on-target effects and anti-cancer effects when used at clinically achievable concentrations. **Methods:** The effects of DCA (≤ 5 mM) on MM cell growth at concentrations in the range of the inhibitory constants (K_i) for the targets of DCA (PDKs) were tested in MM cell lines by measuring total viable cell number (neutral red uptake assay), proliferation (CFSE staining), apoptosis (Annexin V/7AAD) and cell cycle distribution (BrdU/PI). The effects of DCA on extracellular lactate and glucose levels were measured by lactate or glucose meters. The metabolic phenotypes of MM cells and the modulatory effects of DCA on glycolysis and mitochondrial respiration were measured by Seahorse XF analyser. The on-target effects of DCA on pPDH, at clinically achievable concentrations, were measured by western blot. MM cell expression of the targets of DCA (PDKs) was measured by western blot. **Results:** DCA at clinically relevant concentrations inhibited MM cell growth and proliferation without inducing apoptosis, and was accompanied by inhibition of glycolysis in the glycolytic cell lines. DCA acts on-target by reducing the levels of the inactive, phosphorylated form of PDH (pPDH) even when used at lower, clinically achievable concentrations, and these effects were cumulative over time. **Conclusions:** DCA had a cytostatic effect when used at mechanistically relevant concentrations. DCA acted on-target when used at clinically relevant concentrations in MM cell lines, but this did not always directly correlate with its cytostatic effects.

2.1 Introduction

Multiple myeloma (MM) is an incurable B-cell malignancy with unsatisfactory conventional therapies, and new treatments are needed. MM presents with a glycolytic phenotype, which can be used as a potential target. About half of MM cell lines present with a glycolytic phenotype [11]. The malignant plasma cells of MM patients also have a glycolytic phenotype where genes associated with glycolysis, such as *PDK1*, *LDHA*, and oncogene *MYC*, are upregulated compared to the pre-myeloma condition known as monoclonal gammopathy of undetermined significance (MGUS) [12]. MM patients have complex cytogenetic abnormalities [262] and targeting the glycolytic phenotype of myeloma could bypass these complexities and inhibit MM growth by disrupting the downstream metabolic changes. Dichloroacetate (DCA) is a pyruvate dehydrogenase (PDH) kinase (PDK) inhibitor that can reverse the glycolytic phenotype by diverting the pyruvate flow from being transformed to lactate into mitochondrial respiration. DCA has anti-cancer effects in various human cancer types *in vitro* and *in vivo* such as breast, prostate, lung, cervical, and brain cancer [222]. Our laboratory showed that DCA can inhibit breast tumour growth and that it caused a 58% reduction in the number of lung metastases in a rat model [10]. DCA at high doses (≥ 10 mM) induced apoptosis in MM; however, these doses used were much higher than the inhibitory constant (K_i) (concentration of DCA needed to reduce half of the targeted PDK enzyme activity) and thus these observed anti-cancer effects may not be due to the on-target effects of DCA [11, 12]. The four isoforms of PDKs have different K_i values for inhibition by DCA, ranging from the most sensitive PDK2 (K_i: 0.2 mM), to the least sensitive PDK3 (K_i: 8 mM), with PDK1 (K_i: 1 mM) and PDK4 (K_i: 0.5 mM) in between [4]. In the *in vitro* studies presented in this thesis, DCA was used in the range of the K_i values, which were defined as the mechanistically relevant concentrations. Clinically achievable concentrations in cancer patients (taking 6.25 mg/kg, *b.i.d.*) have been reported in the range of 0.05-0.7 mM [235]. It is yet unknown whether the clinically achievable concentrations of DCA are sufficient to inhibit all of the PDK targets of DCA in patients.

We hypothesize that DCA, at clinically achievable concentrations, acts on-target and inhibits MM cell growth. This study aimed to analyse the effects of DCA on MM cell lines and investigate the on-target effects of DCA when used at mechanistically relevant

concentrations. This study also identified metabolism-related factors that could be contributing to the different sensitivities of MM cells to DCA treatment.

2.2 Material & Methods

2.2.1 Cell culture

Three independent human MM cell lines, RPMI 8226, U266, NCI-H929, and two isogenic human MM cell lines (MM.1S (dexamethasone sensitive) and MM.1R (dexamethasone resistant)) were purchased from American Type Culture Collection (ATCC). The basic characteristics of these cell lines are summarised in **Table 2.1**.

Table 2.1 Characteristics of MM cell lines

Cell Lines	Represented Disease	Biogenetics Characteristics [332-334]
RPMI8226	Ig G/ λ MM	14q+, 22q-
U266	Ig E/ λ MM	Deletion of 13 and 17p, p53 mutant
MM.1S	Ig A/ λ MM	t(14;16), glucocorticoid receptor(GR) expressed; p53 wild type
MM.1R	Ig A/ λ MM	t(14;16), GR not expressed, p53 wild type
NCI-H929	Ig A/ κ MM	del(1)(p11p25), del(9)(p13), del(12)(p12); p53 wide type

MM.1S, MM.1R and RPMI 8226 were cultured in RPMI-1640 media (31800, Thermo Fisher) recommended by ATCC at 37°C in a humidified 5% CO_2 atmosphere. The complete RPMI-1640 media was supplemented with 10% or 15% (volume/volume) heat-inactivated fetal bovine serum (FBS), 2 mM L-glutamine, 10 mM HEPES, 1 mM sodium pyruvate and 100 μg/ml antibiotics (penicillin and streptomycin). The glucose concentration in the RPMI-1640 media is ~11.11 mM (full formula in appendix). U266 was cultured in the complete RPMI-1640 media supplemented 15 % FBS. NCI-H929 was cultured in the complete RPMI-1640 media supplemented with 10 % FBS with additional supplementation of 2-mercaptoethanol (2-ME) to a final concentration of 0.05 mM. The cell culture media was replaced by centrifugation (Eppendorf, 5810R) and cells were passaged twice a week. Cells were maintained at concentrations between 5×10^5 and 1×10^6 viable cells per ml. The number of viable cells in suspension was determined using Countess II FL Automated Cell Counter (Life technologies, USA).

Cells ranging in sizes from 5 μm to 60 μm were counted, and 0.2% trypan blue dye was used to distinguish viable cells from dead cells.

2.2.2 DCA preparation

DCA (99% pure, Sigma) was diluted in 1× phosphate-buffered saline (PBS) to produce a stock solution of 100 mM and adjusted to pH 7.4. The stock solution was stored for long-term at 4°C and was stable. DCA was diluted in assay media on the day of use and the vehicle (PBS) was diluted to less than 5% of the total volume per well.

The half maximal effective concentration (EC_{50}) of DCA was calculated by fitting a nonlinear regression dose-response curve using GraphPad Prism's (version 6.0f) dose-response equations. EC_{50} in this thesis refers to the concentration of a drug that induces a response halfway between the baseline and maximum after a specific exposure time.

2.2.3 *In vitro* viability assay

Neutral red staining was used to quantitatively estimate the total number of viable cells after treatment in culture. It is based on the ability of viable cells to incorporate and bind the supravital dye neutral red in the lysosomes [335]. Cells were seeded in 96-well round bottom plates at densities of 25,000-50,000 cells per well. Cell densities were optimized through serial dilutions to ensure reliable neutral red measurements. Drug treatments were performed after a randomized choice of well position in plates (quadruplicate wells per treatment). After treatment for the desired period, the plates were centrifuged at 520 ×g for 5 minutes, and the media was flicked away swiftly and the cells were incubated for 3 hours in media containing neutral red (33 μg/mL). Cells were spun down (520 ×g, 5 minutes) and washed once with 1× PBS and then lysed with destain buffer (75% methanol: 25% acetic acid). The absorbance of the neutral red extract was measured at 540 nm with a microplate reader (BioRad). The total viable cell number of treated cells was expressed as a percentage of the untreated control. At least three independent experiments were performed for each treatment.

2.2.4 Cell proliferation assay

Carboxyfluorescein diacetate succinimidyl ester (CFSE) staining was used to measure cell proliferation. CFSE covalently labels long-lived intracellular molecules with the

fluorescent dye, carboxyfluorescein. Thus, when a CFSE-labeled cell divides, its daughter cells are endowed with half the amount of carboxyfluorescein-tagged molecules and so each cell division can be measured by the corresponding decrease of cell fluorescence via flow cytometry [336]. The total cell number needed for each experiment was collected. Cells were centrifuged at 150 ×g for 5 minutes and resuspended in 1 ml serum-free RPMI (SF-RPMI) media in a 15 ml tube. CFSE staining solution (to a final concentration of 5 μM) was added to the dry part of each tube and vortexed immediately for 30 seconds for even labeling. After incubation at 37°C for 5 minutes, cells were resuspended and washed in 5 ml 1×PBS or SF-RPMI twice. Cells were seeded at a density of 1×10^5 cells/well in a volume of 1 ml per well in 12-well plates. Cells were harvested after DCA (1, 3, 5 mM) treatment and then washed twice in 1×PBS supplemented with 1% FBS. Then cells were resuspended in 1×PBS supplemented with 1% FBS to a total volume of 100 μl and analysed with fluorescence-activated cell sorting (FACS) using LSR II (Becton-Dickinson). At least 10,000 events were acquired for each sample. Data analysis was performed using FlowJo software (FLOWJO, LLC, version 10.0.8). Results presented were from three independent experiments with duplicate wells for each treatment.

2.2.5 Cell population-doubling time calculation

MM.1S and MM.1R were seeded at a density of 2×10^5/ml in T-25 flasks and cultured either in normal RPMI-1640 media as control groups, or in the same media supplemented with 5 mM DCA (1×PBS, pH=7.4) as treatment groups. Cells were passaged once a week and seeded in new flasks at a density of 2×10^5/ml. Viable cell numbers were measured by trypan blue dye exclusion. The treatment groups were exposed to DCA-supplemented media for 12 weeks. The population-doubling time (PDT) was calculated using the exponential growth equation (Roth V. 2006 Doubling Time Computing. http://www.doubling-time.com/compute.php):

$$PDT = \frac{cell\ culture\ duration\ (hours) \times \log 2}{\log final\ cell\ density\ - \log initial\ cell\ density}$$

2.2.6 Apoptosis and cell death assay

Apoptosis and cell death were measured using AnnexinV-FITC (BD Biosciences Pharmingen, 556419) and 7AAD (BD Biosciences Pharmingen, 559925) staining followed by FACS analysis. Cells were seeded at 25,000 cells per well in 96-well round bottom plates. Cells treated with 500 nM staurosporine overnight were used as the positive control for apoptosis induction. Samples were plated in duplicates. Three additional wells of highest drug treatment were plated as unstained, AnnexinV-FITC only and 7AAD only controls. After desired treatment, plates were centrifuged at 520 ×g for 5 minutes at room temperature and the media was discarded by flicking the plates. Cells were washed once by adding 200 μL 1×PBS to each well and centrifuged at 520 ×g for 5 minutes at room temperature. Cells were stained with 2 μL AnnexinV-FITC diluted in 50 μL 1× AnnexinV Binding Buffer (10× buffer formula: 0.1 M HEPES, pH 7.4, 1.4 M NaCl, 25 mM $CaCl_2$) per well. Plates were incubated at room temperature in the dark for 15 minutes, then cells were stained with 7AAD (0.25 μg/10^6 cells) in AnnexinV Binding Buffer per well. Cells were transferred to FACS tubes and then analysed for apoptosis by flow cytometry in LSR II (Becton-Dickinson). At least 10,000 events were acquired from each sample. Data analysis was performed using FlowJo software. Results presented were from three independent experiments with duplicate wells for each treatment.

2.2.7 Cell cycle analysis

BrdU (Bromodeoxyuridine)/propidium iodide (PI) staining was used to analyse cell cycle distribution. Cells were seeded at 5×10^5 cells/ml, in a volume of 2 ml per well in 6-well plates. After drug treatments, cells were pulse labelled with 10 μM BrdU (10 mM stock, Sigma-Aldrich) for 30 minutes at 37℃ 5% CO_2. Cells were collected into sterile 15 ml Falcon tubes and spun down at 150 ×g for 5 minutes and washed with 2 ml 1×PBS. Then cells were gently resuspended in 0.5 ml ice-cold PBS. Ice-cold 80% ethanol (tissue culture grade) was added dropwise into each tube while vortexing. Fixed cells were stored at 4℃ for a minimum of 3-4 hours and for up to 2 weeks before further staining.

Fixed cells were centrifuged at 520 ×g for 5 minutes. Cell pellets were loosened by briefly vortexing and then resuspended in 1 ml 2 N HCl (32% HCl = 10.2 N) containing

0.5% (v/v) Triton X-100 to denature the DNA. Cells were incubated at room temperature for 30 minutes. The supernatant was removed after centrifugation at 520 ×g for 5 minutes. Each sample was neutralized by 1 ml 0.1 M $Na_2B_4O_7.10H_2O$ (pH 8.5). The supernatant was removed after centrifugation at 520 ×g for 5 minutes. Cell pellets were resuspended in 100 μl PBS containing 2% FBS and 0.5% Tween-20 and 20 μl /ml anti-BrdU antibody (BD Biosciences clone B44, Catalogue number 347580) and incubated for 30 minutes at room temperature. Cells were washed with 1 ml of PBS containing 2% FBS by centrifugation at 520 ×g for 5 minutes. Master mix (100 μl) containing fluorescein-labelled (FITC) anti-mouse IgG (Invitrogen, Lot No. 1810918, 2 mg/mL) at a 1:100 dilution in PBS containing 2% FBS and 0.5% Tween-20 was added to each tube. Cells were incubated in the dark for 30 minutes at room temperature and washed as stated above. Then cells were resuspended in 200 μl PBS containing 2% FBS and 10 μg/ml PI, transferred into FACS tubes and incubated in the dark for 15 minutes prior to flow cytometry in the LSR II (Becton-Dickinson). At least 100,000 events were acquired from each sample. Data analysis was performed using FlowJo software. Results presented were from three independent experiments.

2.2.8 Extracellular glucose and lactate level measurement

Extracellular glucose levels were measured using a FreeStyle Optium glucose meter (TrueMeasure Technology, Abbot Japan, test range 1.1-27.8 mmol/L). The glucose meter test principle is based on the chemical reaction of glucose in the samples and glucose dehydrogenase, NAD+, and phenanthroline quinone on the test strips. The reaction created a small electrical current and was measured and displayed on the glucose meter. The reading on the meter is proportional to the glucose concentration in the sample. The extracellular lactate levels were measured using Lactate Pro2 meter (ARKRAY, Inc, test range 0.5-25 mmol/L). The lactate meter electronically analyses potassium ferrocyanide converted from ferricyanide by lactate and the chemical reaction also creates the current that can be measured and displayed by the device. Cells were maintained in complete RPMI-1640 media before experiments and were washed with fresh media before seeding into plates. MM cell lines were seeded at 5×10^5 /ml in a volume of 5 ml per well in 6 well plates and cultured in complete RPMI-1640 media. Media glucose and lactate levels were measured shortly after seeding and measured

once every day for 4 days. As the lactate meter was optimised for measurements on whole blood and were strongly influenced by haemoglobin (which is abundant in blood but not in tissue culture media), the lactate meter readings were calibrated for our purposes by comparison to a lactate standard curve prepared in RPMI-1640 media with 10% FBS. The lactate production was calculated by subtracting the day-1 lactate levels as background from all readings. Data was calculated based on a standard curve. Cell numbers were counted at 24 hours, 48 hours and 72 hours. Results were representative of three independent experiments.

2.2.9 Extracellular acidification and oxygen consumption rates

Metabolism profiling of cell lines was measured using Seahorse XFe96 analyser (Seahorse Bioscience, MA, USA). The XFe96 analyser measures *in vitro* changes in cellular bioenergetics by simultaneously measuring the oxygen consumption rate (OCR, indicating mitochondrial respiration) and the extracellular acidification rate (ECAR, indicating glycolysis). MM cell lines were cultured in RPMI 1640 complete media at a density of 1×10^5/ml, 5 ml per well, in a 6-well plate before the seahorse assay. The cell density for seahorse assay was optimized to reach an OCR value between 50-150 pmol/min. Suspension cell lines were stuck to the bottom of the Seahorse XF96 cell culture microplate using Cell-Tak (BD Biosciences, CN 354240) at a concentration of 22.4 μg/mL diluted in 0.1 M $NaHCO_3$ (pH: 8.0) solution. The diluted Cell-Tak solution (25 μL) was added to each well and incubated for 20 minutes at room temperature, and then each well was washed twice using 200 μL of sterile water. Cell lines were seeded at 80,000 cells/well in XFe96 culture plates (Seahorse Bioscience, North Billerica, MA, USA) in 50 μL of unbuffered assay media (Seahorse Bioscience) (pH: 7.4 ± 0.01). Cells were centrifuged at 200 × g (zero braking) for 1 minute and then the plate was transferred to a 37°C incubator without CO_2 for 25-30 minutes to ensure the cells had completely attached. Treatment drugs were pipetted into the injection ports of the cartridge during this time, then an extra 125 μL warm seahorse assay media was slowly added to the cell culture plate along the side of each well. The sensors calibration was completed after loading the cartridge to the seahorse analyser. The utility plate used for calibration was replaced by the cell plate after the calibrations. The cells were checked for confluence shortly after the assay using Incucyte Zoom (ESSEN Bioscience, USA).

Each cell line's morphology and cell size were predetermined using software Zoom 2016A. The incucyte data was used as a guide to confirm that the cell numbers in each well remained homogenous after the assay and to exclude wells with cells being flushed off in the assay.

2.2.9.1 Glycolysis stress test

To measure the maximum glycolytic capacity and glycolytic reserves, the Seahorse XF Glycolytic Stress Test kit (Seahorse Bioscience) was used. Assay media used in this assay was pyruvate free and glucose free but supplemented with 2 mM glutamine. Measurements were taken over a 3-minute period, followed by 3 minutes of mixing and re-oxygenation of the media. Three measurements were done after each injection. The baseline metabolism and non-glycolytic acidification were measured 3-4 times before glucose was injected from port A to fuel the glycolytic pathway. ECAR was measured using the extracellular flux analyser (Seahorse Biosciences) by sequential injection of glucose (final concentration of 10 mM), oligomycin A (final concentration 0.75 or 1μM, concentrations were predetermined by optimization according to experiment protocol) (**Table 2.2**) and 2-deoxyglucose (2-DG, final concentration 30 mM). Results presented are from 3-4 independent experiments, with 5-6 replicate wells for each treatment.

Table 2.2 Optimised conditions for Seahorse analyser

Cell Lines	**Cell density** (per well)	**Oligomycin A final concentrations** (μM)	**FCCP final concentrations** (μM)
RPMI8226	80,000	0.75	0.125
U266	80,000	1	0.25
MM.1S	80,000	0.75	0.5
MM.1R	80,000	0.75	0.5

2.2.9.2 Mitochondrial respiration stress test

To further investigate the alteration of the mitochondrial respiration pathway by DCA, mitochondrial function was measured using a Seahorse XF 96 cell mitochondria stress test (Seahorse Biosciences, North Billerica, MA, USA) were carried out. As per manufacturer's instructions, oligomycin A, carbonyl cyanide-4 (trifluoromethoxy) phenylhydrazone (FCCP) (final concentration in **Table 2.2**), a mixture of rotenone

(final concentration 1 μM) and antimycin A (final concentration 1 μM) targeting different components of the ETC in the mitochondria were injected sequentially to determine the basal respiration, ATP production, maximal respiration, and non-mitochondrial respiration, respectively. Results presented were from 3-4 independent experiments with 5-6 replicated wells for each treatment.

2.2.10 Western blotting

Cells (~1×10^6 cells) were collected and washed with PBS and lysed with radioimmunoprecipitation assay (RIPA) buffer (50 mM Tris-Cl (pH 7.4), 1% NP-40, 40 mM NaF, 10 mM NaCl, 10 mM Na_3VO_4, 1 mM phenylmethylsulfonyl fluoride, 10 mM dithiothreitol, and 1 μg/ml each of leupeptin and aprotinin). The lysate was then sonicated under low power for 5 seconds and spun down at 13,000 ×g for 20 minutes at 4°C. The supernatant was collected and total protein was measured using BCA assay kit (Pierce, Rockford, IL, USA). Proteins (30 μg/sample) were separated by 10% SDS-PAGE according to BioRad standard protocol and transferred to PVDF membranes (BioRad) by wet transfer method (transfer at 500 mA current, 100 V constant voltage for 1 hour) [337]. The membranes were blocked with either 5% non-fat dry milk (NFM) or 3% bovine serum albumin (BSA) dissolved in 1×TBST (10×TBS: pH 7.5, 10 mM Tris, 100 mM NaCl; 1×TBST: 1×TBS supplemented with 0.1% Tween 20) for one hour at room temperature, and then probed with specific primary antibodies, diluted in their specific blocking buffers, overnight at 4°C. The details of antibody information, dilutions and specific blocking buffers are given in **Table 2.3**. After primary antibody incubation, membranes were incubated with specific horseradish peroxidase-conjugated (HRP) secondary antibodies (**Table 2.3**) for one hour at room temperature.

The membranes were washed again and developed by enhanced chemiluminescence using Clarity Western ECL Substrate (Bio-Rad) reagent for one minute prior to image acquisition. The chemiluminescent blots were imaged with the ChemiDoc MP imager (Bio-Rad). Densitometric analysis was done using ChemiDoc MP imager software. Images are representative of at least three independent experiments for each condition.

When investigating PDKs, each PDK was examined separately on different membranes; the primary and secondary antibodies were then removed by a harsh stripping protocol

(Abcam, buffer formula and protocol in Appendix Table 3) before re-probing for *β*-actin as loading control. When investigating pPDH/tPDH ratio, pPDH was detected first, and tPDH was probed on the same blot after a mild stripping protocol (Abcam, buffer formula and protocol in Appendix Table 3). With this approach, a loading control is not necessary for the pPDH/tPDH investigations (representative blots including *β*-actin loading control are provided in Appendix Figure 2.5).

Table 2.3 Summary of primary antibodies used in western blot

Antibody	Company	Catalogue number	Lot number	Stock (mg/ml)	Dilution rate	Blocking buffer
PDK1	Enzo life science	ADI-KAP-PK112-F	11051415	1.00	1:500	5% NFM
PDK2	ABGENT	AP7039b	SH030422G	0.25	1:500	5% NFM
PDK3	Abnova	H00005165-M01	F2101-2B11	0.50	1:500	5% NFM
PDK4	ABGENT	Ap7041b	SH030422K	0.25	1:500	5% NFM
pPDH	abcam	ab92696	GR196570-1	1.00	1:1000	3% BSA
tPDH	abcam	ab168379	GR121944-9	0.35	1:1000	3% BSA
β-actin	abcam	ab8227	GR245058-1	1.00	1:5000	5% NFM
Polyclonal goat anti-rabbit HRP	Dako	P0448	20010775	0.25	1:8000	
Polyclonal goat anti-mouse HRP	Dako	P0447	00071312	1.00	1:8000	

HRP: horseradish peroxidase. NFM: non-fat dry milk. BSA: bovine serum albumin.

2.2.11 Statistical methods

Numeric data were presented as mean ± standard deviation (SD). T-test was applied to test the differences between two groups. One-way ANOVA with Tukey's multiple comparison test was used to compare single mean among groups. Two-Way ANOVA with Tukey's multiple comparison test was used to compare multiple means among different groups. A probability level of $p < 0.05$ will be considered statistically significant. GraphPad Prism (version 6.0f) was used for all statistical analysis.

2.3 Results

2.3.1 DCA inhibited MM cell line growth without inducing apoptosis or cell cycle arrest

To investigate the effect of DCA on MM cell lines, neutral red uptake assay was used to measure the total viable cell number. DCA treatment significantly reduced the total viable cell number compared to the untreated control in 4 out of 5 cell lines analysed; however, there were considerable differences in their sensitivities to DCA (**Figure 2.1 A**). RPMI 8226 was the most sensitive cell line to DCA treatment with a 43% reduction in total viable cell number, U266 was not responsive and the rest of the cell lines had intermediate sensitivities (**Figure 2.1 A**). The DCA treatment at concentrations up to 5 mM did not reach the 50% inhibitory effect on cell growth in the MM cell lines, so the EC_{50} cannot be accurately calculated (**Figure 2.1 A**).

The contribution of cell proliferation, apoptosis and cell cycle distribution to the reduction of total viable cell number induced by DCA treatment was investigated. MM cell proliferation was measured by CFSE dye dilution followed by FACS analysis. DCA treatment groups had significantly higher CFSE signal compared to their untreated control, thus indicating less proliferation (**Figure 2.1 B**). AnnexinV/7AAD staining after DCA treatment followed by FACS analysis was used to investigate if DCA treatment can induce apoptosis. There was no significant induction of apoptosis by DCA in the MM cell lines that had decreased total viable cell number after DCA treatment (**Figure 2.1 C**). Earlier time points (6 hours, 16 hours, 24 hours) of DCA treatment in MM.1S and MM.1R were also tested but there was no induction of apoptosis (**Appendix Figure 2.1**). Cell cycle analysis in MM.1S and MM.1R indicated that the reduction in total viable cell number was also not due to cell cycle arrest (**Figure 2.1 D**).

DCA is likely to be used in patients chronically (**Chapter 4**) thus the effects of DCA over 3 months of treatment was examined. MM.1S and MM.1R were treated with 5 mM DCA for 3 months and population-doubling time was measured. The average population doubling time of the MM cell lines is about 70 hours (**Table 2.4**). Compared to the untreated control groups, chronic DCA treatment increased population-doubling times from 67±9 to 105±9 hours for MM.1S cells and 80±4 to 109±8 hours for MM.1R

cells (**Figure 2.1 E**). MM cells stopped growing after being exposed to 5 mM DCA for 10 weeks as indicated by cell number count (**Appendix Figure 2.2**). Trypan blue exclusion indicated that DCA was primarily inhibiting cell growth, not inducing cell death.

Table 2.4 MM cell line population doubling times

Cell Lines	Doubling time
RPMI8226 *	*ca.* 70 hours
U266 *	*ca.* 55 hours
MM.1S +	*ca.* 70 hours
MM.1R +	*ca.* 72 hours
NCI-H929 *	*ca.* 70 hours

* Data from German Collection of Microorganisms & Cell Cultures.
+ Calculated from data in Figure 2.1 E.

To conclude, DCA treatment reduced the total viable cell number by slowing cell proliferation and increasing the cell population doubling time without altering cell cycle distribution or inducing apoptosis.

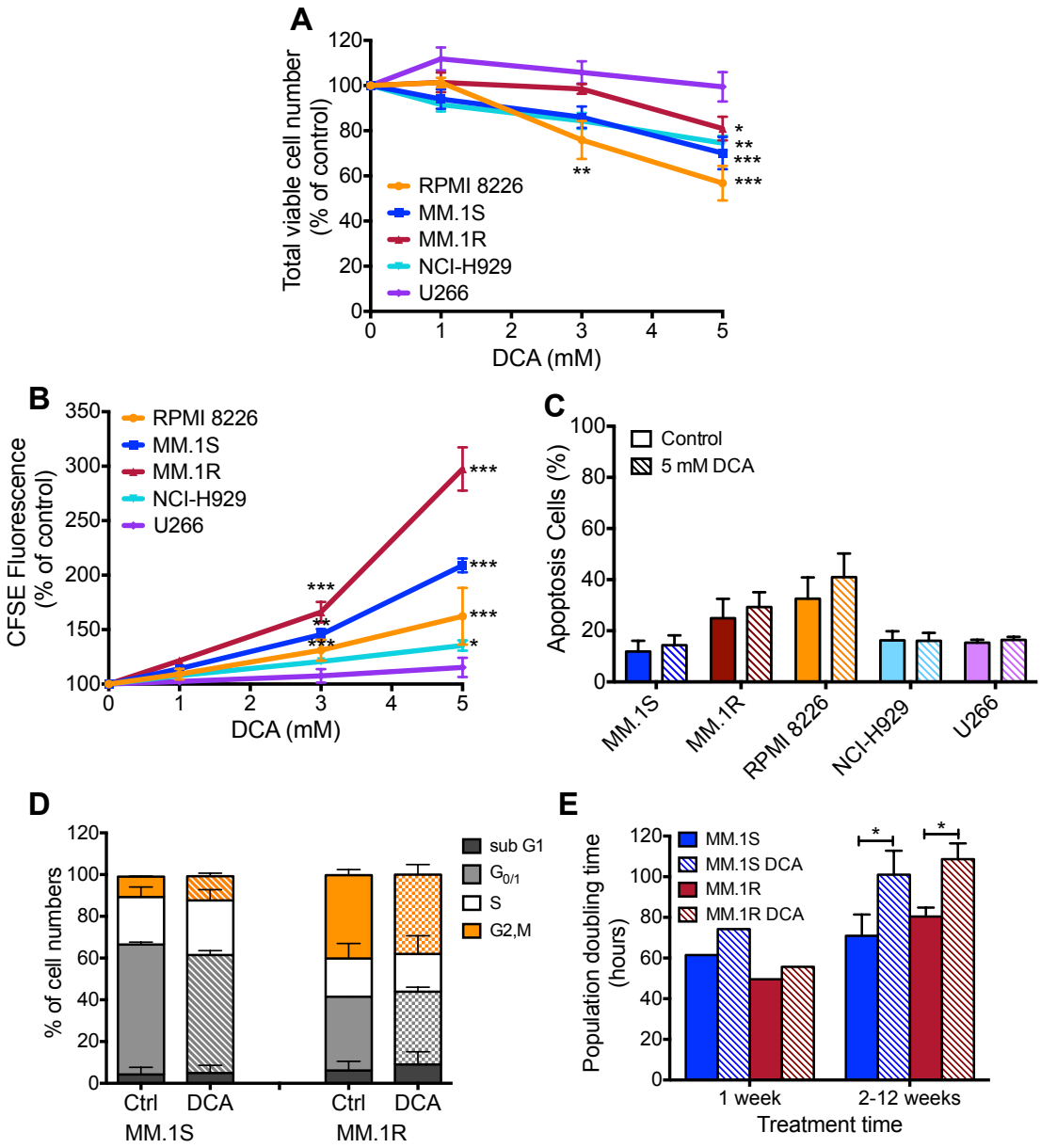

Figure 2.1 The effect of DCA on MM cell growth and viability. (A) DCA (72 hours) treatment significantly reduced the total viable cell number compared to no-DCA control in 4/5 cell lines. (B) Cell proliferation was inhibited in 3/5 cell lines. (C) DCA (48 hours) treatment did not induce apoptosis. Staurosporine (500 μM, overnight) was used as positive control for apoptosis. (D) Cell cycle distribution analysis did not show cell cycle arrest after DCA treatment (72 hours). (E) Chronic DCA treatment (5 mM) increased population-doubling times for MM.1S and MM.1R. Each data point represents mean ± standard deviation (SD), n ≥ 3 independent experiments. *p <0.05, **p <0.01, ***p <0.001. In panels A and B, statistics are with respect to 0 mM DCA control groups.

2.3.2 MM cell lines have heterogeneous metabolic profiles

To further understand the contributing factors to the different responses to DCA across the MM cell lines, experiments were carried out to evaluate the metabolic profiles of the MM cells.

Glucose consumption and lactate production

Glucose consumption was measured by monitoring glucose levels in cell culture media over 4 days of culture. In complete RPMI-1640 media, glucose levels decreased over 4 days of culture (**Figure 2.2**) but differences among cell lines were observed despite similar cell population doubling times (**Table 2.4**). RPMI 8226 and MM.1S both have similar cell population-doubling times (ca.70 hours); however, RPMI 8226 consumed more glucose compared to the rest of the cell lines (~90% decrease at day 3) while MM.1S consumed the least (~13% decrease at day 3) (**Figure 2.2 A**).

The lactate production, as measured by the changes in media lactate levels, were all increased within 1 to 4 days, but the amount by which they increased varied among cell lines and correlated with the reduction in glucose levels. The lactate level in the culture media of RPMI 8226 had the highest increase (to 21.7±3.9 mM at day 4), while MM.1S cells had the lowest lactate production (4.2±2.1 mM at day 4) (**Figure 2.2 B**).

Interestingly, MM.1S (dexamethasone (DEX) sensitive) and MM.1R (DEX resistant), derived from one patient before and after the development of glucocorticoid (GC) resistance, showed different metabolic properties. Response to GC is dependent on the glucocorticoid receptor (GR) which is expressed in the GC-sensitive cell line MM.1S but significantly down-regulated in the GC-resistant derivative cell line MM.1R [286]. MM.1R had higher lactate production and lower glucose consumption compared to that of MM.1S. This is consistent with the literature suggested that GC resistance is correlated with upregulated glycolysis [325], and will be explored further in this chapter.

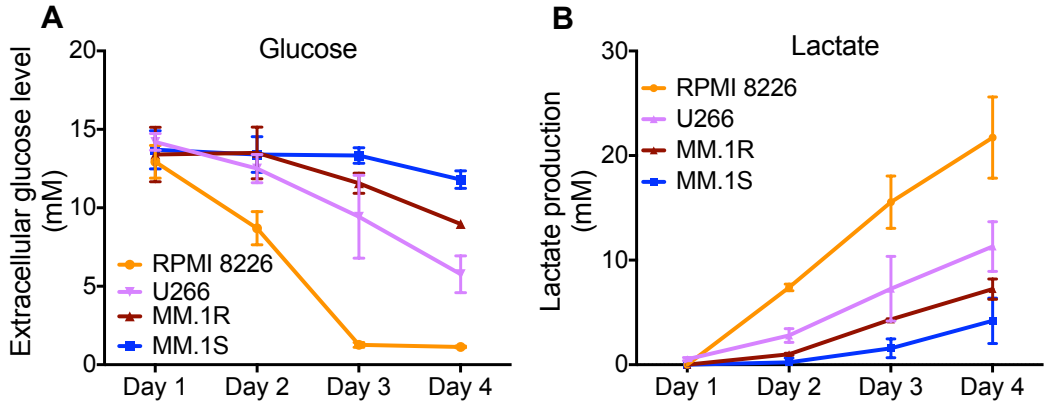

Figure 2.2 MM cell lines are metabolically heterogeneous. (A) Media glucose level was monitored using a glucose meter and (B) media lactate level was monitored using a lactate meter once per day for 4 days in 6-well cell culture plates. The lactate production was calculated by subtracting the day-1 lactate levels as background from all readings. Each data shown represents mean ± SD, n=3 biological repeats. Note: 2-ME was supplemented in NCI-H929 as required to maintain the growth. 2-ME can act as a biological antioxidant by scavenging hydroxyl radicals, thus can offer advantages to NCI-H929, so it was taken out in experiments on metabolism.

Monitoring glucose and lactate levels in the culture media provided a basic understanding of the heterogeneous metabolism phenotypes and substrates preferences of the MM cell lines. Seahorse glycolysis stress and mitochondria stress tests were carried out to analyse the *in vitro* changes of cellular bioenergetics by simultaneously measuring the mitochondrial respiration indicated by oxygen consumption rate (OCR) and glycolysis activities indicated by the extracellular acidification rate (ECAR).

Glycolytic flux and glycolytic capacity

Glycolytic flux and glycolytic capacity of the MM cell lines were studied using the standard Seahorse XF Glycolytic Stress Test assay (**Figure 2.3 A**). Glucose was injected to initiate the glycolysis pathway. The cells metabolise glucose through the glycolytic pathway to pyruvate, ATP, NADH, water and protons. Protons are pumped out of the cell to maintain the intracellular pH. The efflux of the protons into the extracellular space or media is the main cause of extracellular acidification. This first injection increases the ECAR reading and represents the rate of glycolysis; and it is an indicator of the basal glycolytic activities (**Figure 2.3 A**). Media acidification may also result from the CO_2 produced in the TCA cycle from non-glycolytic substrates, which can be catalysed by carbonic anhydrase into bicarbonate and protons. This non-

glycolytic caused acidification is detected before glucose injection [338]. The following injection of oligomycin A, a mitochondrial ATP synthase inhibitor, stimulates cells to utilize glycolysis to their maximum capacity, then subsequently increases the ECAR reading as an indicator of the maximum cellular glycolytic capacity. In this assay, the glycolytic capacity is calculated as the difference between measurement 7 (the first reading after oligomycin A injection) and measurement 3 (the basal ECAR reading before glucose injection). The third injection of 2-DG, a competitive inhibitor for glucose uptake by binding to glucose hexokinase, shuts down the glycolytic pathway and confirms the ECAR produced before is due to glycolysis. The difference between the maximum glycolytic capacity and the basal glycolysis is reported as the glycolytic reserve, which indicates the capability of cells to respond to an energetic crisis, and measures if the cells' glycolytic capacities are at the theoretical maximum (**Figure 2.3 A)** (**Figure 2.3 A**) [338].

In MM cell lines, the glucose injection successfully triggered increased glycolysis flux where RPMI 8226 had the greatest increase, indicating the highest glycolytic activities (**Figure 2.3 B, Figure 2.4 A**). The basal glycolysis of RPMI 8226 cells (151.0±12.3 pmol/min) is 5.2-fold higher than that of U266 (29.3±4.8 pmol/min), with MM.1S (36.6±4.9 pmol/min) and MM.1R (58.8±8.3 pmol/min) being intermediate (**Figure 2.4 A**). The high glycolysis flux result correlates well with the high lactate production and rapid glucose consumption of RPMI 8226 (**Figure 2.2**). It is worth noting that the most glycolytic cell line, RPMI 8226, is also the most sensitive cell line to DCA treatment (**Figure 2.1 A**). The mitochondrial activities (as indicated by OCR) in response to glucose injection were monitored simultaneously with glycolytic activities (**Figure 2.3 C**). The OCR level was decreased after glucose injection in all MM cell lines. RPMI 8226 had the greatest decrease in OCR level compared to the rest of the cell lines, which indicates that RPMI 8226 metabolises preferably through glycolysis rather than mitochondrial respiration.

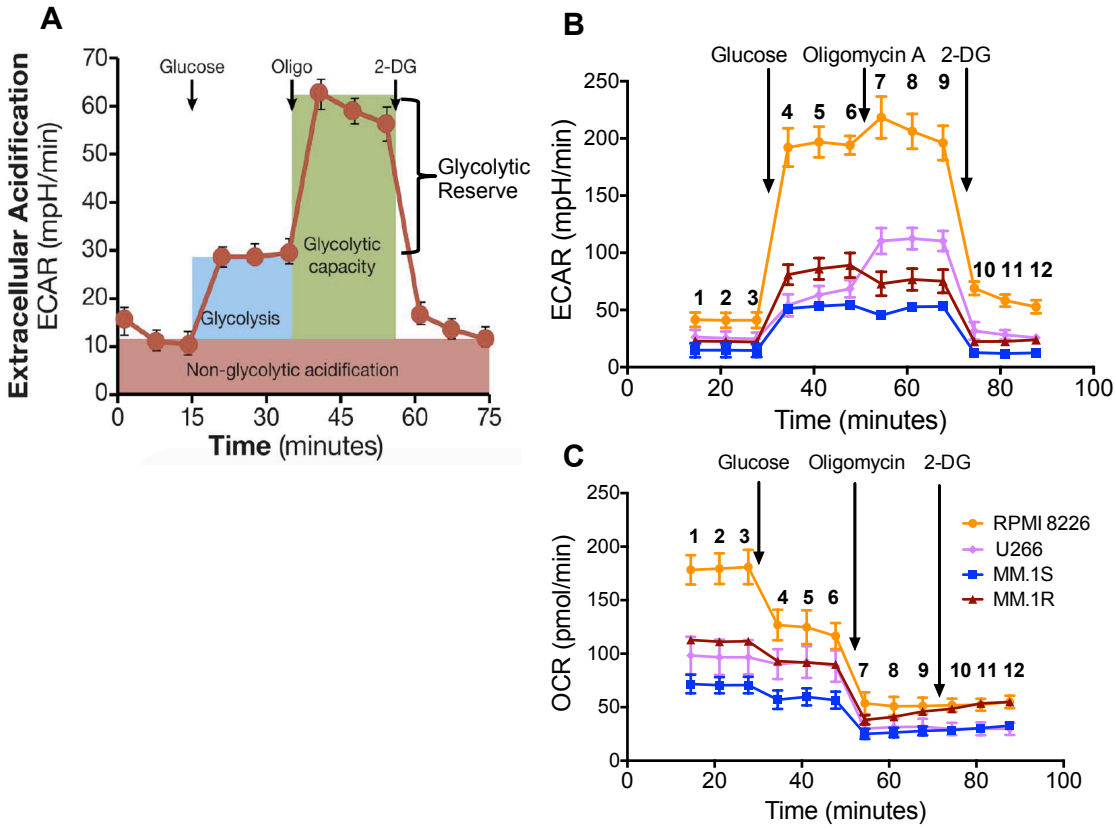

Figure 2.3 Analysing glycolytic flux and glycolytic capacity in MM cells. (A) The cellular glycolytic activity is examined by the Seahorse glycolytic stress assay [338]. Schematic graph was from Agilent Seahorse glycolytic stress kit manual guide. Glucose injection reveals the basal glycolytic activity of MM cells. The non-glycolytic acidification is the ECAR level before glucose injection. Oligomycin A (ATP synthase inhibitor) injection is used to reveal the maximum cellular glycolytic capacity. 2-DG shuts down the glycolytic pathway and confirms the ECAR produced before is due to glycolysis. The difference between the maximum glycolytic capacity and the basal glycolysis rate is reported as the glycolytic reserve. (B, C) ECAR and OCR changes in MM cell lines after glucose (10 mM), oligomycin A (0.75 or 1 μM) and lastly 2-DG (30 mM) injections (black arrows). Numbers above the graph indicate the measurement sequences. Data represents 3-4 independent biological repeats (mean ± SD); each treatment in every biological repeat consists of 5-6 wells (technical replicates). ECAR: extracellular acidification rate; OCR: oxygen consumption rate.

In addition to having the highest basal glycolytic rate, RPMI 8226 had the highest glycolytic capacity, whereas U266, with the lowest basal glycolysis, had the highest glycolytic reserve among the MM cell lines (**Figure 2.4 A, B)**. Despite the addition of oligomycin A, a substantial increase in ECAR (glycolytic reserve) was observed only in U266 (**Figure 2.3 B, 2.4 C**). This result indicated that the other three MM cell lines were already at maximum glycolytic capacity, and inhibiting ATP production through

oxidative phosphorylation could not further stimulate cells to utilize the glycolysis pathways. MM.1R had higher basal glycolysis (p=0.015) and glycolytic capacity (p=0.029) than MM.1S (**Figure 2.4 A, B**), which correlates with published papers suggesting that DEX resistance is associated with upregulated glycolysis [325].

The final injection of 2-DG abolished overall glycolysis by competitively inhibiting glucose uptake through the glucose transporter. The ECAR readings decreased after 2-DG injection, to levels similar to those prior to glucose addition, confirming that the increased ECAR was due to glycolytic activities (**Figure 2.4 D**).

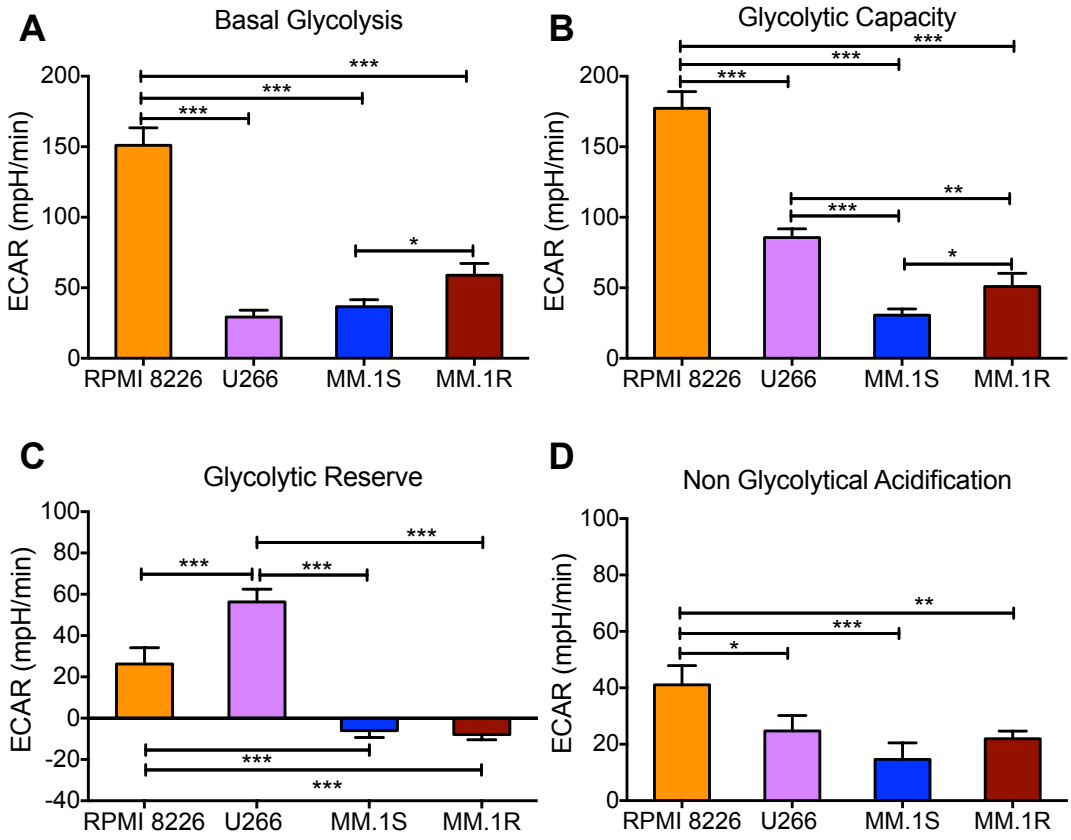

Figure 2.4 Heterogeneous glycolytic activities of MM cell lines This figure shows (A) basal glycolysis, (B) glycolytic capacity, (C) glycolytic reserve, (D) non-glycolytic acidification, as defined in **Figure 2.3**. Data represents 3-4 independent biological repeats (mean ± SD); each treatment in every biological repeat consisting 5-6 wells (technical replicates). *p <0.05, **p <0.01, ***p <0.001. One-way ANOVA Tukey's multiple comparison test was used to compare differences among cell lines.

Oxygen consumption and mitochondrial respiration

Oxygen consumption rate (OCR) is an indicator of oxygen consumption and reflects the mitochondrial activities. Key cellular mitochondrial activities of MM cell lines such as basal respiration, ATP production, proton leak, maximal mitochondrial respiration, and spare respiration capacity were evaluated by the Seahorse standard mitochondria stress test (**Figure 2.5 A**). Oligomycin A, an ATP synthase (complex V) inhibitor, can shut down mitochondrial ATP production and thus decrease OCR. This decreased amount of OCR is linked with ATP production and reflects basal cellular ATP production [339].

At the end of the electron transport chain (ETC), protons return to the mitochondrial matrix through the ATP synthase; the energy stored in the proton gradient drives the phosphorylation of ADP to produce ATP. But the oxidative phosphorylation is not entirely coupled to mitochondrial respiration. Protons can re-enter the matrix through proton channels, bypassing ATP synthase without producing ATP. This process is known as proton leak, which has been considered a protection mechanism from oxidative damage by reducing ROS produced by the ETC [338, 339]. The basal mitochondrial respiration OCR is composed of both the ATP linked OCR and the proton leaked OCR (**Figure 2.5 A**).

Carbonyl cyanide-4 (trifluoromethoxy) phenylhydrazone (FCCP) is an uncoupler of oxidative phosphorylation in mitochondria. It is capable of depolarizing mitochondrial membranes by collapsing the proton gradient and allowing the electrons to flow through the ETC freely, and thus enables the ATP synthase to consume oxygen to the maximum capacity, regardless of ATP levels (**Figure 2.5 B**). The FCCP-stimulated OCR can reveal the maximum mitochondrial respiration capacity. The spare respiratory capacity is calculated as the difference between maximal respiration and basal respiration and it is a measure of the ability of the cell to respond to increased energy demand. The last injection shuts down the ETC by a mixture of rotenone (complex I inhibitor) and antimycin A (complex III inhibitor), thus enabling the calculation of OCR by non-mitochondrial oxygen-consuming processes such as protein folding, lipid and collagen synthesis, demethylation reactions, and hydroxylation reactions [338, 340].

The basal respiration rate reflects the energy demand of cells under normal conditions, which is calculated as the basal OCR (measurement 3) minus the non-mitochondrial oxygen consumption OCR (measurement 10). ECAR was also monitored simultaneously in this assay to reveal the glycolytic activity responses to the injections (**Figure 2.5 D**).

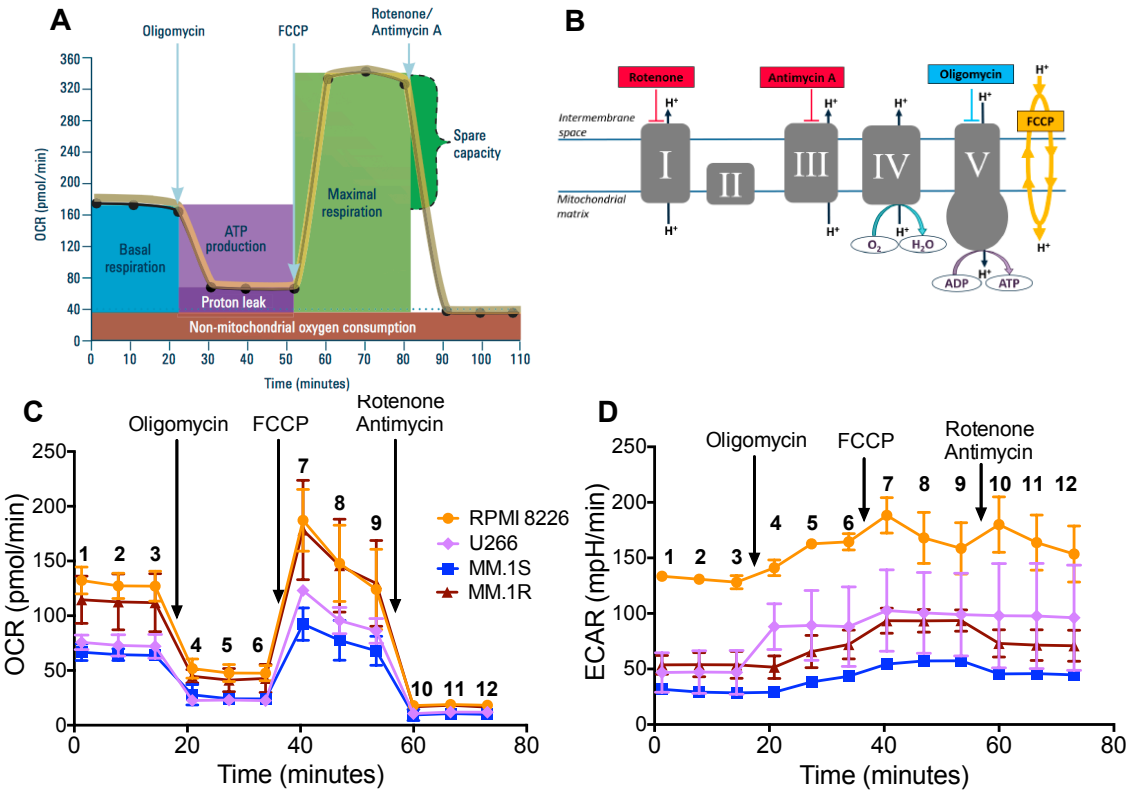

Figure 2.5 Analysing mitochondrial respiration. (A, B) The mitochondrial respiration activities were measured using the Seahorse mitochondrial stress test. The mechanisms of action of the compounds used in this kit are illustrated in (B). Oligomycin A, an ATP synthase (complex V) inhibitor, shuts down mitochondrial ATP production and thus decrease OCR. FCCP, an uncoupler of oxidative phosphorylation, allows the electrons to flow through the ETC freely, and enables complex V to consume oxygen to its maximum capacity. The mixture of rotenone (complex I inhibitor) and antimycin A (complex III inhibitor) was used to shut down the ETC to enable the calculation of non-mitochondrial respiration. Assay media was supplemented with 10 mM glucose, 2 mM glutamine, and 1 mM pyruvate. Schematic graphs were adapted from Agilent Seahorse XF cell mito stress kit manual guide. (C, D) OCR and ECAR response of MM cell lines to oligomycin A (0.75 or 1 μM), FCCP (0.5, 0.25 or 0.125 μM) and a mixture of rotenone (1 μM) and antimycin (1 μM) injections. Black numbers above the data points in the graph indicate the measurements sequences. Each injection is marked as a vertical arrow. Data represents 3-4 independent biological repeats (mean ± SD); each treatment in every biological repeat consists of 5-6 replicates. ECAR: extracellular acidification rate; OCR: oxygen consumption rate.

The differences in the basal levels of OCR and ECAR among different cell lines were a genuine reflection of different energy demands and the metabolic heterogeneity among MM cell lines. RPMI 8226 (109±9.8 pmol/min) had the highest OCR among the cell lines while MM.1S had the lowest OCR (53.3±1.5 pmol/min) (**Figure 2.5 C, 2.6 A**). Consistent with the basal respiration rate, ATP production was highest in RPMI 8226 cells (75.3±4.5 pmol/min), almost double that of the MM.1S (35.7±5.9 pmol/min) (p=0.019), which produced the least ATP among the cell lines (**Figure 2.6 A, B**). These results indicated that RPMI 8226 was the most metabolically active cell line and MM.1S was the least metabolically active one among the tested MM cell lines.

RPMI 8226 also had the highest maximum mitochondrial respiration capacity (169.0± 25.1 pmol/min) while MM.1S had the lowest capacity (81.7±15.9 pmol/min) (p=0.013). Comparing the isogenic cell lines, MM.1R (DEX resistant) had almost 2-fold higher levels of spare respiration capacity (p=0.045**)**, maximal respiration (**p**=0.023), ATP production and basal respiration (p=0.028**)** compared to its isogenic counterpart, MM.1S (DEX sensitive) (**Figure 2.6)**.

U266 had the highest spare respiratory capacity (73.3±27.4 pmol/min), which is 1.2 times higher than that of the most energetic cell line RPMI 8226 (59.3±12.6 pmol/min) (**Figure 2.6 D**).

Examination of ECAR under the conditions of the Mito Stress Test kit gave results in line with that of the previous glycolysis stress test (**Figure 2.4**). U266 had the highest increase in ECAR from its baseline, more than 8 times higher than that of RPMI 8226 (p<0.01**)**, indicating that U266 had the greatest potential to switch to the glycolytic pathway under mitochondria-stressed conditions (**Figure 2.7**). There was no significant difference in non-mitochondrial respiration among the MM cell lines (**Appendix Figure 2.3 B**).

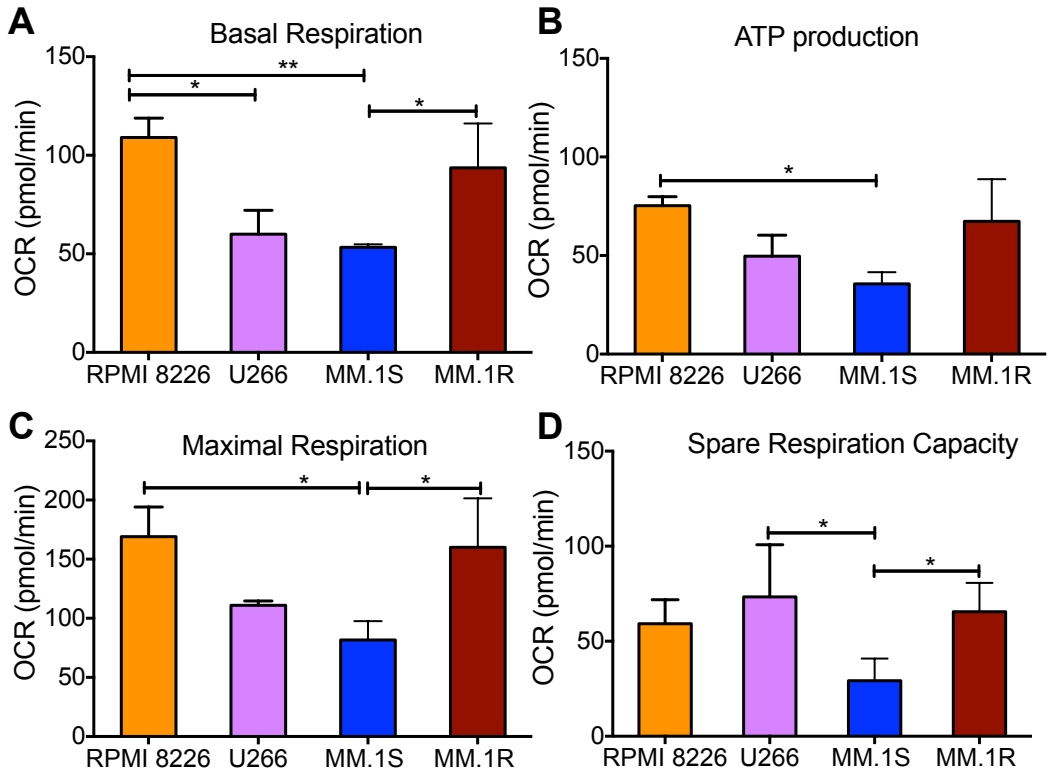

Figure 2.6 Heterogeneous mitochondrial respiration activities of MM cells This figure shows (A) basal respiration, (B) ATP production, (C) maximal respiration, and (D) spare respiratory capacity as defined in **Figure 2.5**. Each data point represents mean ± SD from 3-4 biological repeats, each consisting of 5-6 wells (technical repeats). *p <0.05, **p<0.01, ***p<0.001. One-way ANOVA Tukey's multiple comparison test was used to compare differences among cell lines.

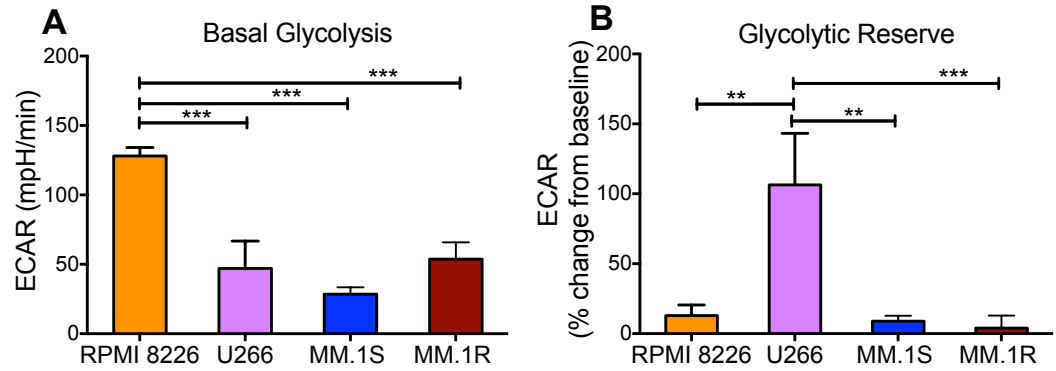

Figure 2.7 Glycolytic activity of MM cells in response to mitochondrial stress (A) Basal glycolysis of MM cells. (B) Glycolytic reserve in this graph is defined as percentage change from the baseline (the raw data was baselined to its basal ECAR). Each data point represents mean ± SD, from n = 3-4 biological repeats, each treatment of each repeat had 5-6 technical replicates. *p <0.05, **p <0.01, ***p <0.001. One-way ANOVA Tukey's multiple comparison test was used to compare difference among cell lines.

2.3.3 DCA diverted the metabolic flux from glycolysis to mitochondrial respiration

The effects of DCA on MM cell growth were mainly cytostatic (**Figure 2.1**). Having established the metabolic characteristics of the cell lines, the effect of DCA on the metabolism of MM cells was evaluated by measuring extracellular lactate production, flux of glycolysis and mitochondrial respiration. As DCA inhibits PDKs and activates PDH (**Figure 1.11**), a decrease in lactate production, decreased glycolytic rate/ECAR and increased mitochondrial respiration rate/OCR would be expected.

The lactate level in the media was measured before and after DCA treatment. RPMI 8226, the cell line with the highest rate of lactate production, showed a significantly reduced lactate production in the presence of DCA. This trend was also observed in MM.1R and U266 (**Figure 2.8 A**).

To evaluate the effects of DCA on glycolysis activity in real time, ECAR was measured within minutes of DCA injections by Seahorse flux analysis. Because pyruvate can fuel the TCA cycle to increase oxygen consumption and can also be converted by LDHA into lactate to increase media acidification, a pyruvate supplement can potentially interfere with the effects of DCA. Thus, ECAR was measured in the presence of glucose and glutamine but without pyruvate according to standard Seahorse protocol. DCA significantly reduced ECAR in U266 by 29± 3.6% (p<0.001), and reduced ECAR in RPMI 8226 by 11.5±3.2% (p<0.001) compared to the basal levels, but there was no reduction of ECAR by DCA in MM.1S or MM.1R (**Figure 2.8 B**). To evaluate the effect of DCA treatment on oxygen consumption in real time, OCR was measured within minutes of DCA injection. DCA successfully increased OCR levels in RPMI 8226 (p<0.001) and U266 (p<0.001) while there was no increase in MM.1S and MM.1R. U266 also had the greatest OCR increase of 12.7±1.2% after DCA injection among the MM cell lines (**Figure 2.8 C**). Thus, the cell line U266 with no change in total viable cell number in response to DCA treatment in normoxia (**Figure 2.1**) was the cell line with the greatest change in metabolic flux following DCA treatment, as measured by OCR and ECAR.

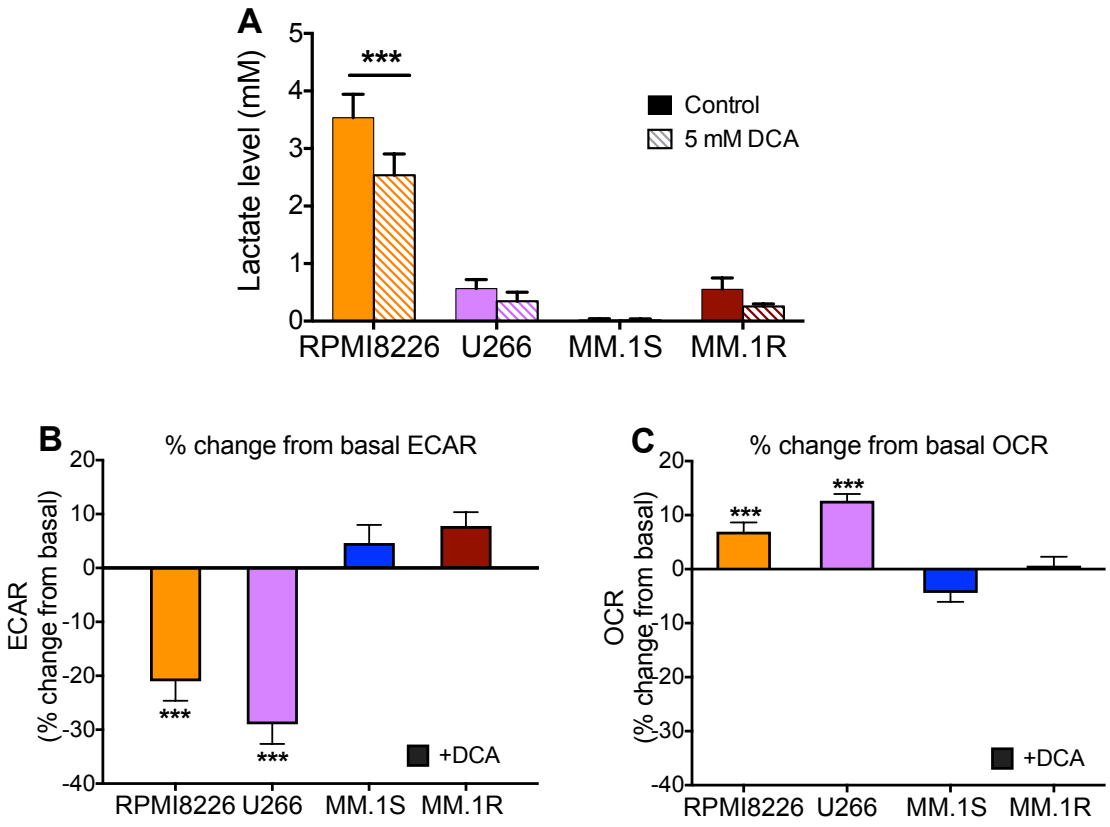

Figure 2.8 DCA reduced extracellular lactate level and glycolytic flux of MM cells (A) Extracellular lactate levels were measured and normalised based on lactate standard curve. ***p <0.001. Two-way ANOVA Tukey's multiple comparison test was used to compare difference among groups, (mean ± SD, n=3). (B, C) OCR and ECAR response of MM cell lines to DCA (5 mM) when supplemented with glucose (10 mM) and glutamine (2 mM) but without pyruvate. Vehicle control for this experiment was the Seahorse assay media used in preparing the DCA dilution; the vehicle control did not cause significant changes for the ECAR and OCR readings (Appendix Figure 2.4). Data was baselined to the last basal reading of OCR or ECAR and the percentage change from basal (100%) was calculated, (mean ± SD, n=3-4); each treatment of every biological repeat consisting 5-6 wells (technical replicates). In Figure 2.8 B and C, T-test was used to analyse the statistical difference between normalised basal levels (ECAR, OCR) and levels after DCA addition for each cell line (***p <0.001).

2.3.4 The pPDH response to DCA correlated with PDK expression profiles

Total PDH (tPDH) and the inactivated phosphorylated form of PDH (pPDH) were evaluated in the MM cell lines by western blotting to test whether DCA acts on-target by inactivating PDKs.

DCA treatment decreased pPDH levels in RPMI 8226 and MM.1S cells which correlated with the growth inhibition by DCA, indicating that successful inhibition of PDK activity (**Figure 2.9**); however, the DCA treatment also reduced pPDH levels in U266 cells which were resistant to DCA growth inhibition. This may indicate that the on-target effect of DCA of reducing pPDH is insufficient to inhibit growth in U266 cells, or that the reduction in pPDH was not sustained long enough in the growth assay.

The MM cell lines had different patterns of response to DCA as revealed by their different degrees of pPDH/tPDH reduction with U266 having the fastest decrease of the pPDH/tPDH after DCA treatment (**Figure 2.9 B**). In U266, the pPDH/tPDH ratio was rapidly decreased by DCA to 25.4±10.7% after 15 minutes of DCA treatment and maintained at a low level over the 24 hours of DCA treatment. In contrast, the pPDH/tPDH ratio in RPMI 8226 was reduced to 51.4±9.8% after 15 minutes of DCA treatment and then further to 27.4 ±15.1% after 24 hours DCA treatment. (**Figure 2.9 B**).

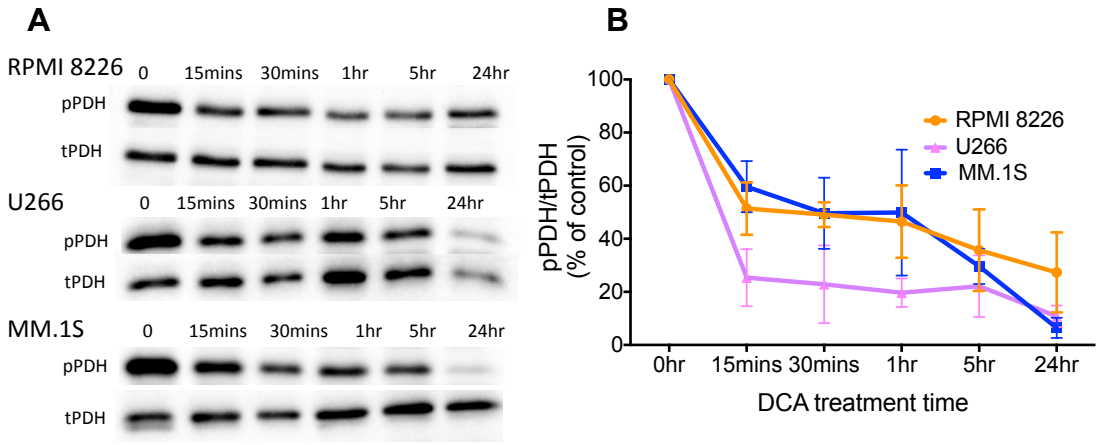

Figure 2.9 pPDH/tPDH of MM cell lines was reduced by DCA. (A) Representative western blots of at least three independent experiments showed the pPDH and tPDH protein levels after DCA treatment (5 mM). (B) Quantification showed the decrease of pPDH/tPDH ratio after DCA treatments compared to no-treatment control (normalized as 100%). Quantification of blot bands was calculated based on the results from three independent biological repeats, each data point represents mean ± SD. pPDH antibody recognises the phosphorylated site S293 of the human pyruvate dehydrogenase E1-alpha subunit. The antibody immunogen of tPDH is recombinant full-length human PDH E1-alpha subunit that can recognise both active and inactive forms of PDH. tPDH: total pyruvate dehydrogenase. pPDH: phosphorylated PDH.

The PDK profiles on MM cell lines were examined as a possible cause of the different pPDH response patterns. There are four PDK isoforms, which vary in their sensitivity to DCA (K_i of 1.0, 0.2, 8.0 and 0.5 mM for PDK 1-4, respectively. Section 1.4.1) [4]. The constitutive isoform PDK2 was expressed to a similar extent in all cell lines, but the other isoforms differed in their levels of expression (**Figure 2.10**). Based on the K_i values, hypothetically, the cell line that could best respond to DCA treatment would express PDK2 but have lower levels of expression of PDK1 and PDK3. In U266, there was less PDK1 or PDK3 expressed compared to other MM cell lines, suggesting that this cell line would not require a high level of DCA to inhibit its PDKs (**Figure 2.10).** This correlated with it having the fastest reduction of pPDH after DCA treatment (**Figure 2.9**) and greatest extent of OCR and ECAR changes as a result of DCA treatment (**Figure 2.8)**. RPMI 8226 had a higher protein level of PDK2 and a moderate level of PDK1 expression, which correlated with a slower response to DCA in reducing pPDH (**Figure 2.9, 2.10**). MM.1S had a higher PDK1 expression, which may require a higher concentration of DCA to be inhibited, and this correlated with the slowest response of pPDH reduction by DCA (**Figure 2.9, 2.10**). U266 expresses the least

amount of PDK1, 2 and 3, which may indicate that the glycolysis pathway of this particular cell line may not be upregulated under normoxia.

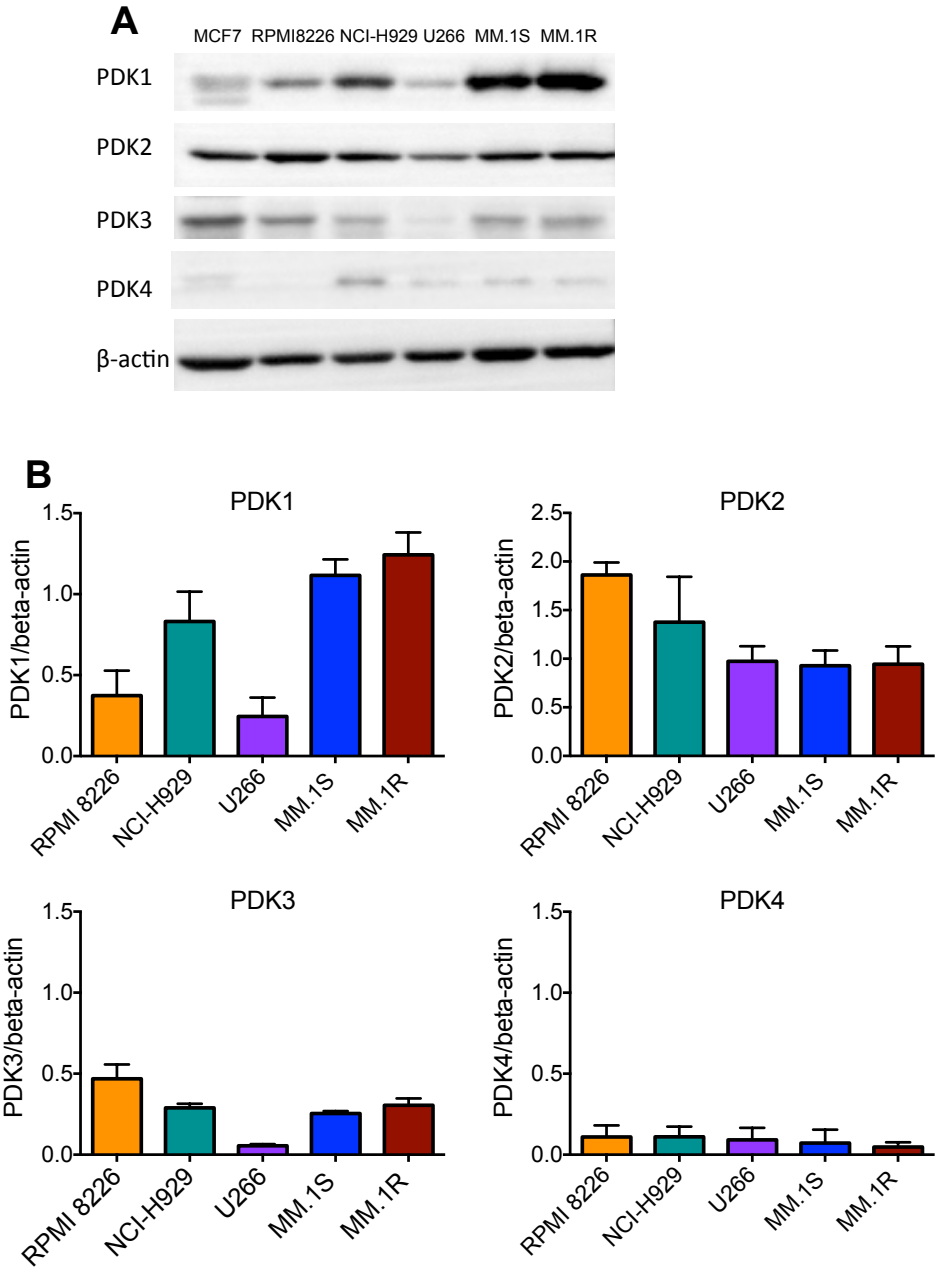

Figure 2.10 PDK expression profiles in MM cell lines (A) PDK 1-4 protein levels were measured by western blot. MCF7 breast cancer cells express all 4 PDKs and are used here as a positive control. Blot shown is representative of 3 independent biological repeats. (B) Quantification of PDK blots. Band intensity is expressed as a ratio compared to *β*-actin on the same blot. Each data point represents mean ± SD, n = 3 biological repeats.

2.3.5 Clinically achievable concentrations of DCA can act on-target by reducing pPDH

While published studies have shown the effects of high levels of DCA (≥ 10 mM) *in vitro*, these concentrations are unlikely to be achievable in patients and there is very limited information about whether DCA can act on-target when used at clinically achievable levels. Based on our DiCAM phase 2 clinical trial data, MM patients' serum DCA (6.25 mg/kg *b.i.d*) trough level was in the range of 0.04-0.79 mM and the average peak level was 0.59 mM (**Chapter 4**). The DCA (6.25 mg/kg *b.i.d*) plasma levels from the published clinical trial were in the range of 0.05-0.7 mM [235].

Based on the above information, a range of clinically achievable DCA concentrations (0.1, 0.3, 1 mM) was tested *in vitro* for the ability to reduce the level of pPDH. In RPMI 8226 cells, low level DCA (0.1 mM) reduced pPDH after 24 hours of treatment. However, there was no effect after 5 hours indicating low trough level DCA can act on-target only after longer DCA exposure (**Figure 2.11**). DCA treatments at 0.3 mM and 1 mM reduced pPDH after 5 hours, and the levels were further reduced after 24 hours of treatment (**Figure 2.11**). These results demonstrated that clinically achievable DCA concentrations can act on-target, and that the effect is cumulative over time.

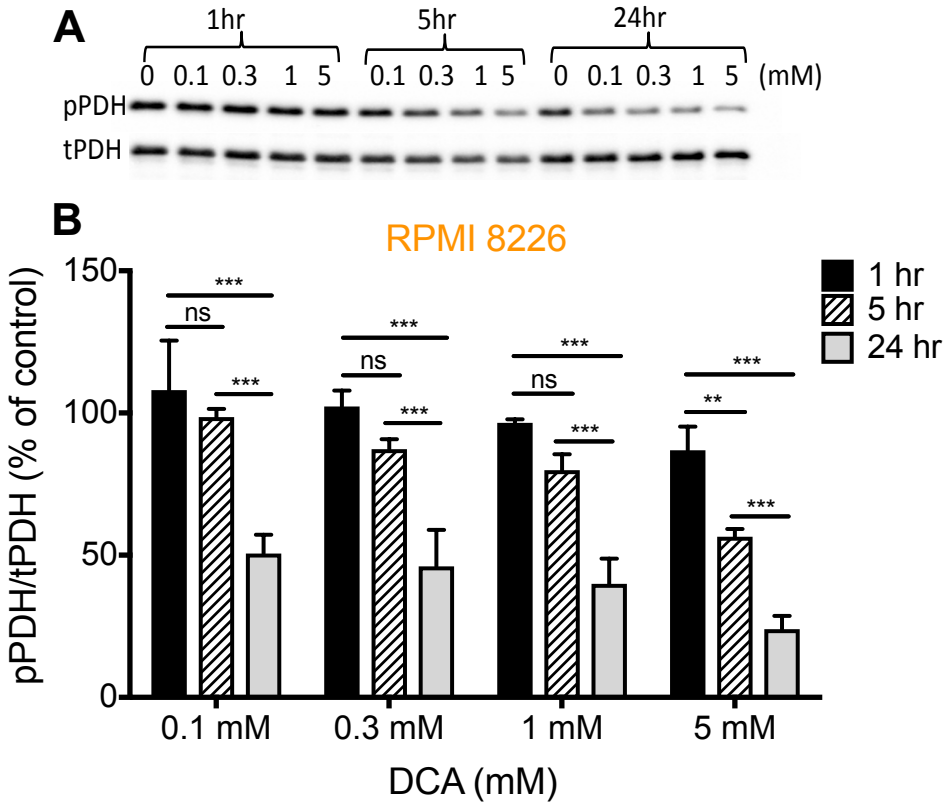

Figure 2.11 DCA at clinically achievable levels can act on-target by reducing pPDH. (A) Western blot showed the pPDH and tPDH protein levels of RPMI 8226 after DCA treatments (0.1, 0.3, 1, 5 mM) at 1 hour, 5 hours and 24 hours. The blots shown are representative of three independent experiments. (B) Quantification of western blots bands. DCA at 0.1 mM (DiCAM maintenance dose trough level) significantly reduced pPDH after 24 hours (p<0.001) but not after 5 hours. DCA at 0.3 mM (DiCAM maintenance dose peak level) and at 1 mM (DiCAM high dose peak level) showed a similar trend and also significantly reduced pPDH after 24 hours but not after 5 hours (p<0.001). Quantification of blot bands was calculated based on the results from three independent biological repeats, each data point represents mean ± SD; data was expressed as a percentage of untreated control (100%) on each blot.

2.4 Discussion

This chapter aimed to target the glycolytic phenotype of MM using DCA as a potential therapeutic approach. To address this, the anti-cancer and on-target effects of DCA at mechanistically relevant concentrations were tested on MM cell lines. In addition, the metabolic phenotypes of MM cells were evaluated and contributing factors to the sensitivity to DCA were analysed. The results of this chapter showed that DCA mainly had cytostatic effects rather than cytotoxic effects on MM cell lines when used at mechanistically relevant concentrations, where DCA (≤ 5 mM) can reduce the total viable cell number by slowing down cell proliferation, increasing the cell population doubling time without inducing apoptosis under normoxia (**Figure 2.1**). The sensitivities to DCA treatment vary significantly among the MM cell lines which may be affected by the heterogeneous metabolic profiles (**Figure 2.2, 2.4, 2.6, 2.8**) and PDK expression levels (**Figure 2.9, 2.10**). This chapter also confirmed the on-target effect of DCA of inhibiting PDKs at clinically achievable concentrations *in vitro* which was found to be cumulative over time (**Figure 2.11**).

Mechanistically relevant and clinically relevant concentrations of DCA were used in our studies. The mechanistically relevant concentrations were defined as concentrations in the range of the inhibition constant (K_i) values of DCA, which are the concentrations of DCA needed to reduce the activity of the targeted enzyme (the PDKs) by half. The four PDK isoforms vary in their K_i values to DCA (1.0, 0.2, 8.0 and 0.5 mM for PDK 1-4 respectively) [4]. The PDK profile of MM cells may contribute to their sensitivity to DCA. MM cell lines studied here expressed various amount of PDK3 (**Figure 2.10**), and the relatively low concentrations of DCA selected in this study may have not been high enough to completely inhibit PDK3 activity. This could explain why there was still residual pPDH after 24 hour 5 mM DCA treatment (**Figure 2.9**). High PDK3 expression could explain a lack of growth inhibition by DCA; however, this is not the case in U266 cells which showed the lowest PDK3 level among the 5 studied MM cell lines. Thus an alternative explanation for the insensitivity of U266 to the growth inhibition by DCA is still needed.

In previous studies of DCA in cancer, DCA was generally used at high concentrations (10-50 mM) [222], which were not only considerably higher than the mechanistically

relevant concentrations but also unachievable in patients based on data gathered from DCA pharmacokinetics studies (**Chapter 4**) and other clinical trials [5, 235]. DCA at concentrations less than 5 mM did not induce apoptosis but had growth inhibitory and metabolic modulatory effects on MM cell lines (**Figure 2.1**). However, in two previous studies of myeloma, the anti-cancer effects of DCA were not observed when used at concentrations lower than 5 mM in cell lines RPMI 8226 and U266, but the apoptosis effects shown in their studies were only seen when DCA was used in non-mechanistically relevant concentrations (10-40 mM). My results are supported by several other studies in human breast cancer, human colorectal cancer and canine mammary cancer which all showed that DCA when used at lower concentrations can only inhibit cell proliferation without inducing apoptosis [9, 10, 223, 224].

MM cells had different sensitivities to DCA treatment. In order to understand what factors contribute to the growth response to DCA, the metabolic profile of MM cell lines and the biochemical changes caused by DCA were analysed. These results clearly showed that the most glycolytic cell line (RPMI 8226) was also the most sensitive to the growth inhibition by DCA (**Figure 2.2, 2.4**). However, for the cell lines that don't fully depend on glycolysis, the results were complex. In contrast to RPMI 8226 cells, U266 cells growth was not affected by DCA (**Figure 2.1 A, B**); but DCA treatment still diverted the metabolic flux from glycolysis to mitochondrial respiration (**Figure 2.8**). Sanchez et al. also identified RPMI 8226 as a typical glycolytic cell line while U266 was non-glycolytic and showed that DCA had metabolic modulatory effects such as reducing lactate production, suppressing glycolysis and improving cellular respiration; however, only high concentrations of DCA were investigated in their study [11]. U266 was found to have the highest glycolytic reserve when mitochondrial respiration was inhibited with ETC inhibitors (**Figure 2.4 C, 2.7 B**), which correlated with its high spare respiration capacity (**Figure 2.6 D**). These data indicate that U266 had greater potential to adapt to mitochondrial stressed condition (such as in hypoxia) (**Chapter 3**). U266 was not a typical glycolytic cell line like RPMI 8226 (Figure 2.8); thus it could have a preference for other nutrients such as glutamine or fatty acids (**Chapter 3**) to fulfil its biological needs. This may explain why the metabolic modulatory effect of DCA on U266 was not sufficient to cause growth inhibition.

These results showed correlation of the different sensitivity to DCA and their heterogeneous metabolic profiles, which are in agreement with studies demonstrating that DCA as an agent to promote mitochondrial respiration can confer selective toxicity against cancer cells that are dependent on glycolysis or having deficiency in mitochondrial respiration. For example, DCA caused pro-apoptotic effects on glycolysis-dependent oral squamous cell carcinomas (OSCC) cells but not on OSCC cells with an efficient mitochondrial respiration [341]. DCA was found to be cytotoxic towards mitochondrial DNA (mito-DNA)-deficient MOLT4 and MCF7 cancer cells, and synergize with mito-DNA damaging agents (cisplatin and topotecan) *in vitro* [226]. This characteristic of DCA has been harnessed by co-targeting mitochondria and glycolysis at the same time. The combination of DCA and arsenic trioxide (inhibitor of the complex IV) was more effective in inducing apoptosis than either agent alone in breast cancer cell lines [9]. A mitochondrial toxin (PENAO) currently in early phase clinical trials also showed enhanced cytotoxicity when combined with DCA in breast cancer cells [232]. Due to the metabolic heterogeneity of the MM cells lines, the preference of MM cells for different nutrient fuels and their abilities to adapt under mitochondrial respiration stressed conditions need to be taken into consideration (**Chapter 3**).

This chapter also characterised the metabolic profiles of two isogeneic MM cell lines that have not been reported on previously. MM.1R (DEX resistant) shows a more glycolytic phenotype than its isogeneic counterpart MM.1S (DEX sensitive), as MM.1R showed higher lactate production and glucose consumption levels, greater basal glycolysis rate and glycolytic capacity (**Figure 2.2, 2.4**). These results are consistent with the hypothesis proposed that glucocorticoid resistance is correlated with upregulated glycolysis [325]. This leads to the question of whether DCA can reduce the resistance to DEX in MM.1R cells, which has been investigated in Chapter 4.

In addition to studying the metabolic profile and biochemical changes, a further examination of the protein expression of the targets of DCA (the PDKs) was carried out to elucidate different sensitivities to DCA. Previous research in this lab showed that the sensitivity of breast cancer cells to DCA is correlated with their PDK profiles. The breast cancer cell line T-47D expressed high PDK2 level but with low levels of other

isoforms, and it was the most sensitive to growth inhibition by DCA. In contrast, MCF7 expressed high PDK3 level and was not sensitive to DCA treatment, but PDK3 siRNA knockdown led to considerably increased sensitivity to DCA [232]. In MM cell lines, the PDK expression levels correlated with their sensitivity to DCA to some degree, but could not fully explain why the growth of U266, which had less PDK expression and should be theoretically easier to be inhibited by DCA (**Figure 2.10**), was not inhibited by DCA. The PDK profiles may, however, correlate better with the metabolic modulatory effects of DCA instead of the biological growth outcomes. For example, U266 expressed less PDK1 and PDK3 compared to other MM cell lines (**Figure 2.10),** and this PDK profile correlated well with having the fastest reduction of pPDH after DCA treatment (**Figure 2.9**). The speed of reduction of pPDH levels in U266 also correlated with having the greatest extent of OCR and ECAR changes by DCA in the Seahorse assay due to the very short timeframe of this assay (**Figure 2.8**). A similar finding was shown in a study where human colorectal cancer cell line SW480 had the lowest PDK expression but was not sensitive to the growth inhibition by DCA, and the effects of DCA in reducing pPDH correlated with changes of mitochondrial activity, but these metabolic modulatory effects also did not lead to significant changes in cellular growth [342]. These results indicate that DCA can successfully modulate metabolism and act on-target but this function may not directly correlate to reduced cancer cell proliferation. A summary of the response patterns of RPMI 8226 and U266 to DCA treatment is displayed in Table 2.5. This table shows the relationship among the on-target effects of DCA (pPDH, OCR), the impact on glycolysis pathway (ECAR, lactate), and the biological outcomes (cell growth and apoptosis).

Table 2.5 Summary of response patterns to DCA in normoxia (N)

	On-target effects: Mitochondrial Respiration		Biological outcome		Feedback regulation (upstream of targets): Glycolysis	
Readout	**pPDH**	**OCR**	**Growth**	**Apoptosis**	**ECAR**	**Lactate**
Conditions	**N**	**N**	**N**	**N**	**N**	**N**
RPMI8226	↓	↑	↓	→←	↓	↓
U266	↓	↑	→←	→←	↓	→←

↓: decrease. ↑: increase. →←: no effect.

This chapter has identified a series of factors that can contribute to the sensitivity to DCA of MM cells, but there are more components that could potentially affect the sensitivity, which can be studied in the future. A possible obstacle for DCA to act on-target effectively is its possible inefficiencies in the process of transportation from the extracellular environment into its target location - the mitochondria. This chapter has provided evidence that argues in favour of DCA being transported quickly into the mitochondria. As the results showed that in RPMI8226 and U266, DCA changed the flux from glycolysis to mitochondrial respiration within minutes of injection (**Figure 2.8**), and in all cell lines tested reduced the pPDH protein level within an hour (**Figure 2.9**). DCA is ionized and cannot pass through the plasma membrane by passive diffusion, but studies showed that DCA as a haloacid, was able to be effectively transported to the cytosol through haloacids transporters, such as sodium-coupled monocarboxylate transporter (MCT1/SLC5A8) [343, 344]. DCA is a pyruvate mimetic that can be transported into the mitochondrial matrix through the mitochondria pyruvate carrier (MPC) [345-347]. However, cancer cells often have altered expression of MCT and MPC [344], so resistance to DCA may be mediated through the lack of DCA transporters. However, the time course results of the pPDH in this chapter suggest that with prolonged exposure, as would happen in patients, DCA will be able to enter the cells to inhibit PDKs.

The amount of pyruvate dehydrogenase phosphatases (PDP) present in mitochondria may also influence the effects of DCA. In the mitochondrial matrix, PDPs have the opposite function to PDKs, that is to dephosphorylate and activate PDH [348]. DCA inhibits PDKs to reduce the new phosphorylation of PDH but needs PDP to be present in mitochondria to dephosphorylate and reactivate the PDH complex. The deficiency of PDP is a rare mitochondrial disorder featured with cellular low native PDH complex activity. It has clinically heterogeneous symptoms such as fatal infantile lactic acidosis, neonatal hypotonia, and intolerance to exercise. DCA incubation can partially restore the activity of the PDH complex in skin fibroblasts of patients with PDP deficiency, but the degree of the restoration varies, possibly due to the different levels of PDP deficiency [200]. In an extreme case of lethal infant null PDP mutation where the PDP1 protein in mitochondria was completely absent, DCA failed to activate the PDH complex in skin fibroblasts [349]. Thus, in order for DCA to activate PDH, some

amount of PDP is required to be present in mitochondria. Lower levels of PDPs may confer relative resistance or a slower response time to DCA.

DCA can divert the pyruvate flow from glycolysis to mitochondrial respiration but it does not directly inhibit the conversion of pyruvate to lactate. LDHA, that converts pyruvate to lactate, is upregulated in many different human cancers thus also needs to be considered in the holistic picture of intervening in the glycolysis pathway [350, 351]. The LDHA expression level of the MM cells could be a contributing factor to their sensitivity to DCA, as LDHA mRNA level was positively correlated with the expression of genes associated with glycolysis such as *PDK1*, *GLUT1*, and oncogene *MYC* in MM cells [12], thus a high level of LDHA may play a role in the degree of dependence of MM cells on glycolysis, and then affect their response to DCA. U266 was found to have no LDHA mRNA expression but RPMI 8226 has high LDHA expression. In RPMI 8226 cells, a higher LDHA expression level was associated with higher glycolytic activity, which was reflected by greater glucose consumption and lactate production [12]. In this chapter, RPMI 8226 was also found to be a highly glycolytic cell line and to be the most sensitive to growth inhibition by DCA while U266 was not glycolysis-dependent and did not respond to the growth inhibition by DCA. The expression levels of LDHA could be further investigated as a factor contributing to the growth inhibition by DCA on MM cells.

In conclusion, this study demonstrated that DCA at mechanistically relevant concentrations mainly had cytostatic effects on MM cells, and that DCA at clinically achievable concentrations can act on-target by inhibiting PDKs *in vitro*. However, the on-target effect of DCA did not always correlate with the inhibition of MM cell growth. Among the factors that could contribute to the different sensitivities to DCA, the degree of dependence of MM cells on glycolysis surfaced as the most likely factor.

Chapter 3

Impact of metabolic stress on the effects of DCA

Abstract

Background: Multiple myeloma (MM) originates from the bone marrow (BM). The nutrient supply and oxygen distribution in the BM microenvironment (BMM) are heterogeneous. The hypoxic niches are crucial for MM development, progression, and drug resistance; and the hypoxic environment promotes glycolysis. DCA is a PDK inhibitor that can promote mitochondrial respiration over glycolysis. Targeting MM cell metabolism using DCA needs to consider the interaction between MM cells and the BMM. Studying the effects of DCA under nutrient deprivation and hypoxic conditions may offer insight into the clinical use of DCA and how well DCA can act in BMM. **Methods:** The effects of DCA on MM total viable cell number under nutrient stressed conditions (glucose or glutamine deprivation) were measured by neutral red uptake assay, the effect on glycolysis and mitochondrial respiration under glucose or glutamine deprived conditions was measured by Seahorse XF analyser. The mRNA and protein levels of the DCA targets (PDK1, 2 and 3) in hypoxia were measured by RT-PCR and western blot. In hypoxia, the effects of DCA on MM cells were measured through examination of the extracellular lactate levels, total viable cell numbers, and apoptosis. **Results:** MM cells displayed variable dependence on glucose or glutamine. DCA cannot further reduce the total viable cell number when glucose was not present or when glucose uptake was inhibited by 2-deoxyglucose. The effect of DCA in promoting mitochondrial respiration and suppressing glycolysis was also abolished when glucose was absent. Under hypoxia, DCA can induce apoptosis in a non-glycolytic cell line, which had the greatest glycolytic reserve and the highest increase of PDK1 and PDK3. **Conclusions:** The anti-growth effect of DCA requires glucose to be present and an active glycolysis pathway. DCA can have cytotoxic effects in hypoxia in cell lines that had greater glycolytic reserve. DCA may be useful in the treatment of hypoxic cancers.

3.1 Introduction

The previous chapter demonstrated DCA had on-target and anti-growth effects on MM cells when used at mechanistically relevant concentrations. This warranted further investigations in this chapter to test if metabolic stress conditions that mimic the BMM can impact on the effects of DCA on MM cells. The BMM presents with a nutrient stressed condition due to the complicated structure and different vascular perfusions, similar to that of a solid tumour (Section 1.5.3.2). MM cells have heterogeneous metabolic phenotypes, which extend beyond the glycolytic phenotype and contributes to the plasticity of MM cells, promoting survival [12, 25, 125, 179, 262, 280, 281]. This metabolic heterogeneity was also reflected in previous results that only a subset of MM cells is sensitive to glycolysis inhibitors. The resistance to glycolysis inhibitors was developed through compensation by alternative metabolic pathways such as glutamine metabolism [13, 352]. When glucose access is limited, cancer cells can upregulate glutamine metabolism to replenish the precursors for the macromolecular biosynthesis such as lipids, proteins, and nucleic acids [280, 353]. Hypoxia inducible factors (HIFs) are important to ensure cancer cell survival under stressed conditions. They can be activated by hypoxia, but also by growth factors, oncogene activation, or tumour suppressors mutations [27, 29, 34, 35, 37, 38]. HIFs enhance glycolysis by altering expression of the downstream effectors such as glucose transporters and glycolytic enzymes such as LDHA and PDK [48, 276], which contribute to an increased rate of glycolysis.

Dichloroacetate (DCA) can reverse the glycolytic phenotype by inhibiting pyruvate dehydrogenase (PDH) kinase (PDK) [222]. To repurpose DCA for the treatment of MM, evidence is needed to confirm that DCA can have anti-growth effects in conditions that may arise in the BMM, such as limited nutrient or oxygen supply. Reports of the effects of DCA under hypoxia in cancer cells have had conflicting results ranging from enhanced cytotoxicity in glioma cells [354] to the cytoprotective effects in colorectal cancer cells [355]. In this chapter, the MM cells were screened for their preference for different nutrients, and the effects of DCA under nutrient deprivation or hypoxic conditions were investigated. This chapter hypothesized that the effects of DCA on MM cells may depend on an active glycolysis pathway, and DCA may have greater effects on MM growth under hypoxic conditions.

3.2 Material & Methods

3.2.1 Nutrient deprivation assay

MM.1S, MM.1R and RPMI 8226 were cultured in recommended RPMI-1640 media (31800, Thermo Fisher) supplemented by 10% (volume/volume) heat-inactivated fetal bovine serum (FBS), 2 mM L-glutamine, 10 mM HEPES, 1 mM sodium pyruvate and 100 μg/ml antibiotics (penicillin and streptomycin) at 37℃ in a 5% CO_2 atmosphere. U266 was cultured in RPMI-1640 media with 15% FBS (**Chapter 2**). For growth in glutamine/glucose free conditions, normal growth media was removed; cells were washed and resuspended with either glutamine-free (#21870 Invitrogen) or glucose-free (#11879 Invitrogen) RPMI-1640 media. 2-Deoxyglucose (2-DG, Sigma, Lot No. 99C-5026), a glucose analogue, was used in this study to simulate glucose deprivation as it can competitively inhibit glucose uptake. 2-DG was diluted in 1× PBS to produce a stock solution of 100 mM. The stock solution was stored for long-term at 4°C and was stable. 2-DG was diluted in assay media on the day of use and the vehicle (PBS) was diluted to less than 5% of the total volume per well. MM cells were seeded in 96-well round bottom plates at optimized cell densities. Neutral red staining (**Chapter 2, section 2.2.3**) was used to quantitatively estimate the number of total viable cells after the nutrient deprivation treatments. The total viable cell number of treated cells was expressed as the percentage of the untreated control. Each treatment was performed in quadruplicate wells on each plate; three independent experiments were carried out.

3.2.2 Glycolysis and mitochondrial respiration measurements under different nutrient conditions

Metabolism profiling of cell lines was measured using Seahorse XFe96 analyser (Seahorse Bioscience, MA, USA) (**Chapter 2, section 2.2.8**). The XFe96 analyser measures *in vitro* changes in cellular bioenergetics by simultaneously measuring the oxygen consumption rate (OCR, indicating mitochondrial respiration) and the extracellular acidification rate (ECAR, indicating glycolysis). Cells were maintained in RPMI-1640 media before the assay, which was replaced with Seahorse assay media with different nutrient supplements. The media nutrient conditions included 10 mM glucose only or 2 mM glutamine only, or both combined. Cell lines were seeded at 80,000 cells/well in XFe96 culture plates (Seahorse Bioscience, North Billerica, MA,

USA) in 50 μL of unbuffered assay media (Seahorse Bioscience) (pH: 7.4 ± 0.01). The experiments followed the same protocol from **Chapter 2**. After 4 basal readings of cells exposed to the above mentioned nutrient conditions, the first injection was 5 mM DCA followed by oxamate (20 mM, LDHA inhibitor), FCCP, then a mixture of rotenone and antimycin A that target different components of the ETC in the mitochondria (**Chapter 2, Figure 2.5 B**). The cells (adhered with Cell-Tak) were checked shortly after the assay using Incucyte Zoom (ESSEN Bioscience, USA) to confirm that the cell numbers in each well remain uniform after the assay, allowing exclusion of wells with cells being flushed off in the assay (**Chapter 2**). Each treatment had 5-6 replicate wells on each plate, and 3-4 independent experiments were performed.

3.2.3 Hypoxia and total viable cell number assay

For hypoxic conditions, cells grown in T-25 flasks or 96 well plates were kept in a sealed hypoxic chamber (Billups-Rothenberg, Delmar, CA, USA) with humidified condition. Oxygen was flushed out with beta gas (95% nitrogen, 5% CO_2) at 20 L/min for 4 minutes and the gas inside the flasks was allowed to equilibrate for 3 hours. The chamber was then flushed multiple times until an atmosphere of 0.3% O_2 condition was obtained (the number of flushes required was estimated based on the flask/plate volume within the chamber), after that the flasks/plates were incubated for 24 hours at 37℃. Total viable cell numbers under hypoxia were measured using neutral red assay (**Chapter 2**). Assays were carried out in two identical replicate plates; one plate was used as normoxia control for each hypoxia plate. Each treatment condition was quadruplicated in each experiment and three independent experiments were carried out.

3.2.4 Apoptosis

Cell apoptosis and cell death were measured using AnnexinV-FITC (BD Biosciences Pharmingen, 556419) and 7AAD (BD Biosciences Pharmingen, 559925) staining followed by FACS analysis (**Chapter 2, section 2.2.6**). Cells were seeded at 30,000/well in U-bottom 96-well plates and treatment plates were duplicated, one plate was used as normoxia control, the other one was used as hypoxia treatment. Each treatment condition was duplicated in each experiment and four independent experiments were performed.

3.2.5 Extracellular lactate level under hypoxia

The extracellular lactate levels were measured using Lactate Pro2 meter (ARKRAY, Inc, test range 0.5-25 mmol/L) (**Chapter 2, section 2.2.7**). Cells were seeded at 30,000 cells /well (200 μL/well) in 96-well plates. Each treatment condition was duplicated in each experiment and three independent experiments were performed.

3.2.6 Western blot

PDK protein expression under normoxia and hypoxia was measured by western blot according to the same protocol in Chapter 2. Proteins (30 μg/sample) were separated by 10% SDS-PAGE and transferred to PVDF membranes (Bio-Rad) by wet transfer method (**Chapter 2, section 2.2.9**). Blots were incubated with the primary antibodies at 4°C overnight, the specific information were listed in **Table 2.3**. Three independent experiments were carried out. The final results were presented here as the percentage of each cell lines' normoxia control (normalized to 100%).

3.2.7 Real-Time Polymerase Chain Reaction

3.2.7.1 RNA extraction from cells

RNA from cells was isolated according to the manual instructions (PureLink RNA Mini Kit, Life technologies). Approximately 1×10^6 cells were collected into an RNase-free tube and centrifuged at 2,000 × g for 5 minutes at 4°C. Growth media was discarded and 300 μl fresh lysis buffer containing 1% 2-mercaptoethanol was added. Cells were vortexed at high speed until the cell pellet was completely dispersed and fully lysed. The cell lysates were passed 5-10 times through a 21-gauge needle attached to an RNase-free syringe. One volume of 70% ethanol was added to each volume of cell homogenate, and then was mix thoroughly. Up to 700 μL of the mixture was transferred to the spin cartridge with the collection tube and was centrifuged at 12,000 ×g for 15 seconds at room temperature. The flow-through was discarded and the spin cartridge was reinserted back into the same tube. This washing process was repeated once. Wash Buffer I (700 μL) was added to the spin cartridge and centrifuged at 12,000 ×g for 15 seconds at room temperature. The flow-through was discarded and the spin cartridge was inserted into a fresh collection tube. Tubes were centrifuged at 12,000 ×g for 15 seconds at room temperature after 500 μL Wash Buffer II with ethanol was added to the

spin cartridge. The same washing steps were carried out as described above and repeated once. The cartridge was spun at 12,000 ×g for 1-2 minutes to dry the membrane. The spin cartridge was inserted into a recovery tube, 30 μL RNase–Free water was added to the centre of the cartridge and incubated at room temperature for 1 minute. The spin cartridge was centrifuged for 2 minutes at 12,000 ×g at room temperature to elute the RNA.

3.2.7.2 DNase treatment

DNA contamination was removed from the RNA samples using Ambion® TURBO DNA-free™ DNase Treatment and Removal Reagents (TURBO DNA-free kit, life technologies). 0.1 volume of 10× TURBO DNase Buffer and 1 μL TURBO DNase were added to the RNA and mixed gently, then incubated at 37°C for 20-30 minutes. 0.1 volume of resuspended DNase inactivation reagent was added and incubated for 5 minutes at room temperature, the content was mixed by flicking every minute. The supernatant containing RNA was transferred to fresh tubes after centrifugation at 10,000 ×g for 1.5 min. Then the purified RNA was aliquoted and stored at -80°C. RNA concentrations were quantified using Nanodrop (Spectrophotometer, ND-1000).

3.2.7.3 cDNA synthesis

SuperScript III Reverse Transcriptase (Invitrogen) was used to synthesize first-strand cDNA. 250 ng RNA was reverse transcribed. A 20 μl reaction mixture contains 1 μl of oligo(dT)$_{12\text{-}18}$; 250 ng mRNA; 1 μl 10 mM dNTP Mix (10 mM each dATP, dGTP, dCTP and dTTP at neutral pH) and sterile distilled water. Mixture was heated to 65°C for 5 minutes and incubated on ice for at least 1 minute. The content of the tube was collected by brief centrifugation and a mixture containing 4 μl 5 × First-Strand Buffer; 1 μl 0.1 M DTT; 1 μl RNaseOUT™ Recombinant RNase Inhibitor (Cat. no. 10777-019, 40 units/μl) and 1 μl of SuperScript™ III RT (200 units/μl) was added. The sample was mixed gently by pipetting and incubated at 50 °C for 30-60 minutes. The reaction was heat-inactivated at 70°C for 15 minutes. The cDNA was dilute to 2.5 ng/μl for use as a template for amplification in polymerase chain reaction (PCR). A total of 10 ng cDNA was used per reaction.

3.2.7.4 Real-Time PCR

Power SYBR Green PCR Master Mix (Applied Biosystems) was used for relative quantification of gene expression in 384 well plates on the Fast Real-Time PCR Detection System (AB Applied Biosystems, Model No. 7900HT). A total amount of 10 μl-reaction mixture composed of 5 μl *Power* SYBR Green PCR Master Mix, 300 nM reverse primer and forward primer separately (original concentration was 200 μM in nuclease-free water) and 4 μl template cDNA. PDK1, PDK2, PDK3, HPRT1 (hypoxanthine- phosphoribosyltransferase 1) and GAPDH real-time PCR primers (Integrated DNA Technologies) for mRNA expression are listed in the table below (F.: forward primer; R.: reverse primer).

Table 3.1 Summary of the primers

Name	Gene symbol	Primer sequence
Hypoxanthine phosphoribosyltransferase1 (Human)	HPRT1	F. 5'-CCTGGCGTCGTGATTAGTGAT-3' R. 5'-AGACGTTCAGTCCTGTCCATAA-3'
Glyceraldehyde-3-phosphate dehydrogenase (Human)	GAPDH	F. 5'-CATGAGAAGTATGACAACAGCCT-3' R. 5'-AGTCCTTCCACGATACCAAAGT-3'
Pyruvate dehydrogenase kinase 1 (Human)	PDK1	F.5'-CTATGAAAATGCTAGGCGTCT-3' R.5'-AAC-CACTTGTATTGGCTGTCC-3'
Pyruvate dehydrogenase kinase 2 (Human)	PDK2	F.5'-AGGACACCTACGGCGATGA-3' R.5'-TGCCGATGTGTTTGGGATGG-3'
Pyruvate dehydrogenase kinase 3 (Human)	PDK3	F.5'-GCCAAAGCGCCAGACAAAC-3' R.5'-CAACTGTCGCTCTCATTGAGT-3'

PCR efficiency of the gene of interest and the internal control genes were optimized before experiments [356]. The thermal-cycling conditions consisted of an enzyme activation step at 95°C for 10 mins followed by 40 PCR cycles of 15 seconds at 95°C and 60 seconds at 60°C. RT-PCR data were analysed using comparative Ct (threshold cycle) method also known as the $2^{-\Delta\Delta Ct}$ method to compare the expression of interested genes relative to the internal control in the treatment group compared with the untreated group [356]. The equation used is shown below:

$2^{-\Delta\Delta Ct}$ = {(Ct gene of interest – Ct internal control) Group A

– (Ct gene of interest – Ct internal control) Group B)}

Each treatment was performed in triplicate on the same 384-well plate, and three independent experiments were carried out.

3.2.8 Statistical analysis

Numerical data were presented as mean ± standard deviation (SD). T-test was applied to test the difference between two groups. One-way ANOVA with Tukey's multiple comparison test was used to compare single mean among groups. Two-Way ANOVA with Tukey's multiple comparison test was used to compare multiple means among different groups. A probability level of $p<0.05$ will be considered statistically significant. The EC_{50} for 2-DG treatment was calculated by fitting a nonlinear regression dose-response curve using dose-response equations. GraphPad Prism (version 6.0f) was used for all statistical analysis.

3.3 Results

3.3.1 The effect of DCA on total viable cell number depends on the presence of glucose

Metabolism study in Chapter 2 showed different glycolytic and mitochondrial respiration capacities among MM cell lines and identified the most glycolytic cell line (RPMI 8226) being the most sensitive one to DCA treatment. Further experiments were carried out to investigate the dependency of the MM cells on glucose or glutamine, and to analyse the effects of DCA under these different nutrient conditions. The neutral red uptake assay was carried out to investigate if the different nutrient supplements can affect the total viable cell numbers with or without the presence of DCA. RPMI 8226 was the most sensitive cell line to glucose-free media compared to other MM cell lines as indicated by the significant 58% decrease in the total viable cell number (**Figure 3.1 A**), and consistent with it having the most glycolytic phenotype (Chapter 2). In standard media, DCA was able to reduce cell growth by 29%. In contrast, DCA was unable to further reduce growth when added to the glucose-free media. The growth of RPMI 8226 was reduced to a lesser extent in glutamine-free media (23% decrease) and, although the decrease was not statistically significant, DCA was able to further reduce the total viable cell number in the glutamine-free media by 12% (p=0.35) (**Figure 3.1 A**). These results indicate RPMI 8226 cells have a stronger preference for glucose over glutamine, and that the effects of DCA on cell growth are dependent on the presence of glucose in the media.

U266's total viable cell numbers were unaffected by glutamine or glucose deprivation indicating the ability of U266 cells to use both nutrient sources, and DCA was unable to impact on cell growth in any media (**Figure 3.1 B**). The total viable cell numbers of MM.1S and MM.1R were not significantly reduced by glutamine or glucose deprivation, but DCA treatment of MM.1R cells significantly reduced the total viable cell numbers in glutamine-free media (p<0.05). These results indicated different cell lines had different nutrient preferences. The results showed that DCA cannot further decrease total viable cell number in the glucose-free condition indicating the effects of DCA on growth inhibition requires the presence of glucose.

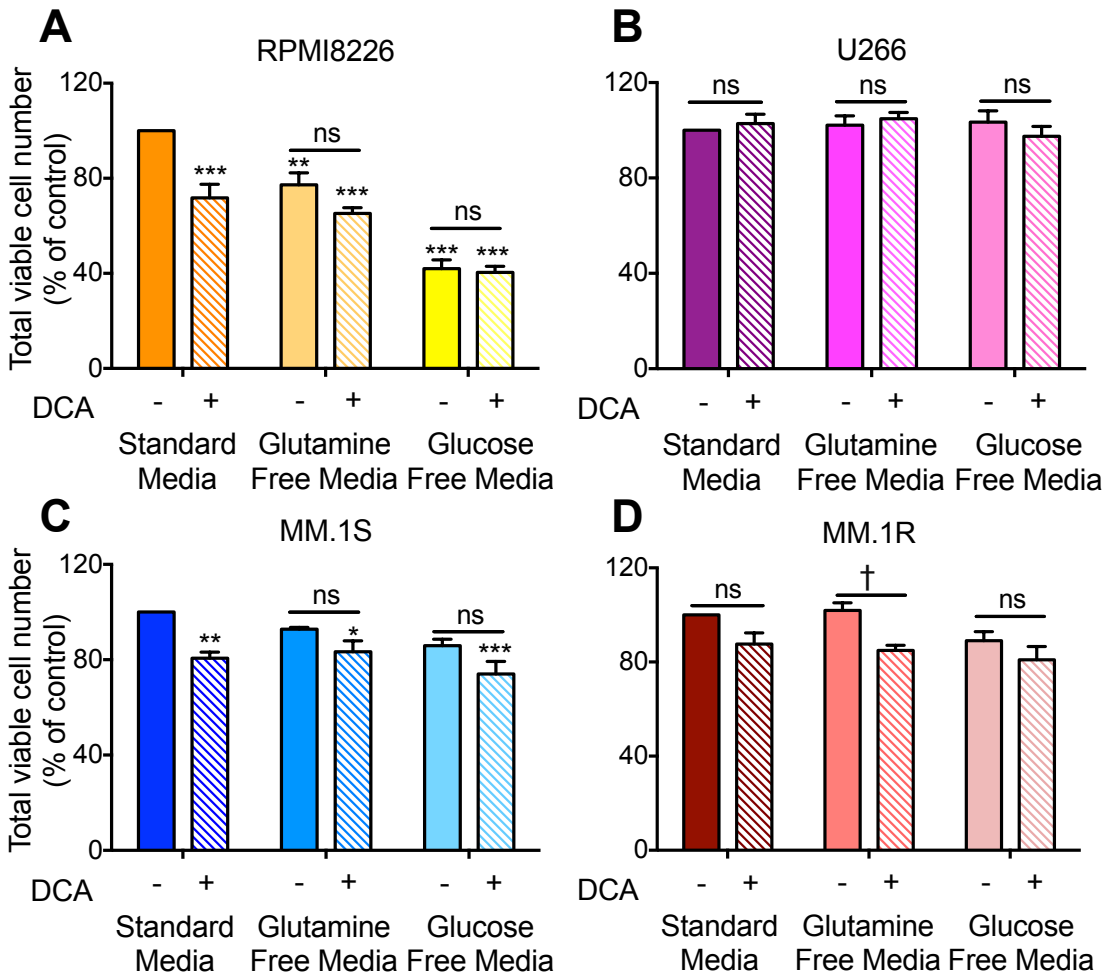

Figure 3.1 The effect of DCA on total viable cell number in different nutrient conditions. MM cell lines were maintained in different media with or without DCA (5 mM) for 72 hours. Neutral red assay was used to measure total viable cell numbers. *Statistical comparisons represent treatment groups compared to Standard Media without DCA treatment group; *$p < 0.05$, ** $p < 0.01$, ***$p < 0.001$. † Statistical comparisons between DCA treatment group to the corresponding media without DCA treatment group; † $p < 0.05$. Each treatment was quadruplicated. All data points shown represented mean ± SD from at least 3 independent experiments.

To further confirm the glucose-dependence of the effect of DCA, glucose deprivation on MM cells, 2-DG was used to simulate glucose deprivation. 2-DG is a glucose analogue that can competitively inhibit glucose uptake and can be phosphorylated by hexokinase to 2-deoxyglucose-6-phosphate but cannot be further metabolized, thus it inhibits glycolysis and can cause ATP depletion (Section 1.3.1). The growth inhibition effect of 2-DG alone on MM cell lines was variable (**Table 3.2, Figure 3.2 A**), and RPMI 8226 was the most sensitive to 2-DG while U266 was the least sensitive, correlating with sensitivity to glucose deprivation and DCA (**Figure 3.1, 2.1**). Treatment of cells with the combination of DCA and 2-DG showed that DCA cannot further decrease the total viable cell number in MM cells when treated with 2-DG (**Figure 3.2 B**), indicating that the effect of DCA is lost when glucose uptake is inhibited.

Table 3.2 2-deoxyglucose EC_{50}

Cell Lines	*EC_{50} (mM)	95% confidence intervals
MM.1S	3.3	3.0 - 3.6
MM.1R	4.8	3.6 - 6.3
RPMI8226	2.3	1.9 - 2.9
U266	11.6	8.9 -15.1

* Derived from data in Figure 3.2 A.

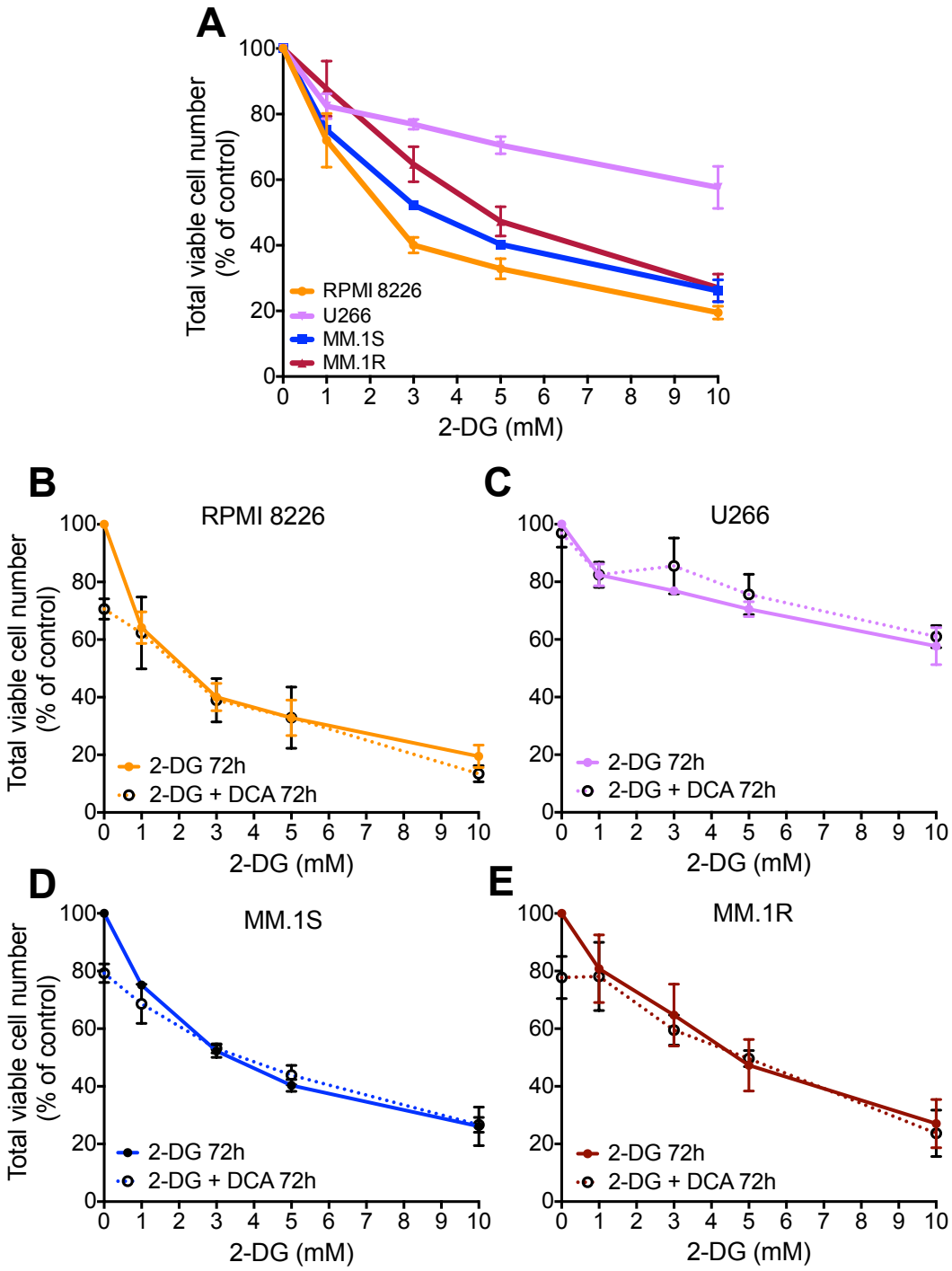

Figure 3.2 DCA cannot further reduce the total viable cell number when combined with 2-DG (A) MM cell lines sensitivities to 2-DG alone. (B-E) DCA and 2-DG combination treatment cannot further decrease total viable cell number compared to 2-DG alone in all MM cell lines. Each treatment was quadruplicated per experiment. All data points shown represented mean ± SD from at least 3 independent experiments;

3.3.2 Nutrient supply alters the effect of DCA on glycolysis and mitochondrial respiration

To analyse the contribution of different nutrients to the glycolysis and mitochondrial respiration of MM cells, basal OCR (mitochondrial respiration indicator) and ECAR (glycolysis indicator) were measured in standard, glutamine-free and glucose-free conditions (**Figure 3.3 A, B**). Glucose was mainly contributing to ECAR while glutamine was mainly contributing to the OCR when MM cells were tested in deficient media conditions (**Figure 3.3 A, B**). The ECAR levels were reduced significantly in MM cell lines in media supplemented with glutamine but without glucose. RPMI 8226's OCR levels were increased by 50% and ECAR levels decreased by 3-fold in media only supplemented with glutamine without glucose indicating a dynamic switch between mitochondrial respiration and glycolysis. However, when glucose was present either in standard or glutamine-free media, the OCR and ECAR were not significantly different under these two conditions indicating RPMI 8226 preferably utilized glucose over glutamine. A similar trend can be seen in other MM cell lines but the degree of the changes was trivial (**Figure 3.3 A, B)**.

RPMI 8226 was identified as the most glycolytic cell line while U266 did not present a glycolytic phenotype but had the highest glycolytic reserve (**Chapter 2**). In this chapter, when glucose was present, RPMI 8226 and U266 both responded to the effect of DCA in redirecting glycolysis to mitochondrial respiration indicated by the increased OCR and decreased ECAR levels compared to the basal levels ($p<0.001$). U266 had greater response to this metabolic modulatory effect of DCA as it had the highest OCR increase by 12.7% and highest ECAR decrease by 29% compared to other MM cells in standard media (**Figure 3.3 C, D**). When glucose was present in the media, this metabolic modulatory effect of DCA remain effective in RPMI 8226 and U266, but this effect was abolished when glucose was absent from the media (**Figure 3.3 C, D**). DCA treatment in MM.1S and MM.1R did not demonstrate similar changes of OCR and ECAR observed in that of RPMI 8226 and U266. This result indicated that the effect of DCA in promoting mitochondrial respiration over glycolysis requires glucose to be present.

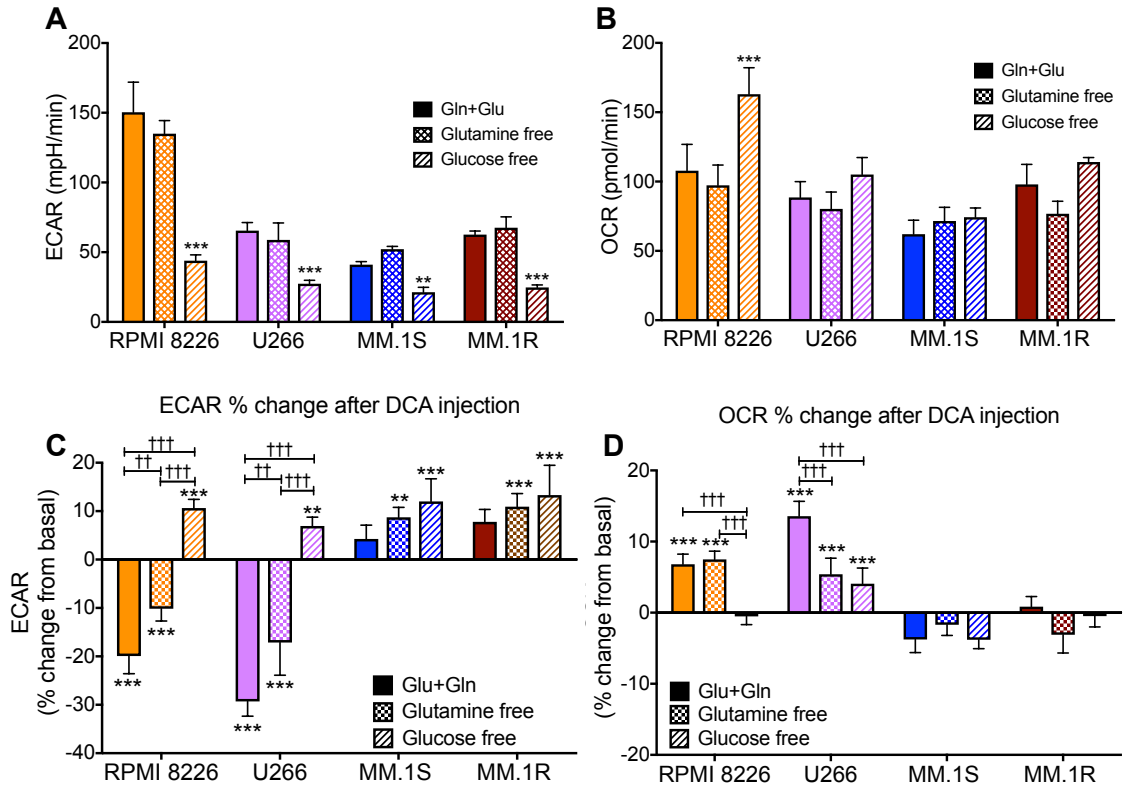

Figure 3.3 The effect of DCA on OCR and ECAR levels under different nutrient conditions. (A, B) Basal ECAR and OCR levels of each cell line under different nutrient conditions. * Statistical comparisons between each cell line's conditioned media groups to its standard media group. (C, D) Percentage change of ECAR and OCR after DCA (5 mM) injection compared to basal OCR and ECAR levels. T-test was used to analyse the difference between normalised basal levels (ECAR, OCR) and levels after DCA addition for each cell line (*). Two-way ANOVA was used to analyse the difference in percentage change after DCA treatment in different media conditions for each cell line (†). Each treatment had 5-6 replicates wells per experiment. All data points shown represent mean ± SD from at least 3 independent experiments; ** $p < 0.01$, *** $p < 0.001$, †† $p < 0.01$, ††† $p < 0.001$.

LDHA is an enzyme converting pyruvate into lactate. Many malignant tumours express higher LDHA levels compared to normal tissues (section 1.3.1) [122]. As an inhibitor of LDHA, sodium oxamate can inhibit lactate production, so it can have similar effect as DCA of redirecting pyruvate into TCA cycle. Thus, the effects of oxamate with or without DCA on glycolysis and mitochondrial respiration were examined to investigate the impact of the pyruvate flux into the TCA cycle to the effects of DCA. Oxamate treatment caused similar changes to OCR and ECAR compared to DCA in RPMI 8226 and U266 cells, increasing OCR and significantly decreasing ECAR when glucose was present; however, this effect was diminished or even reversed when glucose was absent (**Figure 3.4 A, B**). When glucose was present, oxamate decreased ECAR in MM.1S and MM.1R but there was no significant effect on OCR; the above effect was reversed in the absence of glucose (**Figure 3.4 C, D**). These results indicated that oxamate maximized the effect on promoting mitochondrial respiration over glycolysis. DCA and oxamate had a similar effect in diverting glycolysis to mitochondrial respiration; however, in order to achieve this effect, glucose presence is essential and the glycolysis pathway needs to be activated.

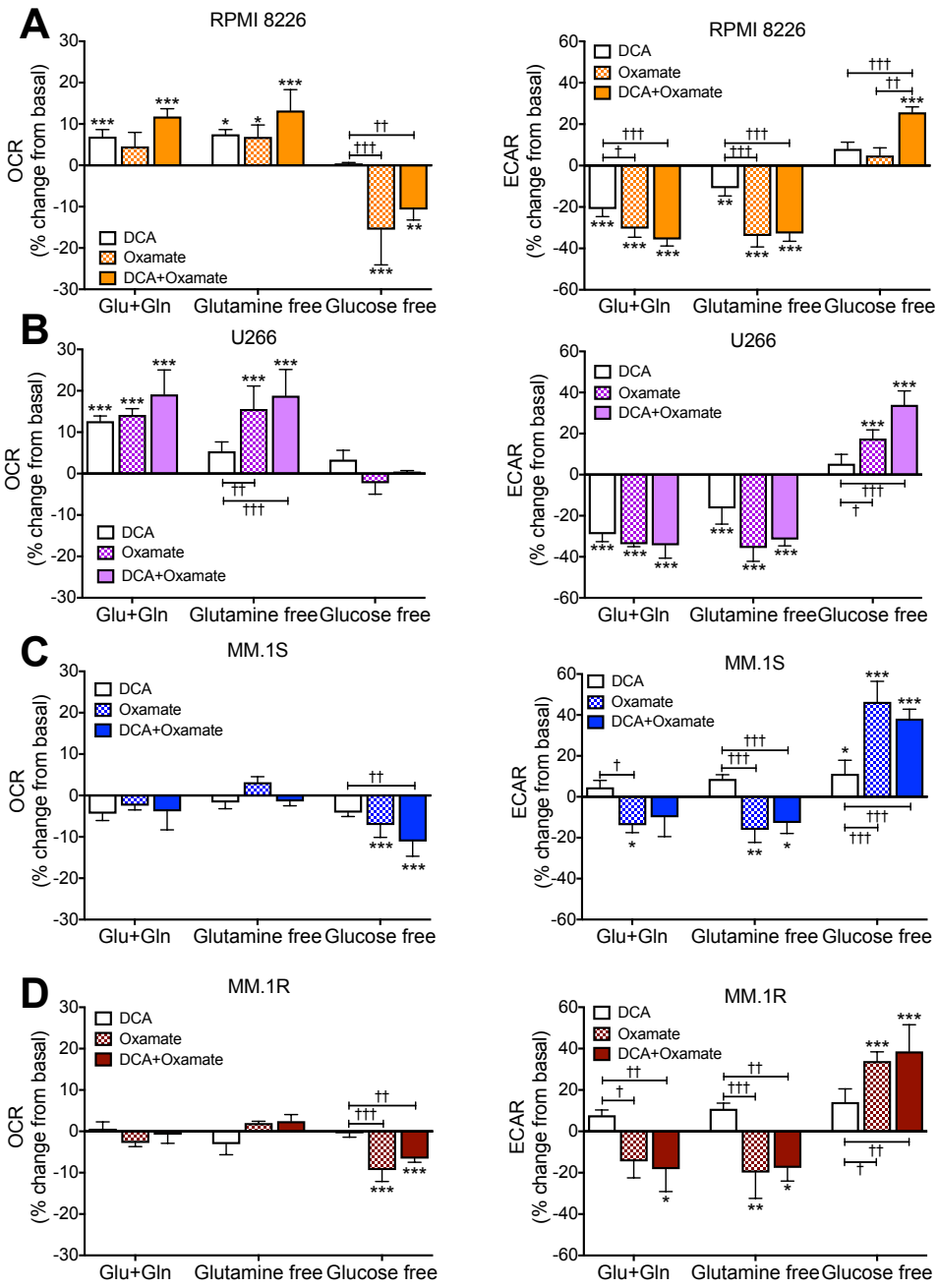

Figure 3.4 The impact of oxamate on the effects of DCA on OCR and ECAR levels of MM cells in different nutrient conditions. OCR and ECAR values were normalised to the non-treatment basal levels (100%). DCA (5mM final) was injected followed by oxamate (20 mM). Percentage changes from basal (displayed as 0 line) were displayed. T-test was used to analyse the difference between normalised basal levels (ECAR, OCR) and levels after treatments for each cell line (*). Two-way ANOVA was used to analyse the difference in percentage change between treatments for each different media condition (†). Each treatment had 5-6 replicates wells per experiment. All data points represented mean ± SD from at least 3 independent experiments; * $p < 0.05$, ** $p < 0.01$, *** $p < 0.001$, † $p < 0.05$, †† $p < 0.01$, ††† $p < 0.001$.

3.3.3 DCA had greater effects in hypoxic condition

The effects of DCA in 24-hour-hypoxia (< 0.3% O_2) were evaluated by measuring total viable cell numbers and extracellular lactate levels. In normoxia, DCA reduced total viable cell number at various levels in all cell lines except U266. Despite hypoxia alone reduced total viable cell number, DCA in hypoxia can further reduce total viable cell number in U266, MM.1S, and MM.1R to various levels but not in the glycolytic cell line RPMI 8226 compare to hypoxia no-treatment control (**Figure 3.5 A**).

The total viable cell number of RPMI 8226 was reduced significantly by hypoxia treatment alone (p=0.016) but it was not significant in other cell lines. In normoxia, DCA reduced the total viable cell number of RPMI 8226 significantly; however, DCA did not have any effect in reducing the total viable cell number in hypoxia (**Figure 3.5 A**). Correlating with results from chapter 2 (Figure 2.2, 2.4), these results indicated that RPMI 8226 was already at its maximal glycolytic capacity in normoxia and had a low glycolytic reserve to cope with the stress caused by hypoxia.

In contrast to RPMI 8226, DCA treatment in hypoxia reduced the total viable cell numbers at various levels on other cell lines. In particular, U266, which is not responding to DCA in normoxia but had a 30% reduction in total viable cell number in response to DCA in hypoxia compared to normoxia control group (p=0.008) (**Figure 3.5 A**). DCA in hypoxia further decreased the total viable cell number by 19% compared to hypoxia control. Previous metabolic phenotype studies in Chapter 2 demonstrated that U266 had the highest glycolytic reserve among the tested MM cell lines (Figure 2.2, 2.4), indicating U266 was not rely on glycolysis in normoxia, and had greater ability to adapt to hypoxia.

Hypoxic treatment significantly increased the extracellular lactate level in all tested MM cell lines with that of RPMI 8226, U266 and MM.1S being statistically significant. DCA significantly reduced RPMI 8226 extracellular lactate level both in normoxia and hypoxia. DCA cannot reduce the extracellular lactate level of U266 in normoxia, but the lactate level of U266 in hypoxia was reduced significantly in response to DCA treatment (p=0.041) (**Figure 3.5 B**).

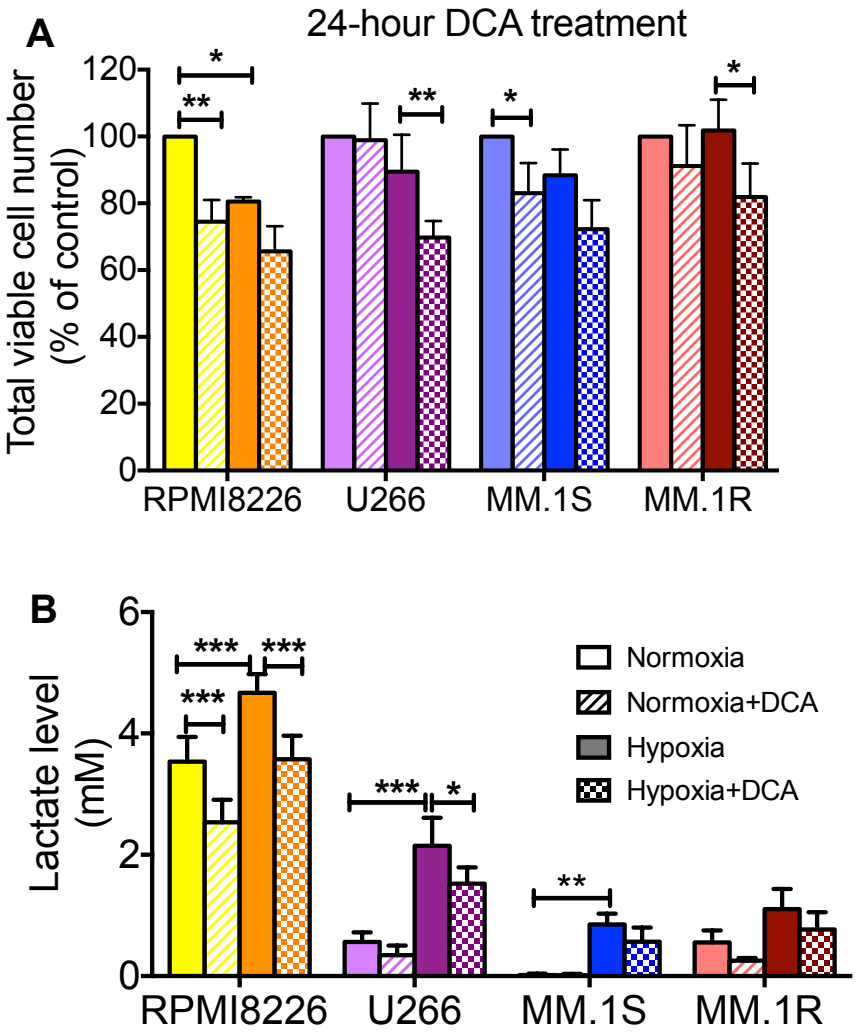

Figure 3.5 DCA enhanced the hypoxia-induced reduction in total viable cell number and reduced hypoxia-induced lactate level. (A) DCA (24 hours, 5 mM) treatment further reduced the total viable cell numbers in hypoxia conditions. (B) DCA significantly reduced hypoxia-induced lactate levels in RPMI 8226 and U266 cells. Each treatment was quadruplicated per experiment. All data points shown represent mean ± SD from at least 3 independent experiments; * $p < 0.05$, ** $p < 0.01$, *** $p < 0.001$.

To further evaluate what causes the reduction of the total viable cell number, cell apoptosis in hypoxia was measured. Experiments were performed in U266 and RPMI 8226 cells as these two cell lines had distinctive metabolic profiles and reacted differently to DCA under hypoxia. While hypoxia alone can induce apoptosis in both RPMI 8226 and U266 cells, DCA treatment in hypoxia can further increase the percentage of apoptotic cells in U266 (**Figure 3.6 A**), but not in RPMI 8226 cells (**Figure 3.6 B**). DCA treatment (24 hours) in hypoxia induced 31% apoptotic cells in U266. This data corresponded with the 28% total viable cell number decrease under the same treatment condition, indicating that DCA under hypoxia can induce apoptosis in a non-glycolytic cell line. Further analysis of the apoptotic cell population showed that it was the early apoptosis (defined as Annexin V+, 7AAD-) population of U266 that was significantly increased after 24 hours of DCA treatment in hypoxia.

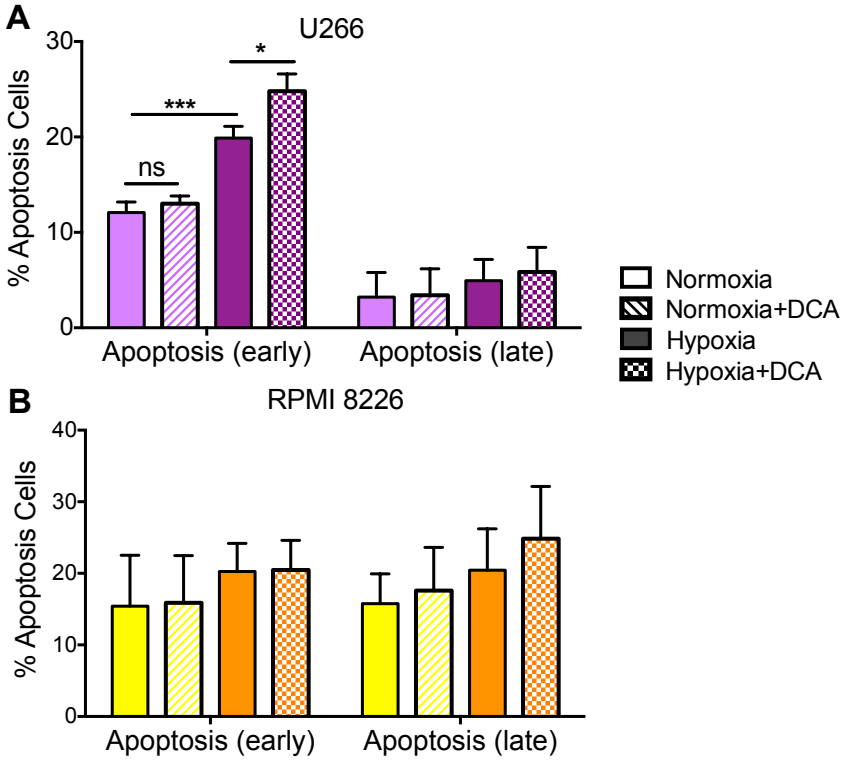

Figure 3.6 DCA increased early apoptosis in U266 but not in RPMI 8226. (A, B) Cells were treated with or without DCA (24 hours, 5 mM) in both normoxia and hypoxia conditions. Apoptosis cells were analysed by FACS. Early apoptosis was defined as Annexin V+/7AAD- cells, late apoptosis was defined as Annexin V+/7AAD+ cells. Each treatment was duplicated per experiment. All data points shown represented mean ± SD from 4 independent experiments; * $p < 0.05$, ** $p < 0.01$, *** $p < 0.001$.

3.3.4 The targets of DCA were upregulated in hypoxia in non-glycolytic cell lines

The mRNA levels of the targets of DCA (PDK 1, 2 and 3) were measured after 24 hours hypoxia treatment. The corresponding protein levels of PDK1, PDK2 and PDK3 were examined by western blot. PDK2 is constitutively expressed while PDK1 and PDK3 are hypoxia-inducible [48, 50]. GAPDH was used as a positive control for the induction of hypoxia. Hypoxia treatment significantly induced the expression of GAPDH to different degrees among MM cell lines indicating a successful hypoxia induction (**Figure 3.7 A**).

Hypoxia treatment upregulated the mRNA expression of PDK1 and PDK3 in U266, a non-glycolytic cell line. U266 had a 5.8-fold increase of PDK3 mRNA level in hypoxia, while its PDK1 mRNA expression was increased only 2.2-fold. The increases of both PDK1 and PDK3 in U266 were the highest compared to other MM cell lines (**Figure 3.7 A**). U266 PDK protein expressions in normoxia were the lowest among the MM cell lines (**Chapter 2, Figure 2.10**). In hypoxia, PDK3 protein level of U266 increased by 64% ($p < 0.001$) compared to PDK3 level in normoxia (normalized as 100%) and PDK1 protein level was increased by 38% ($p=0.073$) compared to corresponding normoxia level. The protein expression of PDK1 and PDK3 in U266 positively correlated with their mRNA expression levels (**Figure 3.7 B**). RPMI 8226 PDK1 and PDK3 protein levels were decreased in hypoxia, which negatively correlated with their mRNA expression. Hypoxia treatment induced the mRNA expression of PDK1 and PDK3 in RPMI 8226, a highly glycolytic cell line, but failed to induce corresponding protein expression (**Figure 3.7**). Hypoxia induced mRNA expression of PDK1 and PDK3 in MM.1S and MM.1R compared to normoxia control, the PDK1 and PDK3 proteins expression in these two cell lines were increased, positively correlating to their mRNA expression in hypoxia (**Figure 3.7**).

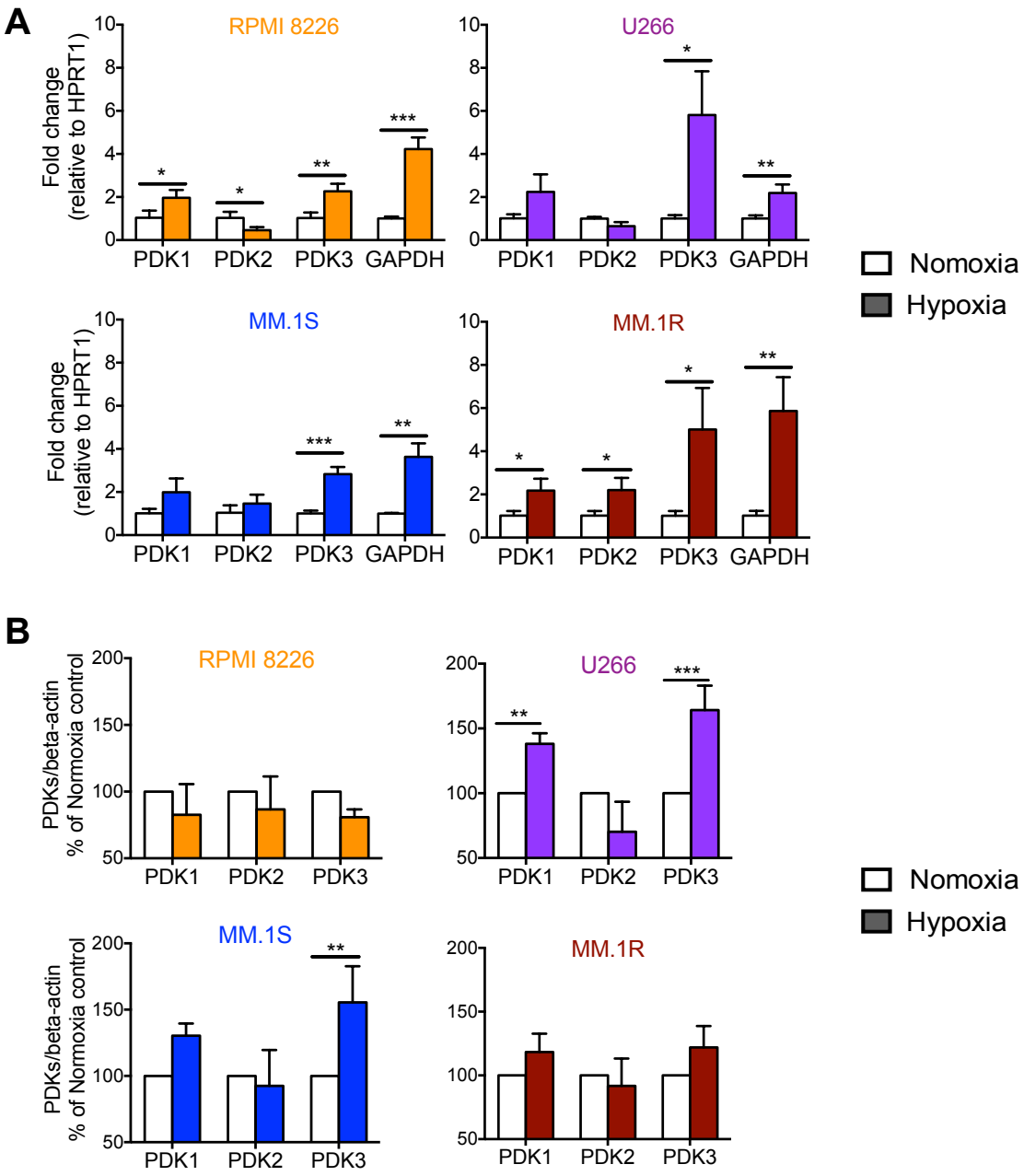

Figure 3.7 PDK mRNA and protein levels under hypoxia. (A) Fold changes of PDK1, PDK2, PDK3, and GAPDH mRNA relative levels normalized to HPRT1 in hypoxia compared to that of normoxia. GAPDH was used as positive control for hypoxia induction. HRPT1 was used as internal control. Each treatment was triplicated per experiment. (B) Percentage change in PDK1, 2 and 3 protein levels were normalized to *β*-actin in hypoxia compared to that of normoxia. Percentage change of protein expression under hypoxia was standardized based on each cell line's normoxia control (100%). Multiple t-test was used for analysis of the differences between normoxia and hypoxia in each cell line. All data points shown represented mean ± SD from 3 independent experiments; * $p < 0.05$, ** $p < 0.01$, *** $p < 0.001$. Representative western blots were shown in Appendix Figure 3.2.

3.4 Discussion

MM originates from the bone marrow (BM), and the BM microenvironments (BMM) are metabolically heterogeneous and hypoxic. The heterogeneous BMM, the heterogeneous metabolic profile of MM cells (Chapter 2), and the contribution of alternative metabolic pathways can potentially impact on the therapeutic outcomes of DCA. This chapter aimed to investigate the impact of the nutrient deprived or hypoxic conditions that mimic the BM on the effects of DCA in MM cells. It was found that MM cells have different preferences for glucose and glutamine (**Figure 3.1**), which complemented the results showing MM cells display heterogeneous metabolic phenotypes (Chapter 2). It was also demonstrated that while both the glycolytic cell line (RPMI 8226) and the non-glycolytic cell line (U266) have functional mitochondrial respiration (Chapter 2), they have varying degrees of plasticity to switch between the different metabolic pathways (**Figure 3.1, 3.3)**. Adequate cellular access to glucose in the media was found to be a precondition of DCA exerting its anti-growth and metabolic modulatory effects in MM cells (**Figure 3.1, 3.2, 3.3**). Furthermore, in hypoxia, DCA had greater anti-growth effect and cytotoxicity in U266 than in normoxia and these effects were accompanied by the upregulation of DCA's targets PDK1 and PDK3 (**Figure 3.5, 3.6, 3.7**).

Cells needed glucose to be present and to have an active glycolysis pathway for DCA to exert its effects. DCA cannot further reduce total viable cell number in glucose-free condition (**Figure 3.1**). When the glycolysis pathway was inhibited at the second step by 2-DG (2-DG is metabolised by HK into 2-DG-6-phosphate, which cannot be further metabolised in glycolysis [357]), DCA cannot further reduce the total viable cell number of MM cells (**Figure 3.2).** In addition to cell growth effects, the metabolic modulatory effect of DCA was also abolished in glucose-deprived conditions (**Figure 3.3 C, D**). These different results proved from multiple angles that anti-growth and metabolic modulatory effects of DCA in MM cells required glucose and an activate glycolysis pathway. These findings also suggested the DCA could exert anti-cancer effects on a subgroup of cancer cells that rely on glycolysis and have active glycolysis pathways. Similar to these findings, in a study of pancreatic cancer the glycolysis inhibitor 2-DG showed selective cytotoxicity to highly glycolytic pancreatic cancer cell lines while it had less effect in non-glycolytic cell lines [358].

The heterogeneous metabolic profiles of MM cells are further demonstrated in this chapter where they showed different dependence on glucose and glutamine. RPMI 8226 was the most sensitive cell line to glucose deprivation while other cell lines (U266, MM.1S, MM.1R) were sensitive to neither glucose nor glutamine deprivation (**Figure 3.1**). These results are in line with a study where MM cell lines (KMS11, L363, and JJN3) showed varying preferences for glucose and glutamine [352]. Compared to RPMI 8226, U266 was also less sensitive to the growth inhibition by 2-DG (**Figure 3.2**), which is in line with a study showing U266 to be relatively insensitive to the growth inhibition of 8-aminoadenosine, a purine analogue that can reduce glucose consumption by inhibiting expression of GLUTs [359]. These results correlated with the results in Chapter 2 where RPMI 8226 was the most glycolytic cell line and U266 was the least glycolytic one. The insensitivity of U266 to the deprivation of glucose or glutamine may also indicate that U266 has higher flexibility to utilize other nutrient source such as fatty acid. Disruption of the fatty acid metabolism pathway by orlistat (fatty acid synthase inhibitor) (**section 1.3.4**) showed to reduce the total viable number of U266 significantly (**Appendix Figure 3.1**). These results indicated that MM cells have different dependence on different metabolic pathways. In a different study, Dalva-Aydemir et al. found that the resistance of MM cells to another glycolysis inhibitor (ritonavir) could lead to reliance on glutamine metabolism and the switch to utilize mitochondrial respiration. Targeting both glycolysis (ritonavir) and mitochondrial respiration (metformin, complex I inhibitor) in their study showed a synergistic cytotoxic effect both in MM cell lines and malignant plasma cells isolated from patient BM aspirates [352]. Combination therapy that targets at multiple metabolic pathways should be considered in future studies of MM treatment.

MM cells also demonstrated to be readily switch between glycolysis to mitochondrial respiration in this chapter (**Figure 3.3 A, B**). This flexible metabolic switch was also supported by an RNA interference (RNAi) screen study, where glycolytic pathway genes were enriched when cancer cells were cultured in high glucose condition (10 mM), in contrast, in low glucose condition (< 0.75 mM), genes of the components of mitochondrial respiration pathway were enriched [360]. The ability of cancer cells metabolically adjusting to the heterogeneous microenvironment proved to be important for the cancer cell survival. In a ^{13}C-isotopomers magnetic resonance spectroscopy

study of breast cancer cells found that the highly metastatic breast cancer cells had higher glycolytic and TCA cycle flux, more capable of switching between glycolysis and mitochondrial respiration and was more capable of adjusting its metabolism to respond to nutrient and hypoxic stress than non-metastatic cancer cells [361]. The glycolytic phenotype of cancer cells is found to be readily interchangeable into non-glycolytic metabolism under lactic acidosis condition, which is an inevitable consequence of the high rate of glycolytic phenotype [104]. This shows that MM cells may switch between glycolysis and mitochondrial respiration in response to the nutrient conditions in their microenvironments. Thus, this finding also supports the rationale of combination treatment that target both glycolysis and mitochondrial respiration pathways.

U266 and RPMI 8226 were different in terms of their metabolic profiles and their responses to growth inhibition by DCA (**Chapter 2, Figure 2.4, 2.6**), these results indicated that the glycolytic pathway of U266 is functional and U266 had greater flexibility to adapt to mitochondrial stressed condition. The impaired mitochondrial function was identified as a condition to sensitize cells to DCA, which suggests that forcing cells to utilize defective mitochondrial respiration is detrimental [362]. Hypoxia can also simulate a situation where the mitochondria function is impaired as the mitochondrial function is downregulated and glycolysis upregulated to cope with the oxygen deprivation. Thus it is hypothesized that using DCA to divert the pyruvate flow into TCA cycle and forcing cells to utilize the already oxygen-deprived mitochondria may lead to further cellular damage and possibly cell death. DCA was found to have greater effects in hypoxia on U266 than in normoxia (**Table 3.3**). DCA cannot reduce the total viable cell number or the lactate level in U266 in normoxia, but there was a significant reduction in both measurements under hypoxia (**Figure 3.5, Table 3.3**). Further analysis of the reduced viable cells indicated the induction of apoptosis by DCA under hypoxia in U266. In contrast, DCA treatment did not further reduce the total viable cell number on RPMI 8226 under hypoxia (**Figure 3.5**). The enhanced DCA cytotoxicity in hypoxia is supported by a study showing that DCA had enhanced cytotoxicity in glioma cells under hypoxia through enhanced ROS production and necrosis [354]. But an opposite result has also been reported, a study showed that while DCA induced apoptosis on colorectal cancer cells in normoxia, it reduced apoptosis of

these cells in hypoxia [355]. The results of this chapter showed that DCA had enhanced anti-cancer effects on U266 in hypoxia and did not display a reduced effect on RPMI 8226 in hypoxia. An expanded summary of the response patterns to DCA (from Table 2.5), including a comparison of the hypoxic and normoxic conditions, is presented in Table 3.3. Thus, the effects of DCA under hypoxia may be cell type specific. Gaining a better understanding of what influences the effects of DCA will be important to using DCA most effectively in the clinic.

Table 3.3 Summary of response patterns to DCA in normoxia (N) and hypoxia (H)

	On-target effects: Mitochondrial Respiration		Biological outcome				Feedback regulation (upstream of targets): Glycolysis		
Readout	pPDH	OCR	Growth		Apoptosis		ECAR	Lactate	
Conditions	N	N	N	H	N	H	N	N	H
RPMI8226	↓	↑	↓	↓	→←	→←	↓	↓	↓
U266	↓	↑	→←	↓	→←	↑	↓	→←	↓

↓: decrease. ↑: increase. →←: no effect.

We hypothesised that the greater effects of DCA observed in MM cells in hypoxia correlated with the activation of glycolysis pathway as indicated by upregulation of PDK expression. Hypoxia can stabilize HIF1, and HIF1 can promote glycolysis over mitochondrial respiration through binding to the hypoxic response elements (HREs) of genes encoding proteins involved in glucose uptake and glycolysis [363, 364]. HIF1 can directly induce PDK1 and PDK3 mRNA by binding to the HRE element in the promoter regions of PDK1 and PDK3 [48, 50]. Thus, MM cells exposed to hypoxia showed that the mRNA expression of PDK1 and PDK3 was upregulated in all tested cell lines but to various degrees, with U266 showing the highest increase of PDK1 and PDK3 mRNA expression levels (**Figure 3.7**). This successful induction of PDK1 and PDK3 in U266 correspond with the highest glycolytic reserve of U266 among the MM cell lines (**Chapter 2, Figure 2.7**), which suggests that U266 did not rely on glycolysis under normoxia, but under hypoxia, it was forced to use glycolysis and consequently

became more sensitive to DCA under hypoxia. This consistent with other reports that the PDK1 siRNA knockdown led to apoptosis in MM cells [12], and suppressed lactate excretion in hypoxia to the normoxia levels in head and neck squamous cancer cells [365]; furthermore, PDK3 siRNA knockdown can inhibit hypoxia-induced glycolysis and induce cell death in HeLa cells, and the double knockdown of PDK3 and PDK1 had additive effects in inducing cancer cell death and overcoming drug resistance [50]. Thus, inhibiting PDK1 and PDK3 warrants further exploration as a therapeutic approach for hypoxic cancers. PDK1 is inhibited relatively more easily than PDK3 by DCA [4]. As PDK3 has the greatest binding affinity to PDH E2 domain among all known isoforms [201], and the PDK3 enzyme activity (1250 nmol/min per mg) is also the highest (25-fold higher than the activity of the least active PDK2) [202], thus it is difficult to overcome PDK3 activities in cancer. Further, DCA is unlikely to achieve the concentrations necessary in humans to inhibit PDK3 (K_i: 8 mM) effectively based on the serum DCA concentrations achieved in our clinical trial (**Chapter 4**) as well as other DCA clinical trials [5, 235]. More potent PDK3 inhibitors need to be developed to better target the enhanced glycolytic phenotype in hypoxic cancers.

The greater effects of DCA in hypoxia could be also due to its ability at inhibiting HIF-1α expression. DCA was found to inhibit HIF-1α either by inducing the production of the mitochondrial-derived α-KG that leads to HIF-1α degradation, or by increasing p53 activity through stimulation of mitochondrial-derived H_2O_2 production [5, 229-231] (Section 1.4.3). The HIF-1 protein level of MM cells was measured in my study using western blot, however even after hypoxia, elevated HIF-1α protein levels was not detected. The reason maybe that MM cells are suspension cells, and after the necessary steps of centrifugation and collecting the cells, HIF-1α protein may already be degraded as it has a very short-half life when exposed in normoxia (5-8 minutes) [366].

To conclude, the anti-cancer and metabolic modulatory effects of DCA requires adequate cellular access to glucose and an active glycolysis pathway in MM cells. DCA had enhanced cytotoxic effects in non-glycolytic cell lines in hypoxia. It has potential in targeting MM in the BM hypoxic environment.

Chapter 4

GSTZ1 genotypes correlate with DCA levels and chronic side effects in MM patients

Abstract

Background: MM is a B-cell malignancy that displays a glycolytic phenotype. DCA is a PDK inhibitor that can reverse the glycolytic phenotype and has potential as an anti-cancer agent. Four clinical trials of DCA in solid tumours demonstrated that DCA is well tolerated, but there is limited efficacy information. GSTZ1 is the only known enzyme that metabolises DCA, and DCA inhibits its own metabolism. GSTZ1 protein coding and promoter sequences may alter a patient's ability to metabolise DCA thus a genetic-based individualised dosing of DCA is needed. **Methods:** Our world-first trial (phase 2, non-randomised) of DCA in plateau phase MM tested if oral DCA could cause a 25% disease readout reduction and established the achievable maximum DCA levels and the safety of DCA with our dosing schedule. The study also correlated *GSTZ1* genotype with DCA levels. Patients were given sodium DCA in addition to standard maintenance therapies for 12 weeks; disease burden was monitored monthly. DCA levels were measured by LC/MS or GC/MS and *GSTZ1* genotyping was analysed by PCR-RFLP. Safety assessment was monitored by physical and biochemical tests. **Results:** The patients tolerated DCA well despite having pre-existing grade 1 neuropathy. Although there was a small increase of the neuropathy score during DCA treatment, none of the patients' side effects were serious enough to require DCA dose reduction. Disease burden was reduced on day 28 in 2/6 patients where it reached the response criteria but was not maintained. DCA was quickly absorbed and maintained at mechanistically relevant concentrations for 3 months. *GSTZ1* promoter polymorphism maybe the driving variant in the chronic usage of DCA. **Conclusions:** While the efficacy of DCA in MM patients could not be accurately assessed due to limited numbers of patients, this trial was able to demonstrate the safety of DCA in patients with neuropathy. DCA maintenance dose can be increased to achieve a better outcome.

4.1 Introduction

Multiple myeloma (MM) is an incurable B-cell malignancy characterized by a multifocal neoplastic proliferation of monoclonal plasma cells in the BM [367]. The malignant plasma cells secrete a monoclonal immunoglobulin product known as paraprotein, which can be used as a biomarker. The most common clinical features of MM are bone pain, hypercalcaemia, immune deficiency, anaemia and renal failure [242]. The standard treatment for MM depends on the stage of the disease. For symptomatic MM, treatment often includes chemotherapy agents with the combination of a novel agent (thalidomide, lenalidomide (LEN), bortezomib) and high dose of dexamethasone (DEX) [284]. The conventional MM chemotherapies are unsatisfactory, leading to cycles of remission and relapse, and ultimately treatment failure. DEX resistance is common among MM patients. When used as single agents in patients, thalidomide and LEN have only a 30% or 47% response rate respectively [306, 307]; when used in combination with DEX or cyclophosphamide, the response rate improved yet eventually all patients develop acquired drug resistance [260, 307, 368-370]. New treatments are needed.

MM displays a glycolytic phenotype that is feasible to target. The key glycolysis relevant genes such as *MYC*, *LDHA*, and *PDK1* were upregulated in patient myeloma cells and correlated with MM progression [12]. Dichloroacetate (DCA) has been used for treatment of lactic acidosis and mitochondrial malfunction for decades. It is an inexpensive and bioavailable candidate that can reverse the glycolytic phenotype by inhibiting pyruvate dehydrogenase (PDH) kinases (PDKs) [3, 4, 48, 49, 132]. By inhibiting PDKs, DCA restores PDH activity and increases the flux of pyruvate into the mitochondria, reversing the glycolytic phenotype and arresting the growth advantage of glycolytic cancer cells [24, 196]. There is cumulative *in vitro* and *in vivo* evidence of the anti-cancer effects of DCA in many cancer types such as glioblastoma, colorectal cancer, endometrial cancer and breast cancer [5-10]. Studies in MM cells showed that DCA could suppress glycolysis and exert anti-growth effects in MM cell lines [11, 12]. DCA could re-sensitize a bortezomib resistant MM cell line to bortezomib, and the combination of DCA and bortezomib improved the survival of myeloma-bearing mice [11]. An increased glycolytic ratio (glycolysis/mitochondrial respiration) was associated with drug resistance in leukaemia and MM, and manipulations of glycolysis overcome

the resistance to glucocorticoids, bortezomib and melphalan [125, 324, 325]. However, the combinations of DCA with glucocorticoids such as DEX or immunomodulatory drugs have not been well studied in MM.

DCA pharmacokinetics studies in humans showed that DCA was rapidly and completely absorbed after oral administration [211]. GSTZ1 (glutathione transferase Zeta) is the only enzyme known to metabolise DCA [209]. DCA is an inhibitor of its own metabolism by inhibiting GSTZ1, explaining why the subsequent doses had longer half-life compared to the initial dose [208]. The *GSTZ1* polymorphisms in both the protein-coding and promoter sequences have significant influence on enzyme expression and functions *in vitro* [219]. *In vitro* experiments showed that *GSTZ1* polymorphisms in promoter sequences (-1002 G>A and -289 C>T) alter promoter activities [218], and different *GSTZ1* polymorphisms in the protein-coding region also corresponded with various activities in metabolising DCA [215, 217-220]. The *GSTZ1* polymorphism is hypothesized to play a determining role in the GSTZ1 enzyme activities and alterations to the function of GSTZ1 can consequently affect the pharmacokinetics of DCA. Thus the knowledge of *GSTZ1* genotype is proposed to be important when assigning dosing regimens to patients participating in clinical trials of DCA.

There have been several early phase clinical trials to study the efficacy and safety of DCA in solid tumour types such as recurrent glioblastoma [5, 234], metastatic breast cancer and advanced stage lung cancer [236]. These early phase trials on DCA showed that chronic DCA treatment was feasible and tolerated well when taken orally using the doses for treating metabolic diseases [234], and the main side effect of DCA was a dose-limiting, reversible peripheral neuropathy without haematological, hepatic, renal, or cardiac toxicity [5, 235]. It was suggested that DCA doses should be individualized based on patients' *GSTZ1* genotypes and DCA study should be carried out in patients with longer life expectancy [236]. The recommended phase-2 dose in 24 patients with advanced solid tumours suggested 6.25 mg/kg *b.i.d.* [235]. Inspired by these early phase trials of DCA in patients with solid tumours, a phase-2 clinical trial in the haematological cancer MM was conducted to investigate if there is any potential of using DCA as an addition to the chemotherapy of MM patients.

4.2 Methods & Materials

4.2.1 Clinical Trial Information

4.2.1.1 Rationale of DCA dosing regimen and patient selection

In order to rapidly achieve and maintain DCA in our predicted therapeutic range, our DCA dosing regimen included administering a high loading dose (25mg/kg) to increase the half-life of DCA, followed by a lower maintenance dose (6.25mg/kg). An initial oral dose of 25mg/kg sodium DCA was given to eligible patients on day 1 and pharmacokinetics (PK) serum samples were taken, with the same measurements repeated on day 8. Patients took the 25 mg/kg high dose on the following day 2 and day 3 of the trial. Then patients took a lower maintenance dose (6.25 mg/kg, *b.i.d*) for the rest of the 12-weeks DCA treatment (**Table 4.1**). To avoid the problems encountered by Garon et al. in metastatic tumours [236], our MM patient selection criteria were designed based on the likelihood of a longer life expectancy and a steady plateau phase, but with measurable disease burden to better evaluate the therapeutic effect of DCA in patients.

Table 4.1 Summary of DCA dosing regimen.

	Day 1	**Day 2-3**	**Days 4-7**	**Day 8**	**Day 9 onward**
Dose (mg/kg)	25, single	25, *b.i.d*	6.25, *b.i.d*	25, single	6.25, *b.i.d*

4.2.1.2 Study design

A Simon's Mini-max 2-stage design was used to conduct the trial. This trial design would optimise safety by exposing fewer patients to a potentially inactive treatment. This clinical trial was undertaken as a prospective two-stage, phase 2, non-randomised study of the efficacy of DCA in plateau phase myeloma. The plateau phase was defined as where patients had achieved a maximal response to conventional glucocorticoid, immunomodulatory drug, and proteasome inhibitor based therapy but showed evidence of residual disease based on the persistence of a residual serum paraprotein or free light chain difference. Patients were given sodium DCA in addition to their standard maintenance therapies for 12 weeks, and free light chain and/or paraprotein levels were monitored routinely as readout of response to DCA. The patient follow-up continued for an additional 6 months. The first stage of the trial was aiming to recruit 15 patients. If there were any proven efficacy, the number would be expanded to 25 in total.

Patients continued treatment until consent was withdrawn, disease relapsed, or unacceptable toxicity occurred during the three-month treatment of DCA. In the event of any grade III toxicity attributable to sodium DCA, medical interventions to alleviate toxicity would be instituted where such a medically appropriate intervention exists. The toxicity must resolve to grade II or lower after 3 weeks of medical intervention. If failed, the participant would be withdrawn from the study. In the event of grade III toxicity, where no supportive medical intervention exists, the study drug would be withheld for 14 days, and at the end of this period, if that toxicity had resolved to less than or equal to grade II, the study drug would be recommenced at 75% of the previously administered dose.

This trial was registered as "A Phase 2 Clinical Trial of Dichloroacetate in Plateau Phase Myeloma – DiCAM" (Trial ID: ACTRN12615000226505). All experiments met Australian Capital Territory Human Research Ethics Committee (ACT HREC) approval. Patients were recruited through the Clinical Haematology department of The Canberra Hospital.

4.2.1.3 Study objectives

(1). Establish if there was evidence of clinical efficacy of DCA in myeloma patients in plateau phase as measured by at least a 25% reduction in serum paraprotein or free light chain (FLC) levels (difference between the involved and uninvolved FLC) over 12 weeks in at least 30% of participants treated with the study drug.

(2). Establish the achievable maximum drug levels of DCA *in vivo* with the dosing schedule and confirm the tolerability and safety of DCA at these doses.

(3). Genotype patients for GSTZ1 and correlate with serum DCA levels and tolerability.

4.2.1.4 Patient eligibility

Eligible patients for this study (**Table 4.2**) are the ones who have been at the plateau phase, which is a phase of stable disease where patients have achieved a maximal response to conventional chemotherapy but with residual disease [371]. The expected life expectancy of the eligible patients ideally should be likely to exceed 6 months in the

opinion of the treating physician. The plateau phase is a period of neither progression nor response for at least 28 days following the last change in myeloma treatment.

According to the International Myeloma Working Group (IWMG), progression is defined as an increase in the paraprotein by ≥ 25% from at least 5 g/L; or in light chain only patients, >25% increase in difference between involved and uninvolved light chain level, with an absolute increase of >0.1g/L; development of new lytic lesions; development of new end organ damage (renal disease, marrow failure, lytic lesions, hypercalcaemia) attributable to myeloma. Response was defined as reduction in the paraprotein by ≥ 25% or in the case of light chain only myeloma, 25% decrease in the difference between the involved and uninvolved light chain. The ineligible criteria of patients are summarized in Table 4.3, patients who have one or more of these below criteria are ineligible for our study.

Table 4.2 Summary of key eligible criteria.

	Eligible criteria
Consent	Able to give informed consent
Myeloma category	Stable myeloma/plateau phase of myeloma with measurable disease, which defined as quantifiable serum paraprotein (⩾ 2g/L on electrophoresis) or elevated free kappa (>21mg/L) or lambda light chains (>30mg/L) and an abnormal serum free light chain ratio (normal κ : λ = 0.26-1.26).
Patients performance and physical status	Age ⩾ 18 years; Eastern Co-operative Oncology Group Performance status ⩽2; Adequate normal cardiac function; adequate hematologic, renal and hepatic function

Table 4.3 Summary of key ineligible criteria.

	Ineligible criteria
Consent	Unable to give informed consent
Myeloma category	Non-secretory myeloma
Co-treatment	Receipt of any active anti-myeloma therapy within the last 16 weeks, except that patients on stable long-term maintenance therapy; major surgery within the last 28 days
Other clinical trial	Enrolled in another trial or discontinued from another clinical trial within the last 14 days
Comorbidities	Peripheral motor or sensory neuropathy; Patient on thalidomide with pre-existing neuropathy score ≥ 2; Neuralgia or paraesthesia (of grade 3 or worse); Liver disease or abnormal liver function within the last 14 days; Renal impairment; Uncontrolled or serious active fungal, bacterial and/or known active viral infection; Second malignancy which may affect the interpretation of results

4.2.1.5 Study assessment

Efficacy assessment of the study was determined by Overall Response Rate (ORR), which was defined as the proportion of participants achieving at least 25% and at least 1g/L reduction in paraprotein or at least a 25% reduction in the difference between involved and uninvolved light chains. This trial was focused on a particular population (plateau phase) of myeloma patients, who present with very low disease burden. Where a 50% reduction in disease burden is more commonly used in trials with active or progressive myeloma patients, a 25% reduction in patients in plateau phase was considered enough to indicate a response to DCA.

Safety assessments of this study were monitored regularly. The vital signs, blood tests, serum biochemistry tests, and neuropathy assessment (Total Neuropathy Score, TNSc) results of the patients were recorded in physical examinations performed before the study and repeated on day 1 (if more than 14 days had elapsed from the screening day), 8, 28, 56, 84, 112 (4 months), 168 (6 months) and 252 (9 months) of the trial. Disease readout paraprotein level or free light chain levels were measured at days 28, 56, 84, 112, 168, and 252 (**Table 4.4**).

Table 4.4 Summary of study assessment.

Assessment	Before trial or Day 1	Day 8	Days 28, 56, 84	Days 112, 168, 252
Vital signs	✓	✓	✓	✓
Neuropathy score	✓	✓	✓	✓
Haematology	✓	✓	✓	✓
Biochemistry	✓	✓	✓	✓
Disease readout			✓	✓

4.2.1.6 Patient serum pharmacokinetic sampling

Measurements of serum sodium DCA levels were made for determination of pharmacokinetics (PK) of DCA on day 1 and day 8 of the study. Blood samples were collected at time 0, 1, 2, 3, 4, 5, 6 and 24 hours after administration of sodium DCA. On day 15 and day 22, blood samples were taken before sodium DCA administration to measure maintenance dose trough level. On day 28, day 56, and day 84, blood samples were taken before and after 2 hours of sodium DCA administration to monitor the maintenance dose trough level and peak level (**Table 4.5**).

4.5 Summary of serum pharmacokinetics (PK) sampling.

Serum samples	Day 1	Day 8	Day 15, 22	Days 28, 56, 84
Tests	PK	PK	Trough level	Trough/Peak levels
Hours after DCA	0, 1, 2, 3, 4, 5, 6, 24 hours	0, 1, 2, 3, 4, 5, 6, 24 hours	0 hour	0, 2 hours

4.2.1.7 Statistical considerations

With this study design a total of 25 patients were needed to achieve 80% power with an alpha of 0.05. The null hypothesis is that less than 10% of patients respond to the DCA treatment. The alternative hypothesis is that at least 30% of patients respond to the DCA. Two-tailed P-values would be used for all comparisons, and all statistical tests would be performed two-sided using a significance level of 0.05.

4.2.2 DCA Pharmacokinetics Study

4.2.2.1 Serum preparation

Blood samples were collected in plain tubes and left undisturbed at room temperature for 15 -30 minutes after collection. The clot was removed by centrifuging at 3000 g for 15 minutes at 4°C. Following centrifugation, the supernatant (serum) was immediately transferred and apportioned in 500 μl aliquots into clean eppendorf tubes. The samples

were kept on ice while handling and transported back to JCSMR on ice. The serum samples were stored at -20 °C for short term and transferred to -70 °C freezer for long-term storage.

4.2.2.2 Sodium DCA extraction and LC/MS conditions

Powder form of sodium DCA (purchased from TCI, USA) used in the clinical trial was used to make 20 mM sodium DCA stock solution in water and 0-20 mM sodium DCA standards were diluted from this stock solution. Control human serum was used and spiked with DCA to make the standards. Difluoroacetic acid (DFA, 100 μM) was used as an internal standard. Serum protein was removed by spinning at 13,000 ×g at 25°C for 30 minutes in filter spin tubes (Pall Life Sciences, Cat# OD010C35). The elute (40 μl) was collected and DCA was extracted by mixing with 200 μl HPLC-grade acetonitrile. After centrifugation at 13,000 ×g at 4°C for 10 minutes, 100 μl of the top acetonitrile layer of the extract was transferred into inserted tubes in mass spectrometry brown glass vials (protect from light) for analysis on a liquid chromatography–mass spectrometry (LC/MS) system (Agilent Technologies). Sample (7 μl) was injected by auto-sampling with needle-washing mode. The temperature of the sampling chamber was kept at 20°C. The LC column and guard column system (Macherey-Nagel) were used which consisted of 1× HPLC column (EC 50/2 Nucleodur HILIC, 50×2mm, 1.8 μm), 1× column protector system (guard column holder), 1× HPLC guard column (EC 4/2 Nucleodur HILIC, 1.8 μm).

The gradient mobile phase was composed of phase A (1% diethylene glycol methyl ether in acetonitrile) and phase B (60 mM ammonium formate in water) with vacuum degas enabled and a flow rate at 0.2 ml/min. Column temperature was 30°C. The initial phase was composed of 96% A and 4% B, followed by linear gradient to 75% A and 25% B in 7 minutes, then returned to the initial phase condition at 7.1 minutes. The Micromass Quattro Micro detector was running in negative electrospray mode. A standard curve was drawn using sodium DCA dilution to determine if the patient samples were within a linear phase of the standard curve and to calculate patient serum DCA levels.

4.2.3 DCA Pharmacogenetics Study

4.2.3.1 DNA isolation

After patients' serum had been removed, clotted blood was used for DNA extraction using QIAamp DNA Blood Mini Kit (QIAGEN, Cat.No.51106). The blood clot (≈500 μl) was transferred from the serum collection tube into an eppendorf tube and was pipetted into smaller pieces. The clot (200 μl) was then transferred into a fresh eppendorf tube containing 20 μl QIAGEN Proteinase K. Buffer AL (200 μl) was added to the tube and mixed thoroughly by pulse-vortexing for 15 sec. The mixture was incubated at 37°C overnight. After incubation, 200 μl 100% ethanol was added, and mixed by pulse-vortexing for 15 second. The mixture was then transferred into the QIAGEN mini spin column and centrifuged at 13,000 ×g for 1 min, then washed with Buffer AW1 and Buffer AW2. After centrifugation, the mini column was inserted in a fresh 1.5 ml eppendorf tube. AE buffer (200 μl) was added to the mini column and incubated at room temperature for 3-5 mins, and then centrifuged at 6000 ×g for 1 minute. The eluted liquid with DNA was transferred into a fresh eppendorf tube, and the DNA concentration was determined by absorbance at 260 nm measured by Nano Drop Spectrophotometer (Biolab, ND-1000). DNA was stored at 4°C for a short term or -20°C for longer term.

4.2.3.2 *GSTZ1* genotyping

GSTZ1 genotyping was performed using polymerase chain reaction restriction fragment length polymorphism (PCR-RFLP) using the published methods in the lab [218, 220]. PCR was performed using a programmable thermal controller PTC-200 (MJ Research Inc, USA). Restriction enzymes and buffers were purchased from MBI Fermentas (NY, USA) (*Alw*26I, *Bsh*1236I) and New England Biolabs (MA, USA) (*Fok*I, *Mlu*CI). PCR product purity was checked by 1% agarose gel electrophoresis (in 1× TBE buffer). Restriction enzyme digestion fragments were separated by 2.5% agarose gel electrophoresis or 8% polyacrylamide gel electrophoresis (PAGE) (Exon 5). ChemiDoc MP imaging system (Bio Rad) was used to analyse gel.

Protein coding region: To amplify exon 3, PCR was performed with 25-50 ng genomic DNA with 375 pmol/ml of ZseqA8 and Zexon3B primers [220] in a 20 μl reaction volume containing 1× reaction buffer IV, 1.5 mM $MgCl_2$, 200 μM dNTPs, 0.5 units of

Taq polymerase (5U/ μl, Thermo Scientific, #AB-0192/A). PCR cycling conditions is summarised in Table 4.6. The resulting 308-bp PCR product was digested with *Alw*26I and *Fok*I separately for the determination of A to G transitions at position 94 and 124 (Appendix).

To amplify exon 5, PCR was performed with 25-50ng genomic DNA with 375 pmol/ml of Zexon5A and Zexon5B2 primers in a 20 μl reaction containing the same formula of that of exon 3 [220]. PCR cycling conditions is summarised in Table 4.6. The resulting 262-bp PCR product was digested with *Bsh*1236I for the determination of the nucleotide present at position 245 (Appendix).

Promoter region: To amplify promoter region containing nucleotide -1002, PCR was performed with 25-50 ng genomic DNA with primers (375 pmol/ml) in a 20 μl reaction volume containing the same formula of that of exon 3. PCR cycling conditions is summarised in Table 4.6. The resulting 216-bp PCR product was digested with *Mlu*CI for the determination of the nucleotide present at position -1002 (Appendix). The PCR product (5 μl) was digested at 37°C overnight in a 15-μl reaction contained 1 unit *Mlu*CI (10,000 U/ml), 1× NEB buffer. The resulting fragments were separated by 2.5% agarose gel electrophoresis [218].

Table 4.6 Summary of PCR cycling conditions

GSTZ1 gene region	Initial Cycle	Cycle (× 35)	Final Cycle
Exon 3	95°C 2 mins	95 °C 20 s 60 °C 15 s 72 °C 30 s	72 °C 3 mins
Exon 5	94 °C 2 mins	94 °C 20 s 60 °C 20 s 72 °C 30 s	72 °C 2 mins
Promoter -1002	95°C 3 mins	95 °C 30 s 58 °C 20 s 72 °C 30 s	72 °C 3 mins

Table 4.7 Restriction enzymes and buffers

Buffers and reagents	Manufacturer	Formula
1× reaction buffer IV	Advanced Biotechnologies, Epsom, Surrey, UK	20mM $(NH_4)_2SO_4$, 75 mM Tris-HCl (pH 9.0), 0.01% Tween 20
1× TBE buffer		0.09M Tris-borate, 2mM EDTA
1× NEB buffer	New England Biolabs	10 mM Bis-Tris-Propane-HCl, 10 mM $MgCl_2$, 1 mM DTT
Taq polymerase (5U/ μl)	Thermo Scientific, #AB-0192/A	
$MgCl_2$	Advanced Biotechnologies	
dNTPs	Advanced Biotechnologies	

Table 4.8 Summary of primers for *GSTZ1* genotyping

GSTZ1 gene region	Primer	Sequence
Exon 3	ZseqA8	5'-TGACCACCCAGAAGTGTTAG-3'
	Zexon 3B	5'-AGTCCACAAGACACAGGTTC-3'
Exon 5	Zexon5A	5'-AAGAGGTGTAGTGATGGTGC-3'
	Zexon5B2	5'-GGTGCAAGTGTACAAGTGCC-3'
Promoter -1002	-1002 forward	5'-CCATTTCTGACACCCAGTAT-3'
	-1002 reverse	5'-TTCTAAGGCCTGAGTTCCTA-3'

4.2.4 *In vitro* chemotherapy and DCA combination

4.2.4.1 Dexamethasone

DEX (Sigma-Aldrich, 100 mg/bottle) was dissolved in 100 % ethanol to make a stock of 10 mM. DEX stock solution was aliquoted in eppendorf tubes and stored at – 20 °C. MM cell lines were treated with DEX alone or in combination with DCA (5 mM). Total viable cell number was measured by neutral red uptake assay. The concentration of DEX and the treatment time was determined through literature research. A range of 0-100 μM of DEX was used in this experiment. Cells were seeded at 25,000 -50,000/well in U-bottom 96-well plates after expansion in 6-well plates overnight. All wells of treatment plates had equal amount of ethanol vehicle (0.01%).

4.2.4.2 Lenalidomide (LEN)

LEN used in this study was manufactured and provided by Celgene Company. LEN is in powder form in brown glass vials, 5 mg per bottle, weighted to 0.01mg accuracy. LEN was dissolved in DMSO directly to make a 100 mM stock solution. LEN powder vials were kept at – 20 °C, LEN stock solution was kept at – 80 °C. MM cell lines were

treated with LEN alone or in combination with DCA. Total viable cell number was measured by neutral red uptake assay. The concentration of LEN and the treatment time was determined through literature research [372, 373]. A range of 0-100 μM of LEN was used in this experiment. Cells were seeded at 25,000 per well in U-bottom 96-well plates after expansion in 6-well plates overnight. All wells of treatment plates had equal amount of DMSO vehicle (0.01%).

4.2.4.3 Neutral red assay

Neutral red uptake assay was used to evaluate total viable cell number after combination treatment (Chapter 2, section 2.2.3). Cells were seeded in 96-well round bottom plates at densities of 25,000-50,000 cells per well. Drug treatments were performed after a randomized choice of well position in plates. Each treatment had quadruplicate wells per plate and three independent experiments were carried out.

4.2.4.4 Combination index calculation

The Chou-Talalay method was used to analyse if the drug combination is synergistic. The calculation was based on the median-effect equation used in biochemistry and biophysics. The results were shown as the combination index (CI), which quantitatively defines different drug combination effects as an additive effect (CI = 1), synergism (CI < 1), and antagonism (CI > 1) [374, 375].

4.2.4.5 Statistical analysis

Numeric data were presented as mean ± standard deviation (SD). Multiple t-test with Holm-Sidak method was applied to determine the significant differences between two treatments within one cell line. Two-Way ANOVA Tukey's multiple comparison was used to compare multiple means among different groups. A probability level of $p < 0.05$ was considered statistically significant. The EC_{50} was calculated by fitting a nonlinear regression dose-response curve using GraphPad Prism's (version 6.0f) dose-response equations. The data was transformed to convert the X values to logarithms before calculations.

4.3 Results

4.3.1 Patient Characteristics

Six Caucasian patients were enrolled in this study between May 2015 and June 2016. Patient demographics, baseline disease, prior treatments and co-morbidities are listed in Table 4.9. Four out of these six patients had myeloma with intact paraproteins while two patients had free light chain myeloma (001, free kappa; 002 free lambda). The average age of the patients enrolled in the study was 65.6 years (range 52-77) and the average age for the initial diagnosis of myeloma was 61.8 years (range 49-75). The DiCAM patients went through rounds of prior myeloma treatment. Five out of six patients were on co-maintenance treatments during the study (**Table 4.9**). P002's maintenance treatment (CyBortD) was stopped at study day 30 due to severe side effects of the chemotherapy. Patients were compliant in this study.

One of the six patients had confirmed complex cytogenetics while the rest had normal results indicating our patient cohort might not be representative of the full spectrum of the high percentage of complex genetic abnormalities of the whole myeloma population. P004 was withdrawal from the study due to rapid disease progression. P004 had a complex cytogenetics background (**Table 4.9**) compared to the rest of the patients. P004's cytogenetics results showed a complex male karyotype with multiple structural and numerical changes in 19/20 cells examined, including chromosome 1 abnormalities, 14q32 rearrangements and monosomy 13 which are observed in myeloma and associated with poor prognosis [259, 376].

4.3.2 Patient Outcomes

Two of the six patients (P001, P002) responded to DCA treatment at day 28 according to our response definition where the measurable paraprotein readout or the difference between affected and unaffected free light chain (FLC) achieved a 25% reduction (**Section 4.2.1.4**), however, the response was not sustained during the low-dose DCA maintenance (6.25 mg/kg *b.i.d*) therapy. P001 reached a 25% reduction at day 28 of the trial, but this was not sustained. P002 had the longest response to DCA as the disease readout remained below or close to the response line from day 28 till day 84 of the trial. P002 also had the greatest response to DCA treatment compared to other patients, as the disease burden of P002 reduced by 37% on day 28, 29% on day 56 and 24% on day 84.

P003 had a 23% paraprotein reduction at day 28 but the effect was not sustained. P004 was taken off the trial due to rapid disease progression, which may be a consequence of the patient's complex cytogenetics background. P005 had a 25% increase of paraprotein on day 56, but the reading dropped to the baseline level (4 g/L) and remained at that level throughout the rest of the trial. P006 had a gradual increase of paraprotein during the trial, with a 22% increase of paraprotein on day 56, and a 44 % increase on day 84, the last day of DCA treatment (**Figure 4.1)**.

Table 4.9 Patients Characteristics Summary

Patient ID	P001	P002	P003	P004	P005	P006
Age of enrolment	70	72	77	61	62	52
Gender	Male	Male	Female	Male	Male	Male
Age of diagnosis	65	62	75	60	60	49
Diagnosis (year)	2010	2005	2013	2014	2013	2012
Ethnicity	Caucasian	Caucasian	Caucasian	Caucasian	Caucasian	Caucasian
Cytogenetics	Normal	Unknown	Normal	Complex*	Normal	Normal
Light chain only myeloma (κ/λ)	No	λ	No	No	No	No
Intact paraprotein (HC/LC Isotypes)	*IgA/κ	No	IgG/κ	IgG/ λ	IgG/ λ	IgG/κ
Baseline disease	FLC (λ-κ) 45 mg/L	FLC (λ-κ) 239 mg/L	Paraprotein 9 g/L	Paraprotein 4 g/L	Paraprotein 4 g/L	Paraprotein 10 g/L
Co-maintenance treatment	None	CyBortD(until study day 30)	Thalidomide	Thalidomide, DEX	Thalidomide	Lenalidomide, DEX
Best response received after 1st therapy	VGPR	VGPR	SD	PR	PR	PR
Lines of prior therapy	3	7	2	3	3	3
Co-morbidities	Deep vein thrombosis/ pulmonary embolism; kidney stones	Unknown	Dyslipidaemia	No	Gastro-oesophageal reflux	Deep vein thrombosis/ pulmonary embolism

***P001:** P001 showed an IgA paraprotein at diagnosis in 2010, but the IgA paraprotein was not detected after 5 years on the screening day for the trial in 2015, thus his disease readout was presented as free light chain myeloma.

Abbreviations: CyBortD, Cyclophosphamide+ Bortezomib + Dexamethasone; sCR, stringent complete response; CR, complete response; VGPR, very good partial response; PR, partial response; SD, stable disease. FLC: free light chain. HC: heavy chain; LC: light chain. DEX: dexamethasone. ***P004 cytogenetics results:** (43,X, Y, add (1)(q21), add (2)(p23), add (2)(q33), add (4)(p15), der (8) t (8; 17)(p21; q11.2), del (11)(p12), add (12)(q13), -13, t (14; 22)(q32; q12), -16, -16, -17, -20, +mar1-3[12]/sdl, del (6)(q25)[5]/46, XX [36].

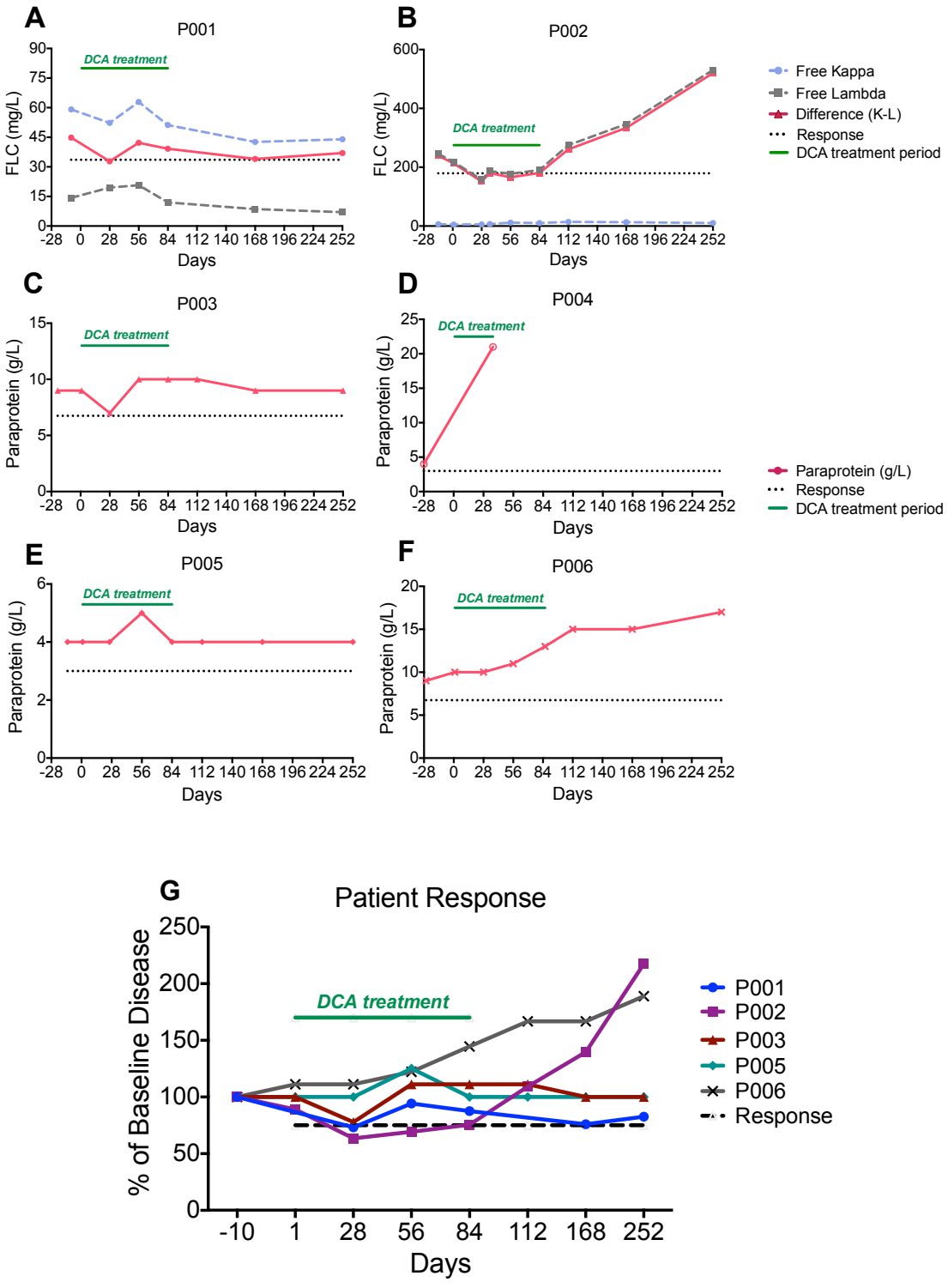

Figure 4.1 Patients disease outcomes. Paraprotein level or FLC levels were measured at days 28, 56, 84, 112, 168 and 252 of study. (A) P001 FLC levels. P001 had free kappa light chain myeloma. (B) P002 FLC levels. 002 had free lambda light chain myeloma. (C-F) The paraprotein levels of P003, P004, P005, and P006. (G) Patients disease readout percentage change calculated based on their baseline level (standardized as 100%) before DiCAM clinical trial. Green line used here is an indicator for DCA treatment period.

4.3.3 Toxicity and adverse events

There were no patients in this study who were withdrawn from the trial due to DCA induced toxicity. The safety monitoring protocol for this trial included the regular evaluation of patients' vital signs, total neuropathy score (TNSc), full blood count, white blood cell differentiations and live and kidney functions. There were no abnormal changes observed of these aspects during the 3-month DCA treatment and the 6-month follow up period (data not shown).

Based on other clinical trials data, peripheral neuropathy was one of the major side effects of DCA in cancer patients. Grade-3 toxicity (defined as any of the 7 aspects of TNSc had a score greater than 3, **Figure 4.2 (A-F)**) was considered as an indication of severe neuropathy; the patient would be taken off study if the symptoms were not alleviated after supportive treatments. P001, P002, P003 showed different degrees of increased TNSc while on DCA during the trial but the TNSc decreased after the trial indicating the peripheral neuropathy aggravated by DCA during the trial was reversible (**Figure 4.2 G**). P002 had an accumulative higher TNSc compared to other patients on the trial. The strength and motor symptoms of P002 both had a score of 3 on the last day of DCA treatment (day 84), but the symptoms were alleviated and the TNSc of P002 was decreased after the DCA treatment (**Figure 4.2 B**). Similarly, P006 had a score of 3 in vibration sensibility on the last day of DCA treatment (**Figure 4.2 F**), but the symptoms were alleviated after the completion of DCA treatment. Thus, both P002 and P006 remained eligible for the trial.

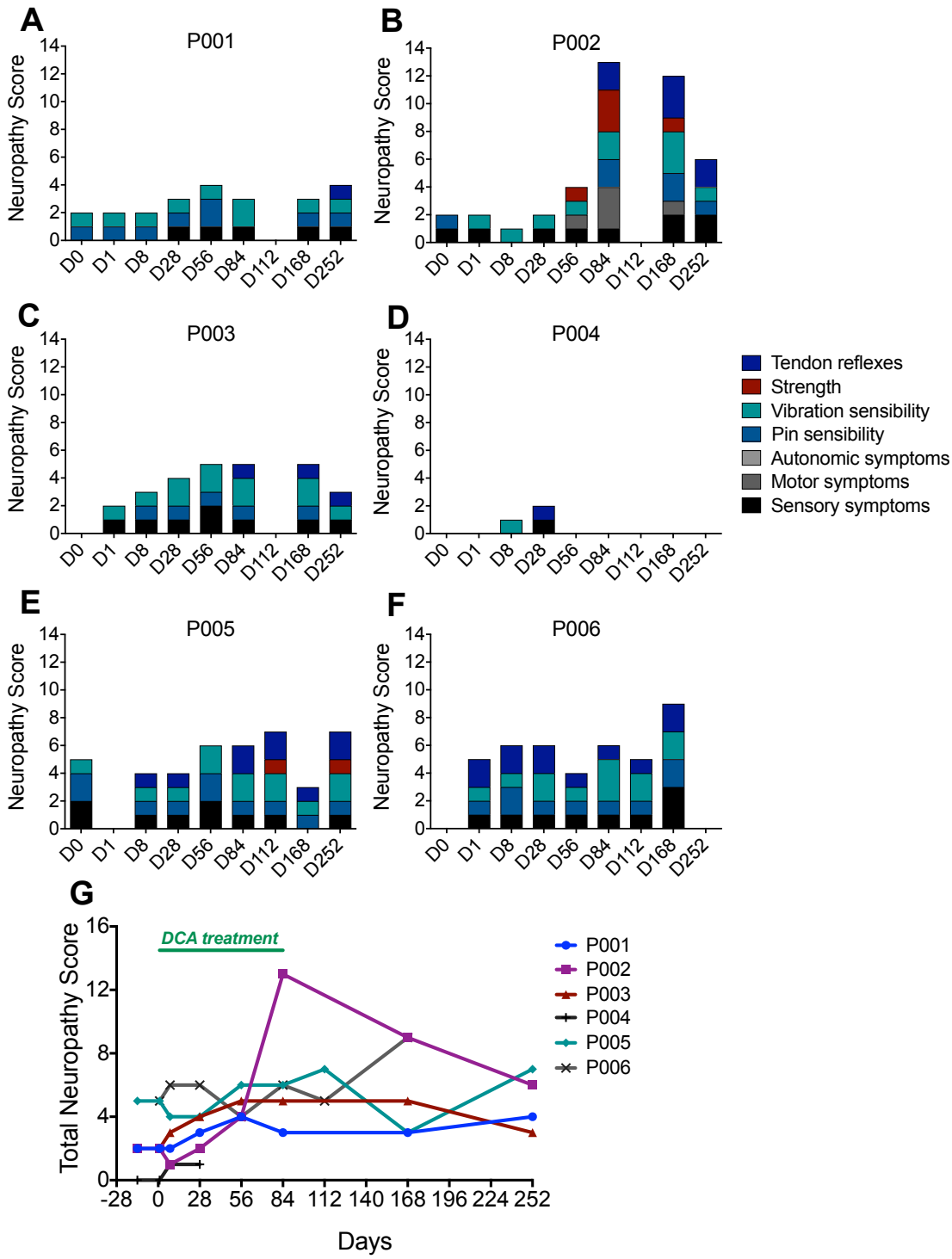

Figure 4.2 Patients Total Neuropathy Score (TNSc). (A-F) The peripheral neuropathy score of each patient was assessed through 7 aspects: sensory symptoms, motor symptoms, autonomic symptoms, pin sensibility, vibration sensibility, strength and tendon reflexes. (G) The TNSc of patients. Patients were examined on screening day (day 0), days 1(if ≥14 days elapsed from screening day), 8, 28, 56, 84, 112, 168 and 252 of the study. Green line indicates the DCA trial period.

4.3.4 Pharmacokinetics

LC/MS method was used to measure the DCA serum levels of P001-P004; GC/MS (gas chromatography–mass spectrometry) method (Appendix) was used to measure P005 and P006 serum DCA levels because the LC/MS machine was no longer available during my study. Although the DCA serum levels were measured by two different methods, the range of the concentrations was similar and thus the data are highly comparable (**Figure 4.3 A, B**). On day 1 of the trial, patients took 25 mg/kg (loading dose) sodium DCA orally. Sodium DCA serum concentrations rapidly reached peak level after 1 hour for P001, P005, and P006; and 2 hours for patients P002, P003, and P004. P001 had a faster clearance rate of DCA compared to other patients with a half-life of 45 mins while the other patients' DCA half-life was greater than 90 mins (**Figure 4.3, Table 4.11**). On day 8 of the study, the peak levels of serum DCA (25 mg/kg) increased about 2-fold (average 0.59 mM, range 0.50-0.66 mM) compared to that of day 1 (average 0.33 mM, range 0.15-0.68 mM) (**Figure 4.3**). These dosages indicate that DCA serum levels had reached concentrations capable of inhibiting PDK2 and PDK4 by DCA (K_i: PDK2, 0.2 mM, PDK4: 0.5 mM), partially inhibiting PDK1 and but not PDK3 (K_i: PDK1, 1 mM, PDK3: 8 mM). The serum DCA concentration remained at high levels 6 hours post DCA administration (half-life > 6 hours).

The average DCA trough level of patient P001-P006 on 6.25 mg/kg (maintenance dose) dose increased from day 8 (0.074 mM) to day 84 (0.309 mM) (**Table 4.10, Figure 4.3 C**). This trough level range is very close to the data reported by Chu et al. [235]. The DCA peak levels of P001-P006 ranged from 0.04-0.69 mM when patients were on maintenance dose (**Table 4.10, Figure 4.3 D**), which reached mechanistically relevant concentrations of inhibiting PDK2 by DCA. Strikingly, P002 had DCA trough levels 2-3 fold higher compared to the average of the other patients on day 56 and day 84 of the trial (**Figure 4.3 C**). This correlated with the increased total neuropathy score (**Figure 4.2 G**).

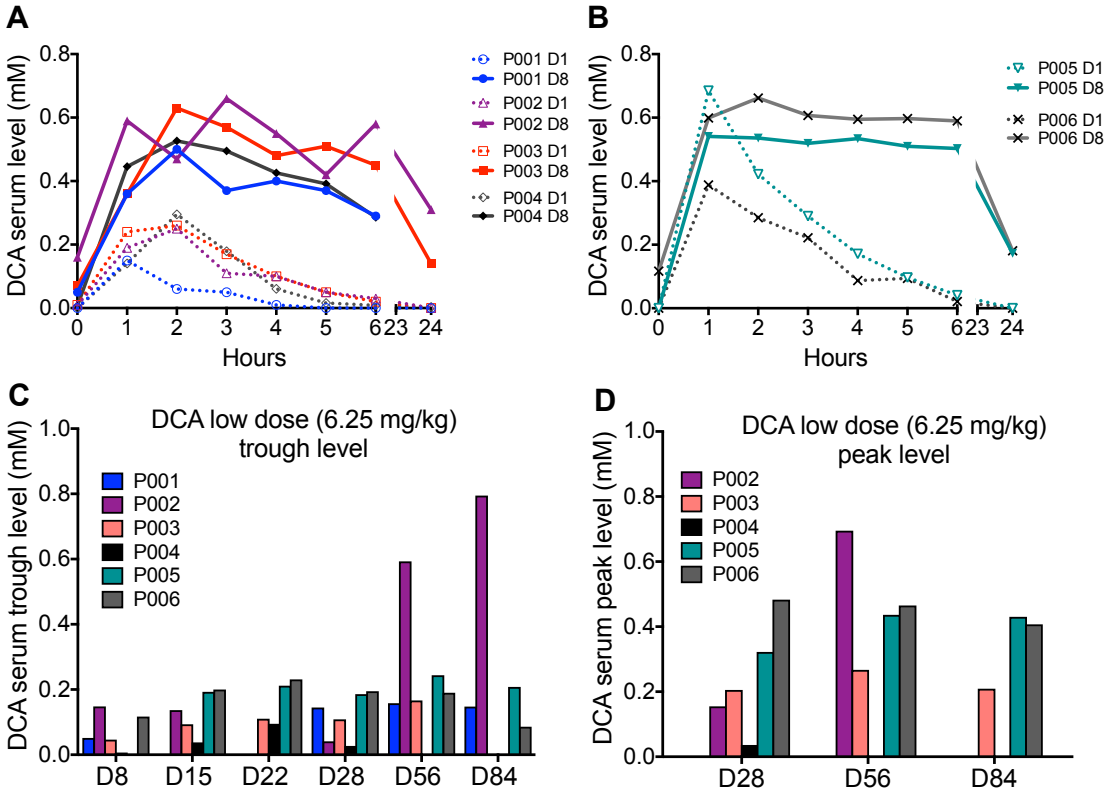

Figure 4.3 Patients serum DCA levels. (A) DCA serum levels measured by LC/MS on day 1 and day 8 of the trial. The loading dose (25 mg/kg, 5 doses) scheme was given to patients. The results showed a longer half-life of DCA after 1 week of therapy. (B) The DCA serum levels of P005 and P006 measured by GC/MS on day 1 and day 8 of the trial. The change of the method was due to LC/MS machine no longer available. (C) DCA serum trough levels when on maintenance dose of DCA (6.25 mg/kg). (D) DCA serum peak levels on maintenance dose of DCA throughout the trial.

Table 4.10 Patients serum DCA (6.25 mg/kg *b.i.d.*) trough and peak level (mM)

	Day 8	Day 15	Day 22	Day 28		Day 56		Day 84	
	Trough	Trough	Trough	Trough	Peak	Trough	Peak	Trough	Peak
P001	0.052	a	a	0.145	N.M	0.158	a	0.148	a
P002	0.148	0.137	N.M	0.041	0.155	0.593	0.695	0.795	b
P003	0.046	0.093	0.110	0.108	0.205	0.166	0.267	b	0.209
P004	0.007	0.038	0.095	0.027	0.036	c	c	c	c
**P005*	d	*0.193*	*0.212*	*0.186*	*0.322*	*0.244*	*0.436*	*0.208*	*0.430*
**P006*	*0.117*	*0.200*	*0.231*	*0.195*	*0.483*	*0.190*	*0.465*	*0.086*	*0.407*
Mean	0.074	0.132	0.162	0.117	0.240	0.270	0.466	0.309	0.349

a-d: levels not measured for the following reasons:
a. Trial protocol design changed after P001, the peak levels of P001 while on maintenance dose were not measured. b. P002 and P003's missing data were due to omission in blood sample collection. c. P004 was withdrawn from the trial after D28. d. P005 took his first dose before tough level blood sample taking.
* P005 and P006 serum DCA levels were measured by GC-MS methods by Ms. Pouryousef and Dr Tea (method in Appendix) due to the unavailability of the LC/MS machine that was used to measure P001-P004 serum levels.

4.3.5 GSTZ1 genotype

Dunbar et al. suggested the importance to consider a patient's *GSTZ1* genotype when determining the suitable dose for chronic DCA administration as evidence showed *GSTZ1* genotypes affected DCA metabolism and thus consequently its toxicity [234]. P001 was heterozygous A/G at both Exon 3 nucleotide position (nt) 94 and 124. P001 haplotype was determined as *GSTZ1*A/Z1*C* based on the categorization methods established by Blackburn et al. (that all alleles containing an A at nt 124 also contained an A at nt 94 and $G^{94}A^{124}$ was not present in the population) [219]. The GSTZ1a-1a recombinant protein variant analysed *in vitro* had a 3.6-fold higher activity towards metabolizing DCA compared to other recombinant GSTZ1 proteins [220]. P001 had a faster clearance rate of DCA compared to other patients on day 1 of the study indicating that the *GSTZ1A* allele's activity maybe the underlying cause. However, at day 8 of the study, there was no difference between P001 and the rest of the patients in terms of the elevated DCA peak level and the longer DCA half-life (**Table 4.11**). Patient 002 was homozygous A/A at *GSTZ1* promoter -1002 who also had the highest average DCA trough level and had the highest accumulative neuropathy score compared to other patients (**Table 4.11**).

Table 4.11 Patient GSTZ1 genotype

	Promoter -1002	Exon3 nt 94	Exon3 nt 124	Exon5 nt 245	Haplotype	Average DCA trough level (mM)	DCA half-life (mins)
P001	G/A	A^{94}/G^{94}	A^{124}/G^{124}	C/C	Z1*A/Z1*C	0.13 (n=4)	45
P002	**A/A**	A^{94}/A^{94}	G^{124}/G^{124}	C/C	Z1*B/Z1*B	**0.34 (n=5)**	**>90**
P003	G/G	G^{94}/G^{94}	G^{124}/G^{124}	C/T	Z1*C/Z1*D	0.10 (n=5)	>90
P004	G/G	G^{94}/G^{94}	G^{124}/G^{124}	C/C	Z1*C/Z1*C	0.04 (n=4)	>90
*P005	G/G	G^{94}/G^{94}	G^{124}/G^{124}	C/T	Z1*C/Z1*D	*0.21 (n=5)*	*>90*
*P006	G/G	G^{94}/G^{94}	G^{124}/G^{124}	C/C	Z1*C/Z1*C	*0.17 (n=6)*	*>90*

* P005 and P006 DCA serum levels were determined by Ms N. Pouryousef and and Dr I. Tea through a GC/MS method due to the unavailability of the LC/MS machine that was used to measure P001-P004 DCA serum levels.

4.3.6 DCA combined with chemotherapy agents can further reduce total viable cell numbers

Five of six of the DiCAM patients enrolled in our study were on maintenance therapy during the trial. To better understand the effects of DCA on the representative chemotherapy agents at a cellular level, a series of drug combination assay were carried out in MM cell lines.

DEX is the backbone of myeloma chemotherapy and commonly used in combinations. The response to DEX or DEX and DCA combination were tested on MM cell lines by measuring total viable cell numbers (**Figure 4.4**), apoptosis (Appendix Figure 4.1 A), and cell cycle distribution (Appendix Figure 4.1 B). MM cell lines had different sensitivity to DEX with MM.1S being the most sensitive while MM.1R and U266 were resistant to DEX (**Figure 4.4, Table 4.12**). MM.1S and MM.1R are two isogeneic cell lines derived from one patient before and after the development of DEX resistance [290]. Previous chapters of this study showed that MM.1S and MM.1R displayed different metabolism profiles. MM.1R demonstrated a higher degree of glycolysis compared to MM.1S as reflected by its higher extracellular lactate level, higher glucose consumption levels, and higher basal ECAR levels compared to MM.1S (**Chapter 2**). Studies showed that the elevated glycolytic phenotype may associate with DEX resistance [125, 324, 325]. In line with established publications, our data showed that MM.1S was the most sensitive to DEX, and MM.1R indeed was resistant to DEX (**Figure 4.4**). DCA and DEX combination significantly reduced the total viable cell number of MM.1R compared to DEX treatment alone, but this effect was mainly contributed by DCA, and there was no synergy between DCA and DEX on MM.1R (**Figure 4.4**). DCA can further reduce the total viable cell number significantly in RPMI 8226 and MM.1R compared to DEX single agent treatment (**Figure 4.4**). DCA (5 mM) had synergistic or additive effect (CI $\leq$ 1) with lower DEX concentrations (< 1μM) in RPMI 8226. U266 was not responsive to DEX and this result was consistent with published results [289].

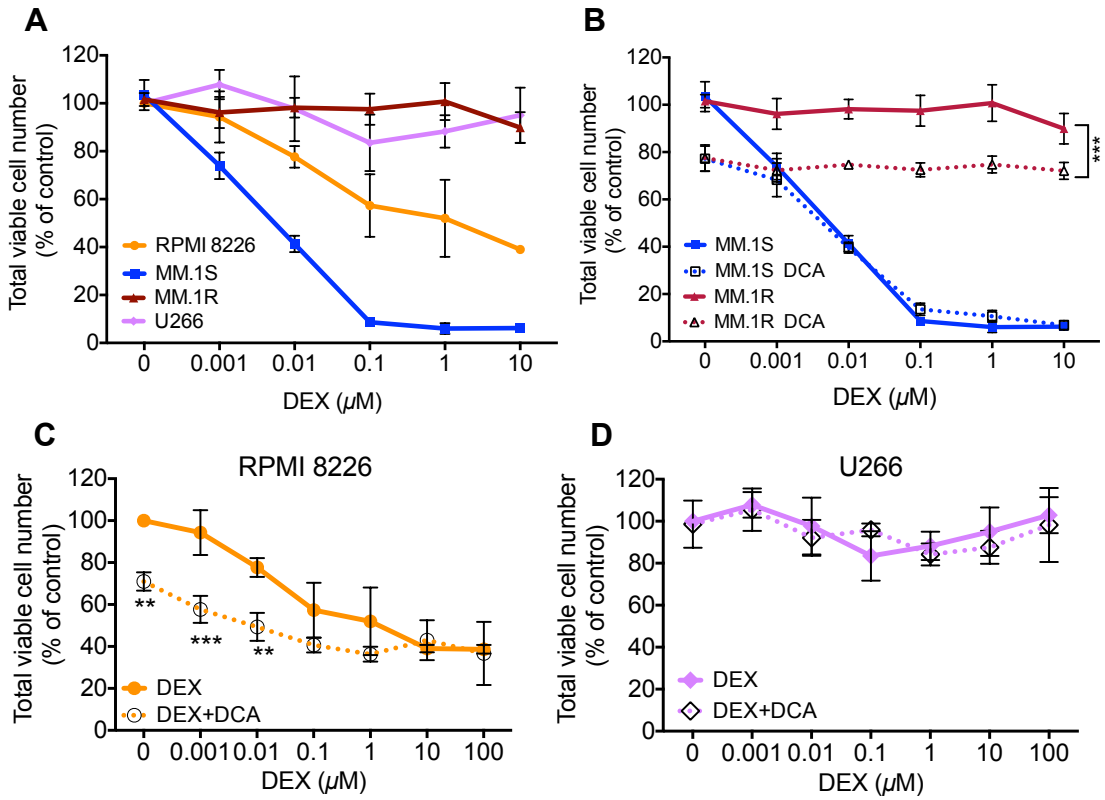

Figure 4.4 DEX and DCA co-treatments can further reduce the total viable cell number in MM cell lines. (A) The different sensitivities of MM cell lines to DEX (0-10 μM, 72 hours) alone. (B) The response of MM.1S and MM.1R to DCA (5 mM) and DEX (0-10 μM) co-treatment. The response of RPMI 8226 (C) and U266 (D) to DCA (5 mM) and DEX (0-100 μM) combination treatments. *Statistical comparisons represent DEX and DCA combination treatment compared to DEX only treatment. Each treatment was quadruplicated. All data points shown represented mean ± SD from at least 3 independent experiments; *$p < 0.05$, ** $p < 0.01$, ***$p < 0.001$.

Table 4.12 The EC_{50} of dexamethasone (DEX)

Cell Lines	EC_{50} (μM)	95% confidence intervals
RPMI8226	1.14	0.34-3.84
U266	*ND	ND
MM.1S	0.007	0.003-0.01
MM.1R	ND	ND

EC_{50}: half maximal effective concentration. *ND: not determined.

Four out of six DiCAM patients were taking immunomodulatory drugs during the trial (**Table 4.9**). LEN represents the immunomodulatory drugs and is often used in combination with DEX in myeloma therapy. The response to single agent LEN, LEN and DCA combination, or LEN, DEX and DCA combination treatments was tested on MM cell lines by measuring total viable cell numbers. MM cells lines had different sensitivities to LEN single agent treatment with MM.1S and MM.1R being sensitive while RPMI 8226 and U266 being resistant (**Figure 4.5 A**). RPMI 8226 was resistant to LEN, which is consistent with published paper; however, U266 in this experiment also showed resistance to LEN, which is inconsistent with the published paper [372]. The sensitivities of MM.1S and MM.1R to LEN were not statistically different indicating the mechanism of resistance to DEX does not affect their sensitivities to LEN (**Figure 4.5 B**). In RPMI 8226, DCA and LEN co-treatment further reduced total viable cell number compared to LEN single agent treatment significantly ($p < 0.001$), and the DEX and LEN co-treatment also significantly reduced the total viable cell number compared to LEN single agent treatment ($p < 0.001$) (**Figure 4.5 C**). While the LEN, DEX and DCA co-treatment showed a significant further reduction of the total viable cell number in RPMI 8226 compared to LEN single agent or LEN and DCA co-treatment, U266 was not responsive to any of the above drugs or any of the drug combinations (**Figure 4.5 D**). The results clearly showed an additive effect of DCA with low concentrations of LEN or DEX. DCA did not further reduce the total viable cell number in LEN plus DEX treatment, which is an existing standard combination for myeloma treatment. To better evaluate the drug combination effects, a full comparison of drugs using the Chou and Talalay method can be further explored. This method uses a range of different concentrations of each drug and can calculate the dose response curve and the combination index to indicate whether a combination is synergistic or not (section 4.2.4.4).

Table 4.13 The EC_{50} of lenalidomide (LEN)

Cell Lines	EC_{50} (μM)	95% confidence intervals
RPMI8226	ND	ND
U266	ND	ND
MM.1S	0.17	0.07-0.43
MM.1R	0.19	0.05-0.81

ND: not determined.

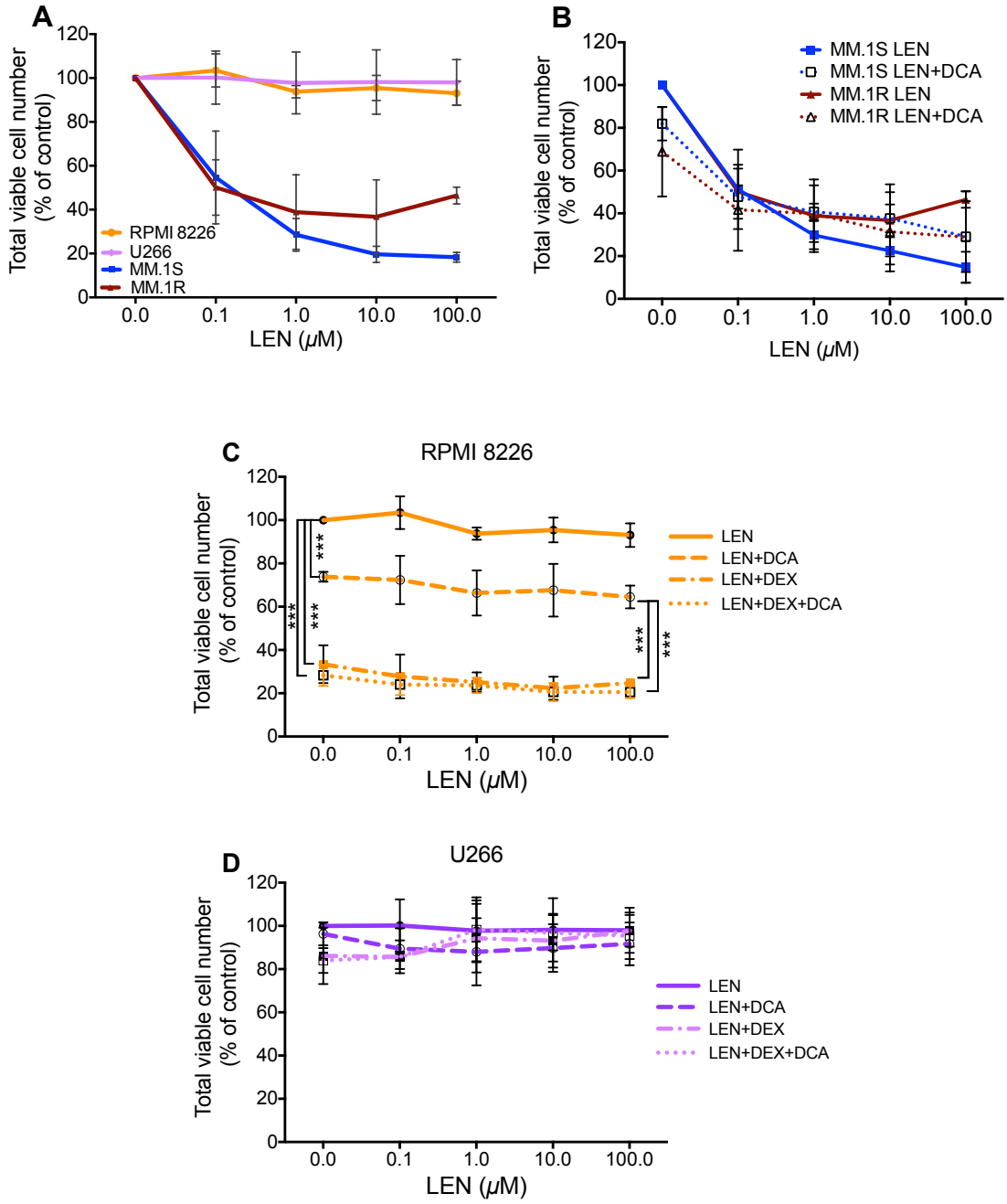

Figure 4.5 Different response to LEN and DCA co-treatments in MM cell lines. (A) The different sensitivities of MM cell lines to LEN (0-100 μM, 96 hours). (B) The response of MM.1S and MM.1R to DCA (5 mM) and LEN (0-100 μM) combination treatment. The response of RPMI 8226 (C) and U266 (D) to DCA (5 mM), LEN (0-100 μM), and DEX (1 μM) combination treatments. *Statistical comparisons represent comparisons among LEN single agent, LEN and DCA combination, LEN, DCA, and DEX combination treatments. Each treatment was quadruplicated. All data points shown represented mean ± SD from at least 3 independent experiments; *** $p < 0.001$.

4.4 Discussion

4.4.1 DCA clinical trial in MM patients

There have been several DCA early phase clinical trials in different solid tumours [5, 234-236], but our study was the first attempt in conducting a phase-2 DCA clinical trial in haematological malignancies, which has provided valuable dosing reference for any further investigation in the field.

The MM patients enrolled in the trial generally tolerated a loading dose of DCA (25 mg/kg) well. No patient was withdrawn due to toxicity caused by DCA. P002 did not take the last dose of DCA (6.25 mg/kg) due to a grade-3 neuropathy on the last day of DCA treatment, but since then the neuropathy symptoms were alleviated so P002 remained eligible for ongoing monitoring and outcome measurement on the trial protocol. The high loading dose regimen was designed to use DCA to inhibit its own metabolism and reduce DCA clearance rate thus to quickly reach ideal DCA serum levels. The recommended phase-2 dose of oral DCA from a published clinical trial in advanced solid tumours was 6.25 mg/kg twice daily [235], but based on the *in vitro* study (**Chapter 2, 3**) and the pharmacokinetics study of this chapter, the serum levels of DCA under this suggested dose regimen is not sufficient to inhibit all PDKs, indicating that future trials should use a higher dosing regimen.

The main concern of using DCA in cancer patients is peripheral neuropathy based on results from a published clinical trial [235]. It is common for cancer patients to experience peripheral neuropathy due to the side effects of chemotherapy or as a paraneoplastic phenomenon. This study successfully showed that high loading dose of DCA (25 mg/kg) was well tolerated even in MM patients who were already experiencing different degrees of mild baseline neuropathy (less than grade 2). There was no severe increase of the TNSc while the patients were given 6 high doses of DCA in the first 8 days of the trial (**Figure 4.2 G**). Furthermore, no patients needed dose reduction in the trial. However, there was a small increase of TNSc for the patients over the 3 months of chronic DCA administration and two out of six patients had grade-3 neuropathy on the last day of DCA treatment. P002 had the highest TNSc of 13 (**Figure 4.2 G**), but this side effect took 3 months to accumulate to a high level, so this side effect was more likely due to chronic DCA administration rather the short high dose of

DCA administration. Moreover, P002's high TNSc was mainly attributed to a high degree of tiredness (measured as strength and motor symptoms) rather than loss of neuron sensibilities (**Figure 4.2 B**). The patients were carefully monitored during the trial. Based on the safety and toxicity assessments through blood tests, liver and kidney function tests, and the Eastern co-operative oncology group performance status evaluation, all patients' quality of life was not affected despite experiencing mild increase of the neuropathy during the DCA treatment. But the neuropathy symptoms were alleviated after the DCA treatment was completed, which further confirmed that the neuropathy caused by DCA was reversible (**Figure 4.2**). These results validated the safety and feasibility of chronic administration of oral DCA for MM patients who had baseline peripheral neuropathy.

In this study, orally administrated DCA quickly reached the peak concentrations in the serum and was maintained at mechanistically relevant concentrations for 3 months. DCA was cleared faster after the first dose administration (**Figure 4.3 A**) with the half-life of DCA being around one hour on day 1, but increasing after subsequent administrations of DCA in all patients (**Figure 4.3 A**). DCA inhibits its own metabolism as seen in the results that the day-8 DCA levels were 2-3 folds higher than that of day 1 (**Figure 4.3 A**).

GSTZ1 protein-coding region polymorphisms correlated with patients' short-term serum DCA levels in this study. *In vitro* protein recombination studies showed that the *GSTZ1*A* haplotype corresponding protein GSTZ1a/1a displayed higher activity to metabolise DCA compared with other haplotypes and this haplotype also had a faster clearance rate of initial dose of DCA in healthy volunteers (**Chapter 1, section 1.4**) [215, 220]. P001 (GSTZ1*A/Z1*C) possesses a *GSTZ1*A* haplotype who had a faster rate of DCA clearance and a shorter DCA half-life than other patients on day 1 of the trial (**Figure 4.3**). However, this faster metabolism pattern was not seen on day 8 where patients were exposed to DCA for a week. This indicated that the GSTZ1 protein coding region polymorphism was responsible for short-term DCA exposure but was not the key manipulator for DCA metabolism when using DCA chronically.

GSTZ1 promoter polymorphisms correlated with patients' serum levels after longer-term DCA exposure in this study. P002 was homozygous A/A at *GSTZ1* promoter

nucleotide position -1002 and this correlated well with the highest DCA trough levels (**Figure 4.3 D**) and highest neuropathy score (**Figure 4.2**) compared to that of other patients. The promoter -1002A allele had significantly lower promoter activities compared to the -1002G allele in HepG2 cells [218]. The presence of -1002A also resulted in a lower cytosolic GSTZ1 protein expression and lower enzyme activities in Caucasian human liver samples [217]. The correlation of P002's genotype, higher DCA trough level and accumulative higher neuropathy score indicated that *GSTZ1* promoter polymorphism may be the driving variant in the chronic use of DCA, by causing changes to GSTZ1 expression and activity, which consequently alters DCA metabolism and its *in vivo* concentrations, thus resulting in different levels of neuropathy.

For future trials, individualized DCA dose based on a patient's *GSTZ1* genotypes can assist in reaching meaningful serum levels to better target the PDKs. For short-term use of DCA, higher dosing of DCA should be given to patients like P001 with a *GSTZ1*A* haplotype that is associated with faster DCA clearance rate. The faster clearance of DCA caused by this *GSTZ1*A* phenotype is only seen when DCA was administered on day 1 of the trial (**Figure 4.3 A**). DCA is more likely to be used chronically in cancer patients. For patients with the promoter -1002 A genotype, a lower chronic dose of DCA should be used to avoid severe peripheral neuropathy. However, as the frequency of homozygous promoter -1002 A genotype only accounts for approximately 11% of the Caucasian population (**Section 1.4.2, Table 1**), the majority of potential patients in Australia would still benefit from DCA treatment without the cumulative side effects. Individualized DCA dose based on each patient's GSTZ1 genotype would be beneficial for patients to achieve optimized DCA drug levels and avoid severe side effects.

The efficacy of DCA on the myeloma disease burden was also evaluated in this study. There was a reduction of the measurable disease burden on day 28 in 33% of patients where it reached a response (**Figure 4.1 G**), but the patients' response was not maintained when patients took lower maintenance dose of DCA. The exception was P002 who had the longest and also the greatest response to DCA compared to other patients. The disease burden of P002 was reduced more than 25% from day 28 till day 56, and on day 84 reduced by 24% (**Figure 4.1, G**). The response of P002 to DCA correlated with the highest DCA trough levels and the highest scores for neuropathy.

One explanation for this response was the *GSTZ1* promoter -1002 A genotype of P002, which can cause a higher serum DCA level. Additionally, P002 was the only patient who received bortezomib as a maintenance therapy during the first 30 days of the trial. *In vitro*, DCA can synergize with bortezomib in myeloma cell lines, and the co-treatment of DCA and bortezomib improved survival of myeloma-bearing mice [11]. Further investigation should be carried out to confirm the synergistic effects of combinational DCA and bortezomib treatment in patients.

Due to the limited number of patients, and the relatively low disease burden of the patients, the efficacy of DCA is still yet to be confirmed. As this trial was designed to protect patients from a potentially inactive treatment, the strict eligibility criteria limited our recruitment of patients with a high measurable disease burden. This may consequently recruited relatively "healthy" patients with only one of them had confirmed abnormal cytogenetic results when the genetic abnormalities are present in 60-70% of patients with progressive disease in the myeloma population [242]. Most of the patients recruited in this study had low quantitative diseases burden, which for some patients were near the detectable limits of the paraproteins measurement methodology (electrophoresis). As such, a result that fluctuates with ± 2 g/L was considered as no change in the actual disease burden. All these conditions made it technically difficult to interpret the efficacy of DCA in some of the recruited patients. Based on the information gained from this study, future clinical trials using DCA can include MM patients with a higher disease burden and a combination of DCA treatment with conventional chemotherapy can be designed instead of using DCA as a single agent.

The results of this trial offer valuable information about the safety and side effects of using DCA chronically in MM patients, determined the DCA pharmacokinetics in myeloma patients and found *in vivo* evidence of the correlation of *GSTZ1* genotypes with the DCA serum levels. The proposed limiting factor for the clinical use of DCA from other studies was the neuropathy, however, this study proved the safety of using DCA in MM patients even with baseline neuropathy. Based on the *in vitro* cell line study and other evidence, the serum DCA levels of the maintenance doses were in the range of inhibiting PDK2 but not sufficient to inhibit PDK1 and PDK3 effectively. Thus, a modified high DCA dose scheme is being carried out in our current clinical trial. DCA

is orally taken at 25-mg/kg *b.i.d* for 5 days, and then followed by a 2-day rest period, and this cycle will be repeated for 3 months. Based on the results from the DiCAM trial, the new trial will determine an optimal dosing guidance for future clinical trial testing DCA in cancer types that also display a glycolytic phenotype.

4.4.2 *In vitro* DCA and chemotherapy agents combination study

This chapter evaluated representative myeloma drugs used in the DiCAM trial in combination with DCA on MM cell lines. The resistance to DEX, the backbone of myeloma therapy, is common among MM patients. There have been various hypotheses to explain the resistance to GCs. The decrease or loss of p53 expression and function leads to MM cell progression and resistance to DEX through Bcl-2-related mechanisms [377, 378]. The results of this chapter showed that U266 was resistant to DEX, and U266 is also a p53 mutant cell line (**Table 2.1**). Many studies also demonstrated that the mutation of the GC receptors (GR) in MM cells is the reason for the GC resistance [285, 379]. MM.1R displayed a truncated mRNA of the GR and the GR protein level was also reduced or non-detectable [380]. However, the screening of the total GR protein expression on MM cell lines does not correlate with these results. MM.1R appeared to still have a certain amount of total GR expressed (**Appendix Figure 4.2**). Future study should investigate the functions and the different isoforms of GR.

The deregulated cancer metabolism phenotype can also contribute to the resistance to GCs. Transcriptional profiling indicated that resistance to GCs in leukaemia was associated with up-regulated glycolysis, cholesterol biosynthesis and glutamate metabolism, and was accompanied by increased proliferation and the activation of PI3K-AKT-mTOR and MYC signalling pathways [381]. GC resistance was demonstrated to be directly associated with a glycolytic phenotype in acute lymphoblastic leukaemia cells, and manipulation of the glycolysis pathways by glycolysis inhibitor (2-DG) and/or the mitochondrial respiration inhibitor (oligomycin) had additive or synergistic effects with methylprednisolone. This suggested that the sensitivity to GC could be restored by targeting the glycolytic phenotype in resistant cells [325]. In line with these above studies, the results of this chapter showed that MM.1R (DEX resistant) had higher glycolysis activities compared to MM.1S (DEX

sensitive) (**Figure 2.2, 2.4, 2.6**). However, while DCA and DEX combination treatment showed synergistic effects on RPMI 8226, a glycolytic cell line, DCA only had additive effects with DEX in MM.1R, suggesting that DEX resistance was due to different mechanisms in these cells (**Figure 4.4**).

Alongside the GCs resistance, the glycolytic phenotype was also found to be contributing to other chemotherapy drug resistance such as bortezomib and melphalan [125, 260]. The resistance correlated with the induction of LDHA and HIF1, and the inhibition of LDHA and HIF1 restored sensitivity to bortezomib and inhibited tumour growth. Consistently, gain-of-function mutations in LDHA or HIF1A induced resistance in bortezomib-sensitive cell lines [125]. The altered cancer cell metabolism is demonstrated to be essential for the regulation of chemotherapy drug resistance in MM cells. More study is needed to test the potential of DCA in reversing chemotherapy drug resistance in MM through manipulating the glycolysis metabolism.

There was limited information on the effects of DCA combined with immunomodulatory agents in MM. The results of this chapter showed that DCA had additive effects with LEN in some of the MM cell lines, but no synergy was observed. Resistance to LEN is common, about 40% of MM cell lines are resistant to LEN treatment [305]. The sensitivities to LEN in this thesis are in line with publications where RPMI 8226 is a LEN resistant cell line [372]. DCA and LEN cotreatment on LEN resistant cell line had a reduced total viable cell number compared to LEN treatment alone (**Figure 4.5**). It may still be useful to know that a LEN resistant cell line can respond to DCA. A study showed that by lowering lactate level and reducing the acidification of the cancer microenvironment using DCA yielded a better outcome for immunotherapy [382]. While DCA alone does not reduce the tumour burden, it increased antitumor immunotherapeutic poly I:C activity in mouse tumour models [382]. Although *in vitro* MM cell line system can only be used to show the direct effects of LEN on MM cells such as cell cycle, apoptosis and total viable cell numbers, but the cell line model is not sufficient to understand the complicated immune modulatory effects of LEN, which require the involvement of immune system.

This chapter demonstrated that the combination of DCA with either DEX or LEN had significant reduction of the total viable cell number compared to single agent treatment

in the DCA-responsive MM cells. Although DCA may not reverse the DEX or LEN resistance phenotype of the MM cell lines, the combination with DCA did not reduce the effectiveness of these commonly used chemotherapy agents. Further studies can be carried out to study the enhanced reduction in total viable cell numbers by DCA. The data shown here demonstrated that further investigations are warranted into the potential benefit of using DCA as an addition to the standard of care for the management of myeloma patients.

Chapter 5 General Discussion

5.1 Significance of Study

Deregulated cancer metabolism is a hallmark of cancer and has been studied for the development of new cancer treatments. The glycolytic phenotype is one of the well-studied metabolic pathways in cancer treatment [1]. Multiple myeloma (MM) displays this glycolytic phenotype but is also a heterogeneous cancer type with complex genetic profiles and metabolic phenotypes [11-13, 262, 352]. DCA has been used as an investigational drug to treat lactate acidosis and mitochondrial malfunction in humans for decades. DCA inhibits PDKs, thus indirectly activates the PDH (the key enzyme convert pyruvate into acetyl-CoA), diverting the flow of glycolysis-derived pyruvate from lactate production into mitochondrial respiration [3]. DCA has been shown to have anti-growth effects both *in vitro* and *in vivo* in various cancer types [5-10]. MM displays a glycolytic phenotype and DCA has anti-proliferative effects on MM cell lines and improved MM-bearing mice model survival when combined with bortezomib [11, 12]. However, the concentrations used in these studies were 10-50 times higher than the ones clinically achievable in humans. Moreover, there have been four DCA clinical trials studying the effects of DCA on malignant solid tumours [5, 234-236], but none on haematological cancer types. The efficacy of DCA has not yet been demonstrated.

In this thesis, the effect of DCA in improving the remission in MM patients with steady disease burden (plateau phase) is investigated in the clinical trial (DiCAM), which is the world first trial using DCA in haematological cancer. Furthermore, it also verified the ability of DCA to inhibit cancer cell growth under clinically relevant conditions; investigated the factors contributing to the different sensitivities to DCA in MM cell lines; and evaluated the effect of combining DCA with various chemotherapy agents with the aim of finding effective combinations for clinical use.

This study demonstrated the safety of using DCA in MM patients with steady disease burden after being treated with conventional chemotherapy (**Chapter 4**). Peripheral neuropathy is the main side effect of DCA and is considered to be the limiting factor for its use in the clinic [383], however, this study showed the safety of using DCA in patients with baseline peripheral neuropathy. GSTZ1 is the only known enzyme to

metabolise DCA, but DCA inhibits GSTZ1 [208, 209]. The dosing regimen of this study innovatively had a high loading dose of DCA to inhibit its own metabolism thus to quickly achieve desirable DCA serum levels in MM patients. The patients *GSTZ1* genotype correlated with their DCA serum levels in this study. This information will be useful in the future to individualize DCA dosage based on patients' *GSTZ1* genotypes in order to achieve a maximum effect and avoid causing severe side effects.

Previously published studies in MM cells did not provide evidence of the effects of DCA when used at clinically achievable levels [11, 12]. Concentrations of DCA used in this thesis were in the range of the inhibitory constant (K_i) values, that is, the concentration of DCA needed to reduce half of the targeted PDK enzyme activity *in vitro*. The four isoforms of PDKs have different K_i values to be inhibited by DCA ranging from 0.2 mM (PDK2) to 8 mM (PDK3) [4]. The results of this thesis found that DCA, at concentrations in the range relevant of the K_i values, had cytostatic effects on MM cells in normoxia and can have cytotoxic effects on MM cells in hypoxia. DCA can act on-target in MM cell line when used at concentrations achieved clinically in our DiCAM trial (**Chapter 2, 4**). These concentrations are 10-50 fold lower than those used in other *in vitro* studies on MM [11, 12]. This thesis also demonstrated that the on-target effect of DCA at these lower concentrations was cumulative over time *in vitro* (**Chapter 2**).

MM is a very heterogeneous disease and the MM cells exhibit varying responses to DCA treatment (**Chapter 2**). This is likely due to the heterogeneity of the MM cells, which was displayed in their preference for nutrients, their degree of dependence on glycolysis, and their glycolytic reserve (**Chapter 2, 3**). Identification of the contributing factors to the sensitivity of cancer cells to DCA is important for the selection of suitable cancer types as well as patients that can benefit from DCA treatment. This study found that the PDK (the targets of DCA) profile under normoxia may correlate with some of the sensitivity to DCA, but the degree of dependence on the glycolytic phenotype and an active glycolysis pathway may be the key contributing factors in determining the sensitivity of cancer cells to DCA. The effects of DCA were abolished when there was no glucose present or when the glycolysis pathway was not activated (**Chapter 2, 3**). While the metabolic modulatory effects of DCA may not cause growth inhibition

effects under normoxia (**Chapter 2**), DCA is able to exhibit greater anti-cancer effects in the non-glycolytic MM cell line in which the glycolysis pathway is activated under hypoxia (**Chapter 2, 3**). DCA was found in this study to be more effective when the glycolysis pathway is upregulated, which offers us insight into which patients would be most likely to benefit from DCA treatment.

5.2 Limitations and Future Directions

5.2.1 DCA clinical trial modification

The DiCAM study was unable to recruit the ideal number of patients due to our strict eligibility criteria. The ideal patient for this trial would be MM patient in remission but still with a considerable amount of residual disease burden. As it turned out, the majority of eligible MM patients in remission had a very low disease burden (**Chapter 4, Table 4.9**) and the levels being close to the limits of the detection methods. The limited number of patients in DiCAM also hindered a statistical analysis on efficacy of DCA. Thus, in this trial, the efficacy of DCA was not determined. In future DCA clinical trials, patients with higher disease burden should be included, for example, MM patients with progressive disease and undergoing active chemotherapy, or patients with other B-cell malignancies can also be considered in DCA clinical trial.

Based on our pharmacokinetics data of DCA from this trial, and correlating with the results from MM cell line study, it has become clear that the dose regimen used in this trial was only high enough to reach the concentrations to inhibit PDK2 (K_i: 0.2 mM), PDK4 (0.5 mM) and partially PDK1 (1 mM) but not PDK3 (8 mM) (**Chapter 4**) [4]. The doses of DCA need to be increased to reach a higher serum level so that all PDKs may be better targeted, but first further investigation is needed into what the optimal doses of DCA in patients are. Recently, a new clinical trial protocol has been approved enabling our laboratory to test a higher DCA dosage regimen for all B-cell malignancies including MM, chronic lymphocytic leukaemia and low-grade lymphoma, at The Canberra Hospital. In this updated protocol, patients will be given 25-50 mg/kg of oral DCA twice daily for 5 days and followed by a 2-day rest period, then this 5-day on, 2-day off regimen will be continued for 12 weeks. As the DiCAM trial data indicated that chronic DCA administration could be associated with increased reversible neuropathy symptoms (**Chapter 4 Figure 4.2**), the new trial has modified the DCA dose schedule

to an intermittent dosing to allow patients to clear all the DCA, preventing accumulation of trough DCA levels, thereby preventing development of further neuropathy. This new study will focus on establishing the lowest effective dose of oral DCA in patients that will achieve serum concentrations of DCA predicted to be sufficient to inhibit PDK 1, 2, and 4, and thus determine a recommended phase-2 dosing (RP2D) schedule for haematological malignancies. This RP2D from our study will be in contrast to the RP2D (6.25 mg/kg, *b.i.d*) determined by Chu et al., which was based on maximum tolerated continuous dosing of DCA [235].

5.2.2 DCA clinical trial in high-risk smouldering myeloma

The repurpose of DCA for MM treatment can be carried out in high-risk smouldering myeloma (SMM). The current standard treatment for SMM is observation. However, SMM is very heterogeneous in terms of disease symptoms, biomarkers and risk to progression to MM. Even after the IMWG updated the MM diagnosis criteria and considered a small subgroup of previous SMM as early-stage MM [248], yet there remain some high-risk subgroups of current SMM with an approximately 50% risk of progression within 2 years, and these patients can be considered for clinical trials that are testing early intervention therapy [384].

There was lack of positive results treating SMM before the introduction of novel agents such as lenalidomide (LEN) and bortezomib. Previous clinical trial designs did not stratify high-risk SMM patients from the low-risk ones. However, a recent randomized clinical trial showed early intervention treatment of high-risk SMM with LEN and DEX, was associated with better progression-free and improved overall survival compared to the no-intervention observation group [283].

To our knowledge, there has not been any study to investigate whether the glycolytic phenotype is present in high-risk SMM. But there has been indirect evidence that SMM does present with a glycolytic phenotype. One of the current definitions of high-risk SMM is that ^{18}F-FDG-PET/CT scan of focal lesion with increased uptake of the^{18}F-FDG tracer without underlying osteolytic bone destruction, which indicates a high-risk of progression to MM [384]. Clinical studies demonstrated that the ^{18}F-FDG-PET/CT scan has diagnostic value in monitoring SMM disease progression as patients with

positive scan results had a higher risk of progression to MM [249, 385, 386]. Through plotting the Oncomine data available from a global gene-expression profiling study [387], we found that many of the glycolysis-related genes had higher expression levels in myeloma cells enriched from SMM biopsy compared to those of the normal plasma cells from healthy people, for example, LDHA mRNA expression is 2.6 fold higher, MYC expression is 3.1-fold higher, GLUT is 1.9-fold higher, and PDK2 is 2-fold higher in SMM compared to healthy plasma cells (**Appendix Table 5.1**).

The evidence suggests that the glycolytic phenotype is present in SMM. Clinical trials can be designed to target this glycolytic phenotype by using DCA in high-risk SMM patients. Patients with high-risk SMM can be grouped into an observation group and an early intervention DCA treatment group in a randomized trial. The end point will be progression to MM, and by comparing the progression time to MM for the two groups, it can potentially reveal whether DCA intervention can lead to a better prognosis or not.

5.2.3 Biomarker of DCA in patients and the effect of DCA on patient myeloma cells

Although the results of this thesis have confirmed the on-target effects of DCA at clinically achievable levels, this was only demonstrated in MM cell lines (**Chapter 2**) and there was no validated biomarker to indicate whether DCA was acting on-target in myeloma cells from the DiCAM MM patients. Our laboratory has explored using pPDH/tPDH (western blot) as a biomarker to evaluate the on-target effects of DCA in MM patients' PBMCs. The results showed a reduced pPDH/tPDH after DCA exposure in the patients (data not shown), which implied that DCA could act on-target in human. But further studies are needed to provide direct evidence of the on-target effects of DCA on myeloma cells in the BM of MM patients.

If we could obtain the permission from the ethics committee, we could directly evaluate the on-target effects of DCA by determining the pPDH/tPDH in the MM patients' BM biopsy myeloma cells ($CD138^+$) both before and after patients receiving a period of DCA treatment. There are a few methods that can be used to measure the on-target effects of DCA. If the yield of the patient's myeloma cells is abundant, a western blot can be performed to evaluate the change of pPDH/tPDH in each patient according to a protocol developed in our laboratory. In order to find a suitable, reliable and easily

detectable biomarker for DCA in patients, I optimized the western blot method to measure pPDH/tPDH as a biomarker in the enriched CD 138^+ MM cells from BM biopsy after *in vitro* DCA treatment. I also evaluated the effects of DCA on pPDH/tPDH and the baseline variation of pPDH/tPDH from different MM patients (newly diagnosed and relapsed) and healthy donors (**Appendix Figure 5.1**). Due to the limited number of donors of BM biopsy and the low myeloma cells count in the acquired biopsies, this result may not be able to draw a conclusion on whether DCA can act on-target in myeloma cells; however, with this optimized method, further recruitment of eligible MM patients can be carried out to validate this biomarker. If the yield of the myeloma cells was too low from the BM biopsy, other methods can be optimised to evaluate the change in the expression of pPDH after DCA treatment, such as using PDH antibody staining followed by flow cytometry analysis or by using immunohistochemistry staining on the BM biopsy smears. But these methods all need optimization and are not as straightforward as western blot.

5.2.4 Predicting a cancer patient's suitability for DCA treatment

The studies of this thesis and other published studies indicate that multiple factors need to be considered to predict whether a cancer patient can be a good candidate for DCA treatment or not. First of all, the results of this thesis confirmed that DCA works best in glycolytic cancer cells and the effect of DCA can be cancelled by inhibiting glycolysis (**Chapter 2, 3**), so it is important to validate whether the cancer type of the patient is glycolytic or not. There are about 24 cancer types, accounting for more than 70% of global cancer cases that have a glycolytic phenotype [2]. Accumulating reports showed that the glycolytic phenotype is associated with cancer progression and that the glycolytic phenotype is targetable. The solid cancers exhibiting the glycolytic phenotype mainly originate from: the brain and nervous system [5]; the digestive system such as colon, stomach, liver, pancreas [388-392]; and reproductive system such as mammary glands, ovary, uterus, prostate [393-396]; as well as lung [397] and skin [2, 398]. Overexpression of glycolysis genes has also been shown to occur in haematological cancers, such as MM, some leukaemia and lymphoma (Hodgkin and non-Hodgkin) [2]. The glycolytic phenotype is associated with drug resistance in acute myeloid leukaemia (AML). The RNA expression of enzymes and transcription factors

associated with the glycolytic phenotype, such as hexokinase, GLUT1, LDHA, and HIF-1α was increased in drug-resistant AML patients compared to AML patients in complete remission and partial remission or healthy individuals [399]. The inhibition of G6PD activity induced anti-leukaemia effects both *in vitro* and *in vivo* [400]. The inhibition of genes driving the glycolytic phenotype such as MYC and PI3K-mTOR decreased lymphoma cell viability through the reduction of the expression of glycolysis-associated genes [401]. Further investigation into the effect of DCA can be carried out in the above described cancer patients with a glycolytic phenotype; however, due to the metabolic heterogeneity of the cancer cells, a personalized screening of the patients' primary cancer cells is needed to better validate the presence of the glycolytic phenotype. There are possible markers that can be screened in the laboratory such as pPDH/tPDH ratio by western blot and OCR/ECAR by Seahorse flux analyser, to predict whether the primary cancer cells of patients can respond to DCA. However, these methods may not be practical or economical in a hospital setting.

These markers may also be suitable for predicting the sensitivities of the cancer cells to DCA in hypoxia. Based on the results from the *in vitro* work of this thesis, the most glycolytic cell line (RPMI 8226) was the most sensitive to DCA treatment, this result correlated with the effects of DCA in reducing the pPDH and ECAR in RPMI 8226. In normoxia, although DCA did not inhibit the growth of non-glycolytic U266, however, it effectively reduced pPDH and ECAR levels; whereas in hypoxia, DCA reduced cell viability and induced apoptosis in U266 (**Chapter 3**). Since myeloma cells develop in the hypoxic BM, so the response to DCA in hypoxic conditions may be more relevant to its clinical use.

The target of DCA, the PDKs, can contribute in predicting whether a patient will be sensitive to DCA treatment. The PDKs vary in their sensitivity to inhibition by DCA, with PDK3 being the least sensitive [4]. The PDK profile correlates with some of the sensitivity to DCA in this thesis (**Chapter 2**). Previous studies in this laboratory have also demonstrated that the magnitude of the sensitivity to DCA correlated with PDK expression. Thus, the PDK expression profile in the cancer cells from patient can be used to predict a patient's sensitivity to DCA. Immunohistochemistry examination of PDK protein expression in patients' BM smears can also be used. PDK1 protein

expression has been studied in different cancer types such as neuroblastoma, lung cancer, head and neck squamous cancer, and breast cancer using immunohistochemistry analysis [365, 402-404]. The ideal patients for DCA treatment would have higher levels of PDK2 and PDK1 expression but lower levels of PDK3 expression since DCA serum levels in our DiCAM trial can achieve the concentrations to inhibit PDK2 and PDK1 but not PDK3 (**Chapter 4**).

When using DCA in patients, one cannot overlook the metabolism of DCA, as this directly affects its serum levels in humans. GSTZ1 is the only known enzyme to metabolise DCA in humans. In the DiCAM trial, the *GSTZ1* promoter polymorphism correlated well with the chronic DCA serum levels in patients and its side effects (**Chapter 4**). Thus, by genotyping the patients, we can predict the ability of a patient metabolise DCA, and based on this information, doctors can adjust the DCA dose to reach an optimized DCA serum level without causing severe side effects.

5.2.5 Chronic low dose DCA treatment in patients

DCA was found to have a cytostatic effect on myeloma cells (**Chapter 2**). There have been several case reports of the chronic use of DCA in cancer patients resulting in disease stabilization and remission. A patient with renal squamous cell carcinoma who was treated with oral DCA (18 mg/kg/day) for 3 months showed no recurrence of the cancer and achieved a complete remission for more than 5 years. This was the first reported long-term complete remission for this aggressive disease with short median survival usually being several months [405]. A stage-4 colon cancer patient experienced disease stabilization by DCA therapy for nearly 4 years. This patient tolerated high doses of DCA well, only experienced mild sedation [406]. Khan et al. (2017) treated a metastatic melanoma patient with oral sodium DCA therapy (17 mg/kg/day) alone, and this resulted in disease stabilization for over 4 years with this patient only experiencing minor peripheral neuropathy [407]. Since DCA is an off-patent chemical, many cancer patients have been purchasing DCA on-line and self-medicating. Strum et al. (2013) contacted self-medicated patients and reported that a non-Hodgkin's lymphoma patient on DCA (1,000 mg/day) achieved a complete remission after disease progression with conventional therapy. This patient's symptoms were alleviated within two weeks of commencing DCA therapy, and by day 71, all systemic symptoms were completely

resolved [408]. These patients were chronically using higher doses of DCA than the maintenance dose (6.25 mg/kg, *b.i.d*) used in our DiCAM trial. Based on these case studies, DCA can be used in patients for long term with minimal side effects that need monitoring.

The chronic DCA treatment in patients caused remission in the case reports, but further study is needed in the laboratory to understand the mechanism of this effect. The results of this thesis showed that the clinically achievable doses of DCA were cumulative in reducing pPDH (**Chapter 2**). Exposure to the lower doses of DCA over long term caused a significant decrease of the pPDH in MM cell line, similar to that achieved with short-term, higher-dose DCA treatment (**Chapter 2**). But investigations are needed to determine whether the long-term exposure to low doses of DCA can yield any on-target effects on MM cell lines with different PDK profiles. Furthermore, it raises the question of whether this low dose regimen causes any growth inhibition outcomes. This would help us to understand how chronic DCA treatment caused remission in patients and how we can best use DCA clinically.

5.2.6 *In vivo* multiple myeloma models

This thesis examined the effects of DCA and tested it in combination with various drugs on MM cell lines. The MM cell lines were found in this thesis to have heterogeneous metabolic profiles and to respond better to DCA in hypoxia (**Chapter 2, 3**). The hypoxia treatment used in this thesis was homogeneous and acute (24 hours) instead of heterogeneous and chronic like that in the BM. The *in vitro* results obtained from myeloma cell lines do not reflect the complexity of the myeloma BMM. Therefore, further study is needed using *in vivo* models which would enable us to observe the interactions between myeloma cells and the BMM, and to test the effects of DCA combination therapy in the BM.

There are different kinds of well-developed murine MM models including the immunocompetent and immunodeficient mouse myeloma models, xenograft murine models of human myeloma, and genetically engineered models which mimic the gene mutations responsible for the development of MM from MGUS in humans [409]. Different models have different advantages and disadvantages. The xenograft murine

myeloma models and the Vk*MYC model can be considered for the purpose of evaluating a new drug combination and studying the effect of DCA on myeloma cells when interacting with the heterogeneous and hypoxic BMM.

To create xenograft myeloma models, human MM cell lines or primary human myeloma cells are injected into immune compromised mice; systemic disease is able to be established via intravenous injection, or local disease via subcutaneous injections. These models can be used to evaluate the homing of MM cells to the BM and to test the efficacy of new therapies against human MM *in vivo* [11, 410, 411]. However, these models are not ideal for studying the immunomodulatory drugs due to the compromised immune system. Another disadvantage is the intravenous injection of xenograft cells can result in cancer that is not restricted to the BM but is also present extensively in extramedullary sites. Although this may represent the rare aggressive type of human MM, it does not reflect the more common but less aggressive types. MM cell lines representing certain types of MM were derived from different MM patients, thus may not be representative of the vast heterogeneity seen in patients [412]. A xenograft model using primary human samples may be more representative of this heterogeneity but it could be difficult to obtain enough myeloma cells from one single biopsy from patients to develop this model. The cost and logistics would need to be considered.

Activation of MYC is associated with the progression of MGUS to MM. The Vk*MYC mouse model was developed by introducing the MYC transgene into the C57BL/KaLwRij mouse strain which has a high rate of spontaneously developed MGUS progressing to MM [413, 414]. The Vk*MYC model resembles many of the biological and clinical characteristics of human MM, for example, it has a high level of monoclonal immunoglobulin (Ig) secretion which can be readily quantified; a progressive monoclonal plasma cell population localized within the BMM; an intact host immune system, and relevant clinical features (anaemia, renal disease, bone fractures). The Vk*MYC model has an indolent disease course and a late onset of MM resembling that of the human MM, thus it can be tested for new therapies that target different phases of MM [414]. These advantages of the Vk*MYC model enable researchers to further study the effects of DCA on myeloma cells in a heterogeneous and chronically hypoxic BMM, and to monitor disease progression and disease burden

through Ig quantification and fluorescent or luminescent signal. The intact host immune system of Vk*MYC can be used to test immunomodulatory drugs combined with DCA as well as combinations of multiple metabolic pathway inhibitors. But this model may not reflect the heterogeneous genetic mutations normally seen among MM patients. These new studies would offer a deeper insight into the potential of DCA and an understanding of its working mechanism in a more complex but realistic setting.

5.2.7 PDKs knockdown in MM cell lines

To confirm that the working mechanism of DCA is by inhibiting PDKs, siRNA knockdown on PDKs should be carried out in a future study. In this laboratory, a PDK siRNA knockdown study was performed successfully in breast cancer cell lines using Lipofectamine reverse transfection method. The effect of DCA on increasing ROS in T-47D (breast cancer cell line that mainly expresses the PDK2 isoform) correlated well with that of the siPDK2 knockdown [232]. Targeting PDK2 with DCA or siPDK2 knockdown yielded similar effects on growth inhibition in T-47D, yet combination of DCA with siPDK2 did not further reduce the growth of T-47D. Thus, the effect of DCA on inhibition of cancer cell growth was confirmed through the inhibition of its target-PDK2 [415].

Knockdown of a specific PDK in cell line and then overexpress it could confirm mechanistically whether any specific PDK isoform expression is contributing to the different sensitivity to DCA. A previous study from this laboratory using the same siRNA knockdown method has demonstrated that the sensitivity to DCA was determined by the PDK profiles. The MCF7 breast cancer cell line expresses high levels of the PDK3 isoform and found to be not sensitive to DCA treatment. The siPDK3 knockdown in MCF7 increased its sensitivity to DCA treatment by 24% [415].

Because MM cell lines grow in suspension or semi-adherently, it is very difficult to manipulated these cells using the above transient transfection methodologies. In our method optimization, the yields of the plasmid-transfected cells were too low to be used for any analysis. There were studies reported or try to develop methods to efficiently deliver siRNAs into MM cells. Although some publications have reported MM cell transfection in their methods [416-419], a robust and widely applied protocol for

efficient transient transfection has not been established. By far, electroporation and viral gene transfer are the relatively more successful siRNA delivery methods in myeloma cells, but each has its limitations. The electroporation method has only been successful in a few myeloma cell lines, and can cause significant cell death; while the viral transfer method is demanding on equipment and time (Dr Amee George, personal communication).

5.2.8 The need for a more potent PDK3 inhibitor

The DCA treatment *in vitro* and in patients showed limited effects in this study. The results of this thesis support the concept of targeting the glycolytic phenotype of the cancer cells, but more potent PDK inhibitors are needed. The mRNA and protein expression of PDK3 was upregulated in hypoxia (**Chapter 3**). Upregulated expression of PDK3 in cancer can contribute to a reinforced glycolytic phenotype and thus contribute to increased cancer cell survival and drug resistance (**Chapter 3 Discussion**). It is difficult to inhibit PDK3 using DCA in patients (PDK3, K_i: 8 mM), thus more potent inhibitors for PDK3 need to be investigated in cancer treatment.

Although there are derivatives of DCA and other molecules that have been developed to inhibit PDKs, many of them lack further preclinical study or have been shown to be too toxic [134]. Besides DCA, the other known PDK inhibitors are AZD7545 and radicicol. AZD7545 inhibits PDK1 and PDK3 by binding to the lipoyl-binding pocket in the N-terminal domain of PDK thus interrupting kinase binding to the pyruvate dehydrogenase complex (PDC) [199]. Similarly, AZD7545 inhibits PDK2 activity by disrupting the binding between PDK2 and lipoyl-bearing domains of the E2 component of the PDC [420]. In contrast, radicicol competes with ATP for the nucleotide-binding site of PDK3 by directly binding to the ATP-binding site in the C-terminal domain of PDK3, thus inhibiting PDK3 activity [199].

Compared to DCA, AZD7545 is relatively more potent at inhibiting PDK1 and PDK3, with an IC_{50} of 0.087 μM for PDK1 and 0.6 μM for PDK3; radicicol exhibits an IC_{50} of 230 μM for the inhibition of PDK1 and an IC_{50} of 400 μM for PDK3 [199]. It takes about 8-times more DCA to inhibit PDK3 than PDK1. Similarly, it takes 7-times more AZD7545 to inhibit PDK3 than PDK1. Thus, AZD7545 does not have a more

specificity for inhibiting PDK3. The dose of radicicol required to inhibit PDK3 is about 1.7 times higher than inhibiting PDK1 so it may be a more specific inhibitor of PDK3.

AZD7545 was demonstrated to activate PDH and stimulate the rate of pyruvate oxidation in rat hepatocytes. AZD7545 was shown to increase the proportion of the activated/dephosphorylated liver PDH form in a dose-related manner in a rat model [421]. Despite promising *in vitro* activity, radicicol is inactive *in vivo* due to its instability in serum. Although there has been research to modify its structure, and the derivatives have potent activity *in vitro* and *in vivo*, these compounds have not been developed further in clinical studies [422]. AZD7545 and radicicol have more potent inhibitory ability against PDKs *in vitro*; however, there is lack of safety and efficacy information in humans. This disadvantage has limited their clinical use. DCA still has the advantage as being a good prototype PDK inhibitor because it can readily be tested in clinical trials.

5.2.9 Targeting the glycolytic phenotype in the treatment of myeloma today

There has been rapid progress in immunotherapy research in myeloma today compared to four years ago. T cell-mediated immunotherapy such as chimeric antigen receptor T-cell (CAR-T, introduced on page 54) is being studied extensively in clinical trials and showing promising results in myeloma patients. However, emerging resistance to CAR-T therapies due to intrinsic immunosuppressive networks remains a major challenge [423]. Moreover, CAR-T therapy faces other challenges such as confronting a highly immunosuppressive cancer microenvironment (CME), and cancer cells with low immunogenicity. Thus, new methods to overcome the resistance and enhance the efficacy of CAR-T therapy are needed [424]. Effector T cell activation requires a rapid metabolic switch to glycolysis, a process common to cancer cells and proliferative cells (Chapter 1 section 1.2.1). Sharing the same metabolic phenotype, T cells and cancer cells compete for key nutrients, such as glucose, glutamine, lipids, and amino acids [425]. The deregulated metabolic phenotype of the cancer cells mediated and regulated the CME, creating a CME characterised by nutrient depletion and acidosis, which is hostile for T cell activation and proliferation, consequently impairing T cell anticancer functions [426].

This thesis supports the concept of targeting cancer glycolytic phenotype in myeloma. DCA single agent treatment showed limited anti-growth effects in myeloma cells (Chapter 2), but the metabolic modulatory effects of DCA can be further explored for reducing the acidic CME (by reducing lactate production) to improve the CME for T cell activation. DCA was demonstrated to improve the immune status in thymoma bearing mouse model and enhance the effects of antitumor immunotherapy (discussed in Chapter 4) [382]. Other metabolic modulatory drugs that inhibit glycolysis, such as LDHA inhibitors or MCT inhibitors can also be studied for their potential to improve immunotherapy in cancer [424]. Targeting the cancer metabolic phenotype may have potential in the improvement of immunotherapy by altering the hostile CME for immune cell activation.

5.3 Conclusions

To conclude, DCA has the potential to be used as a low-toxicity addition to conventional chemotherapy. The safety of DCA treatment in MM patients that present with baseline neuropathy was confirmed. DCA serum levels were maintained at concentrations to inhibit PDK2, PDK4 and partially PDK1 but not PDK3 in patients. The *in vitro* studies presented in this thesis also showed that DCA, at concentrations in the range of inhibitory constant values, can act on-target by reducing the inactive phosphorylated PDH, reverse the glycolytic phenotype, and has anti-growth effects on MM cells. DCA can have greater effects in hypoxic conditions. This thesis provides dosing guidance for future clinical trial testing DCA in cancer treatment. It also opens windows for further investigation into the repurposing of DCA for use against other types of cancer that display a glycolytic phenotype.

References

1. Cairns RA, Harris IS, Mak TW. (2011) Regulation of cancer cell metabolism. *Nature Reviews Cancer* 11, 85-95.

2. Altenberg B, Greulich KO. (2004) Genes of glycolysis are ubiquitously overexpressed in 24 cancer classes. *Genomics* 84, 1014-1020.

3. Whitehous S, Randel PJ. (1973) Activation of pyruvate dehydrogenase in perfused rat heart by dichloroacetate. *Biochemical Journal* 134, 651-653.

4. Bowker-Kinley MM, Davis WI, Wu P, Harris RA, Popov KM. (1998) Evidence for existence of tissue specific regulation of the mammalian pyruvate dehydrogenase complex. *Biochemical Journal* 329, 191-196.

5. Michelakis ED, Sutendra G, Dromparis P, Webster L, Haromy A, Niven E, Maguire C, Gammer TL, Mackey JR, Fulton D, Abdulkarim B, McMurtry MS, Petruk KC. (2010) Metabolic modulation of glioblastoma with dichloroacetate. *Science Translational Medicine* 2, 31-34.

6. Wong JY, Huggins GS, Debidda M, Munshi NC, De Vivo I. (2008) Dichloroacetate induces apoptosis in endometrial cancer cells. *Gynecologic Oncology* 109, 394-402.

7. Bonnet S, Archer SL, Allalunis-Turner J, Haromy A, Beaulieu C, Thompson R, Lee CT, Lopaschuk GD, Puttagunta L, Bonnet S, Harry G, Hashimoto K, Porter CJ, Andrade MA, Thebaud B, Michelakis ED. (2007) A mitochondria-K+ channel axis is suppressed in cancer and its normalization promotes apoptosis and inhibits cancer growth. *Cancer Cell* 11, 37-51.

8. Madhok BM, Yeluri S, Perry SL, Hughes TA, Jayne DG. (2010) Dichloroacetate induces apoptosis and cell-cycle arrest in colorectal cancer cells. *British Journal of Cancer* 102, 1746-1752.

9. Sun RC, Board PG, Blackburn AC. (2011) Targeting metabolism with arsenic trioxide and dichloroacetate in breast cancer cells. *Molecular Cancer* 10, 142-157.

10. Sun RC, Fadia M, Dahlstrom JE, Parish CR, Board PG, Blackburn AC. (2010) Reversal of the glycolytic phenotype by dichloroacetate inhibits metastatic breast cancer cell growth in vitro and in vivo. *Breast Cancer Research and Treatment* 120, 253-260.

11. Sanchez WY, McGee SL, Connor T, Mottram B, Wilkinson A, Whitehead JP, Vuckovic S, Catley L. (2013) Dichloroacetate inhibits aerobic glycolysis in multiple myeloma cells and increases sensitivity to bortezomib. *British Journal of Cancer* 108, 1624-1633.

12. Fujiwara S, Kawano Y, Yuki H, Okuno Y, Nosaka K, Mitsuya H, Hata H. (2013) PDK1 inhibition is a novel therapeutic target in multiple myeloma. *British Journal of Cancer* 108, 170-178.

13. Mashima T, Seimiya H, Tsuruo T. (2009) De novo fatty-acid synthesis and related pathways as molecular targets for cancer therapy. *British Journal of Cancer* 100, 1369-1372.

14. Nelson DL, Cox MM, *Lehninger Principles of Biochemistry* 7th ed.; Macmillan: 2017.

15. Berg J, Tymoczko JL, Stryer L, Glycolysis Is an Energy-Conversion Pathway in Many Organisms In *Biochemistry*, 5th ed.; W H Freeman: New York, 2002.

16. Berg J, Tymoczko JL, Stryer L, The Citric Acid Cycle Oxidizes Two-Carbon Units. In *Biochemistry*, 5th ed.; W H Freeman: New York, 2002.

17. Berg J, Tymoczko JL, Stryer L, The Respiratory Chain Consists of Four Complexes: Three Proton Pumps and a Physical Link to the Citric Acid Cycle. In *Biochemistry*, 5th ed.; W H Freeman: New York, 2002.

18. Berg J, Tymoczko JL, Stryer L, A Proton Gradient Powers the Synthesis of ATP. In *Biochemistry*, 5th ed.; W H Freeman: New York, 2002.

19. Vander Heiden MG, Cantley LC, Thompson CB. (2009) Understanding the Warburg effect: the metabolic requirements of cell proliferation. *Science* 324, 1029-1033.

20. Tennant DA, Duran RV, Boulahbel H, Gottlieb E. (2009) Metabolic transformation in cancer. *Carcinogenesis* 30, 1269-1280.

21. Kroemer G, Pouyssegur J. (2008) Tumor cell metabolism: cancer's Achilles' heel. *Cancer Cell* 13, 472-482.

22. Ganapathy-Kanniappan S, Geschwind J-FH. (2013) Tumor glycolysis as a target for cancer therapy: progress and prospects. *Molecular Cancer* 12, 152-163.

23. Lunt SJ, Chaudary N, Hill RP. (2009) The tumor microenvironment and metastatic disease. *Clinical and Experimental Metastasis* 26, 19-34.

24. Papandreou I, Goliasova T, Denko NC. (2011) Anticancer drugs that target metabolism: is dichloroacetate the new paradigm? *International Journal of Cancer* 128, 1001-1008.

25. Denko NC. (2008) Hypoxia, HIF1 and glucose metabolism in the solid tumour. *Nature Reviews Cancer* 8, 705-713.

26. Talks KL, Turley H, Gatter KC, Maxwell PH, Pugh CW, Ratcliffe PJ, Harris AL. (2000) The expression and distribution of the hypoxia-inducible factors HIF-1alpha and HIF-2alpha in normal human tissues, cancers, and tumor-associated macrophages. *American Journal of Pathology* 157, 411-421.

27. Huang LE, Gu J, Schau M, Bunn FH. (1998) Regulation of hypoxia-inducible factor 1alpha is mediated by an O2-dependent degradation domain via the ubiquitin-proteasome pathway. *Proceedings of the National Academy of Sciences of the United States of America* 95, 7987-7992.

28. Wang GL, Jiang BH, Rue EA, Semenza GL. (1995) Hypoxia-inducible factor 1 is a basic-helix-loop-helix-PAS heterodimer regulated by cellular O2 tension. *Proceedings of the National Academy of Sciences of the United States of America* 92, 5510-5514.

29. Wigerup C, Pahlman S, Bexell D. (2016) Therapeutic targeting of hypoxia and hypoxia-inducible factors in cancer. *Pharmacology & Therapeutics* 164, 152-169.

30. Holmquist-Mengelbier L, Fredlund E, Lofstedt T, Noguera R, Navarro S, Nilsson H, Pietras A, Vallon-Christersson J, Borg A, Gradin K, Poellinger L, Pahlman S. (2006) Recruitment of HIF-1alpha and HIF-2alpha to common target genes is differentially regulated in neuroblastoma: HIF-2alpha promotes an aggressive phenotype. *Cancer Cell* 10, 413-423.

31. Bracken CP, Fedele AO, Linke S, Balrak W, Lisy K, Whitelaw ML, Peet DJ. (2006) Cell-specific regulation of hypoxia-inducible factor (HIF)-1alpha and HIF-2alpha stabilization and transactivation in a graded oxygen environment. *The Journal of Biological Chemistry* 281, 22575-22585.

32. Martin SK, Diamond P, Gronthos S, Peet DJ, Zannettino AC. (2011) The emerging role of hypoxia, HIF-1 and HIF-2 in multiple myeloma. *Leukemia* 25, 1533-1542.

33. Uchida T, Rossignol F, Matthay MA, Mounier R, Couette S, Clottes E, Clerici C. (2004) Prolonged hypoxia differentially regulates hypoxia-inducible factor (HIF)-1alpha and HIF-2alpha expression in lung epithelial cells: implication of natural antisense HIF-1alpha. *The Journal of Biological Chemistry* 279, 14871-14878.

34. Semenza GL. (2003) Targeting HIF-1 for cancer therapy. *Nature Reviews Cancer* 3, 721-732.

35. Semenza GL. (2009) Regulation of cancer cell metabolism by hypoxia-inducible factor 1. *Seminars in Cancer Biology* 19, 12-16.

36. Epstein AC, Gleadle JM, McNeill LA, Hewitson KS, O'Rourke J, Mole DR, Mukherji M, Metzen E, Wilson MI, Dhanda A, Tian YM, Masson N, Hamilton DL, Jaakkola P, Barstead R, Hodgkin J, Maxwell PH, Pugh CW, Schofield CJ, Ratcliffe PJ. (2001) C. elegans EGL-9 and mammalian homologs define a family of dioxygenases that regulate HIF by prolyl hydroxylation. *Cell* 107, 43-54.

37. Weidemann A, Johnson RS. (2008) Biology of HIF-1alpha. *Cell Death & Differentiation* 15, 621-627.

38. DeBerardinis RJ, Lum JJ, Hatzivassiliou G, Thompson CB. (2008) The biology of cancer: metabolic reprogramming fuels cell growth and proliferation. *Cell Metabolism* 7, 11-20.

39. Hu Y, Kirito K, Yoshida K, Mitsumori T, Nakajima K, Nozaki Y, Hamanaka S, Nagashima T, Kunitama M, Sakoe K, Komatsu N. (2009) Inhibition of hypoxia-inducible factor-1 function enhances the sensitivity of multiple myeloma cells to melphalan. *Molecular Cancer Therapeutics* 8, 2329-2338.

40. Marin-Hernandez A, Gallardo-Perez JC, Ralph SJ, Rodriguez-Enriquez S, Moreno-Sanchez R. (2009) HIF-1alpha modulates energy metabolism in cancer cells by inducing over-expression of specific glycolytic isoforms. *Mini-Reviews in Medicinal Chemistry* 9, 1084-1101.

41. Kim JW, Gao P, Liu YC, Semenza GL, Dang CV. (2007) Hypoxia-inducible factor 1 and dysregulated c-Myc cooperatively induce vascular endothelial growth factor and metabolic switches hexokinase 2 and pyruvate dehydrogenase kinase 1. *Molecular and Cellular Biology* 27, 7381-7393.

42. Gordan JD, Thompson CB, Simon MC. (2007) HIF and c-Myc: sibling rivals for control of cancer cell metabolism and proliferation. *Cancer Cell* 12, 108-113.

43. Li F, Wang YY, Zeller KI, Potter JJ, Wonsey DR, O'Donnell KA, Kim JW, Yustein JT, Lee LA, Dang CV. (2005) Myc stimulates nuclearly encoded mitochondrial genes and mitochondrial biogenesis. *Molecular and Cellular Biology* 25, 6225-6234.

44. Dang CV, Kim JW, Gao P, Yustein J. (2008) Hypoxia and metabolism - Opinion - The interplay between MYC and HIF in cancer. *Nature Reviews Cancer* 8, 51-56.

45. Kim JW, Gao P, Liu YC, Semenza GL, Dang CV. (2007) Hypoxia-inducible factor I and dysregulated c-myc cooperatively induce vascular endothelial growth factor and metabolic switches hexokinase 2 and pyruvate dehydrogenase kinase 1. *Molecular and Cellular Biology* 27, 7381-7393.

46. Dang CV, Le A, Gao P. (2009) MYC-induced cancer cell energy metabolism and therapeutic opportunities. *Clinical Cancer Research* 15, 6479-6483.

47. Doherty JR, Cleveland JL. (2013) Targeting lactate metabolism for cancer therapeutics. *Journal of Clinical Investigation* 123, 3685-3692.

48. Kim JW, Tchernyshyov I, Semenza GL, Dang CV. (2006) HIF-1-mediated expression of pyruvate dehydrogenase kinase: A metabolic switch required for cellular adaptation to hypoxia. *Cell Metabolism* 3, 177-185.

49. Papandreou I, Cairns RA, Fontana L, Lim AL, Denko NC. (2006) HIF-1 mediates adaptation to hypoxia by actively downregulating mitochondrial oxygen consumption. *Cell Metabolism* 3, 187-197.

50. Lu CW, Lin SC, Chen KF, Lai YY, Tsai SJ. (2008) Induction of pyruvate dehydrogenase kinase-3 by hypoxia-inducible factor-1 promotes metabolic switch and drug resistance. *Journal of Biological Chemistry* 283, 28106-28114.

51. Bykov VJN, Eriksson SE, Bianchi J, Wiman KG. (2017) Targeting mutant p53 for efficient cancer therapy. *Nature Reviews Cancer* 18, 89-102.

52. Bykov VJN, Zhang Q, Zhang MQZ, Ceder S, Abrahmsen L, Wiman KG. (2016) Targeting of mutant p53 and the cellular redox balance by APR-246 as a strategy for efficient cancer therapy. *Frontiers in Oncology* 6.

53. Vogelstein B, Lane D, Levine AJ. (2000) Surfing the p53 network. *Nature* 408, 307-310.

54. Levine AJ. (1997) p53, the cellular gatekeeper for growth and division. *Cell* 88, 323-331.

55. Schwartzenberg-Bar-Yoseph F, Armoni M, Karnieli E. (2004) The tumor suppressor p53 down-regulates glucose transporters GLUT1 and GLUT4 gene expression. *Cancer Research* 64, 2627-2633.

56. Zhang C, Liu J, Wu R, Liang YJ, Lin MH, Liu J, Chan CS, Hu WW, Feng ZH. (2014) Tumor suppressor p53 negatively regulates glycolysis stimulated by hypoxia through its target RRAD. *Oncotarget* 5, 5535-5546.

57. Bensaad K, Tsuruta A, Selak MA, Vidal MN, Nakano K, Bartrons R, Gottlieb E, Vousden KH. (2006) TIGAR, a p53-inducible regulator of glycolysis and apoptosis. *Cell* 126, 107-120.

58. Contractor T, Harris CR. (2012) p53 negatively regulates transcription of the pyruvate dehydrogenase kinase Pdk2. *Cancer Research* 72, 560-567.

59. Boidot R, Vegran F, Meulle A, Le Breton A, Dessy C, Sonveaux P, Lizard-Nacol S, Feron O. (2012) Regulation of monocarboxylate transporter MCT1 expression by p53 mediates inward and outward lactate fluxes in tumors. *Cancer Research* 72, 939-948.

60. Won KY, Lim SJ, Kim GY, Kim YW, Han SA, Song JY, Lee DK. (2012) Regulatory role of p53 in cancer metabolism via SCO2 and TIGAR in human breast cancer. *Human Pathology* 43, 221-228.

61. Olovnikov IA, Kravchenko JE, Chumakov PM. (2009) Homeostatic functions of the p53 tumor suppressor: regulation of energy metabolism and antioxidant defense. *Seminars in Cancer Biology* 19, 32-41.

62. Wanka C, Brucker DP, Bahr O, Ronellenfitsch M, Weller M, Steinbach JP, Rieger J. (2012) Synthesis of cytochrome c oxidase 2: a p53-dependent metabolic regulator that promotes respiratory function and protects glioma and colon cancer cells from hypoxia-induced cell death. *Oncogene* 31, 3764-3776.

63. Ersahin T, Tuncbag N, Cetin-Atalay R. (2015) The PI3K/AKT/mTOR interactive pathway. *Molecular Biosystems* 11, 1946-1954.

64. Plas DR, Thompson CB. (2005) Akt-dependent transformation: there is more to growth than just surviving. *Oncogene* 24, 7435-7442.

65. Elstrom RL, Bauer DE, Buzzai M, Karnauskas R, Harris MH, Plas DR, Zhuang HM, Cinalli RM, Alavi A, Rudin CM, Thompson CB. (2004) Akt stimulates aerobic glycolysis in cancer cells. *Cancer Research* 64, 3892-3899.

66. Robey RB, Hay N. (2009) Is Akt the "Warburg kinase"?-Akt-energy metabolism interactions and oncogenesis. *Seminars in Cancer Biology* 19, 25-31.

67. Guertin DA, Sabatini DM. (2007) Defining the role of mTOR in cancer. *Cancer Cell* 12, 9-22.

68. Agani F, Jiang BH. (2013) Oxygen-independent regulation of HIF-1: novel involvement of PI3K/AKT/mTOR pathway in cancer. *Current Cancer Drug Targets* 13, 245-251.

69. Rui L. (2014) Energy metabolism in the liver. *Comprehensive Physiology* 4, 177-197.

70. Felig P. (1973) The glucose-alanine cycle. *Metabolism* 22, 179-207.

71. Kim Y, Kim EY, Seo YM, Yoon TK, Lee WS, Lee KA. (2012) Function of the pentose phosphate pathway and its key enzyme, transketolase, in the regulation of the meiotic cell cycle in oocytes. *Clinical and Experimental Reproductive Medicine* 39, 58-67.

72. Lane AN, Fan TW. (2015) Regulation of mammalian nucleotide metabolism and biosynthesis. *Nucleic Acids Research* 43, 2466-2485.

73. McLennan HR, Degli Esposti M. (2000) The contribution of mitochondrial respiratory complexes to the production of reactive oxygen species. *Journal of Bioenergetics and Biomembranes* 32, 153-162.

74. Hayyan M, Hashim MA, AlNashef IM. (2016) Superoxide ion: generation and chemical implications. *Chemical Reviews* 116, 3029-3085.

75. Dickinson BC, Chang CJ. (2011) Chemistry and biology of reactive oxygen species in signaling or stress responses. *Nature Chemical Biology* 7, 504-511.

76. Giannoni E, Buricchi F, Raugei G, Ramponi G, Chiarugi P. (2005) Intracellular reactive oxygen species activate Src tyrosine kinase during cell adhesion and anchorage-dependent cell growth. *Molecular and Cellular Biology* 25, 6391-6403.

77. Circu ML, Aw TY. (2010) Reactive oxygen species, cellular redox systems, and apoptosis. *Free Radical Biology and Medicine* 48, 749-762.

78. Bolisetty S, Jaimes EA. (2013) Mitochondria and reactive oxygen species: physiology and pathophysiology. *International Journal of Molecular Sciences* 14, 6306-6344.

79. Zhou D, Shao L, Spitz DR. (2014) Reactive oxygen species in normal and tumor stem cells. *Advances in Cancer Research* 122, 1-67.

80. Kaplowitz N, Aw TY, Ookhtens M. (1985) The regulation of hepatic glutathione. *Annual Review of Pharmacology and Toxicology* 25, 715-744.

81. Vaughn AE, Deshmukh M. (2008) Glucose metabolism inhibits apoptosis in neurons and cancer cells by redox inactivation of cytochrome c. *Nature Cell Biology* 10, 1477-1483.

82. Kirsch M, De Groot H. (2001) NAD(P)H, a directly operating antioxidant? *The FASEB Journal* 15, 1569-1574.

83. Cho ES, Cha YH, Kim HS, Kim NH, Yook JI. (2018) The Pentose Phosphate Pathway as a Potential Target for Cancer Therapy. *Biomolecules & Therapeutics (Seoul)* 26, 29-38.

84. Patra KC, Hay N. (2014) The pentose phosphate pathway and cancer. *Trends in Biochemical Sciences* 39, 347-354.

85. Gatenby RA, Gillies RJ. (2004) Why do cancers have high aerobic glycolysis? *Nature Reviews Cancer* 4, 891-899.

86. Gottschalk S, Anderson N, Hainz C, Eckhardt SG, Serkova NJ. (2004) Imatinib (STI571)-mediated changes in glucose metabolism in human leukemia BCR-ABL-positive cells. *Clinical Cancer Research* 10, 6661-6668.

87. Chaudhri VK, Salzler GG, Dick SA, Buckman MS, Sordella R, Karoly ED, Mohney R, Stiles BM, Elemento O, Altorki NK, McGraw TE. (2013) Metabolic alterations in lung cancer-associated fibroblasts correlated with increased glycolytic metabolism of the tumor. *Molecular Cancer Research* 11, 579-592.

88. Gillies RJ, Gatenby RA. (2007) Adaptive landscapes and emergent phenotypes: why do cancers have high glycolysis? *Journal of Bioenergetics and Biomembranes* 39, 251-257.

89. Estrella V, Chen TA, Lloyd M, Wojtkowiak J, Cornnell HH, Ibrahim-Hashim A, Bailey K, Balagurunathan Y, Rothberg JM, Sloane BF, Johnson J, Gatenby RA, Gillies RJ. (2013) Acidity generated by the tumor microenvironment drives local invasion. *Cancer Research* 73, 1524-1535.

90. Gatenby RA, Gawlinski ET. (1996) A reaction-diffusion model of cancer invasion. *Cancer Research* 56, 5745-5753.

91. Brahimi-Horn MC, Pouyssegur J. (2007) Hypoxia in cancer cell metabolism and pH regulation. *Essays in Biochemistry* 43, 165-178.

92. Lardner A. (2001) The effects of extracellular pH on immune function. *Journal of Leukocyte Biology* 69, 522-530.

93. Calcinotto A, Filipazzi P, Grioni M, Iero M, De Milito A, Ricupito A, Cova A, Canese R, Jachetti E, Rossetti M, Huber V, Parmiani G, Generoso L, Santinami M, Borghi M, Fais S, Bellone M, Rivoltini L. (2012) Modulation of microenvironment acidity reverses anergy in human and murine tumor-infiltrating T lymphocytes. *Cancer Research* 72, 2746-2756.

94. Chang CH, Curtis JD, Maggi LB, Jr., Faubert B, Villarino AV, O'Sullivan D, Huang SC, van der Windt GJ, Blagih J, Qiu J, Weber JD, Pearce EJ, Jones RG, Pearce EL. (2013) Posttranscriptional control of T cell effector function by aerobic glycolysis. *Cell* 153, 1239-1251.

95. Fischer K, Hoffmann P, Voelkl S, Meidenbauer N, Ammer J, Edinger M, Gottfried E, Schwarz S, Rothe G, Hoves S, Renner K, Timischl B, Mackensen A, Kunz-Schughart L, Andreesen R, Krause SW, Kreutz M. (2007) Inhibitory effect of tumor cell-derived lactic acid on human T cells. *Blood* 109, 3812-3819.

96. Kayani I, Groves AM. (2006) 18F-fluorodeoxyglucose PET/CT in cancer imaging. *Clinical Medicine (London,England)* 6, 240-244.

97. Ben-Haim S, Ell P. (2009) 18F-FDG PET and PET/CT in the evaluation of cancer treatment response. *Journal of Nuclear Medicine* 50, 88-99.

98. Som P, Atkins HL, Bandoypadhyay D, Fowler JS, MacGregor RR, Matsui K, Oster ZH, Sacker DF, Shiue CY, Turner H, Wan CN, Wolf AP, Zabinski SV. (1980) A fluorinated glucose analog, 2-fluoro-2-deoxy-D-glucose (F-18): nontoxic tracer for rapid tumor detection. *The Journal of Nuclear Medicine* 21, 670-675.

99. Challapalli A, Aboagye EO. (2016) Positron emission tomography imaging of tumor cell metabolism and application to therapy response monitoring. *Frontiers in Oncology* 6.

100. Groves AM, Win T, Ben Haim S, Ell PJ. (2007) Non-[(18)F]FDG PET in clinical oncology. *Lancet Oncology* 8, 822-830.

101. Regulal NK, Lubberink M, Jorulf H, Ladjevardi S, Haggman M, Sorensen J. (2017) Dynamic Imaging of Prostate Cancer with 11C-acetate PET/CT. *Journal of Nuclear Medicine* 58.

102. Nazarian A, Sureshbabu S, Andrada ZP, Thomas J, Arreglado A, Berman N, Wolf DJ, Gazda LS, Fahey TJ, Ocean AJ, Smith BH. (2017) 18F-FDG PET/CT evaluation of tumor response to the implantation of RENCA macrobeads (RMB) in phase I and II clinical trials [INDBB 10091] in advanced, treatment-resistant metastatic colorectal cancer (mCRC). *Journal of Clinical Oncology* 35, e15046-e15046.

103. Vander Heiden MG. (2011) Targeting cancer metabolism: a therapeutic window opens. *Nature Reviews Drug Discovery* 10, 671-684.

104. Xie J, Wu H, Dai C, Pan Q, Ding Z, Hu D, Ji B, Luo Y, Hu X. (2014) Beyond Warburg effect-dual metabolic nature of cancer cells. *Scientific Reports* 4, 4927-4939.

105. Talekar M, Boreddy SR, Singh A, Amiji M. (2014) Tumor aerobic glycolysis: new insights into therapeutic strategies with targeted delivery. *Expert Opinion on Biological Therapy* 14, 1145-1159.

106. Barron CC, Bilan PJ, Tsakiridis T, Tsiani E. (2016) Facilitative glucose transporters: Implications for cancer detection, prognosis and treatment. *Metabolism: Clinical and Experimental* 65, 124-139.

107. Melstrom LG, Salabat MR, Ding XZ, Milam BM, Strouch M, Pelling JC, Bentrem DJ. (2008) Apigenin inhibits the GLUT-1 glucose transporter and the phosphoinositide 3-kinase/Akt pathway in human pancreatic cancer cells. *Pancreas* 37, 426-431.

108. Bao YY, Zhou SH, Fan J, Wang QY. (2013) Anticancer mechanism of apigenin and the implications of GLUT-1 expression in head and neck cancers. *Future Oncology* 9, 1353-1364.

109. Xu YY, Wu TT, Zhou SH, Bao YY, Wang QY, Fan J, Huang YP. (2014) Apigenin suppresses GLUT-1 and p-AKT expression to enhance the chemosensitivity to cisplatin of laryngeal carcinoma Hep-2 cells: an in vitro study. *International Journal of Clinical and Experimental Pathology* 7, 3938-3947.

110. Wood TE, Dalili S, Simpson CD, Hurren R, Mao XL, Saiz FS, Gronda M, Eberhard Y, Minden MD, Bilan PJ, Klip A, Batey RA, Schimmer AD. (2008) A novel inhibitor of glucose uptake sensitizes cells to FAS-induced cell death. *Molecular Cancer Therapeutics* 7, 3546-3555.

111. McBrayer SK, Cheng JC, Singhal S, Krett NL, Rosen ST, Shanmugam M. (2012) Multiple myeloma exhibits novel dependence on GLUT4, GLUT8, and GLUT11: implications for glucose transporter-directed therapy. *Blood* 119, 4686-4697.

112. Wu JY, Hu LR, Wu FP, Zou L, He TP. (2017) Poor prognosis of hexokinase 2 overexpression in solid tumors of digestive system: a meta-analysis. *Oncotarget* 8, 32332-32344.

113. Patra KC, Hay N. (2013) Hexokinase 2 as oncotarget. *Oncotarget* 4, 1862-1863.

114. Liu Z, Sun YM, Hong HY, Zhao SR, Zou X, Ma RQ, Jiang CC, Wang ZW, Li HB, Liu H. (2015) 3-bromopyruvate enhanced daunorubicin-induced cytotoxicity involved in monocarboxylate transporter 1 in breast cancer cells. *American Journal of Cancer Research* 5, 2673-2685.

115. El Sayed SM, Mohamed WG, Seddik MAH, Ahmed ASA, Mahmoudi AG, Amer WH, Nabo MMH, Hamed AR, Ahmed NS, Abd-Allah AAR. (2014) Safety and outcome of treatment of metastatic melanoma using 3-bromopyruvate: a concise literature review and case study. *Chinese Journal of Cancer* 33, 356-364.

116. Sobotka O, Endlicher R, Drahota Z, Kucera O, Rychtrmoc D, Raad M, Hakeem K, Cervinkova Z. (2016) Impaired mitochondrial functions contribute to 3-bromopyruvate toxicity in primary rat and mouse hepatocytes. *Journal of Bioenergetics and Biomembranes* 48, 363-373.

117. Zhang DS, Li J, Wang FZ, Hu J, Wang SW, Sun YM. (2014) 2-Deoxy-D-glucose targeting of glucose metabolism in cancer cells as a potential therapy. *Cancer Letters* 355, 176-183.

118. Zhang XD, Deslandes E, Villedieu M, Poulain L, Duval M, Gauduchon P, Schwartz L, Icard P. (2006) Effect of 2-Deoxy-D-glucose on various malignant cell lines in vitro. *Anticancer Research* 26, 3561-3566.

119. Stein M, Lin HX, Jeyamohan C, Dvorzhinski D, Gounder M, Bray K, Eddy S, Goodin S, White E, DiPaola RS. (2010) Targeting tumor metabolism with 2-deoxyglucose in patients with castrate-resistant prostate cancer and advanced malignancies. *Prostate* 70, 1388-1394.

120. Mohanti BK, Rath GK, Anantha N, Kannan V, Das BS, Chandramouli BAR, Banerjee AK, Das S, Jena A, Ravichandran R, Sahi UP, Kumar R, Kapoor N, Kalia VK, Dwarakanath BS, Jain V. (1996) Improving cancer radiotherapy with 2-deoxy-D-glucose: Phase I/II clinical trials on human cerebral gliomas. *International Journal of Radiation Oncology Biology Physics* 35, 103-111.

121. Raez LE, Papadopoulos K, Ricart AD, Chiorean EG, DiPaola RS, Stein MN, Lima CMR, Schlesselman JJ, Tolba K, Langmuir VK, Kroll S, Jung DT, Kurtoglu M, Rosenblatt J, Lampidis TJ. (2013) A phase I dose-escalation trial of 2-deoxy-D-glucose alone or combined with docetaxel in patients with advanced solid tumors. *Cancer Chemotherapy and Pharmacology* 71, 523-530.

122. Goldman RD, Hall TC, Kaplan NO. (1964) Lactic dehydrogenase in human neoplastic tissues. *Cancer Research* 24, 389-399.

123. Girgis H, Masui O, White NMA, Scorilas A, Rotondo F, Seivwright A, Gabril M, Filter ER, Girgis AHA, Bjarnason GA, Jewett MAS, Evans A, Al-Haddad S, Siu KWM, Yousef GM. (2014) Lactate Dehydrogenase A is a potential prognostic marker in clear cell renal cell carcinoma. *Molecular Cancer* 13, 101-111.

124. Huang L, Zheng M, Zhou QM, Zhang MY, Jia WH, Yun JP, Wang HY. (2011) Identification of a gene-expression signature for predicting lymph node metastasis in patients with early stage cervical carcinoma. *Cancer* 117, 3363-3373.

125. Maiso P, Huynh D, Moschetta M, Sacco A, Aljawai Y, Mishima Y, Asara JM, Roccaro AM, Kimmelman AC, Ghobrial IM. (2015) Metabolic signature identifies novel targets for drug resistance in multiple myeloma. *Cancer Research* 75, 2071-2082.

126. Fantin VR, St-Pierre J, Leder P. (2006) Attenuation of LDH-A expression uncovers a link between glycolysis, mitochondrial physiology, and tumor maintenance *Cancer Cell* 9, 425-426.

127. Sheng SL, Liu JJ, Dai YH, Sun XG, Xiong XP, Huang G. (2012) Knockdown of lactate dehydrogenase A suppresses tumor growth and metastasis of human hepatocellular carcinoma. *The FEBS Journal* 279, 3898-3910.

128. Jin L, Chun J, Pan C, Alesi GN, Li D, Magliocca KR, Kang Y, Chen ZG, Shin DM, Khuri FR, Fan J, Kang S. (2017) Phosphorylation-mediated activation of LDHA promotes cancer cell invasion and tumour metastasis. *Oncogene* 36, 3797-3806.

129. Le A, Cooper CR, Gouw AM, Dinavahi R, Maitra A, Deck LM, Royer RE, Jagt DLV, Semenza GL, Dang CV. (2010) Inhibition of lactate dehydrogenase A induces oxidative stress and inhibits tumor progression. *Proceedings of the National Academy of Sciences of the United States of America* 107, 2037-2042.

130. Zhai X, Yang Y, Wan J, Zhu R, Wu Y. (2013) Inhibition of LDH-A by oxamate induces G2/M arrest, apoptosis and increases radiosensitivity in nasopharyngeal carcinoma cells. *Oncology Reports* 30, 2983-2991.

131. El-Sisi AE, Sokar SS, Abu-Risha SE, El-Mahrouk SR. (2017) Oxamate potentiates taxol chemotherapeutic efficacy in experimentally-induced solid ehrlich carcinoma (SEC) in mice. *Biomedicine & Pharmacotherapy* 95, 1565-1573.

132. Patel MS, Nemeria NS, Furey W, Jordan F. (2014) The pyruvate dehydrogenase complexes: structure-based function and regulation. *The Journal of Biological Chemistry* 289, 16615-16623.

133. Lu CW, Lin SC, Chien CW, Lin SC, Lee CT, Lin BW, Lee JC, Tsai SJ. (2011) Overexpression of pyruvate dehydrogenase kinase 3 increases drug resistance and early recurrence in colon cancer. *The American Journal of Pathology* 179, 1405-1414.

134. Stacpoole PW. (2017) Therapeutic targeting of the pyruvate dehydrogenase complex/pyruvate dehydrogenase kinase (PDC/PDK) axis in cancer. *Journal of the National Cancer Institute* 109.

135. Zong WX, Rabinowitz JD, White E. (2016) Mitochondria and cancer. *Molecular Cell* 61, 667-676.

136. Pathania D, Millard M, Neamati N. (2009) Opportunities in discovery and delivery of anticancer drugs targeting mitochondria and cancer cell metabolism. *Advanced Drug Delivery Reviews* 61, 1250-1275.

137. Martinou JC, Youle RJ. (2011) Mitochondria in apoptosis: Bcl-2 family members and mitochondrial dynamics. *Developmental Cell* 21, 92-101.

138. Yip KW, Reed JC. (2008) Bcl-2 family proteins and cancer. *Oncogene* 27, 6398-6406.

139. Gulbins E, Dreschers S, Bock J. (2003) Role of mitochondria in apoptosis. *Experimental Physiology* 88, 85-90.

140. Sharpe JC, Arnoult D, Youle RJ. (2004) Control of mitochondrial permeability by Bcl-2 family members. *Biochimica Et Biophysica Acta-Molecular Cell Research* 1644, 107-113.

141. Armstrong JS. (2007) Mitochondrial medicine: pharmacological targeting of mitochondria in disease. *British Journal of Pharmacology* 151, 1154-1165.

142. Miller WH, Jr., Schipper HM, Lee JS, Singer J, Waxman S. (2002) Mechanisms of action of arsenic trioxide. *Cancer Research* 62, 3893-3903.

143. Jin C, Reed JC. (2002) Yeast and apoptosis. *Nature Reviews Molecular Cell Biology* 3, 453-459.

144. Kang MH, Reynolds CP. (2009) Bcl-2 Inhibitors: targeting mitochondrial apoptotic pathways in cancer therapy. *Clinical Cancer Research* 15, 1126-1132.

145. D'Souza GG, Wagle MA, Saxena V, Shah A. (2011) Approaches for targeting mitochondria in cancer therapy. *Biochimica Et Biophysica Acta* 1807, 689-696.

146. Roberts AW, Huang DCS. (2017) Targeting Bcl2 with BH3 Mimetics: basic science and clinical application of venetoclax in chronic lymphocytic leukemia and related B cell malignancies genome editing techniques and their therapeutic applications. *Clinical Pharmacology & Therapeutics* 101, 89-98.

147. Weinberg SE, Chandel NS. (2015) Targeting mitochondria metabolism for cancer therapy. *Nature Chemical Biology* 11, 9-15.

148. Wheaton WW, Weinberg SE, Hamanaka RB, Soberanes S, Sullivan LB, Anso E, Glasauer A, Dufour E, Mutlu GM, Budigner GRS, Chandel NS. (2014) Metformin inhibits mitochondrial complex I of cancer cells to reduce tumorigenesis. *Elife* 3.

149. Griss T, Vincent EE, Egnatchik R, Chen J, Ma EH, Faubert B, Viollet B, DeBerardinis RJ, Jones RG. (2015) Metformin Antagonizes Cancer Cell Proliferation by Suppressing Mitochondrial-Dependent Biosynthesis. *Plos Biology* 13, e1002309.

150. Chae YK, Arya A, Malecek MK, Shin DS, Carneiro B, Chandra S, Kaplan J, Kalyan A, Altman JK, Platanias L, Giles F. (2016) Repurposing metformin for cancer treatment: current clinical studies. *Oncotarget* 7, 40767-40780.

151. Coyle C, Cafferty FH, Vale C, Langley RE. (2016) Metformin as an adjuvant treatment for cancer: a systematic review and meta-analysis. *Annals of Oncology* 27, 2184-2195.

152. Miskimins WK, Ahn HJ, Kim JY, Ryu S, Jung YS, Choi JY. (2014) Synergistic anti-cancer effect of phenformin and oxamate. *PLOS One* 9, e85576.

153. Zhang XN, Fryknas M, Hernlund E, Fayad W, De Milito A, Olofsson MH, Gogvadze V, Dang L, Pahlman S, Schughart LAK, Rickardson L, Darcy P, Gullbo J, Nygren P, Larsson R, Linder S. (2014) Induction of mitochondrial dysfunction as a strategy for targeting tumour cells in metabolically compromised microenvironments. *Nature Communications* 5, 1-14.

154. Skrtic M, Sriskanthadevan S, Jhas B, Gebbia M, Wang X, Wang Z, Hurren R, Jitkova Y, Gronda M, Maclean N, Lai CK, Eberhard Y, Bartoszko J, Spagnuolo P, Rutledge AC, Datti A, Ketela T, Moffat J, Robinson BH, Cameron JH, Wrana J, Eaves CJ, Minden MD, Wang JCY, Dick JE, Humphries K, Nislow C, Giaever G, Schimmer AD. (2011) Inhibition of mitochondrial translation as a therapeutic strategy for human acute myeloid leukemia. *Cancer Cell* 20, 674-688.

155. Xu ZJ, Yan YL, Li Z, Qian L, Gong ZC. (2016) The Antibiotic Drug Tigecycline: A Focus on its Promising Anticancer Properties. *Frontiers in Pharmacology* 7.

156. Kang BH, Tavecchio M, Goel HL, Hsieh CC, Garlick DS, Raskett CM, Lian JB, Stein GS, Languino LR, Altieri DC. (2011) Targeted inhibition of mitochondrial Hsp90 suppresses localised and metastatic prostate cancer growth in a genetic mouse model of disease. *British Journal of Cancer* 104, 629-634.

157. Kang BH, Plescia J, Song HY, Meli M, Colombo G, Beebe K, Scroggins B, Neckers L, Altieri DC. (2009) Combinatorial drug design targeting multiple cancer signaling networks controlled by mitochondrial Hsp90. *Journal of Clinical Investigation* 119, 454-464.

158. Eagle H. (1955) The specific amino acid requirements of a human carcinoma cell (Stain HeLa) in tissue culture. *Journal of Experimental Medicine* 102, 37-48.

159. Stein WH, Moore S. (1954) The free amino acids of human blood plasma. *Journal of Biological Chemistry* 211, 915-926.

160. Altman BJ, Stine ZE, Dang CV. (2016) From Krebs to clinic: glutamine metabolism to cancer therapy. *Nature Reviews Cancer* 16, 749.

161. Daye D, Wellen KE. (2012) Metabolic reprogramming in cancer: unraveling the role of glutamine in tumorigenesis. *Seminars in Cell and Developmental Biology* 23, 362-369.

162. Le A, Lane AN, Hamaker M, Bose S, Gouw A, Barbi J, Tsukamoto T, Rojas CJ, Slusher BS, Zhang HX, Zimmerman LJ, Liebler DC, Slebos RJC, Lorkiewicz PK, Higashi RM, Fan TWM, Dang CV. (2012) Glucose-independent glutamine metabolism via TCA cycling for proliferation and survival in B cells. *Cell Metabolism* 15, 110-121.

163. Yelamanchi SD, Jayaram S, Thomas JK, Gundimeda S, Khan AA, Singhal A, Prasad TSK, Pandey A, Somani BL, Gowda H. (2016) A pathway map of glutamate metabolism. *Journal of Cell Communication and Signaling* 10, 69-75.

164. Yoo H, Antoniewicz MR, Stephanopoulos G, Kelleher JK. (2008) Quantifying reductive carboxylation flux of glutamine to lipid in a brown adipocyte cell line. *Journal of Biological Chemistry* 283, 20621-20627.

165. Choi YK, Park KG. (2018) Targeting glutamine metabolism for cancer treatment. *Biomolecules & Therapeutics (Seoul)* 26, 19-28.

166. Bhutia YD, Ganapathy V. (2016) Glutamine transporters in mammalian cells and their functions in physiology and cancer. *Biochimica Et Biophysica Acta-Molecular Cell Research* 1863, 2531-2539.

167. Cormerais Y, Massard PA, Vucetic M, Giuliano S, Tambutte E, Durivault J, Vial V, Endou H, Wempe MF, Parks SK, Pouyssegur J. (2018) The glutamine transporter ASCT2 (SLC1A5) promotes tumor growth independently of the amino acid transporter LAT1 (SLC7A5). *Journal of Biological Chemistry* 293, 2877-2887.

168. Todorova VK, Kaufmann YH, Luo SK, Klimberg VS. (2011) Tamoxifen and raloxifene suppress the proliferation of estrogen receptor-negative cells through inhibition of glutamine uptake. *Cancer Chemotherapy and Pharmacology* 67, 285-291.

169. Hassanein M, Qian J, Hoeksema MD, Wang J, Jacobovitz M, Ji XM, Harris FT, Harris BK, Boyd KL, Chen HD, Eisenberg R, Massion PP. (2015) Targeting SLC1a5-mediated glutamine dependence in non-small cell lung cancer. *International Journal of Cancer* 137, 1587-1597.

170. Marshall AD, van Geldermalsen M, Otte NJ, Lum T, Vellozzi M, Thoeng A, Pang A, Nagarajah R, Zhang B, Wang Q, Anderson L, Rasko JEJ, Holst J. (2017) ASCT2 regulates glutamine uptake and cell growth in endometrial carcinoma. *Oncogenesis* 6, e367.

171. Colas C, Grewer C, Gameiro A, Albers T, Singh K, Otte NJ, Shere H, Massimiliano B, Holst J, Schlessinger A. (2015) Ligand Discovery for the Alanine-Serine-Cysteine Transporter (ASCT2, SLC1A5) from Homology Modeling and Virtual Screening. *Biophysical Journal* 108, 54a-54a.

172. Elgogary A, Xu QG, Poore B, Alt J, Zimmermann SC, Zhao L, Fu J, Chen BW, Xia SY, Liu YF, Neisser M, Nguyen C, Lee R, Park JK, Reyes J, Hartung T, Rojas C, Rais R, Tsukamoto T, Semenza GL, Hanes J, Slusher BS, Le A. (2016) Combination therapy with BPTES nanoparticles and metformin targets the metabolic heterogeneity of pancreatic cancer. *Proceedings of the National Academy of Sciences of the United States of America* 113, E5328-E5336.

173. Gross MI, Demo SD, Dennison JB, Chen L, Chernov-Rogan T, Goyal B, Janes JR, Laidig GJ, Lewis ER, Li J, MacKinnon AL, Parlati F, Rodriguez MLM, Shwonek PJ, Sjogren EB, Stanton TF, Wang TT, Yang JF, Zhao F, Bennett MK. (2014) Antitumor activity of the glutaminase inhibitor CB-839 in triple-negative breast cancer. *Molecular Cancer Therapeutics* 13, 890-901.

174. Yuan LQ, Sheng XG, Clark LH, Zhang L, Guo H, Jones HM, Willson AK, Gehrig PA, Zhou CX, Bae-Jump VL. (2016) Glutaminase inhibitor compound 968 inhibits cell proliferation and sensitizes paclitaxel in ovarian cancer. *American Journal of Translational Research* 8, 4265-4277.

175. Jin LT, Li D, Alesi G, Fan J, Kang HB, Zhou L, Boggon T, Magliocca K, He C, Arellano M, Khoury H, Shin D, Khuri F, Kang SM. (2015) Glutamate dehydrogenase 1 signals through antioxidant glutathione peroxidase 1 to regulate redox homeostasis and tumor growth. *Cancer Research* 27, 257-270.

176. Korangath P, Teo WW, Sadik H, Han LF, Mori N, Huijts CM, Wildes F, Bharti S, Zhang Z, Santa-Maria CA, Tsai HL, Dang CV, Stearns V, Bhujwalla ZM, Sukumar S. (2015) Targeting glutamine metabolism in breast cancer with aminooxyacetate. *Clinical Cancer Research* 21, 3263-3273.

177. Ookhtens M, Kannan R, Lyon I, Baker N. (1984) Liver and adipose tissue contributions to newly formed fatty acids in an ascites tumor. *American Journal of Physiology* 247, 146-153.

178. Szutowicz A, Kwiatkowski J, Angielski S. (1979) Lipogenetic and glycolytic enzyme-activities in carcinoma and nonmalignant diseases of the human-breast. *British Journal of Cancer* 39, 681-687.

179. Menendez JA, Lupu R. (2007) Fatty acid synthase and the lipogenic phenotype in cancer pathogenesis. *Nature Reviews Cancer* 7, 763-777.

180. Costello LC, Franklin RB. (2005) 'Why do tumour cells glycolyse?': From glycolysis through citrate to lipogenesis. *Molecular and Cellular Biochemistry* 280, 1-8.

181. Currie E, Schulze A, Zechner R, Walther TC, Farese RV, Jr. (2013) Cellular fatty acid metabolism and cancer. *Cell Metabolism* 18, 153-161.

182. Harjes U, Kalucka J, Carmeliet P. (2016) Targeting fatty acid metabolism in cancer and endothelial cells. *Critical Reviews in Oncology Hematology* 97, 15-21.

183. Pike LS, Smift AL, Croteau NJ, Ferrick DA, Wu M. (2011) Inhibition of fatty acid oxidation by etomoxir impairs NADPH production and increases reactive oxygen species resulting in ATP depletion and cell death in human glioblastoma cells. *Biochimica Et Biophysica Acta* 1807, 726-734.

184. Yao CH, Liu GY, Wang R, Moon SH, Gross RW, Patti GJ. (2018) Identifying off-target effects of etomoxir reveals that carnitine palmitoyltransferase I is essential for cancer cell proliferation independent of beta-oxidation. *Plos Biology* 16, e2003782.

185. Khwairakpam AD, Shyamananda MS, Sailo BL, Rathnakaram SR, Padmavathi G, Kotoky J, Kunnumakkara AB. (2015) ATP citrate lyase (ACLY): a promising target for cancer prevention and treatment. *Current Drug Targets* 16, 156-163.

186. Hatzivassiliou G, Zhao FP, Bauer DE, Andreadis C, Shaw AN, Dhanak D, Hingorani SR, Tuveson DA, Thompson CB. (2005) ATP citrate lyase inhibition can suppress tumor cell growth. *Cancer Cell* 8, 311-321.

187. Migita T, Okabe S, Ikeda K, Igarashi S, Sugawara S, Tomida A, Soga T, Taguchi R, Seimiya H. (2014) Inhibition of ATP citrate lyase induces triglyceride accumulation with altered fatty acid composition in cancer cells. *International Journal of Cancer* 135, 37-47.

188. Kuhajda FP. (2000) Fatty acid synthase and human cancer new perspectives on its role in tumor biology. *Nutrition* 16, 202-208.

189. Takahiro T, Shinichi K, Toshimitsu S. (2003) Expression of fatty acid synthase as a prognostic indicator in soft tissue sarcomas. *Clinical Cancer Research* 9, 2204-2212.

190. Visca P, Sebastiani V, Botti C, Diodoro MG, Lasagni RP, Romagnoli F, Brenna A, De Joannon BC, Donnorso RP, Lombardi G, Alo PL. (2004) Fatty acid synthase (FAS) is a marker of increased risk of recurrence in lung carcinoma. *Anticancer Research* 24, 4169-4173.

191. Liu H, Liu Y, Zhang JT. (2008) A new mechanism of drug resistance in breast cancer cells: fatty acid synthase overexpression-mediated palmitate overproduction. *Molecular Cancer Therapeutics* 7, 263-270.

192. Wang WQ, Zhao XY, Wang HY, Liang Y. (2008) Increased fatty acid synthase as a potential therapeutic target in multiple myeloma. *Journal of Zhejiang University-SCIENCE B* 9, 441-447.

193. Flavin R, Peluso S, Nguyen PL, Loda M. (2010) Fatty acid synthase as a potential therapeutic target in cancer. *Future Oncology* 6, 551-562.

194. Tirado-Velez JM, Joumady I, Saez-Benito A, Cozar-Castellano I, Perdomo G. (2012) Inhibition of fatty acid metabolism reduces human myeloma cells proliferation. *PLOS One* 7, e46484.

195. Loftus TM, Jaworsky DE, Frehywot GL, Townsend CA, Ronnett GV, Lane MD, Kuhajda FP. (2000) Reduced food intake and body weight in mice treated with fatty acid synthase inhibitors. *Science* 288, 2379-2381.

196. Michelakis ED, Webster L, Mackey JR. (2008) Dichloroacetate (DCA) as a potential metabolic-targeting therapy for cancer. *British Journal of Cancer* 99, 989-994.

197. Patel MS, Korotchkina LG. (2006) Regulation of the pyruvate dehydrogenase complex. *Biochemical Society Transactions* 34, 217-222.

198. Knoechel TR, Tucker AD, Robinson CM, Phillips C, Taylor W, Bungay PJ, Kasten SA, Roche TE, Brown DG. (2006) Regulatory roles of the N-terminal domain based on crystal structures of human pyruvate dehydrogenase kinase 2 containing physiological and synthetic ligands. *Biochemistry* 45, 402-415.

199. Kato M, Li J, Chuang JL, Chuang DT. (2007) Distinct structural mechanisms for inhibition of pyruvate dehydrogenase kinase isoforms by AZD7545, dichloroacetate, and radicicol. *Structure* 15, 992-1004.

200. Maj MC, MacKay N, Levandovskiy V, Addis J, Baumgartner ER, Baumgartner MR, Robinson BH, Cameron JM. (2005) Pyruvate dehydrogenase phosphatase deficiency: identification of the first mutation in two brothers and restoration of activity by protein complementation. *The Journal of Clinical Endocrinology and Metabolism* 90, 4101-4107.

201. Tuganova A, Boulatnikov I, Popov KM. (2002) Interaction between the individual isoenzymes of pyruvate dehydrogenase kinase and the inner lipoyl-bearing domain of transacetylase component of pyruvate dehydrogenase complex. *Biochemical Journal* 366, 129-136.

202. Tso SC, Kato M, Chuang JL, Chuang DT. (2006) Structural determinants for cross-talk between pyruvate dehydrogenase kinase 3 and lipoyl domain 2 of the human pyruvate dehydrogenase complex. *Journal of Biological Chemistry* 281, 27197-27204.

203. Dahl HH, Hunt SM, Hutchison WM, Brown GK. (1987) The human pyruvate dehydrogenase complex. Isolation of cDNA clones for the E1 alpha subunit, sequence analysis, and characterization of the mRNA. *Journal of Biological Chemistry* 262, 7398-7403.

204. Rardin MJ, Wiley SE, Naviaux RK, Murphy AN, Dixon JE. (2009) Monitoring phosphorylation of the pyruvate dehydrogenase complex. *Analytical Biochemistry* 389, 157-164.

205. Korotchkina LG, Patel MS. (2001) Site specificity of four pyruvate dehydrogenase kinase isoenzymes toward the three phosphorylation sites of human pyruvate dehydrogenase. *Journal of Biological Chemistry* 276, 37223-37229.

206. Patel MS, Korotchkina LG. (2001) Regulation of mammalian pyruvate dehydrogenase complex by phosphorylation: complexity of multiple phosphorylation sites and kinases. *Experimental and Molecular Medicine* 33, 191-197.

207. James MO, Yan Z, Cornett R, Jayanti VM, Henderson GN, Davydova N, Katovich MJ, Pollock B, Stacpoole PW. (1998) Pharmacokinetics and metabolism of [14C]dichloroacetate in male Sprague-Dawley rats. Identification of glycine conjugates, including hippurate, as urinary metabolites of dichloroacetate. *Drug Metabolism and Disposition* 26, 1134-1143.

208. Stephen H. Curry AL, Pei-I Chu, Marion Limacher, Peter W Stacpoole (1991) Disposition and Pharmacodynamics of dichloroacetate and oxalate following oral DCA doses. *Biopharmaceutics & Drug Disposition* 12, 375-390.

209. Shakil A. Saghir IRS. (2002) Low-dose pharmacokinetics and oral bioavailability of dichloroacetate in naive and GSTZ depleted rats. *Environmental Health Perspectives* 110, 757-763.

210. Chu PI, Stacpoole PW, Curry SH. (1987) Pharmacokinetics of sodium dichloroacetate. *Journal of Pharmaceutical Sciences* 76, S108-S108.

211. Curry SH, Chu PI, Baumgartner TG, Stacpoole PW. (1985) Plasma-concentrations and metabolic effects of intravenous-sodium dichloroacetate. *Clinical Pharmacology & Therapeutics* 37, 89-93.

212. Stacpoole PW, Henderson GN, Yan Z, Cornett R, James MO. (1998) Pharmacokinetics, metabolism and toxicology of dichloroacetate. *Drug Metabolism Reviews* 30, 499-539.

213. Tzeng HF, Blackburn AC, Board PG, Anders MW. (2000) Polymorphism- and species-dependent inactivation of glutathione transferase zeta by dichloroacetate. *Chemical Research in Toxicology* 13, 231-236.

214. Guo X, Dixit V, Liu H, Shroads AL, Henderson GN, James MO, Stacpoole PW. (2006) Inhibition and recovery of rat hepatic glutathione S-transferase zeta and alteration of tyrosine metabolism following dichloroacetate exposure and withdrawal. *Drug Metabolism and Disposition* 34, 36-42.

215. Shroads AL, Langaee T, Coats BS, Kurtz TL, Bullock JR, Weithorn D, Gong Y, Wagner DA, Ostrov DA, Johnson JA, Stacpoole PW. (2012) Human polymorphisms in the glutathione transferase zeta 1/maleylacetoacetate isomerase gene influence the toxicokinetics of dichloroacetate. *Journal of Clinical Pharmacology* 52, 837-849.

216. James MO, Jahn SC, Zhong G, Smeltz MG, Hu Z, Stacpoole PW. (2017) Therapeutic applications of dichloroacetate and the role of glutathione transferase zeta-1. *Pharmacology & Therapeutics* 170, 166-180.

217. Langaee TY, Zhong G, Li W, Hamadeh I, Solayman MH, McDonough CW, Stacpoole PW, James MO. (2015) The influence of human *GSTZ1* gene haplotype variations on GSTZ1 expression. *Pharmacogenetics and Genomics* 25, 239-245.

218. Fang YY, Kashkarov U, Anders MW, Board PG. (2006) Polymorphisms in the human glutathione transferase zeta promoter. *Pharmacogenetics and Genomics* 16, 307-313.

219. Blackburn AC, Coggan M, Tzeng HF, Lantum H, Polekhina G, Parker MW, Anders MW, Board PG. (2001) GSTZ1d: a new allele of glutathione transferase zeta and maleylacetoacetate isomerase. *Pharmacogenetics* 11, 671-678.

220. Blackburn AC, Tzeng HF, Anders MW, Board PG. (2000) Discovery of a functional polymorphism in human glutathione transferase zeta by expressed sequence tag database analysis. *Pharmacogenetics* 10, 49-57.

221. Li W, Gu Y, James MO, Hines RN, Simpson P, Langaee T, Stacpoole PW. (2012) Prenatal and postnatal expression of glutathione transferase zeta 1 in human liver and the roles of haplotype and subject age in determining activity with dichloroacetate. *Drug Metabolism and Disposition* 40, 232-239.

222. Kankotia S, Stacpoole PW. (2014) Dichloroacetate and cancer: new home for an orphan drug? *Biochimica Et Biophysica Acta* 1846, 617-629.

223. Delaney LM, Ho N, Morrison J, Farias NR, Mosser DD, Coomber BL. (2015) Dichloroacetate affects proliferation but not survival of human colorectal cancer cells. *Apoptosis* 20, 63-74.

224. Harting TP, Stubbendorff M, Hammer SC, Schadzek P, Ngezahayo A, Murua Escobar H, Nolte I. (2017) Dichloroacetate affects proliferation but not apoptosis in canine mammary cell lines. *PLOS One* 12, e0178744.

225. Cao W, Yacoub S, Shiverick KT, Namiki K, Sakai Y, Porvasnik S, Urbanek C, Rosser CJ. (2008) Dichloroacetate (DCA) sensitizes both wild-type and over expressing Bcl-2 prostate cancer cells in vitro to radiation. *Prostate* 68, 1223-1231.

226. Stockwin LH, Yu SX, Borgel S, Hancock C, Wolfe TL, Phillips LR, Hollingshead MG, Newton DL. (2010) Sodium dichloroacetate selectively targets cells with defects in the mitochondrial ETC. *International Journal of Cancer* 127, 2510-2519.

227. Zhao Y, Butler EB, Tan M. (2013) Targeting cellular metabolism to improve cancer therapeutics. *Cell Death & Disease* 4, 1-10.

228. Muz B, de la Puente P, Azab F, Azab AK. (2015) The role of hypoxia in cancer progression, angiogenesis, metastasis, and resistance to therapy. *Hypoxia* 3, 83-92.

229. Sutendra G, Dromparis P, Kinnaird A, Stenson TH, Haromy A, Parker JM, McMurtry MS, Michelakis ED. (2013) Mitochondrial activation by inhibition of PDKII suppresses HIF1a signaling and angiogenesis in cancer. *Oncogene* 32, 1638-1650.

230. Schmid T, Zhou J, Kohl R, Brune B. (2004) p300 relieves p53-evoked transcriptional repression of hypoxia-inducible factor-1 (HIF-1). *Biochemical Journal* 380, 289-295.

231. Xuan Y, Hur H, Ham IH, Yun J, Lee JY, Shim W, Kim YB, Lee G, Han SU, Cho YK. (2014) Dichloroacetate attenuates hypoxia-induced resistance to 5-fluorouracil in gastric cancer through the regulation of glucose metabolism. *Experimental Cell Research* 321, 219-230.

232. Gang BP, Dilda PJ, Hogg PJ, Blackburn AC. (2014) Targeting of two aspects of metabolism in breast cancer treatment. *Cancer Biology and Therapy* 15, 1533-1541.

233. Woo SH, Seo SK, Park Y, Kim EK, Seong MK, Kim HA, Song JY, Hwang SG, Lee JK, Noh WC, Park IC. (2016) Dichloroacetate potentiates tamoxifen-induced cell death in breast cancer cells via downregulation of the epidermal growth factor receptor. *Oncotarget* 7, 59809-59819.

234. Dunbar EM, Coats BS, Shroads AL, Langaee T, Lew A, Forder JR, Shuster JJ, Wagner DA, Stacpoole PW. (2014) Phase 1 trial of dichloroacetate (DCA) in adults with recurrent malignant brain tumors. *Investigational New Drugs* 32, 452-464.

235. Chu QSC, Sangha R, Spratlin J, Vos LJ, Mackey JR, McEwan AJB, Venner P, Michelakis ED. (2015) A phase 1 open-labeled, single-arm, dose-escalation, study of dichloroacetate (DCA) in patients with advanced solid tumors. *Investigational New Drugs* 33, 603-610.

236. Garon EB, Christofk HR, Hosmer W, Britten CD, Bahng A, Crabtree MJ, Hong CS, Kamranpour N, Pitts S, Kabbinavar F, Patel C, von-Euw E, Black A, Michelakis ED, Dubinett SM, Slamon DJ. (2014) Dichloroacetate should be considered with platinum-based chemotherapy in hypoxic tumors rather than as a single agent in advanced non-small cell lung cancer. *Journal of Cancer Research and Clinical Oncology* 140, 443-452.

237. Palumbo A, Anderson K. (2011) Multiple myeloma. *The New England Journal of Medicine* 364, 1046-1060.

238. Alexander DD, Mink PJ, Adami HO, Cole P, Mandel JS, Oken MM, Trichopoulos D. (2007) Multiple myeloma: a review of the epidemiologic literature. *International Journal of Cancer* 120 Suppl 12, 40-61.

239. Ferlay J, Soerjomataram I, Dikshit R, Eser S, Mathers C, Rebelo M, Parkin DM, Forman D, Bray F. (2015) Cancer incidence and mortality worldwide: sources,

methods and major patterns in GLOBOCAN 2012. *International Journal of Cancer* 136, E359-386.

240. Costa LJ, Brill IK, Omel J, Godby K, Kumar SK, Brown EE. (2017) Recent trends in multiple myeloma incidence and survival by age, race, and ethnicity in the United States. *Blood Advances* 1, 282-287.

241. Kazandjian D. (2016) Multiple myeloma epidemiology and survival: A unique malignancy. *Seminars in Oncology* 43, 676-681.

242. van Marion AMW, Lokhorst HM, van den Tweel JG. (2003) Pathology of multiple myeloma. *Current Diagnostic Pathology* 9, 322-327.

243. International Myeloma Working G. (2003) Criteria for the classification of monoclonal gammopathies, multiple myeloma and related disorders: a report of the International Myeloma Working Group. *British Journal of Haematology* 121, 749-757.

244. Mateos MV, Landgren O. (2016) MGUS and smoldering multiple myeloma: diagnosis and epidemiology. *Cancer Treatment and Research* 169, 3-12.

245. Korde N, Kristinsson SY, Landgren O. (2011) Monoclonal gammopathy of undetermined significance (MGUS) and smoldering multiple myeloma (SMM): novel biological insights and development of early treatment strategies. *Blood* 117, 5573-5581.

246. Kyle RA, Therneau TM, Rajkumar SV, Larson DR, Plevak MF, Offord JR, Dispenzieri A, Katzmann JA, Melton LJ, 3rd. (2006) Prevalence of monoclonal gammopathy of undetermined significance. *The New England Journal of Medicine* 354, 1362-1369.

247. Kyle RA, Remstein ED, Therneau TM, Dispenzieri A, Kurtin PJ, Hodnefield JM, Larson DR, Plevak MF, Jelinek DF, Fonseca R, Melton LJ, 3rd, Rajkumar SV. (2007) Clinical course and prognosis of smoldering (asymptomatic) multiple myeloma. *The New England Journal of Medicine* 356, 2582-2590.

248. Rajkumar SV, Dimopoulos MA, Palumbo A, Blade J, Merlini G, Mateos MV, Kumar S, Hillengass J, Kastritis E, Richardson P, Landgren O, Paiva B, Dispenzieri A, Weiss B, LeLeu X, Zweegman S, Lonial S, Rosinol L, Zamagni E, Jagannath S, Sezer O, Kristinsson SY, Caers J, Usmani SZ, Lahuerta JJ, Johnsen HE, Beksac M, Cavo M, Goldschmidt H, Terpos E, Kyle RA, Anderson KC, Durie BG, Miguel JF. (2014) International Myeloma Working Group updated criteria for the diagnosis of multiple myeloma. *Lancet Oncology* 15, e538-548.

249. Bhutani M, Landgren O. (2014) [Imaging in smoldering (asymptomatic) multiple myeloma. Past, present and future]. *Radiologe* 54, 1-9.

250. Chesi M, Bergsagel PL. (2013) Molecular pathogenesis of multiple myeloma: basic and clinical updates. *International Journal of Hematology* 97, 313-323.

251. Morgan GJ, Walker BA, Davies FE. (2012) The genetic architecture of multiple myeloma. *Nature Reviews Cancer* 12, 335-348.

252. Chesi M, Brents LA, Fly SA, Bais C, Robbiani DF, Mesri E, Kuehl WM, Bergsagel PL. (2001) Activated fibroblast growth factor receptor 3 is an oncogene that contributes to tumor progression in multiple myeloma. *Blood* 97, 729-736.

253. Xiong W, Wu X, Starnes S, Johnson SK, Haessler J, Wang S, Chen L, Barlogie B, Shaughnessy JD, Jr., Zhan F. (2008) An analysis of the clinical and biologic significance of TP53 loss and the identification of potential novel transcriptional targets of TP53 in multiple myeloma. *Blood* 112, 4235-4246.

254. Chesi M, Nardini E, Brents LA, Schrock E, Ried T, Kuehl WM, Bergsagel PL. (1997) Frequent translocation t(4;14)(p16.3;q32.3) in multiple myeloma is associated with increased expression and activating mutations of fibroblast growth factor receptor 3. *Nature Genetics* 16, 260-264.

255. Hanbali A, Hassanein M, Rasheed W, Aljurf M, Alsharif F. (2017) The Evolution of Prognostic Factors in Multiple Myeloma. *Advances in Hematology* 2017, 1-11.

256. Jian Y, Chen X, Zhou H, Zhu W, Liu N, Geng C, Chen W. (2016) Prognostic impact of cytogenetic abnormalities in multiple myeloma: a retrospective analysis of 229 patients. *Medicine (Baltimore)* 95, e3521.

257. Fonseca R, Monge J, Dimopoulos MA. (2014) Staging and prognostication of multiple myeloma. *Expert Review of Hematology* 7, 21-31.

258. Qiang YW, Ye SQ, Chen Y, Buros AF, Edmonson R, van Rhee F, Barlogie B, Epstein J, Morgan GJ, Davies FE. (2016) MAF protein mediates innate resistance to proteasome inhibition therapy in multiple myeloma. *Blood* 128, 2919-2930.

259. Fonseca R, Blood E, Rue M, Harrington D, Oken MM, Kyle RA, Dewald GW, Van Ness B, Van Wier SA, Henderson KJ, Bailey RJ, Greipp PR. (2003) Clinical and biologic implications of recurrent genomic aberrations in myeloma. *Blood* 101, 4569-4575.

260. Abdi J, Chen G, Chang H. (2013) Drug resistance in multiple myeloma: latest findings and new concepts on molecular mechanisms. *Oncotarget* 4, 2186-2207.

261. Manoj K Pandey, Shantu G Amin, Maurizio Zangari, Talamo G. (2015) Drug resistance in multiple myeloma: how to cross the border. *Annals of Hematology & Oncology* 2, 1025.

262. Hideshima T, Mitsiades C, Tonon G, Richardson PG, Anderson KC. (2007) Understanding multiple myeloma pathogenesis in the bone marrow to identify new therapeutic targets. *Nature Reviews Cancer* 7, 585-598.

263. Liu YJ, Munoz N, Bunnell BA, Logan TM, Ma T. (2015) Density-dependent metabolic heterogeneity in human mesenchymal stem cells. *Stem Cells* 33, 3368-3381.

264. Travlos GS. (2006) Normal structure, function, and histology of the bone marrow. *Toxicologic Pathology* 34, 548-565.

265. Birbrair A, Frenette PS. (2016) Niche heterogeneity in the bone marrow. *Annals of the New York Academy of Sciences* 1370, 82-96.

266. Yu VWC, Scadden DT. (2016) Heterogeneity of the bone marrow niche. *Current Opinion in Hematology* 23, 331-338.

267. He N, Zhang L, Cui J, Li Z. (2014) Bone marrow vascular niche: home for hematopoietic stem cells. *Bone Marrow Research* 2014, 128436.

268. Reagan MR, Rosen CJ. (2016) Navigating the bone marrow niche: translational insights and cancer-driven dysfunction. *Nature Reviews Rheumatology* 12, 154-168.

269. Podar K, Tai YT, Lin BK, Narsimhan RP, Sattler M, Kijima T, Salgia R, Gupta D, Chauhan D, Anderson KC. (2002) Vascular endothelial growth factor-induced migration of multiple myeloma cells is associated with beta(1) integrin- and phosphatidylinositol 3-kinase-dependent PKC alpha activation. *Journal of Biological Chemistry* 277, 7875-7881.

270. Vidriales MB, Anderson KC. (1996) Adhesion of multiple myeloma cells to the bone marrow microenvironment: Implications for future therapeutic strategies. *Molecular Medicine Today* 2, 425-431.

271. Katz BZ. (2010) Adhesion molecules- The lifelines of multiple myeloma cells. *Seminars in Cancer Biology* 20, 186-195.

272. McKeown SR. (2014) Defining normoxia, physoxia and hypoxia in tumours-implications for treatment response. *British Journal of Radiology* 87.

273. Asosingh K, De Raeve H, de Ridder M, Storme GA, Willems A, Van Riet I, Van Camp B, Vanderkerken K. (2005) Role of the hypoxic bone marrow microenvironment in 5T2MM murine myeloma tumor progression. *Haematologica* 90, 810-817.

274. Spencer JA, Ferraro F, Roussakis E, Klein A, Wu J, Runnels JM, Zaher W, Mortensen LJ, Alt C, Turcotte R, Yusuf R, Cote D, Vinogradov SA, Scadden DT, Lin CP. (2014) Direct measurement of local oxygen concentration in the bone marrow of live animals. *Nature* 508, 269-273.

275. Levesque JP, Winkler IG, Hendy J, Williams B, Helwani F, Barbier V, Nowlan B, Nilsson SK. (2007) Hematopoietic progenitor cell mobilization results in hypoxia with increased hypoxia-inducible transcription factor-1 alpha and vascular endothelial growth factor A in bone marrow. *Stem Cells* 25, 1954-1965.

276. Lee JW, Bae SH, Jeong JW, Kim SH, Kim KW. (2004) Hypoxia-inducible factor (HIF-1)alpha: its protein stability and biological functions. *Experimental and Molecular Medicine* 36, 1-12.

277. Martin SK, Diamond P, Williams SA, To LB, Peet DJ, Fujii N, Gronthos S, Harris AL, Zannettino ACW. (2010) Hypoxia-inducible factor-2 is a novel regulator of aberrant CXCL12 expression in multiple myeloma plasma cells. *Haematologica* 95, 776-784.

278. Giatromanolaki A, Bai M, Margaritis D, Bourantas KL, Koukourakis MI, Sivridis E, Gatter KC. (2010) Hypoxia and activated VEGF: receptor pathway in multiple myeloma. *Anticancer Research* 30, 2831-2836.

279. Irigoyen M, Garcia-Ruiz JC, Berra E. (2017) The hypoxia signalling pathway in haematological malignancies. *Oncotarget* 8, 36832-36844.

280. Boroughs LK, DeBerardinis RJ. (2015) Metabolic pathways promoting cancer cell survival and growth. *Nature Cell Biology* 17, 351-359.

281. Tavel L, Fontana F, Garcia Manteiga JM, Mari S, Mariani E, Caneva E, Sitia R, Camnasio F, Marcatti M, Cenci S, Musco G. (2016) Assessing heterogeneity of osteolytic lesions in multiple myeloma by (1)H HR-MAS NMR metabolomics. *International Journal of Molecular Sciences* 17, 1814-1829.

282. Falank C, Fairfield H, Reagan MR. (2016) Signaling interplay between bone marrow adipose tissue and multiple myeloma cells. *Frontiers in Endocrinology* 7.

283. Mateos MV, Hernandez MT, Giraldo P, de la Rubia J, de Arriba F, Lopez Corral L, Rosinol L, Paiva B, Palomera L, Bargay J, Oriol A, Prosper F, Lopez J, Olavarria E, Quintana N, Garcia JL, Blade J, Lahuerta JJ, San Miguel JF. (2013) Lenalidomide plus dexamethasone for high-risk smoldering multiple myeloma. *The New England Journal of Medicine* 369, 438-447.

284. Quach H, Prince HM, Augustson B, Kalff A, Szabo F, Gibson J, Ho J, Harrison S, Horvath N, Jaksic W, Kalro A, Johnston A, Joshua D, Lee C, Ling S, Mollee P, Roberts A, Spencer A, Szer J, Ward C, Talaulikar D, Zannettino A, Clinical practice guidelines for multiple myeloma in Australia. 4 ed.; Myeloma foundation of Australia (MFA): 2017.

285. Moalli PA, Rosen ST. (1994) Glucocorticoid receptors and resistance to glucocorticoids in hematologic malignancies. *Leukemia & Lymphoma* 15, 363-374.

286. Greenstein S, Ghias K, Krett NL, Rosen ST. (2002) Mechanisms of glucocorticoid-mediated apoptosis in hematological malignancies. *Clinical Cancer Research* 8, 1681-1694.

287. Gaynon PS, Carrel AL. (1999) Glucocorticosteroid therapy in childhood acute lymphoblastic leukemia. *Advances in Experimental Medicine and Biology* 457, 593-605.

288. Alexanian R, Dimopoulos MA, Delasalle K, Barlogie B. (1992) Primary dexamethasone treatment of multiple-myeloma. *Blood* 80, 887-890.

289. Sharma S, Lichtenstein A. (2008) Dexamethasone-induced apoptotic mechanisms in myeloma cells investigated by analysis of mutant glucocorticoid receptors. *Blood* 112, 1338-1345.

290. Greenstein S, Krett NL, Kurosawa Y, Ma CU, Chauhan D, Hideshima T, Anderson KC, Rosen ST. (2003) Characterization of the MM.1 human multiple myeloma (MM) cell lines: A model system to elucidate the characteristics, behavior, and signaling of steroid-sensitive and -resistant MM cells. *Experimental Hematology* 31, 271-282.

291. Chauhan D, Hideshima T, Rosen S, Reed JC, Kharbanda S, Anderson KC. (2001) Apaf-1/Cytochromec-independent and Smac-dependent Induction of apoptosis in multiple myeloma (MM) cells. *Journal of Biological Chemistry* 276, 24453-24456.

292. Maniscalco WM, Finkelstein JN, Parkhurst AB. (1985) Dexamethasone increases de novo fatty acid synthesis in fetal rabbit lung explants. *Pediatric Research* 19, 1272-1277.

293. Davies FE, Raje N, Hideshima T, Lentzsch S, Young G, Tai YT, Lin B, Podar K, Gupta D, Chauhan D, Treon SP, Richardson PG, Schlossman RL, Morgan GJ, Muller GW, Stirling DI, Anderson KC. (2001) Thalidomide and immunomodulatory derivatives augment natural killer cell cytotoxicity in multiple myeloma. *Blood* 98, 210-216.

294. Kotla V, Goel S, Nischal S, Heuck C, Vivek K, Das B, Verma A. (2009) Mechanism of action of lenalidomide in hematological malignancies. *Journal of Hematology & Oncology* 2, 36.

295. Anderson KC. (2005) Lenalidomide and thalidomide: mechanisms of action - similarities and differences. *Seminars in Hematology* 42, S3-S8.

296. Shi QL, Chen LJ. (2017) Cereblon: a protein crucial to the multiple functions of immunomodulatory drugs as well as cell metabolism and disease generation. *Journal of Immunology Research* 2017.

297. Greenberg AJ, Walters DK, Kumar SK, Vincent Rajkumar S, Jelinek DF. (2013) Responsiveness of cytogenetically discrete human myeloma cell lines to lenalidomide: lack of correlation with cereblon and interferon regulatory factor 4 expression levels. *European Journal of Haematology* 91, 504-513.

298. Mazumder A, Jagannath S. (2006) Thalidomide and lenalidomide in multiple myeloma. *Best Practice & Research Clinical Haematology* 19, 769-780.

299. Gay F, Hayman SR, Lacy MQ, Buadi F, Gertz MA, Kumar S, Dispenzieri A, Mikhael JR, Bergsagel PL, Dingli D, Reeder CB, Lust JA, Russell SJ, Roy V, Zeldenrust SR, Witzig TE, Fonseca R, Kyle RA, Greipp PR, Stewart AK, Rajkumar SV. (2010) Lenalidomide plus dexamethasone versus thalidomide plus dexamethasone in newly diagnosed multiple myeloma: a comparative analysis of 411 patients. *Blood* 115, 1343-1350.

300. Luo J, Gagne JJ, Landon J, Avorn J, Kesselheim AS. (2017) Comparative effectiveness and safety of thalidomide and lenalidomide in patients with multiple myeloma in the United States of America: A population-based cohort study. *European Journal of Cancer* 70, 22-33.

301. Hideshima T, Raje N, Richardson PG, Anderson KC. (2008) A review of lenalidomide in combination with dexamethasone for the treatment of multiple myeloma. *Therapeutics and Clinical Risk Management* 4, 129-136.

302. Weber D, Wang M, Chen C, Belch A, Stadtmauer EA, Niesvisky R, Yu Z, Olesnyckyj M, Zeldis J, Knight RD, Dimopoulos M. (2006) Lenalidomide plus high-dose dexamethasone provides improved overall survival compared to high-dose dexamethasone alone for relapsed or refractory multiple myeloma (MM): Results of 2 phase III studies (MM-009, MM-010) and subgroup analysis of patients with impaired renal function. *Blood* 108, 1012a-1013a.

303. Rajkumar SV, Hayman S, Lacy MQ, Dispenzieri A, Geyer SM, Kabat B, Zeldenrust SR, Kumar S, Greipp PR, Fonseca R, Lust JA, Russell SJ, Kyle RA, Witzig TE, Gertz MA. (2005) Combination therapy with lenalidomide plus dexamethasone (Rev/Dex) for newly diagnosed myeloma. *Blood* 106, 230a-231a.

304. Benboubker L, Dimopoulos MA, Dispenzieri A, Catalano J, Belch AR, Cavo M, Pinto A, Weisel K, Ludwig H, Bahlis N, Banos A, Tiab M, Delforge M, Cavenagh J, Geraldes C, Lee JJ, Chen C, Oriol A, de la Rubia J, Qiu LG, White DJ, Binder D, Anderson K, Fermand JP, Moreau P, Attal M, Knight R, Chen G, Van Oostendorp J, Jacques C, Ervin-Haynes A, Avet-Loiseau H, Hulin C, Facon T, Team FT. (2014) Lenalidomide and dexamethasone in transplant-ineligible patients with myeloma. *New England Journal of Medicine* 371, 906-917.

305. Maiga S, Gomez-Bougie P, Bonnaud S, Gratas C, Moreau P, Le Gouill S, Pellat-Deceunynck C, Amiot M. (2013) Paradoxical effect of lenalidomide on cytokine/growth factor profiles in multiple myeloma. *British Journal of Cancer* 108, 1801-1806.

306. Baz R, Patel M, Finley-Oliver E, Lebovic D, Hussein MA, Miller KC, Wood M, Sher T, Lee K, Chanan-Khan AA. (2010) Single agent lenalidomide in newly diagnosed multiple myeloma: a retrospective analysis. *Leukemia & Lymphoma* 51, 1015-1019.

307. Kumar S, Gertz MA, Dispenzieri A, Lacy MQ, Geyer SM, Iturria NL, Fonseca R, Hayman SR, Lust JA, Kyle RA, Greipp PR, Witzig TE, Rajkumar SV. (2003)

Response rate, durability of response, and survival after thalidomide therapy for relapsed multiple myeloma. *Mayo Clinic Proceedings* 78, 34-39.

308. Dimopoulos M, Spencer A, Attal M, Prince HM, Harousseau J, Dmoszynska A, San Miguel J, Hellmann A, Facon T, Foa R, Corso A, Masliak Z, Olesnyckyj M, Yu ZN, Patin J, Zeldis JB, Knight RD. (2007) Lenalidomide plus dexamethasone for relapsed or refractory multiple myeloma. *New England Journal of Medicine* 357, 2123-2132.

309. Morgan GJ, Davies FE, Gregory WM, Bell SE, Szubert AJ, Coy NN, Cook G, Feyler S, Johnson PRE, Rudin C, Drayson MT, Owen RG, Ross FM, Russell NH, Jackson GH, Child JA, Oncology NH. (2012) Cyclophosphamide, thalidomide, and dexamethasone as induction therapy for newly diagnosed multiple myeloma patients destined for autologous stem-cell transplantation: MRC Myeloma IX randomized trial results. *Haematologica* 97, 442-450.

310. Crawford LJ, Walker B, Irvine AE. (2011) Proteasome inhibitors in cancer therapy. *Journal of Cell Communication and Signaling* 5, 101-110.

311. Kubiczkova L, Pour L, Sedlarikova L, Hajek R, Sevcikova S. (2014) Proteasome inhibitors - molecular basis and current perspectives in multiple myeloma. *Journal of Cellular and Molecular Medicine* 18, 947-961.

312. Landis-Piwowar KR, Milacic V, Chen D, Yang HJ, Zhao YF, Chan TH, Yan B, Dou QP. (2006) The proteasome as a potential target for novel anticancer drugs and chemosensitizers. *Drug Resistance Updates* 9, 263-273.

313. Jakob C, Egerer K, Liebisch P, Turkmen S, Zavrski I, Kuckelkorn U, Heider U, Kaiser M, Fleissner C, Sterz J, Kleeberg L, Feist E, Burmester GR, Kloetzel PM, Sezer O. (2007) Circulating proteasome levels are an independent prognostic factor for survival in multiple myeloma. *Blood* 109, 2100-2105.

314. Yang H, Zonder JA, Dou QP. (2009) Clinical development of novel proteasome inhibitors for cancer treatment. *Expert Opinion on Investigational Drugs* 18, 957-971.

315. Mateos MV, Hernandez JM, Hernandez MT, Gutierrez NC, Palomera L, Fuertes M, Diaz-Mediavilla J, Lahuerta JJ, de la Rubia J, Terol MJ, Sureda A, Bargay J, Ribas P, de Arriba F, Alegre A, Oriol A, Carrera D, Garcia-Larana J, Garcia-Sanz R, Blade J, Prosper F, Mateo G, Esseltine DL, de Velde HV, San Miguel JF. (2006) Bortezomib plus melphalan and prednisone in elderly untreated patients with multiple myeloma: results of a multicenter phase 1/2 study. *Blood* 108, 2165-2172.

316. Richardson PG, Barlogie B, Berenson J, Singhal S, Jagannath S, Irwin D, Rajkumar SV, Srkalovic G, Alsina M, Alexanian R, Siegel D, Orlowski RZ, Kuter D, Limentani SA, Lee S, Hideshima T, Esseltine DL, Kauffman M, Adams J, Schenkein DP, Anderson KC. (2003) A phase 2 study of bortezomib in relapsed, refractory myeloma. *New England Journal of Medicine* 348, 2609-2617.

317. Richardson PG, Sonneveld P, Schuster MW, Irwin D, Stadtmauer EA, Facon T, Harousseau JL, Ben-Yehuda D, Lonial S, Goldschmidt H, Reece D, San-Miguel JF, Blade J, Boccadoro M, Cavenagh J, Dalton WS, Boral AL, Esseltine DL, Porter JB, Schenkein D, Anderson KC, Investigators A. (2005) Bortezomib or high-dose dexamethasone for relapsed multiple myeloma. *New England Journal of Medicine* 352, 2487-2498.

318. Jagannath S, Richardson PG, Barlogie B, Berenson JR, Singhal S, Irwin D, Srkalovic G, Schenkein DP, Esseltine DL, Anderson KC. (2006) Bortezomib in combination with dexamethasone for the treatment of patients with relapsed and/or refractory multiple myeloma with less than optimal response to bortezomib alone. *Haematologica* 91, 929-934.

319. Orlowski RZ, Voorhees PM, Garcia RA, Hall MD, Kudrik FJ, Allred T, Johri AR, Jones PE, Ivanova A, Van Deventer HW, Gabriel DA, Shea TC, Mitchell BS, Adams J, Esseltine DL, Trehu EG, Green M, Lehman MJ, Natoli S, Collins JM, Lindley CM, Dees EC. (2005) Phase 1 trial of the proteasome inhibitor bortezomib and pegylated liposomal doxorubicin in patients with advanced hematologic malignancies. *Blood* 105, 3058-3065.

320. Berenson JR, Yang HH, Vescio RA, Nassir Y, Mapes R, Lee SP, Wilson J, Yellin O, Morrison B, Hilger J, Swift R. (2008) Safety and efficacy of bortezomib and melphalan combination in patients with relapsed or refractory multiple myeloma: updated results of a phase 1/2 study after longer follow-up. *Annals of Hematology* 87, 623-631.

321. Durie BGM, Hoering A, Abidi MH, Rajkumar SV, Epstein J, Kahanic SP, Thakuri M, Reu F, Reynolds CM, Sexton R, Orlowski RZ, Barlogie B, Dispenzieri A. (2017) Bortezomib with lenalidomide and dexamethasone versus lenalidomide and dexamethasone alone in patients with newly diagnosed myeloma without intent for immediate autologous stem-cell transplant (SWOG S0777): a randomised, open-label, phase 3 trial. *Lancet* 389, 519-527.

322. Niewerth D, Jansen G, Assaraf YG, Zweegman S, Kaspers GJL, Cloos J. (2015) Molecular basis of resistance to proteasome inhibitors in hematological malignancies. *Drug Resistance Updates* 18, 18-35.

323. Zaal EA, Wu W, Jansen G, Zweegman S, Cloos J, Berkers CR. (2017) Bortezomib resistance in multiple myeloma is associated with increased serine synthesis. *Cancer & Metabolism* 5.

324. Zub KA, Sousa MM, Sarno A, Sharma A, Demirovic A, Rao S, Young C, Aas PA, Ericsson I, Sundan A, Jensen ON, Slupphaug G. (2015) Modulation of cell metabolic pathways and oxidative stress signaling contribute to acquired melphalan resistance in multiple myeloma cells. *PLOS One* 10, e0119857.

325. Samuels AL, Heng JY, Beesley AH, Kees UR. (2014) Bioenergetic modulation overcomes glucocorticoid resistance in T-lineage acute lymphoblastic leukaemia. *British Journal of Haematology* 165, 57-66.

326. Borsi E, Perrone G, Terragna C, Martello M, Dico AF, Solaini G, Baracca A, Sgarbi G, Pasquinelli G, Valente S, Zamagni E, Tacchetti P, Martinelli G, Cavo M. (2014) Hypoxia inducible factor-1 alpha as a therapeutic target in multiple myeloma. *Oncotarget* 5, 1779-1792.

327. Storti P, Bolzoni M, Donofrio G, Airoldi I, Guasco D, Toscani D, Martella E, Lazzaretti M, Mancini C, Agnelli L, Patrene K, Maiga S, Franceschi V, Colla S, Anderson J, Neri A, Amiot M, Aversa F, Roodman GD, Giuliani N. (2013) Hypoxia-inducible factor (HIF)-1 alpha suppression in myeloma cells blocks tumoral growth in vivo inhibiting angiogenesis and bone destruction. *Leukemia* 27, 1697-1706.

328. Storti P, Toscani D, Airoldi I, Marchica V, Maiga S, Bolzoni M, Fiorini E, Campanini N, Martella E, Mancini C, Guasco D, Ferri V, Donofrio G, Aversa F, Amiot M, Giuliani N. (2016) The anti-tumoral effect of lenalidomide is increased in vivo by hypoxia-inducible factor (HIF)-1 alpha inhibition in myeloma cells. *Haematologica* 101, E107-E110.

329. Matsumoto T, Jimi S, Migita K, Takamatsu Y, Hara S. (2016) Inhibition of glucose transporter 1 induces apoptosis and sensitizes multiple myeloma cells to conventional chemotherapeutic agents. *Leukemia Research* 41, 103-110.

330. Bartel TB, Haessler J, Brown TL, Shaughnessy JD, Jr., van Rhee F, Anaissie E, Alpe T, Angtuaco E, Walker R, Epstein J, Crowley J, Barlogie B. (2009) F18-fluorodeoxyglucose positron emission tomography in the context of other imaging techniques and prognostic factors in multiple myeloma. *Blood* 114, 2068-2076.

331. Zamagni E, Patriarca F, Nanni C, Zannetti B, Englaro E, Pezzi A, Tacchetti P, Buttignol S, Perrone G, Brioli A, Pantani L, Terragna C, Carobolante F, Baccarani M, Fanin R, Fanti S, Cavo M. (2011) Prognostic relevance of 18-F FDG PET/CT in newly diagnosed multiple myeloma patients treated with up-front autologous transplantation. *Blood* 118, 5989-5995.

332. Fernando RC, Carvalho Fd, Mazzotti DR, Evangelista AF, Braga WMT, Chauffaille MdL, Leme AFP, Colleoni GWB. (2015) Multiple myeloma cell lines and primary tumors proteoma- protein biosynthesis and immune system as potential therapeutic targets. *Genes & Cancer* 6, 462-471.

333. Goldman-Leikin RE, Salwen HR, Herst CV, Variakojis D, Bian ML, Le Beau MM, Selvanayagan P, Marder R, Anderson R, Weitzman S, et al. (1989) Characterization of a novel myeloma cell line, MM.1. *Journal of Laboratory and Clinical Medicine* 113, 335-345.

334. Saha MN, Jiang H, Yang YJ, Zhu XY, Wang XM, Schimmer AD, Qiu LG, Chang H. (2012) Targeting p53 via JNK pathway: a novel role of RITA for apoptotic signaling in multiple myeloma. *PLOS One* 7, e30215.

335. Repetto G, del Peso A, Zurita JL. (2008) Neutral red uptake assay for the estimation of cell viability/cytotoxicity. *Nature Protocols* 3, 1125-1131.

336. Quah BJ, Parish CR. (2010) The use of carboxyfluorescein diacetate succinimidyl ester (CFSE) to monitor lymphocyte proliferation. *Journal of Visualized Experiments*.

337. Towbin H, Staehelin T, Gordon J. (1979) Electrophoretic Transfer of Proteins from Polyacrylamide Gels to Nitrocellulose Sheets - Procedure and Some Applications. *Proceedings of the National Academy of Sciences of the United States of America* 76, 4350-4354.

338. Winer LSP, Wu M. (2014) Rapid Analysis of Glycolytic and Oxidative Substrate Flux of Cancer Cells in a Microplate. *PLOS One* 9.

339. Dranka BP, Benavides GA, Diers AR, Giordano S, Zelickson BR, Reily C, Zou LY, Chatham JC, Hill BG, Zhang JH, Landar A, Darley-Usmar VM. (2011) Assessing bioenergetic function in response to oxidative stress by metabolic profiling. *Free Radical Biology and Medicine* 51, 1621-1635.

340. Banh RS, Iorio C, Marcotte R, Xu Y, Cojocari D, Rahman AA, Pawling J, Zhang W, Sinha A, Rose CM, Isasa M, Zhang S, Wu R, Virtanen C, Hitomi T, Habu T, Sidhu SS, Koizumi A, Wilkins SE, Kislinger T, Gygi SP, Schofield CJ, Dennis JW, Wouters BG, Neel BG. (2016) PTP1B controls non-mitochondrial oxygen consumption by regulating RNF213 to promote tumour survival during hypoxia. *Nature Cell Biology* 18, 803-813.

341. Ruggieri V, Agriesti F, Scrima R, Laurenzana I, Perrone D, Tataranni T, Mazzoccoli C, Lo Muzio L, Capitanio N, Piccoli C. (2015) Dichloroacetate, a selective mitochondria-targeting drug for oral squamous cell carcinoma: a metabolic perspective of treatment. *Oncotarget* 6, 1217-1230.

342. Ho N, Coomber BL. (2015) Pyruvate dehydrogenase kinase expression and metabolic changes following dichloroacetate exposure in anoxic human colorectal cancer cells. *Exp Cell Res* 331, 73-81.

343. Jackson VN, Halestrap AP. (1996) The kinetics, substrate, and inhibitor specificity of the monocarboxylate (lactate) transporter of rat liver cells determined using the fluorescent intracellular pH indicator, 2',7'-bis(carboxyethyl)-5(6)-carboxyfluorescein. *Journal of Biological Chemistry* 271, 861-868.

344. Babu E, Ramachandran S, CoothanKandaswamy V, Elangovan S, Prasad PD, Ganapathy V, Thangaraju M. (2011) Role of SLC5A8, a plasma membrane transporter and a tumor suppressor, in the antitumor activity of dichloroacetate. *Oncogene* 30, 4026-4037.

345. McCommis KS, Finck BN. (2015) Mitochondrial pyruvate transport: a historical perspective and future research directions. *Biochemical Journal* 466, 443-454.

346. Halestrap AP. (1975) The mitochondrial pyruvate carrier. Kinetics and specificity for substrates and inhibitors. *Biochemical Journal* 148, 85-96.

347. Su XB, Li RH, Kong KF, Tsang JSH. (2016) Transport of haloacids across biological membranes. *Biochimica Et Biophysica Acta-Biomembranes* 1858, 3061-3070.

348. Maj MC, Cameron JM, Robinson BH. (2006) Pyruvate dehydrogenase phosphatase deficiency: orphan disease or an under-diagnosed condition? *Molecular and Cellular Endocrinology* 249, 1-9.

349. Cameron JM, Maj M, Levandovskiy V, Barnett CP, Blaser S, Mackay N, Raiman J, Feigenbaum A, Schulze A, Robinson BH. (2009) Pyruvate dehydrogenase phosphatase 1 (PDP1) null mutation produces a lethal infantile phenotype. *Human Genetics* 125, 319-326.

350. Simonsson B, Brenning G, Kallander C, Ahre A. (1987) Prognostic value of serum lactic dehydrogenase (S-LDH) in multiple myeloma. *European Journal of Clinical Investigation* 17, 336-339.

351. Teke HU, Basak M, Teke D, Kanbay M. (2014) Serum level of lactate dehydrogenase is a useful clinical marker to monitor progressive multiple myeloma diseases: a case report. *Turkish Journal of Hematology* 31, 84-87.

352. Dalva-Aydemir S, Bajpai R, Martinez M, Adekola KU, Kandela I, Wei C, Singhal S, Koblinski JE, Raje NS, Rosen ST, Shanmugam M. (2015) Targeting the metabolic plasticity of multiple myeloma with FDA-approved ritonavir and metformin. *Clinical Cancer Research* 21, 1161-1171.

353. DeBerardinis RJ, Mancuso A, Daikhin E, Nissim I, Yudkoff M, Wehrli S, Thompson CB. (2007) Beyond aerobic glycolysis: Transformed cells can engage in glutamine metabolism that exceeds the requirement for protein and nucleotide synthesis. *Proceedings of the National Academy of Sciences of the United States of America* 104, 19345-19350.

354. Kolesnik DL, Pyaskovskaya ON, Boichuk IV, Solyanik GI. (2014) Hypoxia enhances antitumor activity of dichloroacetate. *Experimental Oncology* 36, 231-235.

355. Shahrzad S, Lacombe K, Adamcic U, Minhas K, Coomber BL. (2010) Sodium dichloroacetate (DCA) reduces apoptosis in colorectal tumor hypoxia. *Cancer Letters* 297, 75-83.

356. Schmittgen TD, Livak KJ. (2008) Analyzing real-time PCR data by the comparative CT method. *Nature Protocols* 3, 1101-1108.

357. Zhang DS, Fei Q, Li J, Zhang C, Sun Y, Zhu CY, Wang FZ, Sun YM. (2016) 2-deoxyglucose reverses the promoting effect of insulin on colorectal cancer cells *in vitro*. *PLOS One* 11, 1-14.

358. Cheng G, Zielonka J, McAllister D, Tsai S, Dwinell MB, Kalyanaraman B. (2014) Profiling and targeting of cellular bioenergetics: inhibition of pancreatic cancer cell proliferation. *British Journal of Cancer* 111, 85-93.

359. Shanmugam M, McBrayer SK, Qian J, Raikoff K, Avram MJ, Singhal S, Gandhi V, Schumacker PT, Krett NL, Rosen ST. (2009) Targeting glucose consumption and autophagy in myeloma with the novel nucleoside analogue 8-aminoadenosine. *Journal of Biological Chemistry* 284, 26816-26830.

360. Birsoy K, Possemato R, Lorbeer FK, Bayraktar EC, Thiru P, Yucel B, Wang T, Chen WW, Clish CB, Sabatini DM. (2014) Metabolic determinants of cancer cell sensitivity to glucose limitation and biguanides. *Nature* 508, 108-112.

361. Simoes RV, Serganova IS, Kruchevsky N, Leftin A, Shestov AA, Thaler HT, Sukenick G, Locasale JW, Blasberg RG, Koutcher JA, Ackerstaff E. (2015) Metabolic plasticity of metastatic breast cancer cells: adaptation to changes in the microenvironment. *Neoplasia* 17, 671-684.

362. Sun W, Zhou S, Chang SS, McFate T, Verma A, Califano JA. (2009) Mitochondrial mutations contribute to HIF1alpha accumulation via increased reactive oxygen species and up-regulated pyruvate dehydrogenease kinase 2 in head and neck squamous cell carcinoma. *Clinical Cancer Research* 15, 476-484.

363. Eales KL, Hollinshead KER, Tennant DA. (2016) Hypoxia and metabolic adaptation of cancer cells. *Oncogenesis* 5, e190.

364. Kucharzewska P, Christianson HC, Belting M. (2015) Global Profiling of Metabolic Adaptation to Hypoxic Stress in Human Glioblastoma Cells. *PLOS One* 10.

365. Wigfield SM, Winter SC, Giatromanolaki A, Taylor J, Koukourakis ML, Harris AL. (2008) PDK-1 regulates lactate production in hypoxia and is associated with poor prognosis in head and neck squamous cancer. *British Journal of Cancer* 98, 1975-1984.

366. Berra E, Roux D, Richard DE, Pouyssegur J. (2001) Hypoxia-inducible factor-1 alpha (HIF-1 alpha) escapes O-2-driven proteasomal degradation irrespective of its subcellular localization: nucleus or cytoplasm. *Embo Reports* 2, 615-620.

367. Ziebart T, Walenta S, Kunkel M, Reichert TE, Wagner W, Mueller-Klieser W. (2011) Metabolic and proteomic differentials in head and neck squamous cell carcinomas and normal gingival tissue. *Journal of Cancer Research and Clinical Oncology* 137, 193-199.

368. Borrello I. (2012) Can we change the disease biology of multiple myeloma? *Leukemia Research* 36 Suppl 1, S3-12.

369. Ito S, Oyake T, Murai K, Ishida Y. (2013) Successful use of cyclophosphamide as an add-on therapy for multiple myeloma patients with acquired resistance to bortezomib or lenalidomide. *Case Reports in Hematology* 2013, 651902.

370. Anagnostopoulos A, Dimopoulos MA, Spencer A, Attal M, Prince M, Harousseau JL, Dmoszynska A, San Miguel J, Hellmann A, Facon T, Foa R, Lazzarino M, Masliak Z, Olesnyckyj M, Yu Z, Patin J, Zeldis JB, Knight RD.

(2007) A randomized phase 3 trial of oral lenalidomide and dexamethasone versus placebo and dexamethasone in patients with relapsed or refractory multiple myeloma. Final analysis of MM010 study. *Haematologica* 92, 171-172.

371. Rajkumar SV, Richardson PG, Lacy MQ, Dispenzieri A, Greipp PR, Witzig TE, Schlossman R, Sidor CF, Anderson KC, Gertz MA. (2007) Novel therapy with 2-methoxyestradiol for the treatment of relapsed and plateau phase multiple myeloma. *Clinical Cancer Research* 13, 6162-6167.

372. Lopez-Girona A, Heintel D, Zhang LH, Mendy D, Gaidarova S, Brady H, Bartlett JB, Schafer PH, Schreder M, Bolomsky A, Hilgarth B, Zojer N, Gisslinger H, Ludwig H, Daniel T, Jager U, Chopra R. (2011) Lenalidomide downregulates the cell survival factor, interferon regulatory factor-4, providing a potential mechanistic link for predicting response. *British Journal of Haematology* 154, 325-336.

373. Schmidt M, Kim Y, Gast S-M, Endo T, Lu D, Carson D, Schmidt-Wolf IGH. (2011) Increased *in vivo* efficacy of lenalidomide and thalidomide by addition of ethacrynic acid. *in vivo* 25, 325-334.

374. Chou TC. (2010) Drug combination studies and their synergy quantification using the Chou-Talalay method. *Cancer Research* 70, 440-446.

375. Chou TC. (2006) Theoretical basis, experimental design, and computerized simulation of synergism and antagonism in drug combination studies. *Pharmacological Reviews* 58, 621-681.

376. Avet-Loiseau H, Facon T, Grosbois B, Magrangeas F, Rapp M-J, Harousseau J-L, Minvielle S, Bataille R. (2002) Oncogenesis of multiple myeloma- 14q32 and 13q chromosomal abnormalities are not randomly distributed, but correlate with natural history, immunological features, and clinical presentation. *Blood* 99, 2185-2191.

377. Iyer R, Ding L, Batchu RB, Naugler S, Shammas MA, Munshi NC. (2003) Antisense p53 transduction leads to overexpression of bcl-2 and dexamethasone resistance in multiple myeloma. *Leukemia Research* 27, 73-78.

378. Gazitt Y, Fey V, Thomas C, Alvarez R. (1998) Bcl-2 overexpression is associated with resistance to dexamethasone, but not melphalan, in multiple myeloma cells. *International Journal of Oncology* 13, 397-405.

379. Thomas AL, Coarfa C, Qian J, Wilkerson JJ, Rajapakshe K, Krett NL, Gunaratne PH, Rosen ST. (2015) Identification of potential glucocorticoid receptor therapeutic targets in multiple myeloma. *Nuclear Receptor Signaling* 13, e006.

380. Sanchez-Vega B, Krett N, Rosen ST, Gandhi V. (2006) Glucocorticoid receptor transcriptional isoforms and resistance in multiple myeloma cells. *Molecular Cancer Therapeutics* 5, 3062-3070.

381. Beesley AH, Firth MJ, Ford J, Weller RE, Freitas JR, Perera KU, Kees UR. (2009) Glucocorticoid resistance in T-lineage acute lymphoblastic leukaemia is associated with a proliferative metabolism. *British Journal of Cancer* 100, 1926-1936.

382. Ohashi T, Akazawa T, Aoki M, Kuze B, Mizuta K, Ito Y, Inoue N. (2013) Dichloroacetate improves immune dysfunction caused by tumor-secreted lactic acid and increases antitumor immunoreactivity. *International Journal of Cancer* 133, 1107-1118.

383. Kaufmann P, Engelstad K, Wei Y, Jhung S, Sano MC, Shungu DC, Millar WS, Hong X, Gooch CL, Mao X, Pascual JM, Hirano M, Stacpoole PW, DiMauro S, De Vivo DC. (2006) Dichloroacetate causes toxic neuropathy in MELAS: a randomized, controlled clinical trial. *Neurology* 66, 324-330.

384. Rajkumar SV, Landgren O, Mateos MV. (2015) Smoldering multiple myeloma. *Blood* 125, 3069-3075.

385. Siontis B, Kumar S, Dispenzieri A, Drake MT, Lacy MQ, Buadi F, Dingli D, Kapoor P, Gonsalves W, Gertz MA, Rajkumar SV. (2015) Positron emission tomography-computed tomography in the diagnostic evaluation of smoldering multiple myeloma: identification of patients needing therapy. *Blood Cancer Journal* 5, e364.

386. Zamagni E, Nanni C, Gay F, Pezzi A, Patriarca F, Bello M, Rambaldi I, Tacchetti P, Hillengass J, Gamberi B, Pantani L, Magarotto V, Versari A, Offidani M, Zannetti B, Carobolante F, Balma M, Musto P, Rensi M, Mancuso K, Dimitrakopoulou-Strauss A, Chauvie S, Rocchi S, Fard N, Marzocchi G, Storto G, Ghedini P, Palumbo A, Fanti S, Cavo M. (2016) 18F-FDG PET/CT focal, but not osteolytic, lesions predict the progression of smoldering myeloma to active disease. *Leukemia* 30, 417-422.

387. Zhan FH, Barlogie B, Arzoumanian V, Huang YS, Hollmig K, Pineda-Roman M, Tricot G, van Rhee F, Zangari M, Dhodapkar M, Shaughnessy JD. (2006) A gene expression signature of benign monoclonal gammopathy evident in multiple myeloma is linked to good prognosis. *Blood* 108, 969a-969a.

388. Fang ST, Fang X. (2016) Advances in glucose metabolism research in colorectal cancer. *Biomedical Reports* 5, 289-295.

389. Chan AKC, Bruce JIE, Siriwardena AK. (2016) Glucose metabolic phenotype of pancreatic cancer. *World Journal of Gastroenterology* 22, 3471-3485.

390. Yuan LW, Yamashita H, Seto Y. (2016) Glucose metabolism in gastric cancer: The cutting-edge. *World Journal of Gastroenterology* 22, 2046-2059.

391. Song K, Kwon H, Han C, Zhang J, Dash S, Lim K, Wu T. (2015) Active glycolytic metabolism in CD133(+) hepatocellular cancer stem cells: regulation by MIR-122. *Oncotarget* 6, 40822-40835.

392. Iansante V, Choy PM, Fung SW, Liu Y, Chai JG, Dyson J, Del Rio A, D'Santos C, Williams R, Chokshi S, Anders RA, Bubici C, Papa S. (2015) PARP14 promotes the Warburg effect in hepatocellular carcinoma by inhibiting JNK1-dependent PKM2 phosphorylation and activation. *Nature Communications* 6, 1-15.

393. Schmidt M, Voelker HU, Kapp M, Krockenberger M, Dietl J, Kammerer U. (2010) Glycolytic phenotype in breast cancer: activation of Akt, up-regulation of GLUT1, TKTL1 and down-regulation of M2PK. *Journal of Cancer Research and Clinical Oncology* 136, 219-225.

394. Karantanis D, Allen-Auerbach M, Czernin J. (2012) Relationship among glycolytic phenotype, grade, and histological subtype in ovarian carcinoma. *Clinical Nuclear Medicine* 37, 49-53.

395. Pertega-Gomes N, Felisbino S, Massie CE, Vizcaino JR, Coelho R, Sandi C, Simoes-Sousa S, Jurmeister S, Ramos-Montoya A, Asim M, Tran M, Oliveira E, da Cunha AL, Maximo V, Baltazar F, Neal DE, Fryer LGD. (2015) A glycolytic phenotype is associated with prostate cancer progression and aggressiveness: a role for monocarboxylate transporters as metabolic targets for therapy. *Journal of Pathology* 236, 517-530.

396. Byrne FL, Poon IKH, Modesitt SC, Tomsig JL, Chow JDY, Healy ME, Baker WD, Atkins KA, Lancaster JM, Marchion DC, Moley KH, Ravichandran KS, Slack-Davis JK, Hoehn KL. (2014) Metabolic vulnerabilities in endometrial cancer. *Cancer Research* 74, 5832-5845.

397. Yoshino I, Kameyama T, Shikada Y, Kometani T, Kawano D, Osoegawa A, Yohena T, Yamaguchi M, Maehara Y. (2005) Glycolytic phenotype of non-small cell lung cancer: Implication of anaerobic glycolysis on malignant potential. *Journal of Clinical Oncology* 23, 869s-869s.

398. Laurenzana A, Chilla A, Luciani C, Peppicelli S, Biagioni A, Bianchini F, Tenedini E, Torre E, Mocali A, Calorini L, Margheri F, Fibbi G, Del Rosso M. (2017) uPA/uPAR system activation drives a glycolytic phenotype in melanoma cells. *International Journal of Cancer* 141, 1190-1200.

399. Song K, Li M, Xu XJ, Xuan L, Huang GN, Liu QF. (2016) Resistance to chemotherapy is associated with altered glucose metabolism in acute myeloid leukemia. *Oncology Letters* 12, 334-342.

400. Poulain L, Sujobert P, Zylbersztejn F, Barreau S, Stuani L, Lambert M, Palama TL, Chesnais V, Birsen R, Vergez F, Farge T, Chenevier-Gobeaux C, Fraisse M, Bouillaud F, Debeissat C, Herault O, Recher C, Lacombe C, Fontenay M, Mayeux P, Maciel TT, Portais JC, Sarry JE, Tamburini J, Bouscary D, Chapuis N. (2017) High mTORC1 activity drives glycolysis addiction and sensitivity to G6PD inhibition in acute myeloid leukemia cells. *Leukemia* 31, 2326-2335.

401. Mediani L, Gibellini F, Bertacchini J, Frasson C, Bosco R, Accordi B, Basso G, Bonora M, Calabro ML, Mattiolo A, Sgarbi G, Baracca A, Pinton P, Riva G,

Rampazzo E, Petrizza L, Prodi L, Milani D, Luppi M, Potenza L, De Pol A, Cocco L, Capitani S, Marmiroli S. (2016) Reversal of the glycolytic phenotype of primary effusion lymphoma cells by combined targeting of cellular metabolism and PI3K/Akt/mTOR signaling. *Oncotarget* 7, 5521-5537.

402. Ognibene M, Cangelosi D, Morini M, Segalerba D, Bosco MC, Sementa AR, Eva A, Varesio L. (2017) Immunohistochemical analysis of PDK1, PHD3 and HIF-1 alpha expression defines the hypoxic status of neuroblastoma tumors. *PLOS One* 12, e0187206.

403. Koukourakis MI, Giatromanolaki A, Sivridis E, Gatter KC, Harris AL, Tumor, Angiogenesis Research G. (2005) Pyruvate dehydrogenase and pyruvate dehydrogenase kinase expression in non small cell lung cancer and tumor-associated stroma. *Neoplasia* 7, 1-6.

404. Lin HJ, Hsieh FC, Song H, Lin J. (2005) Elevated phosphorylation and activation of PDK-1/AKT pathway in human breast cancer. *British Journal of Cancer* 93, 1372-1381.

405. Khan A. (2013) Case report of long term complete remission of metastatic renal squamous cell carcinoma after palliative radiotherapy and adjuvant dichloroacetate. *Advances in Cancer: Research & Treatment* 2012, 1-7.

406. Khan A, Andrews D, Blackburn AC. (2016) Long-term stabilization of stage 4 colon cancer using sodium dichloroacetate therapy. *World Journal of Clinical Cases* 4, 336-343.

407. Khan A, Andrews D, Shainhouse J, Blackburn AC. (2017) Long-term stabilization of metastatic melanoma with sodium dichloroacetate. *World Journal of Clinical Oncology* 8, 371-377.

408. Strum SB, Adalsteinsson O, Black RR, Segal D, Peress NL, Waldenfels J. (2013) Case Report: Sodium dichloroacetate (DCA) inhibition of the "Warburg Effect" in a human cancer patient: complete response in non-Hodgkin's lymphoma after disease progression with rituximab-CHOP. *Journal of Bioenergetics and Biomembranes* 45, 307-315.

409. Lwin ST, Edwards CM, Silbermann R. (2016) Preclinical animal models of multiple myeloma. *Bonekey Reports* 5, 1-9.

410. Chauhan D, Hideshima T, Anderson KC. (2006) A novel proteasome inhibitor NPI-0052 as an anticancer therapy. *British Journal of Cancer* 95, 961-965.

411. Freeman LM, Lam A, Petcu E, Smith R, Salajegheh A, Diamond P, Zannettino A, Evdokiou A, Luff J, Wong PF, Khalil D, Waterhouse N, Vari F, Rice AM, Catley L, Hart DN, Vuckovic S. (2011) Myeloma-induced alloreactive T cells arising in myeloma-infiltrated bones include double-positive CD8+CD4+ T cells: evidence from myeloma-bearing mouse model. *Journal of Immunology* 187, 3987-3996.

412. Dalton W, Anderson KC. (2006) Synopsis of a roundtable on validating novel therapeutics for multiple myeloma. *Clinical Cancer Research* 12, 6603-6610.

413. Amend SR, Wilson WC, Chu L, Lu L, Liu PY, Serie D, Su XM, Xu YL, Wang DY, Gramolini A, Wen XY, O'Neal J, Hurchla M, Vachon CM, Colditz G, Vij R, Weilbaecher KN, Tomasson MH. (2015) Whole genome sequence of multiple myeloma-prone C57BL/KaLwRij mouse strain suggests the origin of disease involves multiple cell types. *PLOS One* 10, e0127828.

414. Chesi M, Matthews GM, Garbitt VM, Palmer SE, Shortt J, Lefebure M, Stewart AK, Johnstone RW, Bergsagel PL. (2012) Drug response in a genetically engineered mouse model of multiple myeloma is predictive of clinical efficacy. *Blood* 120, 376-385.

415. Gang B. Targeting cancer metabolism. PhD Thesis. PhD Thesis, The Australian National University, 2014.

416. Zhang HR, Chen JM, Zeng ZY, Que WZ. (2013) Knockdown of DEPTOR inhibits cell proliferation and increases chemosensitivity to melphalan in human multiple myeloma RPMI-8226 cells via inhibiting PI3K/AKT activity. *The Journal of International Medical Research* 41, 584-595.

417. MacCallum DE, Melville J, Frame S, Watt K, Anderson S, Gianella-Borradori A, Lane DP, Green SR. (2005) Seliciclib (CYC202, R-Roscovitine) induces cell death in multiple myeloma cells by inhibition of RNA polymerase II-dependent transcription and down-regulation of Mcl-1. *Cancer Research* 65, 5399-5407.

418. Tiedemann RE, Zhu YX, Schmidt J, Shi CX, Sereduk C, Yin H, Mousses S, Stewart AK. (2012) Identification of molecular vulnerabilities in human multiple myeloma cells by RNA interference lethality screening of the druggable genome. *Cancer Research* 72, 757-768.

419. Steinbrunn T, Chatterjee M, Bargou RC, Stuhmer T. (2014) Efficient transient transfection of human multiple myeloma cells by electroporation--an appraisal. *PLOS One* 9, e97443.

420. Tuganova A, Klyuyeva A, Popov KM. (2007) Recognition of the inner lipoyl-bearing domain of dihydrolipoyl transacetylase and of the blood glucose-lowering compound AZD7545 by pyruvate dehydrogenase kinase 2. *Biochemistry* 46, 8592-8602.

421. Mayers RM, Butlin RJ, Kilgour E, Leighton B, Martin D, Myatt J, Orme JP, Holloway BR. (2003) AZD7545, a novel inhibitor of pyruvate dehydrogenase kinase 2 (PDHK2),activates pyruvate dehydrogenase in vivo and improves blood glucose control in obese (fa/fa) Zucker rats. *Biochemical Society Transactions* 31, 1165-1167.

422. Soga S, Shiotsu Y, Akinaga S, Sharma SV. (2003) Development of radicicol analogues. *Current Cancer Drug Targets* 3, 359-369.

423. Ghosh A, Mailankody S, Giralt SA, Landgren CO, Smith EL, Brentjens RJ. (2018) CAR T cell therapy for multiple myeloma: where are we now and where are we headed? *Leukemia & Lymphoma* 59, 2056-2067.

424. Kouidhi S, Aye FB, Elgaaied AB. (2018) Targeting Tumor Metabolism: A New Challenge to Improve Immunotherapy. *Frontiers in Immunology* 9, 1-11.

425. Menk AV, Scharping NE, Moreci RS, Zeng X, Guy C, Salvatore S, Bae H, Xie J, Young HA, Wendell SG, Delgoffe GM. (2018) Early TCR Signaling Induces Rapid Aerobic Glycolysis Enabling Distinct Acute T Cell Effector Functions. *Cell Reports* 22, 1509-1521.

426. Beckermann KE, Dudzinski SO, Rathmell JC. (2017) Dysfunctional T cell metabolism in the tumor microenvironment. *Cytokine & Growth Factor Reviews* 35, 7-14.

427. Zhan FH, Hardin J, Kordsmeier B, Bumm K, Zheng MZ, Tian EM, Sanderson R, Yang Y, Wilson C, Zangari M, Anaissie E, Morris C, Muwalla F, van Rhee F, Fassas A, Crowley J, Tricot G, Barlogie B, Shaughnessy J. (2002) Global gene expression profiling of multiple myeloma, monoclonal gammopathy of undetermined significance, and normal bone marrow plasma cells. *Blood* 99, 1745-1757.

Appendix

Appendix Table 1. RPMI-1640 cell culture media formula (31800, Thermo Fisher)

Main Component	Concentration (mM)
Amino Acids	
Glycine	0.133
L-Arginine	1.149
L-Asparagine	0.378
L-Aspartic acid	0.150
L-Cystine 2HCl	0.207
L-Glutamic Acid	0.136
L-Glutamine	2.054
L-Histidine	0.096
L-Hydroxyproline	0.152
L-Isoleucine	0.381
L-Leucine	0.381
L-Lysine hydrochloride	0.218
L-Methionine	0.100
L-Phenylalanine	0.090
L-Proline	0.173
L-Serine	0.285
L-Threonine	0.168
L-Tryptophan	0.024
L-Tyrosine disodium salt dihydrate	0.111
L-Valine	0.170
Vitamins	
Biotin	8.1967213E-4
Choline chloride	0.0214
D-Calcium pantothenate	5.24109E-4
Folic Acid	0.0022
Niacinamide	0.0081
Para-Aminobenzoic Acid	0.0072
Pyridoxine hydrochloride	0.0048
Riboflavin	5.319149E-4
Inorganic Salts	
Calcium nitrate ($Ca(NO_3)_2$ $4H_2O$)	0.423
Magnesium Sulfate ($MgSO_4$) (anhyd.)	0.407
Potassium Chloride (KCl)	5.333
Sodium Chloride (NaCl)	103.44
Sodium Phosphate dibasic (Na_2HPO_4-$7H_2O$)	2.985
Other Components	
D-Glucose (Dextrose)	11.111
Glutathione (reduced)	0.003
Phenol Red	0.013

Appendix Table 2. Agilent Seahorse XF base media formula (Agilent)

Main Component	Concentration
Mg^{2+} (as $MgSO_4$)	0.8 mM
Ca^{2+} (as $CaCl_2$)	1.8 mM
NaCl	143 mM
KCl	5.4 mM
NaH_2PO_4	0.91 mM
Phenol Red	3 mg/L

Appendix Table 3. Stripping buffer and protocols used in western blot

Antibody	Buffer composition (100 ml)	Stripping protocol
PDK1-4	Harsh stripping buffer: Mix 20 mL 10% SDS, 12.5 mL 0.5 M Tris HCl (pH 6.8), 0.8 mL β-mercaptoethanol, bring volume to 100 ml with distilled water.	Incubate at 50°C for up to 45 mins with agitation. Rinse the membrane under running water tap for 1-2 mins. Wash extensively for 5 mins in 1×TBST. Block in 5% NFM, 4°C, overnight.
pPDH	Mild stripping buffer: Dissolve 1.5 g glycine, 0.1 g SDS, 1 mL Tween 20, in 80 mL distilled water and adjust pH to 2.2, bring volume to 100 mL with distilled water.	Incubate at room temperature for 10 mins. Repeat incubation for 10 mins with fresh stripping buffer. Then repeat again. Wash in 1×PBS twice, each for 10 mins Wash in 1×TBST twice, each for 5 mins Block in 3% BSA, 4°C, overnight

Chapter 2 Supplementary data

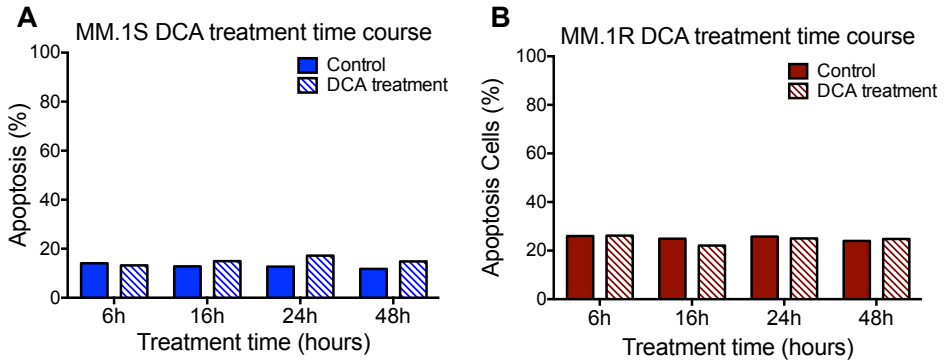

Appendix Figure 2.1 DCA treatment did not induce apoptosis in MM cell lines at different time points. (A, B) Apoptosis (Annexin V positive) cells were measured in MM.1S and MM.1R after treated with or without DCA (5 mM) for various time periods.

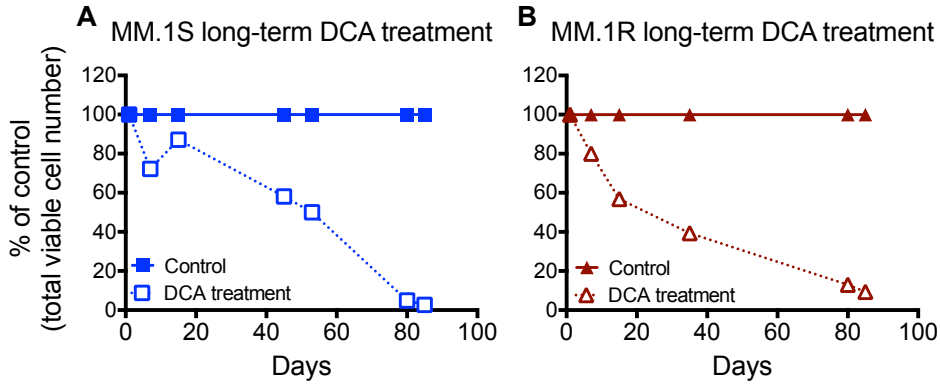

Appendix Figure 2.2 Long-term DCA treatments reduced the total viable cell number of MM cell lines. MM.1S and MM.1R were cultured in normal media and in media supplemented with 5 mM DCA for 3 months. Viable cells were measured by Trypan blue exclusion method. Viable cell number was calculated as percentage of the no-DCA treatment control.

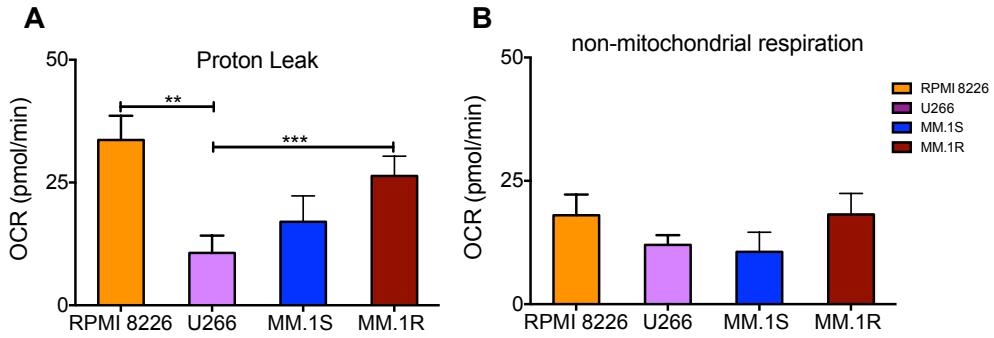

Appendix Figure 2.3 Non-ATP-linked OCR of MM cell lines. This figure shows (A) proton leak, (B) non-mitochondrial respiration, as defined in Figure 2.5. Each data point represents mean ± SD from 3-4 biological repeats, each consisting of 5-6 wells (technical repeats). *p <0.05, **p <0.01, ***p <0.0001. One-way ANOVA Tukey's multiple comparison test was used to compare differences among cell lines.

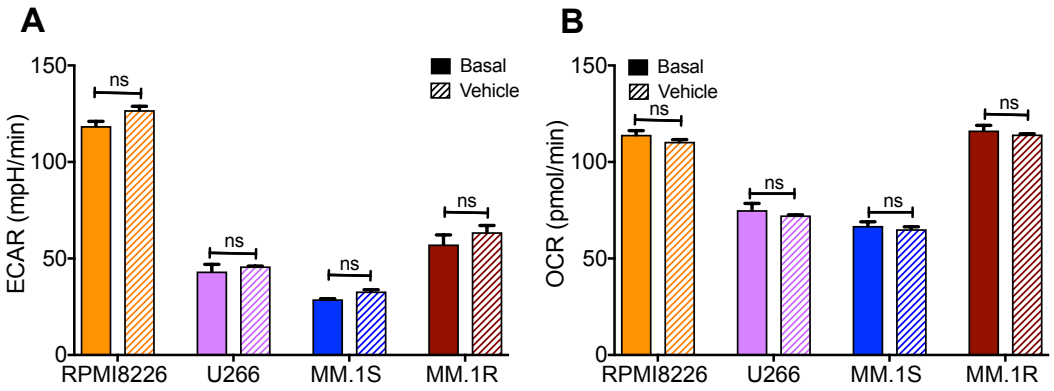

Appendix Figure 2.4 Vehicle control addition did not affect ECAR (A) and OCR (B) readings in MM cells. Vehicle control (0 mM DCA) in the seahorse assay was the media used to prepare DCA dilutions. T-test was used to compare difference of basal ECAR or OCR readings with readings after vehicle control addition in each cell line (mean ± SD, n=1). Each treatment has 5-6 technical replicates. ns: non-significant.

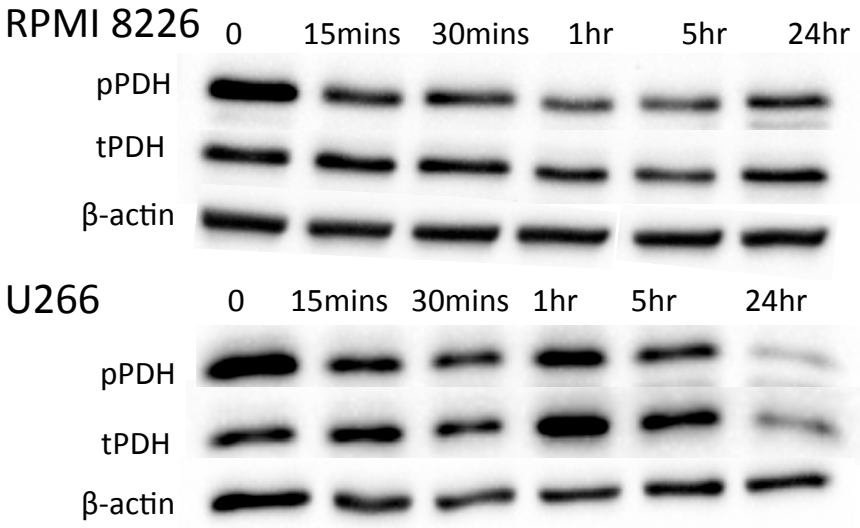

Appendix Figure 2.5 Loading control for pPDH/tPDH western blots in MM cell lines. Representative western blots of *β*-actin as loading control for pPDH and tPDH western blot experiments. *β*-actin was used as loading control in the experiment optimization and other experiments of pPDH (data not included in the thesis), and these results consistently showed an even loading practice. Protein estimation kit BCA was also used to ensure equal protein loading onto the gel. The aim of this particular experiment was to check the changes of the ratio of pPDH and tPDH after DCA treatment, a loading control was not needed for this purpose as pPDH and tPDH were determined on the same blot and so the loading was identical for the two readouts. The quantitative results of pPDH/tPDH ratios were not generated through the *β*-actin loading control.

Chapter 3 Supplementary data

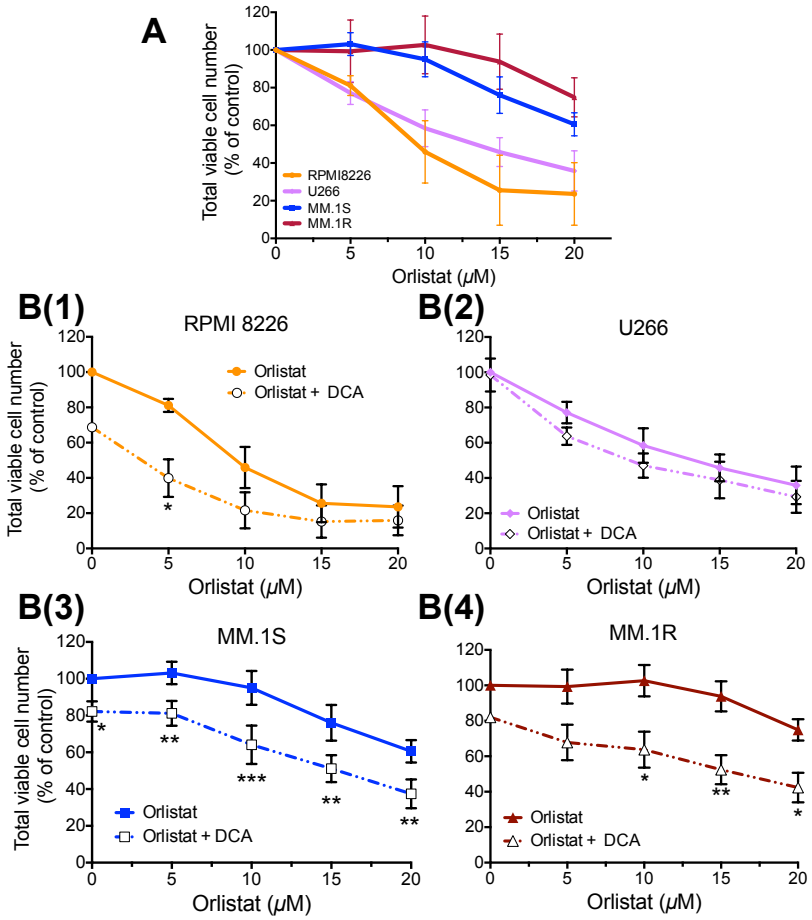

Appendix Figure 3.1 Orlistat and DCA co-treatments further reduced total viable cell number in MM cell lines. (A) Different sensitivities of MM cell lines to orlistat. U266 and RPMI 8226 were sensitive to orlistat. Total viable cell numbers were shown after 72 hours with different concentrations of orlistat (0-20 μM) with or without DCA (5 mM) treatments. **(B, 1-4)** DCA and orlistat combination treatments further decreased total viable cell number compared to orlistat alone in 3 MM cell lines. Orlistat was purchased from Sigma (Cat#O4139, Lot#115M4717V), dissolved in DMSO at a concentration of 15 mM as stock solution. All wells of treatment plates had an equal amount of vehicle DMSO. * Orlistat and DCA combination treatment compared to orlistat treatment group. Each treatment was quadruplicated. All data points shown represented mean ± SD from at least 3 independent experiments; *$p < 0.05$, ** $p < 0.01$, ***$p < 0.001$.

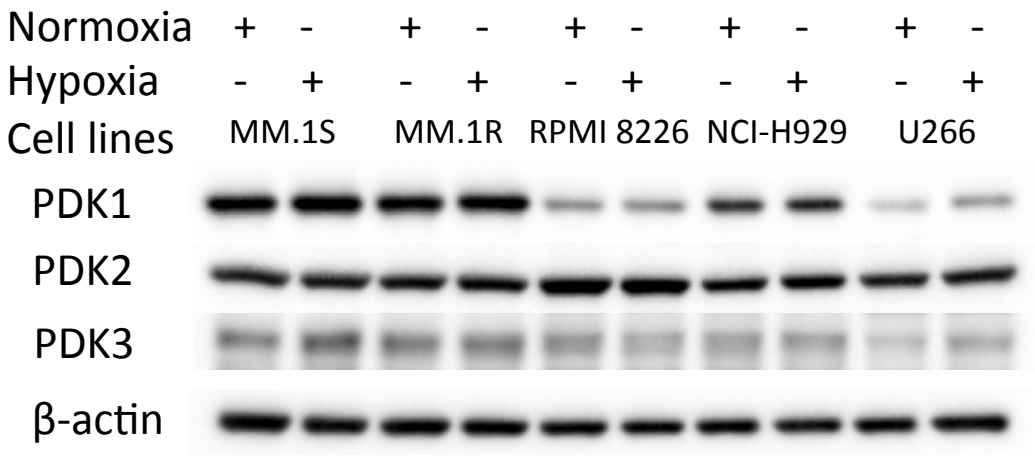

Appendix Figure 3.2 PDKs protein expression in normoxia and hypoxia in MM cell lines. Representative western blot of PDK1, 2, and 3 were shown here. β-actin was used as loading control. Three independent experiments were carried out.

Chapter 4 Supplementary data

4.1 DiCAM patients PCR-RFLP results

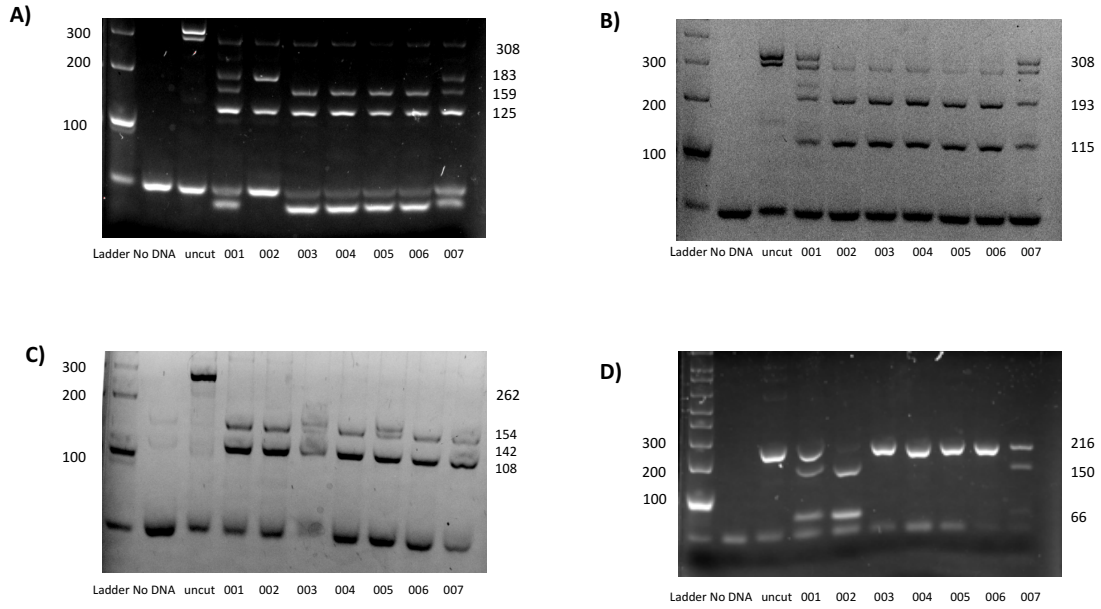

Appendix Figure 4.1. PCR-RLFP results of the GSTZ1 coding regions and -1002 promoter region genotype of patients 001-007. (A) RFLP analysis of the *Alw26I* digestion of exon 3. P 001 and 007 are A^{94}/G^{94}; P 002 is A^{94}/A^{94}; P 003, 004, 005, and 006 G^{94}/G^{94}. **(B)** RFLP analysis of the *FokI* digestion of the exon 3. P 001 and 007 are A^{124}/G^{124}; P 002, 003, 004, 005, and 006 G^{124}/G^{124}. The doublets in uncut and individuals 001 and 007 are thought to be heteroduplex formation. The faint bands in individual P 002, 003, 004, 005, and 006 are undigested residue. C) RFLP analysis of the *Bsh1236*I digestion of exon 5. P 001, 002, 004, 006, and 007 are C^{245}/C^{245}; 003 and 005 C^{245}/T^{245}. D) RFLP analysis the *MlucI* digestion of -1002 promoter region. 001 and 007 G/A; 002 A/A; 003,004,005, and 006 are G/G.

Appendix Table 4.1 Guide for genotyping at Exon 3 nt 94, 124 [220].

	Uncut size (bp)	A/A band sizes (bp)	G/G band sizes (bp)	A/G band sizes (bp)	Invariant size (internal control) (bp)
nt 94	308				
		183		183	
			159	159	
		125	125	125	125
			26	26	
nt 124	308	308		308	--
			193	193	
			115	115	

Appendix Table 4.2 Guide for genotyping at Exon 5 nt 245

	Exon 5 uncut size (bp)	C/C band sizes (bp)	T/T band sizes (bp)	C/T band sizes (bp)	Invariant size (bp)
nt 245	262		154	154	108
		142		142	
		108	108	108	
		12		12	

Appendix Table 4.3 Guide for genotyping at promoter -1002

	Promoter -1002 uncut size (bp)	A/A band sizes (bp)	G/G band sizes (bp)	A/G band sizes (bp)	Invariant size (bp)
-1002	216		216	216	--
		150		150	
		66		66	

4.2 GC-MS method

P005 and P006 serum DCA levels were determined using gas chromatography–mass spectrometry (GC-MS) modified by our lab. Serum aliquots (80 μl) from each patient was mixed with 40 μl of the internal standard (2,2-dimethyl-5-oxohexanoic acid) and 40 μl of distilled water. 500 μl of 12% boron trifluoride-methanol complex (12% BF3-MeOH) was added and mixed by votexing. The samples were heated at 115°C for 30 minutes in a graduated screw top vial. After cooling, 500 μl water and 500 μl methylene chloride (dichloromethane) was added to the reaction solution. The mixture was mixed by shaking vigorously for 15 seconds and centrifuged at 1057×g, 10 ºC for 15minutes. The methylene chloride layer/ the organic phase from each sample was transferred to a fresh micro sampling vial with inserted tubes. Samples were run on 7010QQQ (Agilent Technology) GC-MS. The GC-MS condition of 7010 MS triple Quad (QQQ) machine with a 7890B GC system from Agilent Technologies was set up by Dr Illa Tea. The GC column was a capillary column (from Zebron) ZB-Wax 60 m length, 0.32 I.D mm, 0.5 µm. 1 μl of each organic phase was injected into the GC-MS column. The GC run conditions are: -Injector temperature: 250 ºC with a pressure of 17.729 psi, the oven temperature conditions were: initial temperature 60 ºC, initial time (1 minute), ramp temperature: 10ºC /min until 250 ºC (for 5 minutes). MS conditions: full scan mode, source temperature 230 ºC and impact electronic mode with an Energy of 70eV. The

7010QQQ system is driven by the Xcalibur Data system. The DCA half-life for each patient was calculated from the time of peak level to the time where the DCA level fell to the half amount of the peak level. The formula for calculation of drug half-life was programmed using python programing which was $m(t)=m_0 e^{-kt}$. m=half peak level mass, t=time, m0 = peak level, and e-k = negative exponential rate.

4.3 DCA did not further induce apoptosis or cell cycle arrest when combined with DEX

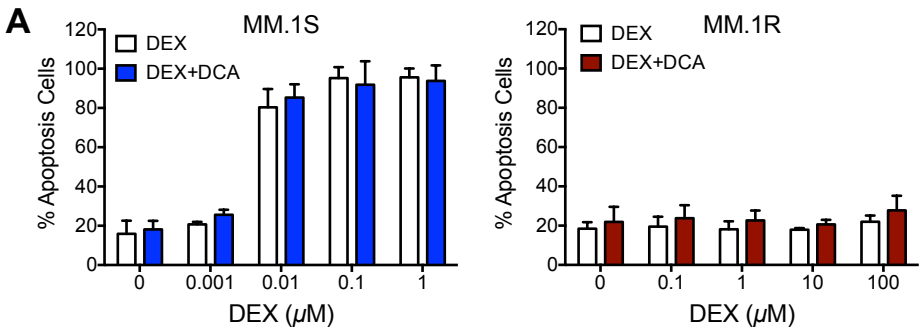

Appendix Figure 4.1 (A) The effects of DCA and DEX co-treatment on MM cells apoptosis. Apoptosis cells (Annexin V positive cells) were measured after 48 hours of DEX (0-100 μM) with or without DCA (5 mM) treatments. Cells were seeded at 25,000/well in U-bottom 96-well plates. Each treatment was duplicated and three independent experiments were carried out. All data points shown represented mean ± SD from at least 3 independent experiments.

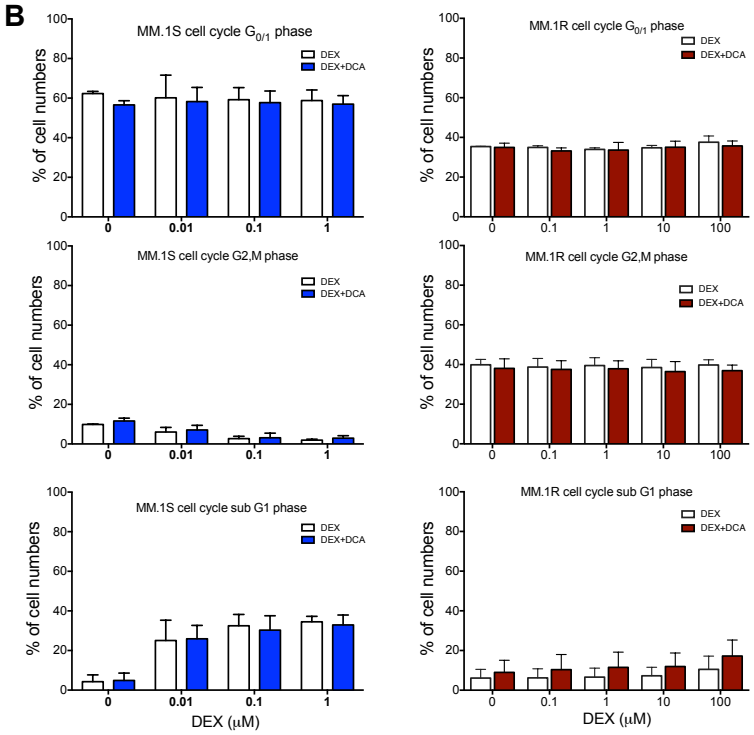

Appendix Figure 4.1 (B) The effects of DCA and DEX co-treatment on MM cell cycle distribution. Cell cycle was analysed after 72 hours of DEX (0-100 μM) with or without DCA (5 mM) treatments. The cell cycle analysis was carried out using the BrdU/PI staining method described in Chapter 2. Cells were seeded at 5×10^5/ well, 2 ml per well in 6-well plates. Each combination treatment was duplicated and three independent experiments were carried out. All data points shown represented mean ± SD from at least 3 independent experiments.

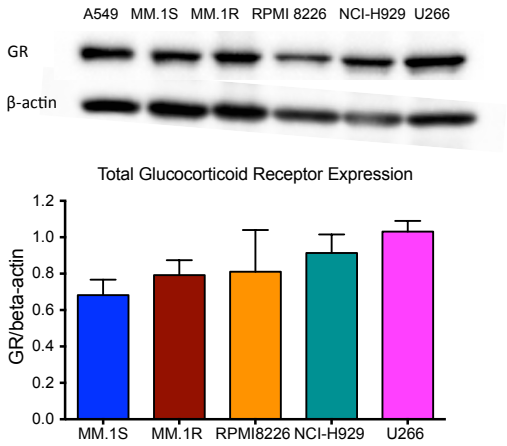

Appendix Figure 4.2 Glucocorticoids receptor (GR) in MM cell lines. GR protein expression levels were analysed by western blot. A549 lung cancer cell line was used as positive control. Blot shown was a representative of three independent experiments. GR antibody (Abcam, Cat# ab109022, Lot# GR47297-21) was diluted to 1:1000 in 3% FBS in 1×TBST and incubated at 4°C overnight, 2nd antibody (Polycolonal goat anti-rabbit HRP, Dako, REF# P0448, Lot# 20010775) was diluted to 1:5000 in 3 % FBS in 1× TBST and incubated for one hour at room temperature. All data points shown in the graph represented mean ± SD from 3 independent experiments.

Chapter 5 Supplementary data

5.1 Oncomine data

Appendix Table 5.1 Summary of fold changes of gene related glycolysis in SMM and normal plasma cells from bone marrow

Gene	Fold change	Samples compared [387, 427]
LDHA	2.6	SMM (12) vs normal PC bone marrow (22) vs MGUS (44)
MYC	3.1	SMM (12) vs normal PC bone marrow (22) vs MGUS (44)
MYC	2.68	MM (74) vs normal PC bone marrow (37)
GLUT	1.86	SMM (12) vs normal PC bone marrow (22) vs MGUS (44)
PDK2	2.03	SMM (12) vs normal PC bone marrow (22) vs MGUS (44)
PDK3	1.05	SMM (12) vs normal PC bone marrow (22) vs MGUS (44)

MGUS: Monoclonal Gammopathy of Undetermined Significance (44); PC: plasma cells; SMM: Smouldering Myeloma.

5.2 pPDH/tPDH western blot on bone marrow plasma cells

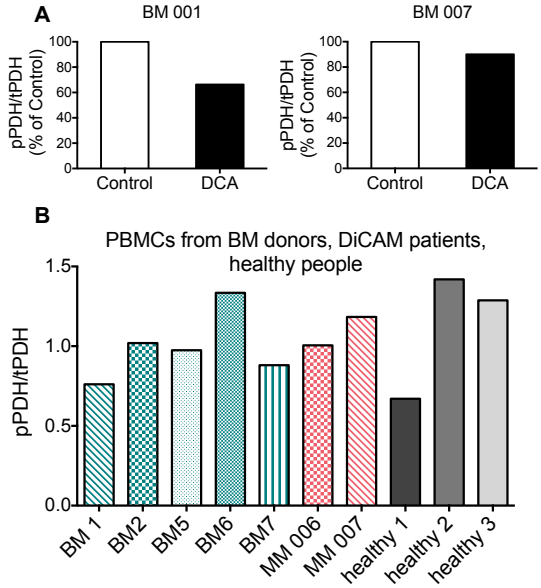

Appendix Figure 5.1 (A) MM newly diagnosed patient 001 (BM001) had 33.7% decrease of pPDH/tPDH of the enriched CD 138^{+} plasma cells from BM biopsy (70% myeloma cells in BM biopsy) after DCA (5 mM, 1 hour) treatment *in vitro* compared to that of the non-treated control group. But there was only 10% decrease of pPDH/tPDH in DCA treatment in MM relapsed patient 007 (BM007). Data was normalized to control as 100%. **(B)** Baseline variation of pPDH/tPDH of PBMCs from MM bone marrow (BM) donors, MM patients in DiCAM and healthy humans. Bone marrow from patient was collected in The Canberra Hospital in EDTA tube and were culture with or without 5 mM DCA for an hour in a 6-well plate. Whole Blood and Bone Marrow CD138+ MicroBeads (MACS) kit was used. Posselwb/Rinse programme was selected from the autoMACS Pro Separator (MACS) This result indicates that there are natural basal variations among individuals regardless of the disease profile. The ratio does not associate with the healthy status. Comparisons or statistic considerations can only be done within each individual's different treatments.